Surface Activation of Rubber to Enhance the Durability and Chemo-Mechanics of Asphalt

by

Sk Faisal Kabir

A Dissertation Presented in Partial Fulfillment
of the Requirements for the Degree
Doctor of Philosophy

Approved July 2020 by the
Graduate Supervisory Committee:

Elham Fini, Chair
Kamil Kaloush
Anthony Lamanna
Anca Delgado
Lily Poulikakos

ARIZONA STATE UNIVERSITY

August 2020

ABSTRACT

It is common to use crumb rubber as modifier in bitumen. Good performance of crumb rubber in bitumen has been reported in terms of improving characteristics like higher skid resistance, reducing noise, higher rutting resistance and longevity. However, due to the vulcanization, the polymeric crosslinked structure of crumb rubber suffers from inadequate dispersion and incompatibility in bitumen where storage stability becomes an issue. To solve this problem, partial surface devulcanization of the rubber via chemical and microbial surface activation was examined in this study showing both method can be effective to enhance rubber-bitumen interactions and subsequently storage stability of the rubberized bitumen. To ensure proper surface activation, it is important to thoroughly understand chemo-mechanics of bitumen containing rubber particles as well as underlying interaction mechanism at the molecular level. Therefore, this study integrates a multi-scale approach using density functional theory based computational modeling and laboratory experiments to provide an in-depth understanding of the mechanisms of interaction between surface activated rubber and bitumen. To do so, efficacy of various bio-modifiers was examined and compared it terms of both surface activation capability and durability of resulting rubberized bitumen. It was found that biomodifiers with various compositions can have either synergistic or antagonistic effect onchemo-mechanics of rubberized bitumen. The study was further extended to study the interplay of Polyphosphoric Acid (PPA) and these biomodified rubberized bitumens showing not all modifiers have high synergy with PPA in bitumens. Finally, durability of

rubberized bitumen was studied in terms of its resistance to Ultraviolet (UV) aging. It was shown that there is a strong relation between composition of biomodified rubberized bitumen and its resistance to UV-aging.

DEDICATION

I dedicate this dissertation to my beloved wife Dr Jannatun Naher, my lovely mother Tajmun Nahar, my cute son Rishav Aditya Faisal and to those who are in the frontline of treating patients of recent pandemic and also to those who are continuously fighting to keep the environment clean.

ACKNOWLEDGMENTS

My first acknowledgment goes to Almighty Allah who has helped me to get an advisor like Dr. Fini. I am blessed to complete my PhD dissertation in Arizona State University with Arizona being the birthplace of rubberized asphalt. I thank my adviser who guided me to work on this topic and Mr. Charles McDonald with city of Phoenix for first coming up with the idea of using rubber from scrap tires in asphalt back in 1950, so today in 2020, I can add to his work by completing my PhD research. The topic is dear and near to my heart and I believe in its positive social, economic, and environmental impacts. I want to thank Dr. Fini who is a motherly figure to me to lead me, guide me, correct me, and inspire me all the way through this dissertation journey and has believed in me in my ups and downs through this whole journey. I am thankful to my wife Jannatun Naher. She has continuously supported me in making my choices no matter how much she had to suffer. I am very thankful to my incredible family specially to my mother Tajmun Nahar and then to my father Sk Abdul Wadud. I am incredibly indebted to my entire research group and colleagues; there is no word to truly describe my appreciation and there is not enough space in this entire document to name them all. Thank you for all your genuine support, advice and assistance enabling me reach to this point of my personal and professional life.

TABLE OF CONTENTS

Page

CHAPTER Page

CHAPTER Page

LIST OF TABLES

Table Page

Table Page

Table Page

Table Page

LIST OF FIGURES

Figure Page

Figure Page

Figure Page

Figure Page

Figure Page

Figure Page

Figure Page

Chapter 1 INTRODUCTION

1.1 Background

The service life of asphalt pavement is greatly affected by traffic loadings and the surrounding environmental conditions, which cause distress to pavements. Based on failure mechanisms, there are five major categories of pavement distresses: rutting, fatigue cracking, low-temperature cracking, moisture damage, and raveling. Researchers have developed modification methods that attempt to improve the properties that delay these pavement distresses and thereby increase the service life of the pavement. Modification of bitumen with elastomers like crumb rubber is one of these approaches that is widely accepted.

The idea of adding rubber to bitumen first developed in the 1950's. Rubberized asphalt was first used in Phoenix, Arizona, by city engineer Charles McDonald. The first use of crumb rubber· modifier (CRM) in flexible pavements did not occur until 1964. In 1968, for the first time, asphalt rubber was applied with chips using an asphalt distributor. But early asphalt rubber had thick consistency and faced difficulty in pumping and distributing. Viscosity was lowered in 1972 when kerosene started to be added to the asphalt rubber. Adding kerosene improved the workability as well as the overall construction quality of asphalt rubber (Brown, 1993). By the end of 2018, producers from 11 states reported the use of waste tire rubber in asphalt mixtures, with an increase of 66 percent from 2017 to 1,621,000 tons in the 2018 construction season (Williams et al., 2019). States such as Arizona, Florida, California, Texas, and Nebraska are presently

using large amounts of asphalt-rubber. States like New Jersey, South Carolina, New York, and New Mexico have also studied rubberized asphalt (Hansen and Copeland, 2015).

A passenger car tire typically contains 48% elastomers or rubber and 22% carbon black. There can be other components like metal, textile cords, and chemical additives (Shulman, 2019). The U.S. Environment Protection Agency (EPA) estimated that nearly 1.7 million tons of rubber in tires were recycled in 2017, whereas approximately 4.22 million tons of rubber in tires was generated that year (EPA, 2019). With an estimated total market of 1.02 million tons, 15 percent (153,100 tons) of this crumb rubber was used in asphalt pavement mixtures and various surface treatments in 2017 (USTMA, 2017).

The most popular method of recycling tire rubber is the grinding process. Ambient grinding and cryogenic grinding are two different methods of producing ground tire rubber, which is also known as crumb rubber (Way et al., 2012). In 2017, 12% of the market for ground tire rubber was consumed by the asphalt industry (USTMA, 2017).

Approximately 315,980 tons of rubber was used for civil-engineering purposes in 2017. However, Figure 1 shows that land disposal of scrap tires is again on the increase in recent years, implying that recycling did not improve in a great way in the last decade.

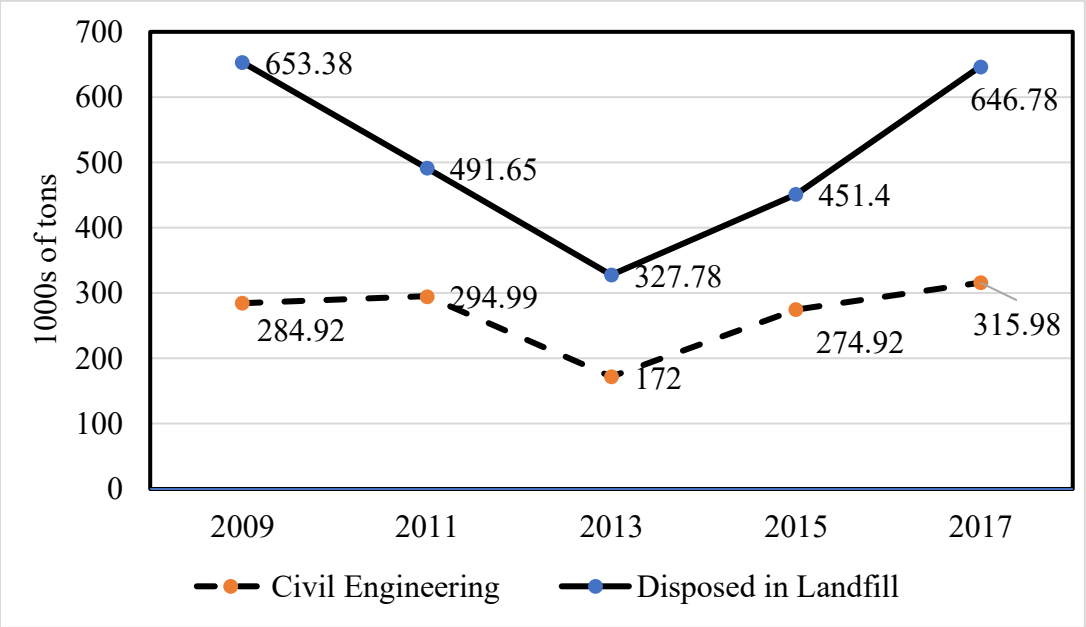

Figure 1-1. Number of Scrap Tire Rubbers Used in Civil Engineering and Disposed in Landfills

Crumb rubber can be incorporated in hot-mix asphalt using either of two major processes: the wet process, and the dry process. In the dry process, rubber is used as a replacement for aggregate. In the wet process, rubber in considered as a binder additive. The wet process can either happen on-site, or it can be blended at a terminal. On-site wet processing has a longer history of practice. On-site blending temperature for wet processing reaches 175 to 200˚C, and blending is done for 45 to 60 minutes. The reaction of rubber with asphalt is affected by the crumb rubber type and size, the temperature, the aromatic type of asphalt binder, and the type and amount of mechanical mixing (Shen et al., 2009). During this reaction time, the rubber particles absorb some of the light fractions of asphalt binder and swell (Way et al., 2012).

1.2 Elastomers for Improved Performance

Good performance has been reported for using rubber in asphalt, such as reducing fatigue cracking and rut depths (Way et al., 2012). It has also been reported that incorporation of crumb rubber in bitumen can enhance performance of asphalt mixture in a wide range of service temperatures: improved rutting resistance at high temperature, increased fatigue resistance at intermediate service temperature, and enhanced stress relaxation properties at low temperature. In addition, it has been reported that using crumb rubber in asphalt mixtures improves the skid resistance, reduces pavement noise level up to 50-70%, improved thermal properties as well as providing a safe method for recycling of scrap tire and reduces construction cost (Xiaowei et al., 2017; Yu et al., 2011).

1.3 Problem Statement

Crumb rubber in a bitumen matrix can have two types of effects: the physical (filler) effect, which is highly dependent on the rubber particles' shape and size; and the polymer contribution effect, which is mainly controlled by rubber-asphalt interaction. The polymer contribution effect can vary with the binder composition and treatment of the rubber surface; both factors are affected by mixing time (Fini et al., 2019a; Li et al., 2017).

The polymeric structure of rubber is mostly vulcanized, which means rubber molecules are crosslinked with sulfur via an irreversible reaction. Mechanism of crosslinking rubber itself dates back to 1839 when Charles Goodyear managed to

enhance thermo-mechanical properties of rubber by mixing rubber with sulfur and heat it. Crumb-rubber asphalt suffers from inadequate dispersion and incompatibility with asphalt binder, which is related to its vulcanized structure (Liang, 2015b; Yu et al., 2011). Devulcanization of the rubber surface can be an effective method of recovering rubber polymer and transforming the structure of waste vulcanized rubber or elastomers for reuse as a virgin rubber substitute. Devulcanization can be performed mechanically or chemically using devulcanizing agents (Isayev, 2005). These are some of the physical techniques for devulcanization: plasma polymerization, plasma chlorination, ultraviolet (UV) radiation, ozone treatment, and corona discharge (Cao et al., 2014; de Sousa et al., 2017; Romero-Sánchez and Martín-Martínez, 2006; Tyczkowski et al., 2003). In the chemical method of devulcanization, a reagent penetrates the crumb rubber and breaks the carbon-sulfur and sulfur-sulfur bonds that cross-link the linear polymers in the crumb rubber (Fan et al., 2013).

The physical effect of rubber is the main contributor to the increase in viscosity of rubber asphalt, which eventually increases the difficulty of pumping and requires continuous agitation (Hosseinnezhad et al., 2014). This problem reduces the workability of rubber asphalt and prevents the use of higher percentages of crumb rubber (Thodesen et al., 2009).

1.4 Specific Aim of This Research

This dissertation aims to address phase separation issue via sound scientific approach which are low-cost and scalable. Therefore, here we investigate the merits of

applying bio-modifiers (with and without microwave treatment) and microbial treatment (using activated sludge) to facilitate partial surface devulcanization of rubber. It further evaluates efficacy of surface activation to improve performance of rubberized bitumen as well as its impact on rubberized bitumen durability.

Therefore, specific objective of this research is to evaluate at different scales the effects of using surface-activated rubber on asphalt binder's rheological properties, chemical characteristics, and mechanical characteristics. Conventional test methods will be used to characterize the impact of surface activation of crumb rubber on asphalt binder by rheological characterization before and after the surface activation of the rubber. The research will also evaluate the impact of a hybrid approach to surface activation and the variation of using different bio-modifiers on crumb rubber. In addition, the research will try to gain a better understanding of how these modifiers fuel the partial breakup of rubber's three-dimensional network and how that affects the asphalt-rubber interaction. A unique contribution of this study will be a link between the rheological and mechanical properties of bitumen and the molecular interactions of its constituents, which will help gain a better understanding of some of the unknown aspects of bitumen behavior.

Another modification process to be studied is microbially desulfurized rubber, which involves usage of activated sludge microbes to feed on crumb rubber containing sulfur. The research will also investigate the synergistic effect of additives like polyphosphoric acid (PPA) with the biomodified rubbers in asphalt. In addition, the research will look into the recycling and rejuvenation of the bio-modified rubber asphalts.

1.5 Research Approach

A summary of the research approach is given in Figure 1-2. To address the objectives of this study, these research questions will be investigated:

- Study the merits of using surface activation of rubber using bio-modifiers to decrease rubber segregation and improve the workability of rubberized asphalt.
    - Does surface activation using bio-modifier(s) increase the surface polarity of rubber particles?
    - Does increased polarity of the rubber surface enhance the interaction of rubber and the asphalt matrix?
    - Does the interaction between the radicals of the bio-modifier and the carbon/sulfur-centered radicals of the rubber lead to grafting bio-molecules to the rubber surface?
    - Does grafting bio-molecules onto rubber particles change the rubber's surface microstructure?
- Study the merits of using surface activation of rubber using microbial treatment to decrease rubber segregation and improve the workability of rubberized asphalt.
    - Does microbial desulfurization occur via activated sludge microbes?
    - Does this microbially desulfurized rubber enhance bitumen's properties?

- Study the synergistic effects of bio-modified rubberized bitumen and polyphosphoric acid.
    - Are there any synergistic effects between bio-modifiers and polyphosphoric acid in bitumen that promote the durability and sustainability of bitumen?
- Study the recycling and rejuvenation of rubberized bitumen after UV aging.
    - Do indices of aging show variations in resistance to UV aging arising from the composition of bio-modifiers used to treat rubber?
    - Does the composition of a bio-modifier affect the dosage required to restore UV-aged rubberized bitumen to its original properties?
- Study the economic viability and market landscape of bio-modified rubberized bitumen.
    - How are the proposed hybrid method, the desulfurization technique, and the use of bio-modifiers relevant to the asphalt market?

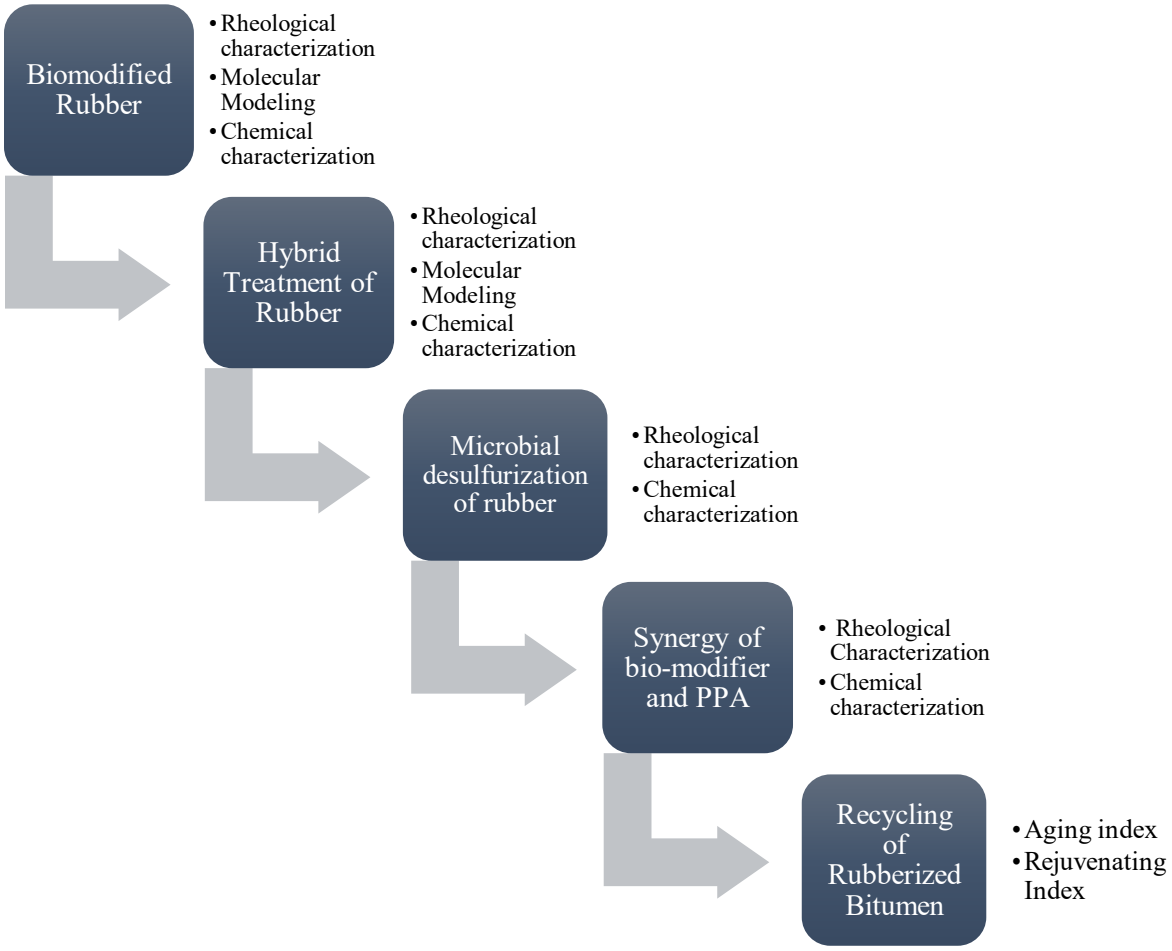

Figure 1-2. Experimental Flow Diagram of Research Plan

1.6 References

Brown, R., 1993. Historical Development Crumb rubber modifier workshop notes: Design procedures and construction practices. Federal Highway Administration Washington, DC.

Cao, X.-W., Luo, J., Cao, Y., Yin, X.-C., He, G.-J., Peng, X.-F., Xu, B.-P., 2014. Structure and properties of deeply oxidized waster rubber crumb through long time ozonization. Polymer degradation and stability 109, 1-6.

de Sousa, F.D., Scuracchio, C.H., Hu, G.-H., Hoppe, S., 2017. Devulcanization of waste tire rubber by microwaves. Polymer Degradation and Stability 138, 169-181.

EPA, 2019. “Rubber and Leather: Material-Specific Data.”.

Fan, L.-T., Shafie, M.R., Tollas, J.M., Lee, W.A.F., 2013. Extraction of hydrocarbons from hydrocarbon-containing materials and/or processing of hydrocarbon-containing materials. Google Patents.

Fini, E.H., Hosseinnezhad, S., Oldham, D., Mclaughlin, Z., Alavi, Z., Harvey, J., 2019a. Bio-modification of rubberised asphalt binder to enhance its performance. International Journal of Pavement Engineering 20(10), 1216-1225.

Hansen, K.R., Copeland, A., 2015. Asphalt pavement industry survey on recycled materials and warm-mix asphalt usage: 2014.

Hosseinnezhad, S., Holmes, D., Fini, E.H., 2014. Decoupling the physical filler effect and the time dependent dissolution effect of crumb rubber on asphalt matrix Rheology.

Isayev, A.I., 2005. Recycling of rubbers. In: Mark JE, Erman B, Eirich FR. editors Science and technology of rubber. 3rd ed Elsevier Inc, p. 663e701.

Li, P., Ding, Z., Zou, P., Sun, A., 2017. Analysis of physico-chemical properties for crumb rubber in process of asphalt modification. Construction and Building Materials 138, 418-426.

Liang, H., 2015b. Characterization and surface modification of rubber from recycled tires.

Romero-Sánchez, M.D., Martín-Martínez, J.M., 2006. Surface modifications of vulcanized SBR rubber by treatment with atmospheric pressure plasma torch. International journal of adhesion and adhesives 26(5), 345-354.

Shen, J., Amirkhanian, S., Xiao, F., Tang, B., 2009. Influence of surface area and size of crumb rubber on high temperature properties of crumb rubber modified binders. Construction and Building Materials 23(1), 304-310.

Shulman, V.L., 2019. Tire recycling, Waste. Elsevier, pp. 489-515.

Thodesen, C., Xiao, F., Amirkhanian, S.N., 2009. Modeling viscosity behavior of crumb rubber modified binders. Construction and Building Materials 23(9), 3053-3062.

Tyczkowski, J., Krawczyk, I., Woźniak, B., 2003. Modification of styrene–butadiene rubber surfaces by plasma chlorination. Surface and coatings technology 174, 849-853.

USTMA, 2017. 2017 U.S. Scrap Tire Management Summary. www.ustires.org/system/files/USTMA_scraptire_summ_2017_072018.pdf. (Accessed 6/19 2020).

Way, G.B., Kaloush, K.E., Biligiri, K.P., 2012. Asphalt-rubber standard practice guide. Rubber Pavements Association, Tempe.

Williams, B.A., Willis, J.R., Ross, T.C., 2019. Asphalt Pavement Industry Survey on Recycled Materials and Warm-Mix Asphalt Usage: 2018.

Xiaowei, C., Sheng, H., Xiaoyang, G., Wenhui, D., 2017. Crumb waste tire rubber surface modification by plasma polymerization of ethanol and its application on oil-well cement. Applied Surface Science 409, 325-342.

Yu, G.-X., Li, Z.-M., Zhou, X.-L., Li, C.-L., 2011. Crumb rubber–modified asphalt: microwave treatment effects. Petroleum Science and Technology 29(4), 411-417.

Chapter 2 BIO-MODIFIED RUBBER

2.1 Abstract

This paper examines the merits of using an amide-rich bio-binder for surface activation of natural rubber through cleavage of some of the disulfide bonds leading to partial surface devulcanization. It further examines the effects of the abovementioned devulcanization on rubberized asphalt properties. To do so, computational modeling and laboratory experiments were used to evaluate the process of partial devulcanization of rubber. We further introduced the resulting partially devulcanized rubber to an asphalt binder and examined its interaction mechanisms and its effect on rheological properties of rubber-modified asphalt binder. Accordingly, we used density functional theory in a systematic multi-scale approach to evaluate the intermolecular interactions between sulfur crosslinked rubber and an amide-based bio-binder. Analyses were performed of the interaction energies, frontier molecular orbitals (HOMO, LUMO), atoms in molecules topological indices, chemical hardness and softness, and natural bond orbitals between natural rubber and the bio-binder. The results indicate a preference for strong non-covalent interactions between the —NH2 site of the bio-binder and the S—S part of natural rubber, inducing partial devulcanization of the natural rubber. It was also found that the interaction of the NH2 functional group of the bio-binder is stronger with the S—S bond than with the C—S bond. This study explains the molecular interactions with sulfur cross-linked natural rubber leading to partial devulcanization in the presence of the bio-binder. The results of laboratory experiments showed the interaction between rubber and asphalt was improved due to partial devulcanization of rubber. This was evidenced in

a 70% reduction in viscosity of rubber-modified asphalt when rubber was partially devulcanized. In addition, the fatigue resistance was increased by 34% and stress relaxation was increased by 4%. The study outcomes help asphalt contractors and designers to develop rubber-modified asphalt with enhanced performance utilizing partially devulcanized rubber while promoting recycling of waste tire rubber and resource conservation.

Keywords: natural rubber (NR); sulfur devulcanization; amide-based bio-binders (BB); density functional theory (DFT); atoms in molecules (AIM); natural bond orbital (NBO) analysis.

2.2 Introduction

The use of recycled tire rubber as an additive to enhanced thermo-mechanical properties of asphalt binder has spread worldwide, particularly in the U.S. The use of chemical additives and stabilizers for surface treatment of rubber to enhance the interaction between the rubber and the asphalt matrix has attracted a great deal of attention in chemical engineering (De et al., 2006; Froese et al., 2007). The use of rubberized asphalt, particularly vulcanized rubber with various modifiers such as styrene-butadiene-styrene, ethylene vinyl acetate, polyvinyl acetate, and styrene-butadiene rubber copolymers, can improve the quality and elastic properties of unmodified asphalt (Fini, 2015; MacLeod et al., 2007; Zhao et al., 2010). The physical features of rubber have a crucial impact on asphalt's composition and viscosity; therefore, the physico-mechanical characteristics of asphalt concrete are under the influence of the rubber polymer contribution, which is mainly controlled by the rubber-asphalt interactions. These types

of interactions are sensitive to environmental conditions and vary depending on the asphalt composition and the rubber surface treatments (Jeong et al., 2010). Fini et al. investigated the effect of bio-binder as an additive on the performance of natural rubber. Their results showed an improvement in the workability and pumpability of rubberized asphalt binder when the rubber was treated with bio-binder. This in turn could alleviate the problems associated with the application of crumb rubber in the asphalt industry, while improving the rheological properties of asphalt binder (Fini et al., 2019a). The bio-binder was made from thermochemical conversion of animal waste (Fini et al., 2011b). Hosseinnezhad et al. investigated surface activation of rubber using a hybrid treatment method using the bio-binder from animal waste and microwave irradiation and results showed significant improvement in phase separation (Hosseinnezhad et al., 2019a). Previously, Bocoum et al. added an amine-based additive to rubberized asphalt and observed reduction in viscosity and improvement in pumpability (Bocoum et al., 2014a).

Mousavi et al. showed that amidyl radical (RCO-N•H) of bio-binder formed with microwave treatment have higher affinity to bind to carbon-centered radicals than to sulfur-centered radicals of rubber (Mousavi et al., 2019b). Kabir et al. used different bio-oils to surface activate crumb rubber and showed that adsorption on the surface of rubber largely depends on chemical composition of bio-oils with bio-oils made from wood pellets having stronger adsorption than other studied bio-oils(Kabir et al., 2019).

The cleavage of the rubber polymer chains (dissolution) to release the backbone polymer of rubber is strongly impacted by environmental factors; the abovementioned

cleavage results in a decrease in the viscosity of asphalt (John B. Macleod et al., 1995; Teixeira, 2015; Zanchet et al., 2009). Due to the highly crosslinked structure of rubber and the presence of stabilizers and other chemical additives, the natural degradation of scrap tires is time-consuming (Adhikari et al., 2000). Thus, the decomposition of the crosslinked structure of vulcanized rubber, as chemically and biologically resistant polymeric materials, is the main challenge in recycling used tires. The reutilization of natural rubber through recycling remains a global environmental challenge (Adhikari et al., 2000; Dubkov et al., 2014; Mohaved et al., 2015).

Before plasticization of the vulcanized rubber, the 3D structure of the vulcanizate has to be cleaved; this can occur at the crosslink sites or in the main chain (backbone). The latter scission generates short polymer chains and causes a degradation of the mechanical properties, while crosslink scission (bond cleavage) results in polymers in their original form. Consequently, the 3D network breakdown (devulcanization) is selective at the crosslinking units (Sutanto, 2006). Devulcanization is the break-down process of the chemical network of a rubber polymer through region-selective homolytic or heterolytic fission of C—C, C—S, and S—S bonds using organic devulcanization agents (Adhikari et al., 2000; De et al., 2006; Knorr, 1994). In the structure of vulcanized rubber, long hydrocarbon chains are linked to sulfur bonds. The lower bond energy of the S—S linkage compared to the C—S linkage will cause chemical surface devulcanization, which preferably destroys the S—S linkages(Goldshtein, 2002; Goldshtein, 2003). Partial or complete devulcanization (the cleavage of sulfur crosslinks formed during vulcanization) is the most desirable technique to reduce the volume of waste tire

rubber(Adhikari et al., 2000; Dubkov et al., 2014; Fukumori et al., 2002; Isayev AI, 2005).

Structurally, natural rubber (NR) can easily deform when heated; the inelastic deformation of non-vulcanized rubber is due to its long polymer chains, and heating can alter their shape(Lo Presti, 2013). Consequently, surface activation within the devulcanization process requires a high energy level to impose suitable pressure and temperature to cleave the C—S or S—S bonds(Warner, 1994). Levin et al.(Levin et al., 1997) identified a large quantity of sulfur-containing molecules in devulcanized rubber particles that are responsible for crosslinking during revulcanization. However, the ideal devulcanization process requires chemical transformations (depolymerization, thermal destruction, or oxidation), with the uncontrolled cleavage of polymer chains in vulcanized rubbers decreasing the process selectivity(Fukumori et al., 2002; Isayev AI, 2005; Kleps et al., 2000).

The non-covalent interactions between the natural rubber and the bio-binder (NR—BB) play a crucial role in determining the 3D structures of complexation in rubber polymers and biomaterials and in understanding their structures and properties in the condensed phase(Jorgensen et al., 1984). Generally, the non-covalent interactions within a NR—BB complex can arise from hydrogen bonding, van der Waals forces, Coulombic interactions from the NR—BB complex, and adhesion strength and orientation. This type of inter-molecular interaction can be enhanced during surface devulcanization of the NR particles using amide-based bio-binders; this is an active area of research that offers opportunities for extensive investigations(Garcia-Hernandez et al., 2006; Kim et al.,

2000). A common approach to determine intermolecular interaction energies of organic molecules is to perform quantum chemical calculations, particularly density functional theory (DFT) (Buckingham et al., 1988; Tsuzuki et al., 1994). Conventional B3LYP density functionals do not account for long-range dispersion interactions (Chai and Head-Gordon, 2008; Garza et al., 2015) and do not provide reliable geometry and physico-chemical properties of separate NR and bio-binder sub-units; these functionals are inadequate to justify the role of intermolecular interactions in the NR—BB complexes. DFT methods with dispersion-corrected density functionals enable atomistic modeling of large systems(Fominykh et al., 2016; Grimme, 2006). To take into account the non-covalent interactions within NR—BB complexes, a suitable dispersion-corrected density functional that includes long-range forces, the DFT including dispersion corrections (DFT—D) such as the B97D functional(Alturk et al., 2017; Burns et al., 2011), with a reasonably large basis set are required to accurately estimate the electron correlation and dispersion interaction as the crucial intermolecular interaction energy terms. The carbonyl oxygen and amine nitrogen atoms of amide-based compounds as Lewis base structures are the two electron-donor centers. Due to their delocalized amide linkage through the formation of tautomeric species (**Figure 2-1**), the amide-based compounds are regarded as a promising candidate for coordination studies(Laidig and Cameron, 1996).

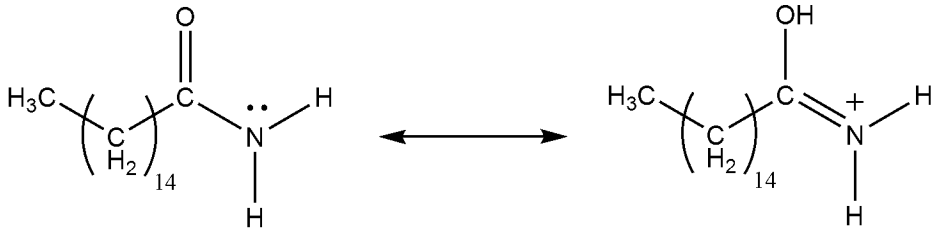

Figure 2-1. Electron Delocalization in An Amide Functional Group of BB1 and BB2 Molecules of Bio-Binders (Mousavi et al., 2016).

The structural planarity of the amide functional group of the BB_1 and BB_2 bio-binders which are the main components of bio-binder (41) leads to the electron delocalization of nitrogen's lone pair and consequently to the electronic structure of amide-based compounds (**Figure 2-1**). This resonance generates a partial double-bond character of the C—N bond, which leads to planarity and stability of the amide functional group. The possibility of the restricted C—N bond rotation, the planarity of the adjacent atoms, and the short C—N bond lengths make the amide-based biomaterials promising compounds for promoting partial devulcanization of natural sulfur vulcanized rubber (**Figure 2-1**) (Kemnitz and Loewen, 2007). The two synthesized compounds (BB_1:$C_{16}NH_{33}O$ and BB_2: $C_{22}NH_{45}O$) derived from swine manure were chemically characterized using GC-MS and NMR(Fini et al., 2011b; Mousavi et al., 2016) and were used as our bio-binder models in the present study. The structures of natural rubber (NR) vulcanized by sulfur crosslinks and two linear amide-based bio-binder models are shown in **Figure 2-2**.

These structures were obtained by geometric optimization of the NR as well as the NR—BB complexes, using a hybrid approach that combines B97D density functional with a semi-empirical method, PM6, in a two-layered ONIOM (B97D/6-31+G*: PM6) model.

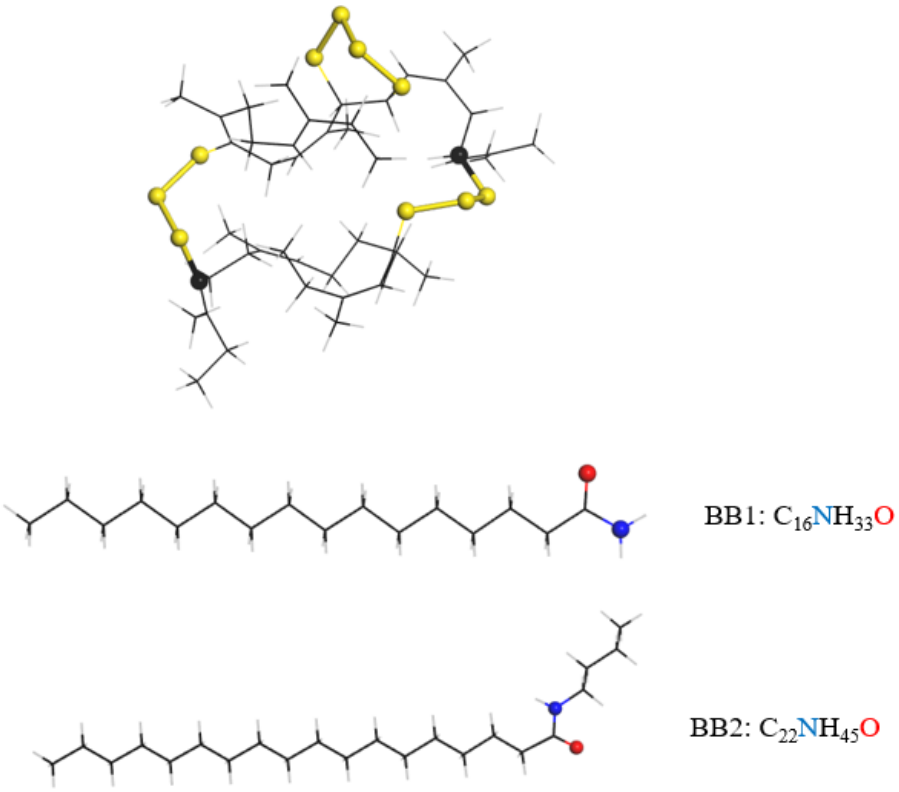

Figure 2-2. The Structure of (a) Natural Rubber (NR) Vulcanized by Sulfur Crosslink and (b) Two Linear Amide-Based Bio-Binder Models Based on Our Earlier Experimental Characterization (Elham H. Fini et al., 2011; Mousavi et al., 2016).

The C—S and S—S bonds considered in the calculation are marked in yellow (S), black (C) and as ball and stick. It is notable that the considered bond lengths corresponding to C—S and S—S, before optimization and after optimization, are presented as $r_{C—S(right)}$: 1.79 Å, $r_{S—S(right)}$: 2.04 Å and $r_{C—S(left)}$: 1.79 Å, $r_{S—S(left)}$: 2.02 Å.

It is understood that the polysulfidic bonds involved in the crosslink unit of NR will be broken, and that free radicals will be generated. The remaining sulfur-containing radicals in the broken sulfur crosslinks then react with the amide-based biomaterials (**BB_1**: palmitic acid amide; **BB_2**: N-(n-butyl) palmitic acid amide). In this context, BB_1/BB_2 act as a quenching agent for the radicals formed from NR at the heating stage to prevent the recombination of free radicals with the rubber assembly. In other words, these amide-based BB_1/BB_2 binders can reinforce the intermolecular interactions between the free radicals of the NR and the amide functional groups to promote the surface devulcanization process and surface activation of the rubber particles by preventing rubber dimerizes, and thereafter to expedite rubber-asphalt chemical integrity and segregation (Pahlavan, 2016; Rooj, 2011; Sutanto, 2006).

Despite comprehensive efforts to study the effectiveness of experimental techniques for the surface devulcanization of sulfur-cured NR (Kanazawa, 2006; Kojima, 2004, 2005; Kojimaa, 2005), little attention has been paid to explain at the molecular level the efficiency of the amide-based bio-binders **(BB_1** and **BB_2)** created through the fractional distillation of bio-oils from swine manure (Chritiansson et al., 1998; Fini et al., 2012; Hosseinnezhad et al., 2019a). This paper shows a high-level theoretical study on the nature of their interactions supported by laboratory results. Here, we used the B97D density functional method of density functional theory (DFT) with the 6-31+G* basis set to investigate the inter-molecular interactions between NR and amide-based bio-binders **(**BB_1 and BB_2**)**. The present work supplements our earlier experiment observations in the partial devulcanization of sulfur crosslink NR in the presence of amide-based BB_1/BB_2

biomaterials (Fini, 2015; Fini et al., 2012; Fini et al., 2015; Fini et al., 2011b) and shows the effect of biomaterial modification in a clear and concise way. Using DFT, the interaction energies (E_{int}), frontier molecular orbitals (HOMO, LUMO), atoms in molecules (AIM), chemical hardness (η) and softness (S), and natural bond orbitals (NBOs) for NR and BB bio-binders were analyzed to investigate the interactions of S—S or C—S bonds of sulfur crosslink units (partial devulcanization) of NR in the presence of BB1/BB2 bio-binder models.

2.3 Materials and Methods

2.3.1 Modeling based on density functional theory

This section has a review of the basic concepts of density functional theory (DFT) and how it is used with the Gaussian 09 package.

Schrödinger's equation can be solved for the one-electron element hydrogen, but there are many elements with more than one electron (Zielinski et al., 2005). Writing an equation for each electron, proton, and neutron and then solving the equation would require more than a decade for the fastest computer. That is when an approximation enters the picture. The Born-Openheimer approximation says electronic wave functions depend on their nuclear positions but not their velocities. Nuclei are heavy, so they have slower motion compared to an electron's motion and can be considered as fixed. The Hohenburg-Kohn density functional theory proposed that the total energy of any system consisting of a set of electrons moving under the influence of an external potential is a unique functional of the electron density. The electron density of any system determines all the ground-state properties of the system, so if we know the electron-density

functional, we know the total energy of that system. In 1965, Kohn-Sham proposed a system of non-interacting electrons and provided Equation 2-1.

$$E[\rho(r)] = T_{ni}[\rho(r)] + V_{ext}[\rho(r)] + V_H[\rho(r)] + V_{xc}[\rho(r)] \qquad (2-1)$$

where

$T_{ni}[\rho(r)]$= Kinetic energy of non-interacting electrons

$V_{ext}[\rho(r)]$= External potential

$V_H[\rho(r)] =$ Hartree potential

$V_{xc}[\rho(r)]$= Exchange correlation potential

The B3LYP approximation cannot explain the reactivity of CR-BB. Since no existing functional can be a 100% match, experiment data gives a better starting picture.

All quantum-chemical calculations were carried out using Gaussian 09 software (Gaussian09, 2020). The structures of the two linear amide-based bio-binder models (BB1 and BB2) were fully geometry-optimized using the B97D density functional and 6-31+G* basis set. The selection of the basis set varies if one deals with molecular properties that depend on regions of the valence shells that are far from the nucleus. In that case, it is necessary to include diffuse basis functions (primitives with very small exponents), which are denoted by '+' or '++'. That is why the basis set chosen has a '+' sign. However, it is highly recommended to choose the most relevant basis set according to the recent literature cited or advice from experts (Hinchliffe, 2005).

In Gaussian 09, there are several steps of building molecules from scratch using GaussView:

- Using templates
- Setting angles between rings
- Using symmetry
- Docking structures
- Using alternate templates

Built molecules are then analyzed by:

- Selecting the correct template/symmetry
- Docking two structures
- Building a skeleton structure with C, then specifying the heteroatoms

In this research, the molecules are built based on gas chromatography-mass spectroscopy (GC-MS) data and NMR data (performed by our laboratory group) as well as recent literature.

Once molecules are built, electrostatic-potential mapping (a map with regions showing electron excess or deficiency) is performed as a rough survey of the molecule. The next task is to provide geometry optimization. By default, Gaussian versions perform geometry optimization in redundant internal coordinates using the Berny Algorithm. This algorithm is based on an earlier program written by H. B. Schlegel. Subsequent improvements from published and unpublished works have been incorporated (Schlegel et al., 1982). Generalized geometry optimization is done using the following steps.

First, an initial estimate is made of a force-constant matrix, which is a second-derivative matrix or Hessian. To calculate force constants, a valence force field (VFF) is used that considers all possible inherent connectivity and flexibility of the

molecule. Estimation of the diagonal force constants is applied for a set of redundant internal coordinates, using empirical rules. This includes all stretches, bends, torsions, or out-of-plane deformations involving bonded atoms. From the redundant internal coordinates, the force constants are then transformed to Cartesian coordinates. After that they are again transferred from Cartesian coordinates to non-redundant internal coordinates (Gaussian09, 2020; Hinchliffe, 2005; Schlegel, 1984).

Second, if a minimum is sought, the trust radius is updated using the method of Fletcher (Fletcher, 1980), while any components of the gradient vector corresponding to frozen variables are projected out. Here, the trust radius is the maximum-allowed Newton-Raphson step. Following that, a linear search is performed between the latest point and the best previous point (the previous point having the lowest energy). Finally, convergence criteria is tested for the maximum force component, root-mean-square force, maximum step component, and root-mean-square step. The details of the optimization example can be found elsewhere (Gaussian09, 2020).

The electronic energy in Kohn-Sham deterministic DFT applications can be generally written as Equation 2-2 (the square brackets denote a functional of the one-electron density P(r)).

$$\varepsilon_{e1}[P] = \varepsilon_1[P] + \varepsilon_J[P] + \varepsilon_X[P] + \varepsilon_C[P] \qquad (2-2)$$

where

ε_1 = the one-electron energy,

ε_J = the Coulomb contribution,

ε_X= the exchange energy,

ε_c = the correlation energy.

The exchange and correlation functionals depend on the density of the α electrons, the density of the β electrons, and their density gradients. Therefore, the energy terms ε_X and ε_c are given by the volume integrals shown in Equations 2-3 and 2-4 (Hinchliffe, 2005).

$$\varepsilon_X = \int f_x(P^\alpha, P^\beta, grad\ P^\alpha, grad\ P^\beta) d_\tau \qquad (2-3)$$

$$\varepsilon_C = \int f_C(P^\alpha, P^\beta, grad\ P^\alpha, grad\ P^\beta) d_\tau \qquad (2-4)$$

After the functionals and electron density are known, the energy can be obtained by integrating over the space of the molecule. Since analytical solutions to these integrals are difficult to obtain, a numerical integration has to be performed for each cycle. To do so, the integral is replaced by a sum over quadrature points, where the first summation is over the atoms and the second is over the numerical quadrature grid points (Equation 2-5) (Hinchliffe, 2005).

$$\varepsilon_{X/C} = \sum_A \sum_i w_{Ai} f(P_1^\alpha, P_1^\beta, grad\ (P_1^\alpha), grad(P_1^\beta);\ \mathbf{r_{Ai}} \qquad (2-5)$$

Here, the w_{Ai} are the quadrature weights and the grid points, $\boldsymbol{r}_{Ai}$ are given by the sum of the position of nucleus A, $\boldsymbol{R}_A$ and a suitable one-center, $\boldsymbol{r}_i$ grid given by Equation 2-6.

$$\boldsymbol{r}_{Ai} = \boldsymbol{R}_A + \boldsymbol{r}_i \qquad (2-6)$$

Gaussian09 offers a wide variety of density functional theory (DFT). Among the density functional approaches, the B97D density functional provides an accurate description of the intramolecular interactions particularly involving sulfur-containing compounds (Li et al., 2014; Morgado et al., 2007). To maintain the optimization accuracy, first BB_1 was fully optimized, then the structure of BB_2 was constructed on the optimized BB_1 model, and then BB_2 was re-optimized. The geometry optimizations of both the natural rubber (NR) vulcanized by sulfur crosslink (**Figure 2-2**) and the NR—BB complexes were performed using a hybrid approach that combines the B97D density functional with a semi-empirical method, PM6, in a two-layered ONIOM (B97D/6-31+G*: PM6) model (Maseras and Morokuma, 1995; Svensson et al., 1996). In this hybrid model, the interactive region between NR and the bio-binder models was treated at a higher theoretical level (B97D/6-31+G*), and the rest of the system was treated with the PM6 method. The harmonic vibrational frequencies were calculated using normal mode frequency analysis (Coropceanu et al., 2002) to ensure each stationary point and local minima on the potential energy surface were based on no negative frequency. The optimized geometries of rubber (**Figure 2-2**) and of the BB_1/ BB_2 bio-binder models (**Figure 2-2**) could provide further insight into the complexation of NR with the BB_1/ BB_2 bio-binder models (**Figure 2-2**). First, the intermolecular interactions of acetamide, the simplest amide-based BB-representative model, with the sulfur crosslink segment of NR were investigated. The structures of acetamide and the BB_1 and BB_2 models were fully optimized using a density functional of the generalized gradient approximation

(GGA), termed B97D(Grimme, 2006), with the 6-31+G* basis set. The B97D density functional is based on Becke's power-series ansatz from 1997, and is explicitly parameterized with damped atom-pairwise dispersion corrections, being recommended as an accurate density functional method for large systems where dispersion forces are of significance (Grimme, 2006). To identify the potential interacting regions of the sulfur vulcanized NR (either S—S or C—S bonds of sulfur crosslink units) with acetamide and the **BB1** and **BB2** models, the locations of the highest occupied molecular orbital (HOMO) and lowest unoccupied frontier molecular orbital (LUMO) were determined. All the atomic and molecular properties were obtained at the optimized geometries using the same level of theory (B97D/6-31+G*). Different probable molecular orientations between the amide units of BB_1/BB_2 and NR were optimized at the B97D level of theory with the 6-31+G* basis set. The interaction energies (E_{int}) of acetamide, BB_1/ BB_2 models with NR were calculated based on Equation (**2-6)**:

$$E_{int} = E_{AB} - (E_A + E_B) \qquad (\mathbf{2-7})$$

where E_{AB} is the total energy of the NR—BB complexes, and E_A and E_B are the energies of two interacting subsystems, i.e., the NR and BB_1/ BB_2 compounds. After exploring and comparing the various possible interactions between acetamide into the rubber's surface (sulfur crosslink units in both sides of NR), the two structural orientations of BB_1/ BB_2 with the promising sulfur crosslink segment of rubber were further characterized. It is worth noting that the interaction energies based on Equation (**2-7**) often lead to severe complications for systems that are bound by the inclusion of intra-molecular dispersion interactions or hydrogen bonds. The implications of the

counterpoise corrected (CP) approach, together with an estimation of basis set superposition error (BSSE), are intimately related to the concept of interaction energy. The accurate strategy to obtain the intermolecular interaction energies is to use the counterpoise correction method. It is notable that the interaction energy (E_{int}) defined in Equation (**2-8**) is BSSE-polluted. After the counterpoise correction, the counterpoise-corrected interaction energies (ΔE_{int}^{CP}) should be expressed as in Equation (**2-8**) (Brandenburg et al., 2013; Paizs and Suhai, 1998):

$$\Delta E_{int}^{CP}(AB) = E_{AB}^{AB} - E_{BSSE}(A) - E_{BSSE}(B) \qquad (\mathbf{2-8})$$

where

$$E_{BSSE}(A) = E_{A}^{AB}(A) - E_{A}^{A}(A) \qquad (\mathbf{2-9})$$

and

$$E_{BSSE}(B) = E_{B}^{AB}(B) - E_{B}^{B}(B) \qquad (\mathbf{2-10})$$

The significance of Equations **(2-8**) and **(2-9**) is indeed due to the arbitrariness of the position of the basis functions belonging to each subunit in the complex. It is also due to the fact that the wave function for one of the components in the complex (NR) overlaps with the basis functions located on the other subunit (BB).

The AIM topological analysis of the charge density (ρ_c) and Laplacian charge density ($\nabla^2\rho_c$) at the intra-molecular charge-density critical points (BCP) for acetamide, BB_1/ BB_2, and a crosslink unit of NR was performed using AIM2000 software (Biegler-

Konig and Bader, 2002). The Laplacian ($\nabla^2\rho_c$) is the sum of three curvatures of the density. The ρ_c value measures the interaction strength, and the sign of $\nabla^2\rho_c$ indicates the bond nature for the covalent interactions ($\nabla^2\rho_c < 0$) and for electrostatic interactions ($\nabla^2\rho_c > 0$) (Bader, 1990). Furthermore, the DFT-based reactivity indicators (Cardenas et al., 2011; Geerlings et al., 2003), such as ionization potential ($IP = E_{cation} - E_{neutral}$), electron affinity ($EA = E_{anion} - E_{nuetral}$), chemical hardness ($\eta = \frac{IP - EA}{2}$) and softness ($S = \frac{1}{2\eta}$) (Ralph G. Pearson, 1963; Robert G. Parr and Ralph G. Pearson, 1983), and dipole moment (μ) and polarizability (α) (Lameira et al., 2006a; Lameira et al., 2006b; Sarasia et al., 2012) for different NR—BB1/BB2 model complexes were calculated. These parameters are used as conceptual DFT descriptors for global reactivity, for deeper understanding of the chemical reactivity of the rubber in the presence of the BB_1/BB_2 biomaterials. Finally, the natural bond orbital (NBO) analysis (Weinhold F and Carpenter J.E., 1988) and the calculation of the stabilization energy, $E^{(2)}$, deduced from the second order perturbation theory analysis of the Fock Matrix (Reed et al., 1988), were performed on the fully optimized molecular assemblies. This was done to provide details about the second-order interactions between the filled orbitals of one subsystem and the vacant orbitals of another subsystem, which are a measure of the charge transfer within the NR—BB_1/BB_2 complexes.

2.3.2 Treatment with biomodification

The crumb rubber used in this study was supplied by crumb rubber manufactures from Mesa, Arizona. The bio-binder (BB) used in this study was produced in the lab through thermochemical liquefaction of swine manure; details of which can be found elsewhere (Fini et al., 2011b). The asphalt binder was PG64-22 commonly used in North Carolina (**Table 2-1**).

Table 2-1. Properties of Asphalt Binder (PG64-22)

Specific Gravity @15.6 ºC	1.039
Cleveland Open Cup method Flash point	335 ºC
Mass change after RTFO	-0.0129
Absolute Viscosity @ 60 ºC	202 Pa.s
Stiffness @-12ºC @ 60s	112.5 MPa

The regular crumb-rubber (non-devulcanized) was first blended to asphalt binder at 15% by weight at 180°C for 30 minutes at 3,000 rpm using a benchtop high shear mixer to prepare crumb rubber modified asphalt referred to as CRM. To prepare the bio-modified rubber (BMR), crumb rubber modified asphalt was preheated at 135°C before the gradual addition of 15% bio-binder by weight (making a 1:1 ratio of rubber and bio-binder). After introducing the bio-binder, the mixed contents were stirred for 30 minutes maintaining the constant temperature. To simulate field aging of asphalt, samples were aged in the lab using rolling thin film oven (RTFO) and pressure aging vessel (PAV) according to ASTM-D2872 (ASTM-D2872, 2019, 2019a).

2.3.3 Rotational Viscometer

Flow properties of the binder was measured using a Brookfield Viscometer RV-DVIII Ultra following ASTM-D-4402 (ASTM-D-4402, 2015). To measure the viscosity as a measure of flow properties, specimens were prepared using 10.5 grams of each sample poured in standard aluminum tube. Tubes and a smooth spindle (SC4-27) were preheated in an oven for 30 minutes before placing them into the preheated thermosel. An additional 10 minutes was taken to ensure thermal equilibrium after loading the specimen in thermosel. A continuous shear at 20rpm was utilized for 10 minutes before reading the viscosity values. Three measurements were taken for each sample at four different temperatures (105°C, 120°C, 135°C, 150°C).

2.3.4 Dynamic Shear Rheometer

Rheological properties of of the binder was studied using a Malvern Kinexus dynamic shear rheometer. Oscillation test was performed at 0.1 strain and frequency of 10 rad/s to represent the typical shearing action that asphalt experiences under traffic speed of 90 km/h (AASHTO-T-315, 2019). The measured data is then used to calculate the complex shear modulus (G*) and phase angle (δ). The complex shear modulus (G*) is a measure of material resistance to deformation when repeatedly sheared and phase angle (δ) is a time lag between stress and strain. Based on the performance grade specifications, the data obtained were used to calculate G*/sin(δ) as an indicator of asphalt's resistance to rutting and G*sin(δ) as an indicator of asphalt's resistance to fatigue(ASTM-D6373-16, 2016).

2.3.5 Bending Beam Rheometer

To study stiffness and stress relaxation capacity of binder, the bending beam rheometer (BBR) was used to measure deflection (d) of the bean over time under a constant load of 980 ± 50 mN applied at the midpoint of an asphalt binder beam.. Prior to testing, a beam of fixed length, width, and height is prepared following standard specification and is conditioned in a bath of ethanol at a selected test temperature. Abovementioned constant load is applied, and deformation of midspan of the bean is recorded as a function of time. Using the deformation data during the loading period, the stiffness is calculated using Equation 2-11 (AASHTO-T-313, 2019b). Stress relaxation capacity is calculated from the slope of stiffness versus loading time.

$$S(t) = \frac{PL^3}{4bh^3\partial(t)} \qquad (\mathbf{2-11})$$

where:

P = applied constant load (100 g or 0.98 N)

L = distance between beam supports (102 mm)

b = beam width (12.5 mm)

h = beam thickness (6.25 mm)

S(t) = binder stiffness at a specific time, MPa

∂(t) = deflection at a specific time, mm

2.4 Results and Discussion

In this section, the electronic structure properties are analyzed to gain insight into the intermolecular interactions in rubber when it is treated with bio-binder and to explore

the effectiveness of amide-based bio-binders on the partial devulcanization process of sulfur crosslinked NR. Laboratory experiments were performed on asphalts containing partially devulcanized rubber to examine extent of improvement due to abovementioned devulcanization enabled by bio-binder.

2.4.1. Interaction energies between rubber and bio-binder

To assess the effectiveness of the amide functional group of bio-binders in terms of forming intermolecular interactions with sulfur crosslink units of natural rubber, two complexes with different molecular orientations between the amide functional group of acetamide (the simplest representative amide-based model) with the NR were compared. Interest was centered on the non-bonding interaction of the amide functional group of acetamide particularly with the S—S and C—S bonds involved in the sulfur crosslink unit of NR.

The electron charge delocalization of the amide functional group of acetamide and BB bio-binders makes these compounds planar; the molecular plane contains the amino group (—NH_2) and the carbonyl's oxygen (C═O) (Mujika et al., 2006; Platts et al., 2012). The NR—acetamide model complexes are (**a**) —NH_2 group of acetamide facing the rubber's surface, and (**b**) oxygen from C═O of acetamide facing the sulfur crosslink units (**Figure 2-3**).

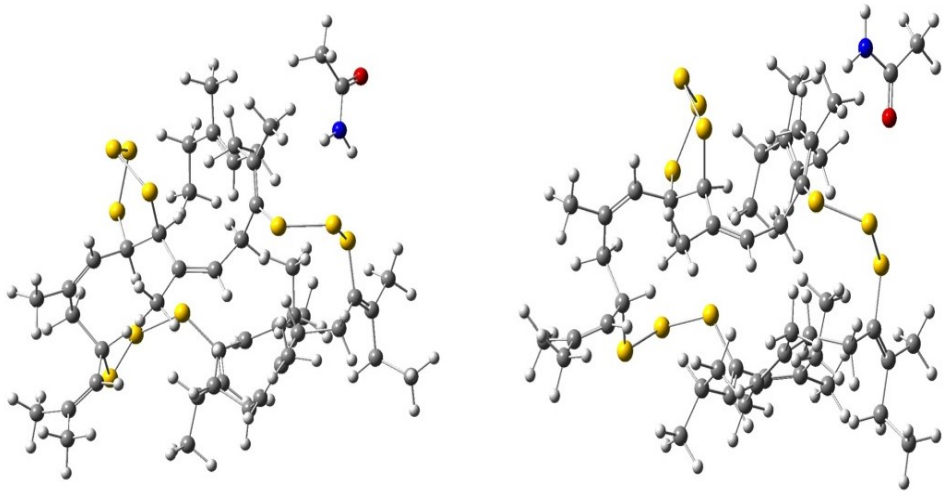

(a) **(b)**

Figure 2-3. The Optimized Structures of The NR—Acetamide Complexes That Are Modeled Based on The Potential Interacting Sites of Sulfur Crosslink Natural Rubber: (a) —NH2 Functional Group of Acetamide Facing The Rubber's Surface, (b) Oxygen From C═O of Acetamide Facing The Sulfur Crosslink Segments (S—S and C—S bonds).

These two model NR—acetamide complexes (**Figure 2-3**) were fully optimized at the B97D level of theory using 6-31G* basis set to local minima. The optimized distances of S-N and S-O are 3.2 Å and 3.7 Å, respectively. Monitoring the obtained intermediate structures within the optimization process revealed that all the geometrical optimizations converged to the situation in which the plane of the amide functional group is in proximity to the S—S and C—S bonds of rubber. This suggests that a possible non-covalent electron—π interaction exists between the delocalized electrons of the molecular orbitals of the S—S and C—S of rubber with the π orbital of the amide group.

The interaction energies (E_{int}), counterpoise-corrected interaction energies, ΔE_{int}^{CP}, and BSSE energies, E^{BSSE}, defined in Equations (2-7)-(2-10) for different considered acetamide—rubber complexes are presented in **Table 2-2.** Table 2-2 compares the

interaction energies of —NH_2 and C═O functionals of acetamide as a simple model of amide-based bio-binder with S—S and C—S of the right-hand and left-hand sides of the sulfur crosslink rubber, S—S (right/left) and C—S (right/left). These interaction energies (E_{int}) revealed the preference of the specifically preferred intermolecular interactions that will be important when the amide functional group of a given bio-binder is interacting with the sulfur crosslink zone of the NR. In all cases, the E_{int} values were obtained by considering the optimized conformations for each component of Equation (2-**7**).

Table 2-2. The Interaction Energies (Eint), Counterpoise-Corrected Interaction Energies (E_{int}), Counterpoise-Corrected Interaction Energies, ΔE_{int}^{CP}, and BSSE Energies, E^{BSSE}

Complexes	**E_{int} (kcal/mol)**	ΔE_{int}^{CP} **(kcal/mol)**	**E^{BSSE}(kcal/mol)**
NH_2 orientation			
C—S (right)	-43.182	-36.590	2.221
S—S (right)	-46.170	-37.774	3.422
C—S (left)	-43.023	-36.964	2.124
S—S (left)	-43.631	-36.873	3.112
C═O orientation			
C—S (right)	-42.453	-38.870	3.611
S—S (right)	-45.040	-37.354	2.712
C—S (left)	-41.982	-36.581	2.883
S—S (left)	-42.572	-37.123	2.244

The E_{int} values derived from Equation (**2-7**) are much more negative than their corresponding counterpoise corrected energies (ΔE_{int}^{CP}) defined in Equation (**2-8**), so it seems that Equation (**2-7**) overestimates the interaction energies (E_{int}) for non-bonded

systems. As the implemented basis sets are of finite size at nuclear configurations, where the two subunits are in equilibrium geometry of the complex AB (A: acetamide; B: rubber), the basis functions centered on A decrease the energy of B and vice versa; this effect is termed 'basis set superposition error' (BSSE)(Xantheas, 1996).

A comparison of the interaction energies (E_{int}) between the two possibilities where acetamide potentially interacts either from its —NH_2 or C═O sites onto the NR surface (**Table 2-2**), revealed that, for the case where the acetamide interacts with the —NH_2 functional group, the average of the E_{int} was 1-2 Kcal/mol more negative than with the carbonyl (C═O). Interestingly, the intermolecular interactions of the both the —NH_2 and carbonyl sites of acetamide with the S—S bond of NR's sulfur crosslink units is about 3 Kcal/mol stronger than the C—S units. Due to such a potential non-covalent interaction of acetamide with NR's S—S bond, surface devulcanization of the S—S bond might be more feasible than surface devulcanization of the C—S bond. This observation can be related to earlier published articles (Fini et al., 2015; Goldshtein, 2002; Goldshtein, 2003). This reconfirms the fact that the energy required to cleave the monosulfidic crosslinks is higher than that required for the polysulfidic crosslinks experimentally reported earlier(Olmsted III and Williams, 1997; Sutanto et al., 2006). This fact could be attributed to the higher stability of C—S bonds as compared to S—S bonds.

Furthermore, the negative average E_{int} values of both C—S and the S—S bonds of the right-hand side of the sulfur crosslink unit of NR (for all orientations) with acetamide implied that the potential intermolecular interactions of sulfur crosslink units localized in the right-hand side of NR with acetamide (particularly the —NH_2 functional group) are stronger than for those in the left-hand side. This observation is consistent with the location of the HOMO frontier molecular orbitals of NR exactly localized in the right-hand side sulfur crosslink unit (**Figure 2-4a**). The higher counterpoise-corrected energy (ΔE_{int}^{CP}) yielded less negative energy values for all the considered complexes than their corresponding systems optimized for E_{int}; this was established in earlier work(Kobko and Dannenberg, 2001). The interaction energies (E_{int}), counterpoise-corrected interaction energies, ΔE_{int}^{CP}, and BSSE energies, E^{BSSE}, defined in Equations (2-**7)-(2-10)** for different NR—BB_1/BB_2 complexes are reported in **Table 2-3**. Earlier in **Table 2-2,** it was observed that the interactions of right-hand side sulfur crosslink units of NR with acetamide are more preferred than left-hand side units; therefore, the right-hand side sulfur crosslink units of natural rubber, S—S (right) and C—S (right), interacting with BB_1/BB_2 were measured.

Table 2-3. The Interaction Energies (E_{int}), Counterpoise-Corrected Interaction Energies, ΔE_{int}^{CP} , and BSSE Energies, E^{BSSE}

NR—BB$_1$	**E_{int} (kcal/mol)**	**ΔE^{CP} (kcal/mol)**	**E^{BSSE}(kcal/mol)**
NH_2 orientation			
C—S	-47.693	-33.644	3.371
S—S	-51.624	-35.753	3.691
C=O orientation			
C—S	-46.214	-37.182	2.353
S—S	-50.341	-37.104	3.343
NR —BB$_2$			
NH_2 orientation			
C—S	-48.351	-35.443	3.362
S—S	-51.912	-35.410	3.160
C=O orientation			
C—S	-46.380	-34.990	3.004
S—S	-50.463	-34.563	4.042

2.4.2. Thermodynamic properties

In this section, the thermochemical quantities of the NR—BB_1/BB_2 complexation, including enthalpies (ΔH), Gibbs free energies (ΔG), and entropies (ΔS), are listed in **Table 2-4** and discussed to gain a deeper insight into the preferred interactive sites of NR with bio-binders and to correlate these parameters to their interaction energies (**Table 2-3**). These data provide information regarding the favorability of NR—BB complexation and also show the rotational, translational, and vibrational contributions to the entropies (ΔS_{Rot}, ΔS_{Trans}, ΔS_{Vib}) for all modeled complexes.

Table 2-4. Thermodynamic Properties for The Intermolecular Interaction of Optimized NR—BB_1/BB_2 Complexes Obtained at The Level of B97D/6-31+G* theory.

NR—BB_1	**ΔH (kcal mol^{-1})**	**ΔG (kcal mol^{-1})**	**ΔS (cal mol^{-1} K^{-1})**	**ΔS_{Rot} (cal mol^{-1} K^{-1})**	**ΔS_{Trans} (cal mol^{-1} K^{-1})**	**ΔS_{Vib} (cal mol^{-1} K^{-1})**
NH_2 orientation						
C—S	-29.979	-13.876	-54.036	30.706	-108.779	19.037
S—S	-36.897	-18.877	-60.469	35.975	-118.233	21.789
C═O orientation						
C—S	-27.505	-11.140	-54.916	30.580	-105.714	20.218
S—S	-34.217	-16.117	-60.738	30.568	-118.715	27.409
NR—BB_2						
NH_2 orientation						
C—S	-30.511	-14.501	-53.724	35.082	-111.962	23.156
S—S	-36.999	-18.999	-60.402	28.170	-98.785	10.213
C═O orientation						
C—S	-27.992	-11.992	-53.691	23.492	-89.429	12.246
S—S	-34.349	-16.749	-62.416	35.884	-114.213	15.913

As for the interaction of the —NH_2 group of BB_1/BB_2 onto the NR surface, the enthalpies (ΔH) and Gibbs free interaction energies (ΔG) for each C—S and S—S involved in the right-hand side of the sulfur crosslink unit of NR are more negative than for the carbonyl (C═O). This fact implies that those complexes at which the plane of the amide functional group (—NH_2) of the BB_1/BB_2 bio-binders are facing the sulfur crosslink unit of natural rubber are thermodynamically more stable than that of the carbonyl functional group. This observation is in good agreement with the more negative interaction energies (E_{int}) obtained for the —NH_2 group of the BB_1/BB_2 bio-binders (**Tables 2-2**, **2-3**). Interestingly, for both the —NH_2 and C═O orientations of BB_1/BB_2, the interaction of BB_1/BB_2 bio-binders with the S—S bond involved in the sulfur

crosslink of rubber is about 7.0 kcal/mol more probable than with the C—S bond, which supports our earlier observation for E_{int} values (**Tables 2-2,** 2-**3**). As for the entropic contribution, all ΔS values were negative (-53 Cal/mol.K and -54 cal/mol.K for **BB_1** and -60 cal/mol.K and -62 cal/mol.K for **BB_2**). This could be understood by considering ΔG= ΔH-TΔS, which caused variation in the entropic part (ΔS). Comparison of the ΔS values of S—S and C—S bonds of sulfur crosslink units of NR interacting with each of the —NH_2 and C═O sites of BB_1/BB_2 revealed that in most cases, the ΔS values for the —NH_2 were less negative than the carbonyl orientation. According to this observation, it can be inferred that the intermolecular interaction of the BB_1/BB_2 bio-binders from the —NH_2 site is more probable; this is consistent with the E_{int} values reported in **Tables 2-2** and **2-3**.

Among the different entropic contributions (ΔS_{Rot}, ΔS_{Trans}, ΔS_{Vib}), the rotational contribution of entropy (ΔS_{Rot}) for the NR—BB_1/BB_2 complexes was more positive and has the largest contribution. It seems that the rotation of the —NH_2 functional group of BB_1/BB_2 bio-binders is considerably contributing in the electrostatic interaction with the sulfur crosslink unit of NR. It can therefore be understood that in this specific NR—BB_1/BB_2 complex, the ΔS_{Rot} contribution has a critical role in the interaction of the BB_1/BB_2 with the natural rubber. All the translational entropy contributions (ΔS_{Trans}) showed close negative values. A comparison of the ΔH and ΔG quantities of the NR—BB_1 complex with the NR—BB_2 complex shows that the ΔH and ΔG values for the NR—BB_2 system are more negative than the NR—BB_1. This observation implies that the

BB_2 bio-binder as a secondary amide has a greater tendency to interact with natural rubber, and it therefore seems that the BB_2 bio-binder might be more effective in the partial sulfur devulcanization of the sulfur crosslinked natural rubber than the BB_1, which is a primary amide compound.

2.4.3. Analysis of frontier molecular orbitals

The molecular polarizability of a single molecule or complex and the atomic electron charge densities are directly referred to the frontier molecular orbitals (HOMO, LUMO)(Dumont, 2014; Jung et al., 2014). The HOMO energy eigenstate (E_{HOMO}) represents the ability of the molecule to donate electrons. The higher the E_{HOMO}, the greater the tendency of the molecule to donate electrons(Monajjemi, M.; et al., 2010; Monajjemi, M. et al., 2010; Rauf, 2015; Sarasia et al., 2012). The HOMO and the LUMO for the sulfur crosslink rubber, acetamide, and bio-binder models (BB_1/ BB_2) in **Figure 2-4** could identify the location of the charge flow and the desired interactive sites of each of these NR and BB molecules. The specific grid points sampled for the HOMO and LUMO frontier orbitals, with viewable surfaces(Szabo Attila. and Ostlund Neil.S., 1989), are shown in **Figures 2-4a** and 2-**4b**.

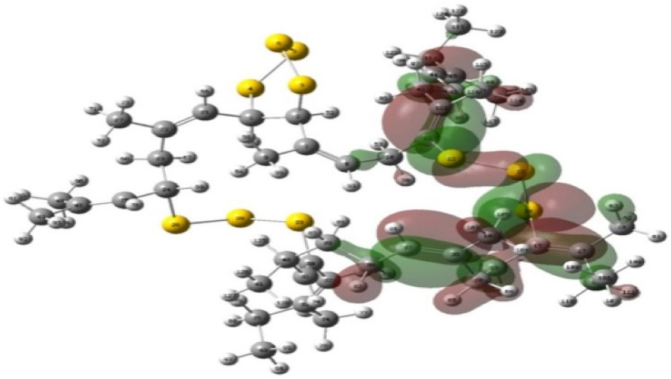

(a)

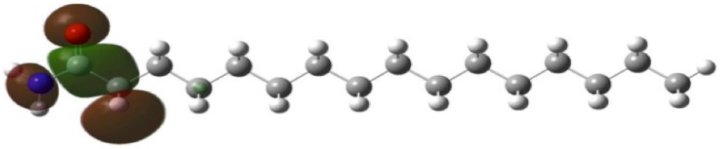

(b)

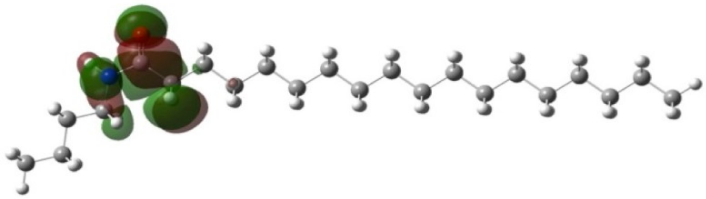

(c)

Figure 2-4. The Frontier Molecular Orbital Surfaces of (a) Natural Rubber Vulcanized by Sulfur Crosslink, Two Linear Amide-Based Bio-Binder Models, (b) BB_1 and (c) BB_2 Obtained at The B97D/6-31+G* Level of Theory.

Inspection of the frontier molecular orbitals of NR and BB1/BB2 revealed that the electron charge density is predominantly localized on the sulfur crosslink unit (right-hand side) of NR (**Figure 2-4a)** and amide functional group of BB_1/ BB_2 bio-binders (**Figures 2-4b** and **2-4c)**. This observation implies that the electron-rich and eventually reactive part of natural rubber, which can potentially interact with the amide functional group of bio-binders, are localized at this region. This fact was also confirmed by our earlier observation of obtaining more negative E_{int} for the acetamide with both the right-hand side sulfur crosslink segments of NR than the left-hand side (**Table 2-2**). The location of the HOMO frontier molecular orbitals of BB_1/BB_2 on their amide moiety (**Figures 2-4b** and **2-4c)** indicates that the amide functional groups of these bio-materials act as potential centers to interact with the sulfur crosslink segment of NR and to accelerate and activate the rubber particles during partial sulfur devulcanization. The calculated energy eigenstates of the highest occupied molecular orbital ($E_{\mathbf{HOMO}}$), the lowest unoccupied molecular orbital ($E_{\mathbf{LUMO}}$), and the $\Delta E_{HOMO–LUMO}$ gap for the studied NR—BB_1/BB_2 complexes at the B97D/6-31+G* level are listed in **Table 2-5**.

Table 2-5. Calculated Energy Eigenstates of The Highest Occupied Molecular Orbital (E_{HOMO}) and The Lowest Unoccupied Molecular Orbital (E_{LUMO}) for The Studied NR—BB_1/BB_2 Complexes at The B97D/6-31+G* Theoretical Level.

NR—BB_1	**E_{HOMO} (eV)**	**E_{LUMO} (eV)**	**$\Delta E_{LUMO-HOMO}$ (eV)**
NH_2 orientation			
C—S	-4.916	-2.389	2.528
S—S	-4.969	-2.484	2.485
C=O orientation			
C—S	-5.105	-2.533	2.572
S—S	-4.802	-2.291	2.511
NR—BB_2			
NH_2 orientation			
C—S	-4.981	-2.464	2.517
S—S	-4.898	-2.427	2.471
C=O orientation			
C—S	-4.961	-2.394	2.567
S—S	-5.036	-2.532	2.504

The energy gap between the E_{HOMO} and E_{LUMO} ($\Delta E_{HOMO–LUMO}$ gap) is an important characteristic of chemical reactivity and complex stability(Diener and Alford, 1998; Pearson, 1989). The large $\Delta E_{HOMO–LUMO}$ energy gap shows less tendency of valence electrons of the molecules to move to the excited state, with such compounds being chemically more inert or the complex of two molecules with non-covalent interactions being more stable(Li Feng-Yu and Zhao Ji-Jun 2010). In our case, smaller $\Delta E_{HOMO–LUMO}$ values could be due to stronger inter-molecular interactions and a higher possibility of

charge transfers between the NR and BB_1/BB_2 binders. This phenomenon can motivate the possible interactions between the radical forms of the sulfur crosslink and polarized amide-based bio-binders.

According to the data reported in **Table 2-5**, among all considered complexes, the lowest $\Delta E_{HOMO-LUMO}$ was observed through the interaction between the BB_1/BB_2 bio-binders with the S—S bond of rubber rather than with the C—S bond. This observation indicates that the inter-molecular orbital interactions between the amide functional group of BB_1/BB_2 and the S—S crosslink of the NR will lead to a higher possibility of the polarization of the amide functional group in the presence of NR. Furthermore, a comparison of the considered interacting sites of BB_1 in **Table 2-5** showed that the complex in which the —NH_2 group of BB_1 is in proximity to NR has a lower $\Delta E_{HOMO-LUMO}$ gap than for the carbonyl (C═O). This fact revealed the interaction of the —NH_2 group with the NR is stronger than that of the carbonyl group. The probability of an amide to interact with the —NH_2 orientation is more preferred than with the carbonyl (C═O) orientation, this could be also observed for the NR—BB2 complex. However, a comparison of the obtained results showed the higher efficiency of BB_2 to promote partial devulcanization of the sulfur crosslinked NR, compared to BB_1. The better functionality of BB_2 than BB_1 in terms of non-covalent interaction with natural rubber was also observed in the calculated thermochemical properties (**Table 2-4**).

2.4.4. AIM analysis

To further investigate the nature of intermolecular interactions in the NR—BB_1/BB_2 complexes, the topological properties of the electron density ρ_c and the

Laplacian charge density $\nabla^2\rho_c$ at the non-bonding critical points between the amide functional group of BB_1/BB_2 bio-materials and sulfur crosslink of NR were explored through AIM analysis. The calculated AIM parameters for the considered orientations of the BB_1/BB_2 bio-binders interacting with the right-hand side sulfur crosslink units of NR at the B97D/6-31+G* level are listed in **Table 2-6**.

Table 2-6. Topological Properties of The Critical Points for The Inter-Molecular Interaction Between BB_1/BB_2 Bio-Binders and The Right-Hand Side Sulfur Crosslink Units of Natural Rubber in The Four Complexes, Obtained at The B97D/6-31+G* Level of Theory.

NR—BB_1	λ_1	λ_2	λ_3	ρ_c	$\nabla^2\rho_c$
NH_2 orientation					
C—S	-0.049	-0.022	0.217	0.125	0.197
S—S	-0.091	-0.053	1.190	0.261	0.368
C═O orientation					
C—S	-0.032	-0.024	0.186	0.119	0.145
S—S	-0.057	-0.035	0.432	0.188	0.249
NR—BB_2					
NH_2 orientation					
C—S	-0.061	-0.033	0.317	0.138	0.197
S—S	-0.087	-0.038	1.203	0.226	0.386
C═O orientation					
C—S	-0.032	-0.015	0.350	0.123	0.157
S—S	-0.023	-0.016	0.579	0.213	0.255

As anticipated, both λ_1 and λ_2 (perpendicular to the bond path) are negative, while λ_3, located along the bond gradient path, is positive. The charge density ρ_c (e a_0^{-3}) measures the electrostatic interaction strength, and the sign of the Laplacian of the charge density $\nabla^2\rho$ (e a_0^{-5}) indicates the nature of the molecular interaction, with $\nabla^2\rho_c < 0$ for the covalent interactions and $\nabla^2\rho_c > 0$ for electrostatic interactions(Bader, 1990).

In both BB_1 and BB_2, the higher average value of charge density ρ_c **(**average of ρ_c between C—S and S—S) of the —NH_2 orientation ($\rho\mathbf{c}_{-NH2}^{BB1}$ =0.193 e a_0^{-3}; $\rho\mathbf{c}_{-NH2}^{BB2}$ = 0.760 e a_0^{-3})**,** in comparison to the carbonyl (C═O) site ($\rho\mathbf{c}_{C=O}^{BB1}$ = 0.153 e a_0^{-3}; $\rho\mathbf{c}_{C=O}^{BB2}$ = 0.168 e a_0^{-3}) revealed the stronger electrostatic interaction of the —NH_2 group with NR's sulfur crosslink unit than the carbonyl (C═O) group. This observation confirmed the preference and stronger non-covalent interactions between the —NH_2 site of BB_1/BB_2 and NR, which is consistent with the more negative interaction energy (stronger electrostatic interactions) in the case where the BB_1/BB_2 were interacting with the sulfur crosslink of NR with the —NH_2 group rather than with the carbonyl (C═O) group (**Tables 2-2** and 2-**3**). In addition, a comparison of two potential interacting points of natural rubber (C—S and S—S) with each —NH_2 and C═O orientation of BB_1/BB_2 showed that for both —NH_2 and carbonyl (C═O), the more ρ_c (the stronger electrostatic interaction) was obtained for the case of the sulfur (S—S) interacting point involved in the sulfur crosslink unit of natural rubber. Interestingly, this is in agreement with the stronger binding interaction energies that are presented in **Tables 2-2** and 2-**3**. These findings are further evaluated and supported with analysis of the DFT-based reactivity indexes such as chemical hardness (***η***) and softness (*S*) upon complexation as well as charge transfer between NR and BB_1/BB_2 molecular orbitals using second-order perturbation theory. In addition, among all considered orientations, the obtained values of ρ_c reconfirmed that the interaction between NR—BB_2 has higher values than NR—BB_1, which indicates a stronger interaction and better performance of BB_2 than BB_1 in promoting partial sulfur devulcanization of NR (**Table 2-6**).

2.4.5. Analysis of reactivity-based quantities of bio-binder

Ionization potential (IP), electron affinity (EA), chemical hardness (η), and softness (S) are reactivity-based parameters for better understanding the intermolecular stabilization and chemical reactivity of the constituent molecules of BB_1/BB_2 bio-binder and rubber models(Hohenberg, 1964; Parr, 1993; Pearson, 1997; Wong, 2014). Chemical hardness fundamentally signifies the structural resistance of the complex system to deformation of electronic distribution and intermolecular charge transfer between the two components of the system (NR and BB_1/BB_2)(Udhayakalaa, 2012). Generally, soft molecules have smaller E_{HOMO} and E_{LUMO} energy gaps, and the complexes with the higher value of $\Delta E_{HOMO-LUMO}$ gap correspond to harder molecules(Pearson, 1987, 1988). The ionization potential (IP), electron affinity (EA), chemical hardness (η), and softness (S) for the selected NR—BB_1/BB_2 models are reported in **Table 2-7**.

Table 2-7. Ionization Potential (IP), Electron Affinity (EA), Chemical Hardness (η) and Softness (*S*) for The Selected NR—BB_1/BB_2 Complexes Obtained at The B97D/6-31+G* Level of Theory.

NR—BB1	**IP (eV)**	**EA (eV)**	***η*(eV)**	***S* (eV)$^{-1}$**
NH_2 orientation				
C—S	7.620	-1.108	4.364	0.116
S—S	7.352	-1.069	4.210	0.119
C═O orientation				
C—S	7.666	-1.228	4.447	0.112
S—S	7.433	-1.143	4.288	0.117
NR—BB2				
NH_2 orientation				
C—S	7.477	-1.195	4.336	0.115
S—S	7.222	-1.004	4.113	0.122
C═O orientation				
C—S	7.566	-1.195	4.380	0.114
S—S	7.351	-1.093	4.222	0.118

Among all considered NR—BB_1/BB_2 model complexes, the smallest values of chemical hardness were observed where the BB_1/BB_2 was interacting with the S—S bond of the NR (4.210 eV, 4.288 eV, 4.113 eV, 4.222 eV) in comparison to the C—S bond (4.364 eV, 4.447 eV, 4.336 eV, 4.380 eV). This lowest value of hardness for BB_1/BB_2 approaches to the S—S bond is directly correlated with the lowest value in interaction energy obtained for all considered —NH_2 and carbonyl (C═O) reactive sites of BB_1/BB_2

(**Table 2-3**). This orientation also has the stronger intermolecular interaction and smallest $\Delta E_{HOMO–LUMO}$ energy gap (**Table 2-5**), which corresponds to the complex with the softest character. These observations confirmed that the more reactive nature of this NR—BB_1/BB_2 interaction originates from the orientations for radical particles of sulfur crosslink involved in NR in the presence of the BB_1/BB_2 bio-binders. This reconfirmed that the devulcanization process of the S—S bond of sulfur crosslink is more probable than for the C—S bond connected to an isoprene unit of NR.

It is also notable that the orientation of BB_1 from the —NH_2 site has a softer nature and is more polarized within the intermolecular NR—BB interactions. These soft, polarized characteristics make the interaction more feasible and stronger than a carbonyl (C═O) interaction, with similar observations being achieved during the interaction of the NR—BB_2 complex. Interestingly, a comparison of the results for both NR—BB_1 and NR—BB_2 indicated that the NR—BB_2 interaction was more polarized and softer, and consequently more efficient, than the NR—BB_1 interaction.

2.4.6. Charge transfer in the NR—BB1/BB2 complexes

NBO analysis(Reed, 1985) deals with the electronic wave functions that are defined based on the occupied and unoccupied localized orbitals. The strengths of the stabilization interactions $E^{(2)}$ of the NR—BB_1/BB_2 complexes, which originate from the charge transfer energies between the donor and acceptor molecular orbitals, can be obtained with second-order perturbation theory(Reed et al., 1988). Larger $E^{(2)}$ values represent stronger molecular orbital interactions between the electron donor and electron

acceptor parts of the system and higher complex stabilization through non-covalent interactions(Honarparvar; Md Abdur Rauf S, 2015; Mosapour Kotena Z, 2014; Mosapour Kotena ZB-A, 2013).

A probable electron charge transfer within the NR—BB_1/BB_2 complexes is demonstrated in **Figure 2-5.** In the case of —NH_2 of BB_1 as the donor, interacting with either S—S bonds or C—S bonds of NR as the acceptor, reasonably high $E^{(2)}$ values (2.71 kcal/mol for S—S bonds and 2.33 kcal/mol for C—S bonds) were obtained in comparison to the $E^{(2)}$ values for the C═O orientation of BB_1 with the S—S (2.45 kcal/mol) and C—S (2.25 kcal/mol) bonds of NR. These results revealed the increase in charge transfer and intermolecular orbital interactions between the S—S molecular orbital of NR—BB_1 with the —NH_2 orientation. Similarly, in the case of the NR—BB_2 complex, a prominent molecular orbital interaction in terms of $E^{(2)}$ (2.85 kcal/mol) for the donor —NH_2 of BB_2 to the acceptor S—S bond of NR) indicated significant molecular orbital overlap in comparison to the C—S bond (2.42 kcal/mol). In the case of the C═O interacting site of the BB_2 to the S—S (2.51 kcal/mol) and the C—S (2.36 kcal/mol) molecular orbitals of the NR, lower $E^{(2)}$ values were observed than for the —NH_2 site. The results implied that among all possible interactive sites (—NH_2 and carbonyl (C═O) groups) of BB_1/BB_2 to S—S and C—S molecular orbitals of NR, the strongest interactions and electron delocalization (charge transfer) were observed between the S—S bond of the NR and the —NH_2 functional group of both BB_1 and BB_2. Interestingly, a comparison of the NR interaction with BB_1 and with BB_2 reveals a higher $E^{(2)}$ value for the intermolecular orbital interaction of the NR—BB_2 complex. This

observation indicates a higher possibility of a charge transfer and electron delocalization, and a stronger intermolecular interaction, of NR—BB_2 compared to NR—BB_1. This observation indicates that the BB_2 bio-binder as a secondary amide is more effective at interacting with natural rubber and can promote the partial sulfur devulcanization of NR better than the BB_1 bio-binder.

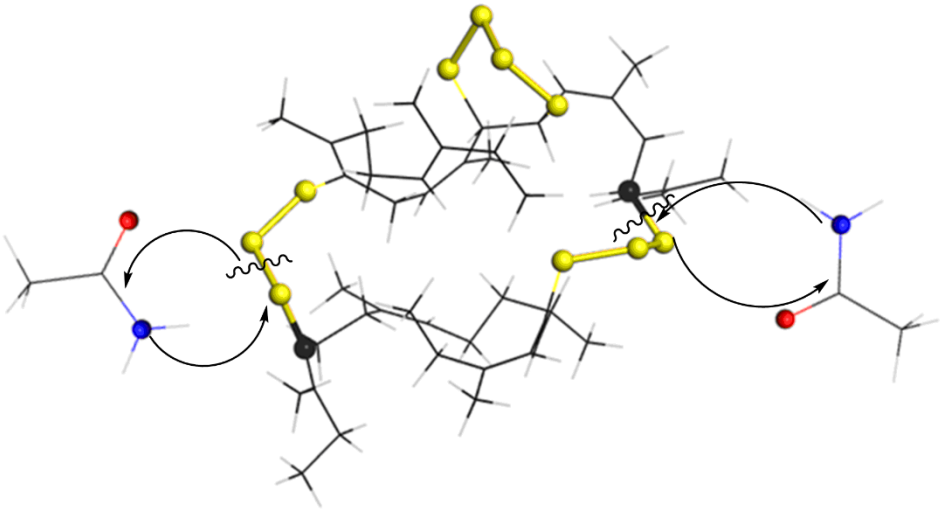

Figure 2-5. Charge Transfer within The NR—BB_1/BB_2 Complexes Calculated at The B97D/6-31+G* Level of Theory.

Overall, the lower $\Delta E_{HOMO\text{-}LUMO}$ band gap and the higher complex stabilization, $E^{(2)}$, provide the possibility of intermolecular orbital interactions and charge transfer between the donor and acceptor segments of the considered NR—BB complexes, which motivate and facilitate the intermolecular interaction between them and will lead to partial devulcanization of the sulfur crosslinked natural rubber.

2.4.7. The driving force for partial devulcanization of natural rubber

The continuous growth of innovative methods for retrieving recyclable polymers such as partial devulcanization of sulfur vulcanized natural rubber (NR) addresses a great need to reduce the effects of waste and ensure a sustainable environment. In addition to experimental synthesis and characterization methods of effective amide-based biomaterials for a partial sulfur devulcanization process of NR, this process can be further investigated by engineering a theoretical model where the effects of the dominant physico-chemical quantities on the inter-molecular interactions of NR—BB complexes are studied at the molecular level. Earlier experiment observations support the hypothesis that the addition of amide-based bio-binders (BB_1/BB_2) to natural rubber can stimulate the partial sulfur devulcanization and surface activation of rubber particles. This will reduce the segregation between the rubber and the asphalt binder matrix, while making more functional polymer available to reinforce the asphalt binder matrix(Fini et al., 2012; Fini et al., 2013; Walters, 2014). The partial devulcanization that activates the surface of rubber particles not only prevents agglomeration (through destabilizing the NR dimerization) but also interacts with the asphaltene side chains, helping them get dispersed within the asphalt matrix and not segregate, which in turn improves the rubberized asphalt binder's stability and performance.

Despite comprehensive efforts made in this field, there is still a need for detailed insight into the partial devulcanization of sulfur crosslink NR in the presence of amide-based bio-binders (BB_1 and BB_2) derived from fractional distillation of bio-oils from swine manure. The present study could computationally illustrate the extent to which the

intermolecular non-covalent interactions in NR-BB complexes can promote the interaction of S—S bonds of NR with bio-binders during the partial devulcanization through the activation of the surface of rubber particles. This fact can provide insight into understanding the partial devulcanization process and surface activation of sulfur crosslink natural rubber in the presence of amide-based bio-modifiers, and it can also address some intermolecular mechanisms at the molecular level. It is notable that the amide group in BB_1 and BB_2 compounds is an important functional group for the intermolecular orbital interactions of the electron lone pairs in the amino group, and the adjacent carbonyl leads to resonance stabilization as shown in **Figure 2-1**.

In this study, BB_1 and BB_2 bio-binder compounds are interacting with the sulfur crosslink zone of natural rubber; this study assessed the influence of amide-based BB molecules upon complexation with rubber to form NR—BB intramolecular interactions within the complexes. According to the observed results, it seems that due to the polarization of a carbonyl functional group in amide-based bio-binders, along with the C—N bond rotation, the coplanarity of the adjacent atoms, and the short C—N bond lengths, these bio-binders can be applied as effective biomaterials for partial sulfur devulcanization of natural rubber. It is likely that the charge transfer between the amide functional group of the bio-binder materials and the sulfur crosslink unit of NR is the driving force in the NR—BB intramolecular interactions, which can further promote the region-selective intermolecular interactions of the preferred S—S bond of the NR (partial devulcanization). It could also be envisaged that adding amide-based bio-binders to NR plays an important role in promoting the interfacial adhesion between the amide

functional groups in BB_1/BB_2 bio-binders and the free radicals generated by the partial sulfur devulcanization of the rubber particles. Furthermore, the outcome of this study can be implemented to propose a possible multiscale mechanism underlying the partial sulfur devulcanization of NR in the presence of amide-based bio-binders, leading to an increase in intermolecular interactions in the NR—BB complexes that are formed.

2.4.8. Laboratory Experiments

Figure 2-6 shows the effect of partial devulcanization of rubber on asphalt binder's properties. It was found that viscosity has increased at any given temperature due to the introduction of regular rubber. However, when the rubber was partially devulcanized, the viscosity was significantly decreased. For instance, viscosity of asphalt containing devulcanized rubber referred to as BMR found to be 70% lower than asphalt having non-devulcanized rubber referred to as CRM.

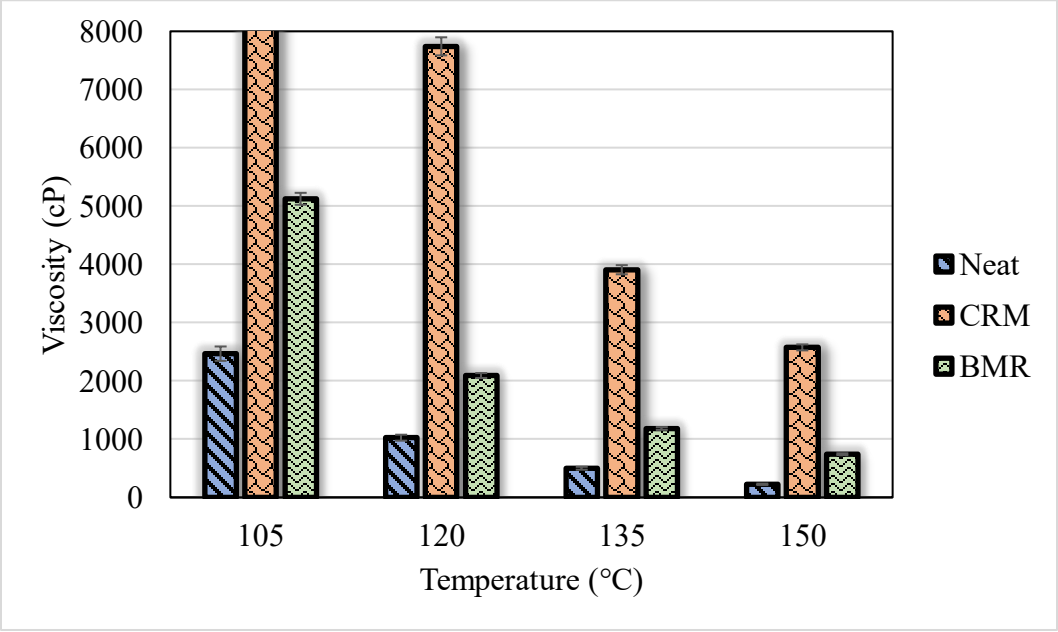

Figure 2-6. Viscosity for Neat, Crumb Rubber Modified Asphalt (CRM) and Biomodified Rubber (BMR) at All Testing Temperature.

The effect of rubber on asphalt binder's G*/sin(δ) value for RTFO aged samples is shown in **Figure 2-7**, which are plotted based on the measurement at 64 ºC at 10 rad/s. The parameter G*/sin(δ) is an indicator for evaluating the rutting resistance of binder per specification. The minimum value of G*/sin(δ) to resist rutting in RTFO-aged binder according to Superpave™ specification is ≥2.2 kPa which is satisfied by neat and all modifiers. It was observed that G*/sin(δ) value is higher in RTFO-aged asphalt containing devulcanized rubber (BMR) than neat asphalt and asphalt containing non-devulcanized rubber (CRM). It complies with the fact found in the DFT based modeling, which showed partial devulcanization of sulfur crosslinking has increased NR—BB intramolecular interactions.

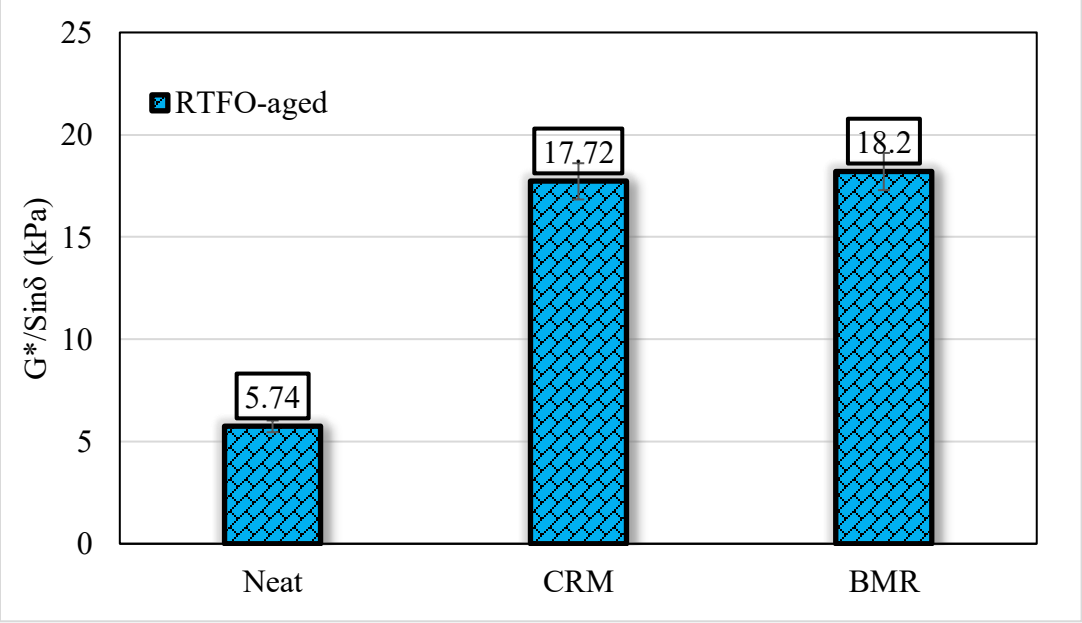

Figure 2-7. G*/sinδ Results for All RTFO Aged Binders at 64˚C

Figure 2-8 shows the G*Sinδ value at 46 ºC at 10 rad/sec for PAV aged binder. The criterion for fatigue resistance is that, G*sinδ value must be ≤5000 kPa. All modification made to binder including neat pass that criterion. The asphalt containing devulcanized rubber (BMR) is more fatigue resistance than asphalt containing non-devulcanized rubber (CRM) and neat binder. This can be attributed to the partial devulcanization of NR due to charge transfer between the amide functional group of the bio-binder materials and the sulfur crosslink unit of NR that triggered enhanced interaction between asphalt and partially devulcanized rubber.

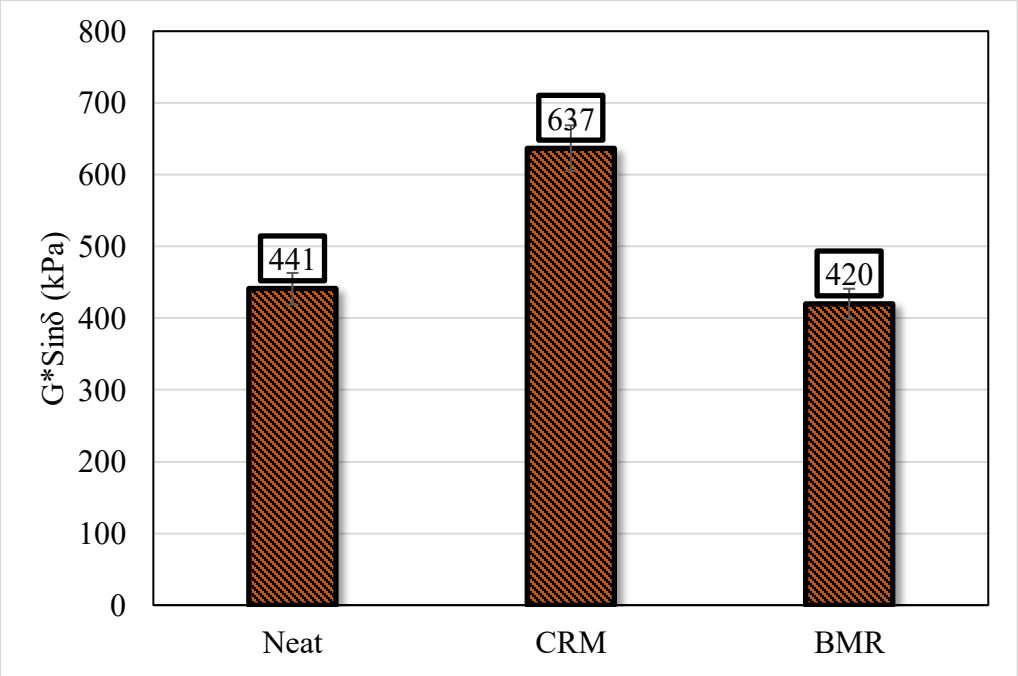

Figure 2-8. G*sinδ Results for All PAV Aged Binders at 46˚C

The bending beam rheometer (BBR) results for PAV aged crumb rubber modified asphalt (CRM) and biomodified rubber (BMR) is shown in **Figure 2-9** respectively. We

can see that asphalt containing devulcanized rubber (BMR) has improved stress relaxation or m-value compared to the control asphalt containing non-devulcanized rubber (CRM) among PAV aged binders. This overall improvement is possible due to a partial devulcanization of rubber network, where increased interaction between asphalt and partially devulcanized rubber reduced stiffness and increased stress relaxation at cold climate temperature.

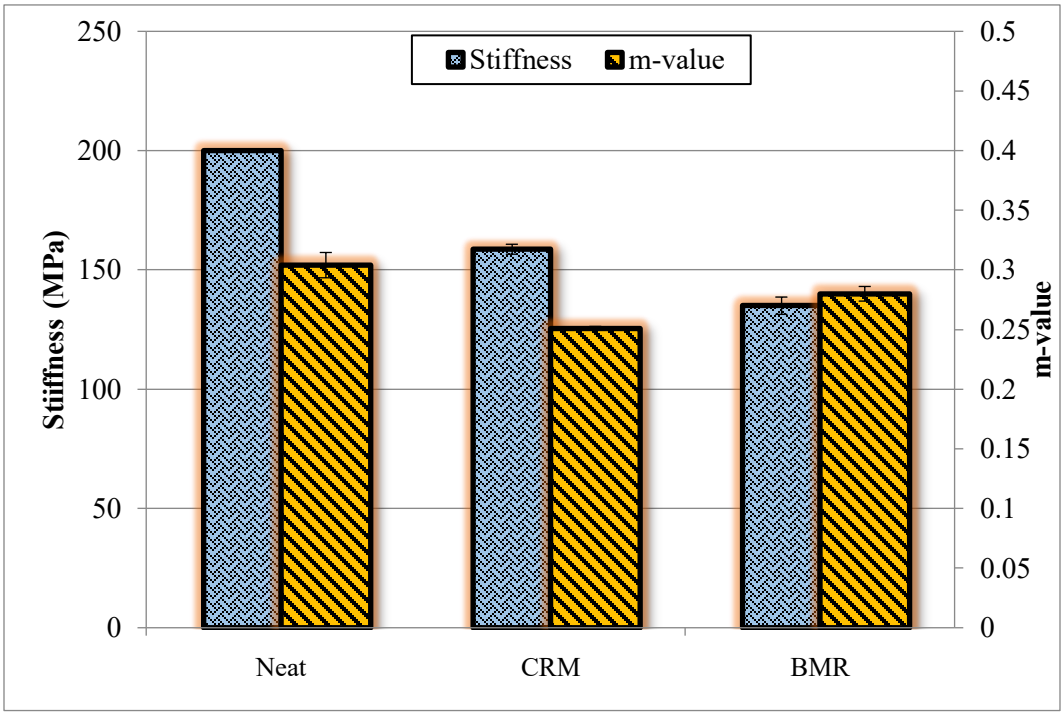

Figure 2-9. BBR Test Results for All PAV Aged Binders at -12˚C

2.5 Conclusions

In this study, intermolecular interactions between an amide-rich bio-binder and sulfur crosslinked natural rubber were studied to explain the observed partial sulfur

devulcanization of natural rubber when exposed to bio-binder molecules. The interaction of the sulfur crosslink unit of the NR with amide-based bio-binders was explored by comparing the interaction energies of the NR—BB_1/BB_2 complexes, together with the electronic structure properties including interaction energies (E_{int}), frontier molecular orbitals (HOMO, LUMO), atoms in molecules (AIM) topological indices, chemical hardness (η) and softness (S), and natural bond orbital (NBO) analysis between NR and bio-binders. The results confirmed that bio-binder has a stronger interaction with natural rubber's S—S bond than with its C—S bond. Furthermore, the charge transfer between NR and the bio-binders within the inter-molecular orbital interactions of the NR—BB_1/BB_2 complexes played a significant role. Our model is able to explain the effectiveness of BB_1/BB_2 during the partial devulcanization of NR. It has shown that the devulcanization process can be promoted within the non-covalent inter-molecular interactions between the amide accelerator and the sulfur crosslink segment or the C—S bond in the isoprene unit (C=C unit connected to C—S) of the natural rubber.

The theoretical model for the NR—BB complexes derived here is mainly based on the results of laboratory experiments; It was observed in laboratory experiments that treatment of natural rubber with amide-rich bio-binder considerably enhances the performance of natural rubber in asphalt binder in terms of workability and pumpability as viscosity decreased by 70% compared to asphalt containing non-devulcanized rubber (CRM). It has been shown that the addition of bio-binder to rubberized asphalt enhances the fatigue resistance by 34% as well as improving stress relaxation value by 4%, which could be attributed to cleavage of some of the sulfur crosslinks. The outcome of this

study could provide insights into the partial devulcanization phenomenon and plausible mechanisms involved in the surface activation of natural rubber in the presence of amide-based bio-binder.

2.6 References

AASHTO-T-313, 2019b. Standard method of test for determining the flexural creep stiffness of asphalt binder using the bending beam rheometer (BBR). American Association of State Highway and Transportation Officials.

AASHTO-T-315, 2019. Standard Method of Test for Determining the Rheological Properties of Asphalt Binder Using a Dynamic Shear Rheometer (DSR).

Adhikari, B., De, D., Maiti, S., 2000. Reclamation and recycling of waste rubber. Progress in Polymer Science 25(7), 909-948.

Alturk, S., Avci, D., Tamer, O., Atalay, Y., 2017. Comparison of different hybrid DFT methods on structural, spectroscopic, electronic and NLO parameters for a potential NLO material. Computational and Theoretical Chemistry 1100, 34-45.

ASTM-D2872, 2019. Standard Test Method for Effect of Heat and Air on a Moving Film of Asphalt (Rolling Thin-Film Oven Test), ASTM International, West Conshohocken, PA.

ASTM-D2872, 2019a. Standard practice for accelerated aging of asphalt binder using a pressurized aging vessel (PAV), USA: Annual Book of ASTM Standards.

ASTM-D6373-16, 2016. Standard Specification for Performance Graded Asphalt Binder. ASTM International, West Conshohocken, PA, 2016, www.astm.org, ASTM International, West Conshohocken, PA, 2016, www.astm.org.

ASTM-D-4402, 2015. Standard test method for viscosity determination of asphalt at elevated temperatures using a rotational viscometer, American Society for Testing and Materials.

Bader, R.F.W., 1990. Atoms in Molecules: A Quantum Theory. Wiley Online Library, Ontario, Canada.

Biegler-Konig, F., Bader, R.F., 2002. AIM 2000, Version 2

Bocoum, A., Hosseinnezhad, S., Fini, E.H., 2014a. Investigating effect of amine based additives on asphalt rubber rheological properties, Asphalt Pavements. CRC Press, pp. 945-956.

Brandenburg, J.G., Alessio, M., Civalleri, B., Peintinger, M.F., Bredow, T., Grimme, S., 2013. Geometrical Correction for the Inter- and Intramolecular Basis Set Superposition Error in Periodic Density Functional Theory Calculations. Journal of Physical Chemistry A 117(38), 9282-9292.

Buckingham, A.D., Fowler, P.W., Hutson, J.M., 1988. THEORETICAL-STUDIES OF VANDERWAALS MOLECULES AND INTERMOLECULAR FORCES. Chemical Reviews 88(6), 963-988.

Burns, L.A., Vazquez-Mayagoitia, A., Sumpter, B.G., Sherrill, C.D., 2011. Density-functional approaches to noncovalent interactions: A comparison of dispersion corrections (DFT-D), exchange-hole dipole moment (XDM) theory, and specialized functionals. Journal of Chemical Physics 134(8).

Cardenas, C., Ayers, P., De Proft, F., Tozer, D.J., Geerlings, P., 2011. Should negative electron affinities be used for evaluating the chemical hardness? Physical Chemistry Chemical Physics 13(6), 2285-2293.

Chai, J.D., Head-Gordon, M., 2008. Long-range corrected hybrid density functionals with damped atom-atom dispersion corrections. Physical Chemistry Chemical Physics 10(44), 6615-6620.

Chritiansson, M., Stenberg, B., Wallenberg, L., Holst, O., 1998. Reduction of surface sulphur upon microbial devulcanization of rubber materials. Biotechnology letters 20(7), 637-642.

Coropceanu, V., Malagoli, M., da Silva Filho, D., Gruhn, N., Bill, T., Brédas, J., 2002. Hole-and electron-vibrational couplings in oligoacene crystals: intramolecular contributions. Physical review letters 89(27), 275503.

De, D., Das, A., De, D., Dey, B., Debnath, S.C., Roy, B.C., 2006. Reclaiming of ground rubber tire (GRT) by a novel reclaiming agent. European Polymer Journal 42(4), 917-927.

Diener, M.D., Alford, J.M., 1998. Isolation and properties of small-bandgap fullerenes. Nature 393(6686), 668-671.

Dubkov, K.A., Semikolenov, S.V., Ivanov, D.P., Babushkin, D.E., Voronchikhin, V.D., 2014. Scrap tyre rubber depolymerization by nitrous oxide: products and mechanism of reaction. Iranian Polymer Journal 23(11), 881-890.

Dumont, R.S., 2014. Effects of charging and polarization on molecular conduction via the source-sink potential method. Canadian Journal of Chemistry-Revue Canadienne De Chimie 92(2), 100-111.

Fini, E., Hajikarimi, P., Rahi, M., and Moghadas Nejad, F., 2015. Physiochemical, Rheological, and Oxidative Aging Characteristics of Asphalt Binder in the Presence of Mesoporous Silica Nanoparticles. J. Mater. Civ. Eng. 28(2), 1-9.

Fini, E.H., Al-Qadi, I.L., You, Z., Zada, B., Mills-Beale, J., 2012. Partial replacement of asphalt binder with bio-binder: characterisation and modification. International Journal of Pavement Engineering 13(6), 515-522.

Fini, E.H., Bocoum, A., Hosseinnezhad, S., Martinez, F.M., 2015. Bio-Modification of Rubberized Asphalt and Its High Temperature Properties.

Fini, E.H., Hosseinnezhad, S., Oldham, D., Mclaughlin, Z., Alavi, Z., Harvey, J., 2019a. Bio-modification of rubberised asphalt binder to enhance its performance. International Journal of Pavement Engineering 20(10), 1216-1225.

Fini, E.H., Kalberer, E.W., Shahbazi, A., Basti, M., You, Z., Ozer, H., Aurangzeb, Q., 2011b. Chemical characterization of biobinder from swine manure: Sustainable modifier for asphalt binder. Journal of Materials in Civil Engineering 23(11), 1506-1513.

Fini, E.H., Oldham, D.J., Abu-Lebdeh, T., 2013. Synthesis and characterization of biomodified rubber asphalt: Sustainable waste management solution for scrap tire and swine manure. Journal of Environmental Engineering 139(12), 1454-1461.

Fletcher, R., 1980. Unconstrained optimization. Practical methods of optimization 1.

Fominykh, O.D., Sharipova, A.V., Balakina, M.Y., 2016. The Choice of Appropriate Density Functional for the Calculation of Static First Hyperpolarizability of Azochromophores and Stacking Dimers. International Journal of Quantum Chemistry 116(2), 103-112.

Froese, R.D.J., Hustad, P.D., Kuhlman, R.L., Wenzel, T.T., 2007. Mechanism of activation of a hafnium pyridyl-amide olefin polymerization catalyst: Ligand modification by monomer. Journal of the American Chemical Society 129(25), 7831-7840.

Fukumori, K., Matsushita, M., Okamoto, H., Sato, N., Suzuki, Y., Takeuchi, K., 2002. Recycling technology of tire rubber. Jsae Review 23(2), 259-264.

Garcia-Hernandez, Z., Flores-Parra, A., Grevy, J.M., Ramos-Organillo, A., Contreras, R., 2006. 2-Aminobenzothiazole phosphorus amides: Molecular and supramolecular structures, hydrogen bonds and sulfur donor-acceptor interactions. Polyhedron 25(7), 1662-1672.

Garza, A.J., Osman, O.I., Asiri, A.M., Scuseria, G.E., 2015. Can Gap Tuning Schemes of Long-Range Corrected Hybrid Functionals Improve the Description of Hyperpolarizabilities? Journal of Physical Chemistry B 119(3), 1202-1212.

Gaussian09, 2020. Optimization

Geerlings, P., De Proft, F., Langenaeker, W., 2003. Conceptual density functional theory. Chemical Reviews 103(5), 1793-1873.

Goldshtein, V., 2002. US Patent, 6 387: 966

Goldshtein, V., 2003. US Patent 6, 541: 526.

Grimme, S., 2006. Semiempirical GGA-type density functional constructed with a long-range dispersion correction. Journal of Computational Chemistry 27(15), 1787-1799.

Hinchliffe, A., 2005. Molecular modelling for beginners. John Wiley & Sons.

Hohenberg, P., Kohn, W., 1964. Inhomogeneous Electron Gas. Physical Review 136(3B), B864-B871.

Honarparvar, B., Pawar, S.A., Alves, C. N., Lameira, J., Maguire, G. E., Silva, J. R., Govender, T, Kruger, H. G., Pentacycloundecane lactam vs lactone norstatine type protease HIV inhibitors: binding energy calculations and DFT study. Journal of Biomedical Science 22(15), 1-15.

Hosseinnezhad, S., Kabir, S.F., Oldham, D., Mousavi, M., Fini, E.H., 2019a. Surface functionalization of rubber particles to reduce phase separation in rubberized asphalt for sustainable construction. Journal of Cleaner Production 225, 82-89.

Isayev AI, 2005. Recycling of rubbers.Science and technology of rubber, Chapter 15,. Elsevier, USA.

Jeong, K.-D., Lee, S.-J., Amirkhanian, S.N., Kim, K.W., 2010. Interaction effects of crumb rubber modified asphalt binders. Construction and Building Materials 24(5), 824-831.

John B. Macleod, M.E.M., Ronald D. Myers, Peter Nicholson, 1995. Rubber devulcanization process, in: Company, E.R.A.E. (Ed.). USA.

Jorgensen, W.L., Madura, J.D., Swenson, C.J., 1984. OPTIMIZED INTERMOLECULAR POTENTIAL FUNCTIONS FOR LIQUID HYDROCARBONS. Journal of the American Chemical Society 106(22), 6638-6646.

Jung, I.H., Lo, W.-Y., Jang, J., Chen, W., Zhao, D., Landry, E.S., Lu, L., Talapin, D.V., Yu, L., 2014. Synthesis and Search for Design Principles of New Electron Accepting Polymers for All-Polymer Solar Cells. Chemistry of Materials 26(11), 3450-3459.

Kabir, S.F., Mousavi, M., Fini, E.H., 2019. Selective adsorption of bio-oils' molecules onto rubber surface and its effects on stability of rubberized asphalt. Journal of Cleaner Production, 119856.

Kanazawa, H., Higuchi, M., Yamamoto, K., 2006. Synthesis and chemical degradation of thermostable polyamide with imine bond for chemical recycling. Macromolecules 39(1), 138–144.

Kemnitz, C.R., Loewen, M.J., 2007. "Amide resonance" correlates with a breadth of C-N rotation barriers. Journal of the American Chemical Society 129(9), 2521-2528.

Kim, K.S., Tarakeshwar, P., Lee, J.Y., 2000. Molecular clusters of pi-systems: Theoretical studies of structures, spectra, and origin of interaction energies. Chemical Reviews 100(11), 4145-4185.

Kleps, T., Piaskiewicz, M., Parasiewicz, W., 2000. The use of thermogravimetry in the study of rubber devulcanization. Journal of Thermal Analysis and Calorimetry 60(1), 271-277.

Knorr, K., 1994. RECLAIM FROM NATURAL AND SYNTHETIC RUBBER SCRAP FOR TECHNICAL RUBBER GOODS. Kautschuk Gummi Kunststoffe 47(1), 54-57.

Kobko, N., Dannenberg, J.J., 2001. Effect of basis set superposition error (BSSE) upon ab initio calculations of organic transition states. Journal of Physical Chemistry A 105(10), 1944-1950.

Kojima, M., Tosaka, M., Ikeda, Y., Kohjiya, S, 2005. Devulcanization of carbon black filled natural rubber using supercritical carbon dioxide. Applied Polymer 95(1), 137–143.

Kojima, M., Tosakaa, M., Ikedab, Y. , 2004. Chemical recycling of sulfur-cured natural rubber using supercritical carbon dioxide. Green Chemistry(6), 84-89.

Kojimaa, M., Kohjiyaa, S., Ikedab,Y. , , 2005. Role of supercritical carbon dioxide for selective impregnation of decrosslinking reagent into isoprene rubber vulcanizate. Polymer 46(7), 2016–2019.

Laidig, K.E., Cameron, L.M., 1996. Barrier to rotation in thioformamide: Implications for amide resonance. Journal of the American Chemical Society 118(7), 1737-1742.

Lameira, J., Alves, C.N., Moliner, V., Silla, E., 2006a. A density functional study of flavonoid compounds with anti-HIV activity. Eur J Med Chem 41(5), 616-623.

Lameira, J., Medeiros, I.G., Reis, M., Santos, A.S., Alves, C.N., 2006b. Structure-activity relationship study of flavone compounds with anti-HIV-1 integrase activity: A density functional theory study. Bioorg Med Chem 14(21), 7105-7112.

Levin, V.Y., Kim, S.H., Isayev, A.I., 1997. Vulcanization of ultrasonically devulcanized SBR elastomers. Rubber Chemistry and Technology 70(1), 120-128.

Li, F., Yan, B., Zhang, Y.P., Zhang, L.H., Lei, T., 2014. Effect of activator on the structure and desulphurization efficiency of sludge-activated carbon. Environmental Technology 35(20), 2575-2581.

Li Feng-Yu, Zhao Ji-Jun 2010. Quantum chemistry PM3 calculations of sixteen mEGF molecules. 1(1), 68-77.

Lo Presti, D., 2013. Recycled Tyre Rubber Modified Bitumens for road asphalt mixtures: A literature review. Construction and Building Materials 49, 863-881.

MacLeod, D., Ho, S., Wirth, R., Zanzotto, L., 2007. Study of crumb rubber materials as paving asphalt modifiers. Canadian Journal of Civil Engineering 34(10), 1276-1288.

Maseras, F., Morokuma, K., 1995. IMOMM - A NEW INTEGRATED AB-INITIO PLUS MOLECULAR MECHANICS GEOMETRY OPTIMIZATION SCHEME OF EQUILIBRIUM STRUCTURES AND TRANSITION-STATES. Journal of Computational Chemistry 16(9), 1170-1179.

Md Abdur Rauf S, A.P.I.A., F., Govender T., Maguire G. E. M., Kruger, H. G., Honarparvar, B., 2015. The effect of N-methylation of amino acids (Ac-X-OMe) on solubility and conformation: a DFT study. Organic & Biomolecular Chemistry 13(39), 9885-10076.

Mohaved, S.O., Ansarifar, A., Nezhad, S.K., Atharyfar, S., 2015. A novel industrial technique for recycling ethylene-propylene-diene waste rubber. Polymer Degradation and Stability 111, 114-123.

Monajjemi, M., Honarparvar, B., Hadad, B.K., Ilkhani, A.R., and Mollaamin, F., 2010. Thermo-chemical investigation and NBO analysis ofsome anxileotic as Nano-drugs. African Journal of Pharmacy and Pharmacology 4 (8), 521-529.

Monajjemi, M., Lee, V.S., Khaleghian, M., Honarparvar, B., Mollaamin, F., 2010. Theoretical Description of Electromagnetic Nonbonded Interactions of Radical, Cationic, and Anionic NH2BHNBHNH2 Inside of the B18N18 Nanoring. Journal of Physical Chemistry C 114(36), 15315-15330.

Morgado, C.A., McNamara, J.P., Hillier, I.H., Burton, N.A., 2007. Density functional and semiempirical molecular orbital methods including dispersion corrections for the accurate description of noncovalent interactions involving sulfur-containing molecules. Journal of Chemical Theory and Computation 3(5), 1656-1664.

Mosapour Kotena Z, B.A.R., Hashim R., 2014. AIM and NBO analyses on hydrogen bonds formation in sugar-based surfactants (α/β-d-mannose and n-octyl-α/β-d-mannopyranoside): a density functional theory study. Liquid Crystals 41(6), 784-792.

Mosapour Kotena ZB-A, R., Hashim, R., Manickam Achari, V., 2013. Hydrogen bonds in galactopyranoside and glucopyranoside: a density functional theory study. Journal of Molecular Modeling 19(2), 589-599.

Mousavi, M., Hosseinnezhad, S., Kabir, S.F., Burnett, D.J., Fini, E.H., 2019b. Reaction pathways for surface activated rubber particles. Resources, Conservation and Recycling 149, 292-300.

Mousavi, M., Pahlavan, F., Oldham, D., Abdollahi, T., Fini, E.H., 2016. Alteration of intermolecular interactions between units of asphaltene dimers exposed to an amide-enriched modifier. RSC Advances 6(58), 53477-53492.

Mujika, J.I., Matxain, J.M., Eriksson, L.A., Lopez, X., 2006. Resonance structures of the amide bond: The advantages of planarity. Chemistry-a European Journal 12(27), 7215-7224.

Olmsted III, J., Williams, G.M., 1997. Chemistry: the Molecular Science, 2nd Edition ed. Wm.C. Brown.

Pahlavan, F., Mousavi, M., Hungb, A., Fini, E. H. , 2016. Investigating molecular interactions and surface morphology of wax-doped asphaltenes Physical Chemistry Chemical Physics

Paizs, B., Suhai, S., 1998. Comparative study of BSSE correction methods at DFT and MP2 levels of theory. Journal of Computational Chemistry 19(6), 575-584.

Parr, R., Zhou, Z., 1993. Absolute hardness: unifying concept for identifying shells and subshells in nuclei, atoms, molecules, and metallic clusters. Accounts of Chemical Research 26(5), 256-258.

Pearson, R., 1987. Recent advances in the concept of hard and soft acids and bases. Journal of Chemical Education 64(7), 561.

Pearson, R., 1988. Absolute electronegativity and hardness: application to inorganic chemistry. Inorganic Chemistry 27(4), 734-740.

Pearson, R.G., 1989. Absolute electronegativity and hardness: applications to organic chemistry. The Journal of Organic Chemistry 54(6), 1423-1430.

Pearson, R.P., 1997. Chemical hardness: applications from molecules to solids. Wiley-VCH, Weinheim.

Platts, J.A., Maarof, H., Harris, K.D.M., Lim, G.K., Willock, D.J., 2012. The effect of intermolecular hydrogen bonding on the planarity of amides. Physical Chemistry Chemical Physics 14(34), 11944-11952.

Ralph G. Pearson, 1963. Hard and Soft Acids and Bases. J. Am. Chem. Soc. 85(22), 3533–3539.

Rauf, M.A., Arvidsson, P., Albericio, F., Govender, T., Maguire, G. E., Kruger, H. G., Honarparvar, B., 2015. The effect of N-methylation of amino acids (Ac-X-OMe) on solubility and conformation: a DFT study. Organic & biomolecular chemistry 13(39), 9993-10006.

Reed, A.E., Curtiss, L.A., Weinhold, F., 1988. INTERMOLECULAR INTERACTIONS FROM A NATURAL BOND ORBITAL, DONOR-ACCEPTOR VIEWPOINT. Chemical Reviews 88(6), 899-926.

Reed, A.E., Weinhold, F., 1985. Natural localized molecular orbitals. Chemical Physics 83(4), 1736-1740.

Robert G. Parr , Ralph G. Pearson, 1983. Absolute hardness: companion parameter to absolute electronegativity. J. Am. Chem. Soc., 105(26), 7512–7516.

Rooj, S., Basak,G. C., Maji, P. K., Bhowmick, A. K., 2011. New Route for Devulcanization of Natural Rubber and the Properties of Devulcanized Rubber. Journal of Polymers and the Environment 19(2), 382-390.

Sarasia, E.M., Soliman, M.E.S., Honarparvar, B., 2012. Theoretical study on the molecular electronic properties of salicylic acid derivatives as anti-inflammatory drugs. Journal of Structural Chemistry 53(3), 574-581.

Schlegel, H.B., 1984. Estimating the Hessian for gradient-type geometry optimizations. Theoretica chimica acta 66(5), 333-340.

Schlegel, H.B., Binkley, J., Pople, J., 1982. Chent Phys. 1984, 80, 1976-1981. Schlegel, HBJ. Comput. Chem 3, 214-218.

Sutanto, P., Laksmana, F.L., Picchioni, E., Janssen, L.P.B.M., 2006. Modeling on the kinetics of an EPDM devulcanization in an internal batch mixer using an amine as the devulcanizing agent. Chemical Engineering Science 61(19), 6442-6453.

Sutanto, P., Laksmana, F.L. ,Picchioni, F. , Janssen, L.P.B.M., 2006. Modeling on the kinetics of an EPDM devulcanization in an internal batch mixer using an amine as the devulcanizing agent. Chemical Engineering Science 61(19), 6442 – 6453.

Svensson, M., Humbel, S., Morokuma, K., 1996. Energetics using the single point IMOMO (integrated molecular orbital plus molecular orbital) calculations: Choices of computational levels and model system. Journal of Chemical Physics 105(9), 3654-3661.

Szabo Attila. , Ostlund Neil.S., 1989. Modern Quantum Chemistry: Introduction to Advanced Electronic Structure Theory. McGraw Hill, Mineola, New York.

Teixeira, J., 2015. Industrial Devulcanization of Rubber. Kgk-Kautschuk Gummi Kunststoffe 68(1-2), 6-9.

Tsuzuki, S., Uchimaru, T., Tanabe, K., Kuwajima, S., 1994. REFINEMENT OF NONBONDING INTERACTION POTENTIAL PARAMETERS FOR METHANE ON THE BASIS OF THE PAIR POTENTIAL OBTAINED BY MP3/6-311G(3D,3P)-LEVEL AB-INITIO MOLECULAR-ORBITAL CALCULATIONS - THE ANISOTROPY OF H/H INTERACTION. Journal of Physical Chemistry 98(7), 1830-1833.

Udhayakalaa, P., Rajendiranb, T. V., Gunasekaranc, S. , 2012. Theoretical approach to the corrosion inhibition efficiency of some pyrimidine derivatives using DFT method. Journal of Computational Methods in Molecular Design 2(1), 1-15.

Walters, R., Fini, E. H., Abu-Lebdeh, T., 2014. Introducing Combination of Nano-clay and Bio-char to Enhance Asphalt Binder's Rheological and Aging Characteristics. International Journal of Pavement Research and Technology 7(6), 451-455.

Warner, W.C., 1994. METHODS OF DEVULCANIZATION. Rubber Chemistry and Technology 67(3), 559-566.

Weinhold F, Carpenter J.E., 1988. The Structure of Small Molecules and Ions, Plenum, New York.

Wong, K.Y., -Mercader, A.G., Saavedra, L. M., Honarparvar, B., Romanelli, G.P., Duchowicz, P. R., 2014. QSAR analysis on tacrine-related acetylcholinesterase inhibitors. Journal of Biomedical Science 21(84), 1-8.

Xantheas, S.S., 1996. On the importance of the fragment relaxation energy terms in the estimation of the basis set superposition error correction to the intermolecular interaction energy. Journal of Chemical Physics 104(21), 8821-8824.

Zanchet, A., Carli, L.N., Giovanela, M., Crespo, J.S., Scuracchio, C.H., Nunes, R.C.R., 2009. Characterization of Microwave-Devulcanized Composites of Ground SBR Scraps. Journal of Elastomers and Plastics 41(6), 497-507.

Zhao, Y., Gu, F., Xu, J., Jin, J., 2010. Analysis of Aging Mechanism of SBS Polymer Modified Asphalt based on Fourier Transform Infrared Spectrum. Journal of Wuhan University of Technology-Materials Science Edition 25(6), 1047-1052.

Zielinski, T.J., Harvey, E., Sweeney, R., Hanson, D.M., 2005. Quantum states of atoms and molecules. ACS Publications.

Chapter 3 HYBRID TREATMENT OF RUBBER

3.1 Abstract

Application of crumb rubber in asphalt has demonstrated many performance advantages for the pavement industry while bringing a solution for the disposal of the scrap tire. However, the introduction of rubber to asphalt binder has challenges associated with rubber segregation and workability. To address the latter issues, continuous agitation and high mixing temperature is commonly used which increases energy consumption, disintegration of crumb rubber, and emission of greenhouse gases. This paper introduces a newly developed surface activated rubber (SAR) prepared via a hybrid method of microwave treatment and bio-modification to alleviate the associated problems. The properties and performance of SAR were compared with those of conventional crumb rubber modified (CRM) and microwave-activated crumb rubber modified (M-CRM) asphalt. Fourier transform infrared spectroscopy (FTIR), Scanning electron microscopy (SEM) and computational analysis using density functional theory (DFT) indicated successful grafting of biomolecules on the rubber particles. SAR showed 86% reduction in segregation index compared to the other CRM scenarios. Such enhancement was also reflected in a significant improvement in workability of SAR modified binder compared to the other CRM scenarios. Mechanical tests showed high fracture energy (167 J/m^2) for SAR modified asphalt, which was approximately three times higher than that of conventional CRM asphalt (57 J/m^2). It further examines how surface activation of rubber promotes its interaction with asphalt molecules to reduce phase separation in rubberized asphalt-binder. Using quantum-based calculations, chain reactions between

an amide-rich bio-modifier and irradiated molecules of rubber is examined. The density functional theory (DFT)-based molecular modeling was performed on amide-type molecules as representatives for the bio-modifier. Comparing interactions of amidyl radical (RCO-N•H) of bio-modifier with sulfur-centered and carbon-centered radicals of rubber showed that amidyl radicals have higher affinity to bind to carbon-centered radicals than to sulfur-centered radicals. While the spine triplet state for –N…S– reaction coordinates encounters the obstacle of spin block and activation barrier, no spin block is observed on the –N…C– reaction pathway. The latter reaction was further observed via FTIR spectra where a new peak appeared at 1040 cm-1 indicating formation of C-N bonds. Aforementioned reactions led to grafting highly polar molecules of bio-modifier onto the surface of rubber increasing rubber's surface polarity. This was evidenced by the increase in acid-base component of rubber's surface energy from 2.9 mJ/m^2 in control rubber to 14.6 mJ/m^2 in treated rubber. The increased polarity increased the interactions of rubber with asphalt molecules reducing the phase separation commonly known as segregation in rubberized asphalt.

Keywords: Crumb rubber, Surface activated rubber, Workability, Segregation, Phase separation, Rheology, Asphalt binder, Density Functional Theory (DFT)

3.2 Introduction

The application of crumb rubber from scrap tire in asphalt industry demonstrated many benefits including extended service life, reduced noise level up to 50-70%, improved thermal properties and skid resistance as well as providing a safe method for recycling of scrap tire (Yu et al., 2011) (Xiaowei et al., 2017). In spite of its benefits for

asphalt, challenges associated with the workability and segregation have limited its application (CalTrans, 2003; Liang, 2015a; Oliveira et al., 2013; Presti et al., 2018; Yu et al., 2011; Yu et al., 2017).

Segregation is the result of high settling rate of crumb rubber in modified asphalt. Rubber particle size, density differences between rubber and asphalt binder, and swelling of rubber particles are the problems associated with the segregation, which consequently has a negative effect on the application of CRM in asphalt (Kocevski et al., 2012; Shu and Huang, 2014). Polymeric structure of rubber is mostly contained of vulcanized rubber, which means rubber molecules are crosslinked with sulfur bonds via an irreversible reaction. Crumb rubber asphalt suffers from inadequate dispersion and incompatibility with asphalt binder which is related to its vulcanized structure (Liang, 2015a) (Yu et al., 2011). The modification of rubber surface performed via a physical process, or a chemical process can alleviate the issue of incompatibility. Different physical techniques such as plasma polymerization, plasma chlorination, ultraviolet (UV) radiation, ozone treatment, and corona discharge have been applied to modify rubber surface to address the problem of crosslinking structure of rubber (Cao et al., 2014; Manhart et al., 2016; Romero-Sánchez et al., 2003; Romero-Sánchez and Martín-Martínez, 2006; Romero-Sánchez et al., 2007; Tyczkowski et al., 2003; Xiang et al., 2018). Chemical treatments on the other hand have some advantages over the physical treatment such as avoiding excessive disintegration of rubber structure while introducing selected chemical groups to the surface of rubber for increasing its feasibility in various applications (Liang, 2015a; Xiaowei et al., 2017). The study by Kocevski et al showed

the effect of functionalizing of the rubber surface by grafting active species such as acrylic acid in modification of asphalt. Their results showed increased the viscosity and failure temperature values of asphalt binder (Kocevski et al., 2012). Treating rubber with an amide-enriched bio-modifier showed an enhancement in overall rheological properties of asphalt (Hosseinnezhad et al., 2015a). Leng et al used bis (2-hydroxy ethylene) terephthalamide (BHETA) for modification of CRM and they found BHET was able to enhance storage stability of CRM binder (Leng et al., 2018).

Microwave treatment has been studied for devulcanization of rubber and it was shown that this method can provide uniform volumetric heat leading to partial devocalization of rubber by cleavage of disulfide bonds (Colom et al., 2018; de Sousa et al., 2017; Yu et al., 2011). Yu et al performed microwave treatment on crumb rubber before mixing with asphalt. According to their research, cleaving the crosslinked networks led to the activation of surface increasing asphalt-rubber interaction. They showed asphalt containing treated rubber has lower temperature susceptibility and improved viscoelasticity and storage stability compared to specimens containing non-treated rubber (Yu et al., 2011). Liang et al. used a commercial microwave oven to perform modification of crumb rubber and later used trans-polyoctenamer (TOR) to increase binder's performance. Their test results showed that microwave-activated CR increases resistance to thermal cracking, but the risk of fatigue cracking also increases (Liang et al., 2017b). Similar research has been carried by De Sousa et al. who studied microwave devulcanized rubber to study structural modifications of crumb rubber (de Sousa et al., 2017). They found that the ultimate temperature during the residence time

plays a major role of the cleavage of the disulfide bonds. They concluded that processing factors can be controlled to balance the rate of cleavage and re-vulcanization during the treatment process. However, none of the above treatment fully addresses the rubber segregation and workability issues.

Accordingly, this paper examines efficacy of a novel sustainable hybrid approach to modify crumb rubber using microwave radiation combined with bio-modification to promote grafting polar bio-molecules onto the surface of rubber to create surface activated rubber in an attempt to reduce aforementioned segregation and workability issues.

Micro-scale study can provide valuable information about the structure-function relationship for microwave irradiated rubber and its treatment effect on asphalt-binder. However, the inherent complexity and molecular diversity of the asphalt-binder as well as the uncertainty of mechanisms involved during the rubber devulcanization process are the main obstacles for molecular-level understanding of these matrices. Accordingly, very few theoretical studies have been performed on the devulcanized rubber or rubberized asphalt-binder. Recently, *ab initio* molecular dynamic simulations and quantum chemistry have been employed to explain some aspects of the bond breaking mechanism of sulfur crosslinks(Gehrke et al., 2017),(Hanson and Martin, 2009),(Hanson and Barber, 2018) and mechanical response of the simulated rubber under tensile or compressive strains.(Hanson et al., 2013),(Hanson, 2011),(Hanson, 2009), In a series of polymer-modified asphalt-binder models, molecular dynamic simulations were

performed to study the physical and transport properties of asphalt-binder modified with poly(styrene-butadiene) rubber.(Berry, 2017)

This paper contributes to the body of knowledge by determining reaction pathways between irradiated crumb rubber and bio-modifier molecules leading to a treated rubber with the reduced phase separation and enhanced compatibility in the matrix of asphalt-binder.

The first part of this paper concentrates on theoretical aspects of the irradiated rubber and bio-modifier while performing density functional theory (DFT) calculations on model systems that simulate representative interactions between molecules of irradiated rubber and bio-modifier. What makes the aforementioned interactions specifically complicated is the emergence of many free radicals due to the microwave irradiation. So, spin unrestricted type calculations are performed to model the free-radical reactions that occur upon irradiation. At the second part, we conduct a series of experiments using Fourier-transform infrared (FTIR) spectroscopy, dynamic shear rheometer (DSR), cigar tube separation test, and inverse gas chromatography (IGC) to further evaluate the chemical and surface properties of the treated rubber.

Accordingly, this study examines efficacy of a novel sustainable hybrid approach to modify crumb rubber using microwave radiation combined with bio-modification to promote grafting polar bio-molecules onto the surface of rubber to create surface activated rubber in an attempt to reduce aforementioned segregation and workability issues.

Therefore, the objective of this chapter is to observe results of surface modification and explain the underlying interactions with density functional theory (DFT).

3.3 Experimental Procedure

3.3.1 Modeling

For modeling part Without imposing any constraint, geometry of all interacting systems were fully optimized at the gradient-corrected BPE(Perdew et al., 1996) density functional, in conjunction with a standard 6-31g(d) basis set, embedded in Gaussian 09. The spin unrestricted self-consistent-field (SCF) calculation of the ground state was performed at each point along with the extension curve of potential energy surface.

Interaction energy (E_{int}), indicative of the thermodynamic stability of the system, was calculated by the energy difference between the total energy of the complex, $E_{complex}$, and sum of the energies of the interacting fragments, $E_{fragment}$, when they are in their lowest energy state;

$$E_{int} = E_{complex} - \left(\sum E_{fragment}\right) \quad (3\text{-}1)$$

3.3.1 Materials

The asphalt binder used in this study is PG 64-22, which is commonly used in North Carolina. The crumb rubber (0.177 mm) was acquired from the Liberty Tire Recycling. Supplied rubber is cryogenic processed, with major source is passenger car tire.

The bio-modifier was synthesized using a bio-oil derived from bio-mass. Bio-oil was produced from thermochemical liquefaction of swine manure at NC A&T farm, the process of production has been reported in elsewhere (Fini et al., 2012). Below tables 1 and 2 show the basic properties of asphalt binder and bio-modifier.

Table 3-1. Physicochemical Properties of Asphalt Binder (PG 64-22)

Name	pH	Specific Gravity	Elemental Composition (wt%)				Absolute Viscosity (Pa.s) at 60 ºC
			C	H	N	O	
PG 64-22	Neutral	1.0-1.10	81.6	10.8	0.77	6.83	202

Table 3-2. Physicochemical Properties of Bio-modifier

Name	pH	Density (g/ml)	Elemental Composition (wt%)				Viscosity (Pa. s) at 60ºC
			C	H	N	O	
Bio-modifier	5.97	0.96	63.44	8.36	3.53	14.33	0.075

3.3.2 Treatment Methods

Microwave Treatment

Microwave-activated crumb rubber (M-CR) was prepared in a microwave oven (2,450 MHz) with microwave power of 400W. To prepare each specimen 60 g of crumb rubber was placed in a 250-ml beaker and exposed to the radiation for 4 minutes. The resulting samples were referred to as microwave activated crumb rubber (M-CR).

Hybrid Treatment with Bio-modifier and Microwave

To enhance the effectiveness of treatment method, crumb rubber was treated with bio-modifier followed by microwave treatment. Crumb rubber particles were immersed in bio-modifier in the ratio of 1:1 for 12 hours, then exposed to microwave irradiation for 4 minutes. The resulting samples referred to as surface activated crumb rubber.

Asphalt binder Modification

Rubberized asphalt binder was produced in the laboratory by incorporating 15% (by the weight of asphalt binder) of rubber samples into PG64-22. The blending of rubber particles into asphalt binder was done using a bench-top high shear mixer at 3000 rpm at 170°C. The crumb rubber was gradually poured into the binder while the shearing was continuously applied for 30 minutes, following the California Department of Transportation specification (Specifications). The shearing speed was maintained constant and the mixing blade was completely submerged into the sample, to prevent whipping of air into the asphalt.

3.4 Testing Methods

3.4.1 Viscosity Measurement

To study the effect of modification on the rheological properties of asphalt binder, the viscosity of each modified asphalt sample was measured using a Brookfield viscometer DVII-Ultra, following the ASTMD4402 specification (ASTM-D4402, 2015). Viscosity was measured by applying continuous shear using a smooth spindle (SC4-27)

for 15 minutes. Measurements were done at four different temperatures (105°C, 120°C, 135°C, 150°C), and shearing speed of 20 rpm.

3.4.2 Dynamic Shear Rheometer (DSR)

A Thermo Scientific HAAKE rheometer from 70°C to 22°C was used to evaluate the elastic and viscous behavior through monitoring the shear stress and shear strain due to application of a specified oscillation rate (10 rad/s), which is typically used to represent the shearing action caused by a traffic speed of 90 km/hr (AASHTO-T315, 2012). The measured data is then used to calculate the complex shear modulus (G*) and phase angle (δ). In addition, the rutting performance of the binder was evaluated using the method of multiple stress creep recovery (MSCR), as outlined in the AASHTO standard (AASHTO-T315, 2012).

3.4.3 Cigar Tube Separation Test

ASTM D7173 – 14 (ASTM-D7173, 2014) was followed to find the separation tendency of rubber particles from the binder. The test also referred to as the Cigar Tube Separation test. To conduct the test, samples were heated to 163°C until they were sufficiently fluid to pour in aluminum tubes, which were then placed vertically in a sample holder rack. Tube tops were sealed to prevent air intrusion. Tubes were then placed inside an oven at 163°C for 48 hours. After 48 hours, the rack was put in a freezer for 4 hours at -18°C. After cooling the tubes were taken out and cut into three equal sections. The middle part was discarded, and bottom and top sections were stored for tests with dynamic shear rheometer at 58°C. The data from the test was used to calculate

complex modulus and phase angle which were further use to obtain the segregation index (SI) according to Equation 3-2 below (Shatanawi et al., 2009).

$$SI = \frac{\left(\frac{G^*}{sin\delta}\right)max - \left(\frac{G^*}{sin\delta}\right)avg}{\left(\frac{G^*}{sin\delta}\right)_{avg}} \quad (3\text{-}2)$$

3.4.5 Attenuated Total Reflectance Fourier Transform Infrared Spectroscopy (ATR-FTIR)

To analyze any change in chemical structure of treated rubber the Thermo Scientific Nicolet iS10 FT-IR Spectrometer was used in absorbance mode; Wavenumbers ranging from 4000cm^{-1} to 400cm^{-1} were covered. The background spectrum was taken after cleaning the diamond prism with methylene chloride.

3.4.6 Inverse Gas Chromatography (IGC)

Inverse gas chromatography was carried out using the IGC-Surface Energy Analyzer, IGC-SEA (Surface Measurement Systems Ltd., Allentown, PA, USA). The samples were loaded in silanized glass columns, with an internal diameter of 4 mm. The samples were held in place by silanized glass wool and the column temperature was kept constant at 30 °C. The dispersive surface energy was determined using four alkane probes (nonane, octane, heptane and hexane) and acid-base energy was determined using two polar probes including dichloromethane was used for Lewis acid and ethyl acetate for Lewis base determination. Each probe was run through the column, with a helium carrier gas, allowing sufficient time for the entire probe to elute through the column. The dispersive component was determined assuming there is no interaction between adsorbate molecules at infinite dilution. After complete elution of solute molecules, retention parameter like net retention time was calculated and using this net retention time another parameter net retention volume and specific retention volume was calculated. Then using

these retention parameters dispersive surface free energy is determined from thermodynamic equations. Similarly, the acid-base component of surface free energy was calculated based on the above-mentioned polar probes. Details of the procedure can be found in these references (Mohammadi-Jam and Waters, 2014; Newell et al., 2001). Prior to the surface energy determination, to remove any impurity and extra bio-modifier from the surface of bio-treated rubber, it was preconditioned for 120 minutes with helium going through the chamber at the rate of 10 scc/m at 0% humidity. Data analysis was done using the IGC-SEA Advanced Analysis Software.

3.4.7 Direct Tension Tester

The direct tension test (DTT) is used to determine the low-temperature performance of asphalt binder. The apparatus manufactured by Interlaken Inc., applies tensile forces to dog-bone-shaped asphalt binder specimens following ASTM D6723 specification (ASTM-D6723, 2012). The binder is heated until it is fluid enough, then it is poured into specific DTT molds, and cooled down to room temperature. Samples are then placed in a freezer for seven minutes before demolding. After demolding, the samples are placed in the DTT methanol bath at -12°C and kept for one hour before running the test. The data collected from the test is used to calculate fracture energy (Equation 3-2). Ductility was also calculated based on the change in length divided by the original length.

$$\text{Fracture Energy} = \frac{\sum Area_{L-D.Curve}}{Area_{C.S.A}} \quad (3\text{-}3)$$

where:

$Area_{L\text{-}D.Curve}$: The area under the load - displacement curve (N.m)

$Area_{C.S.A}$: The cross-section area at fracture (m^2)

3.4.8 Scanning Electron Microscopy (SEM)

To study the effect of treatment methods on the morphology of rubber surface, SEM was conducted. Samples were sputter coated with 3 nm AuPd with a Leica EM ACE200 coating system and imaged with a Zeiss Auriga field emission scanning electron microscope (FESEM) operating at 5 kV accelerating voltage.

3.5 Results and Discussion

3.5.1 Chemical Analysis

Figure 3-1 shows FTIR spectra of activated and non-activated rubber. Chemical analysis of rubber particles showed a significant reduction in intensity of the peak at 710 cm^{-1} and at 870 cm^{-1} which corresponds to C=C and C-H bonds of the main rubber chain in both M-CR and SAR compared to CRM. This can be attributed to breakage of polymeric chains due to the above modifications. In addition, the peak at 1540 cm^{-1} is a peak attributed to the stretching frequency of methyl assisted conjugated double bonds [ν-[CH=CH)n]- where n>6, which is appeared in vulcanized natural rubber one of the constituent of crumb rubber. The disappearance of this peak for M-CR and SAR is an evidence of devulcanization and reducing conjugated double bonds in the rubber (Jana and Das, 2005),(Zhang et al., 2009).

In addition, a new peak was appeared at 1040 cm-1 in treated rubber which can be attributed to the formation of C-N group from an amidyl of bio-modifier reacting with carbon radicals of rubber. Formation of such functional groups on the rubber surface can lead to increased surface polarity. This was further evidenced in increase of acid-base and dispersive surface energy components of rubber measured by Inverse Gas Chromatography (IGC).

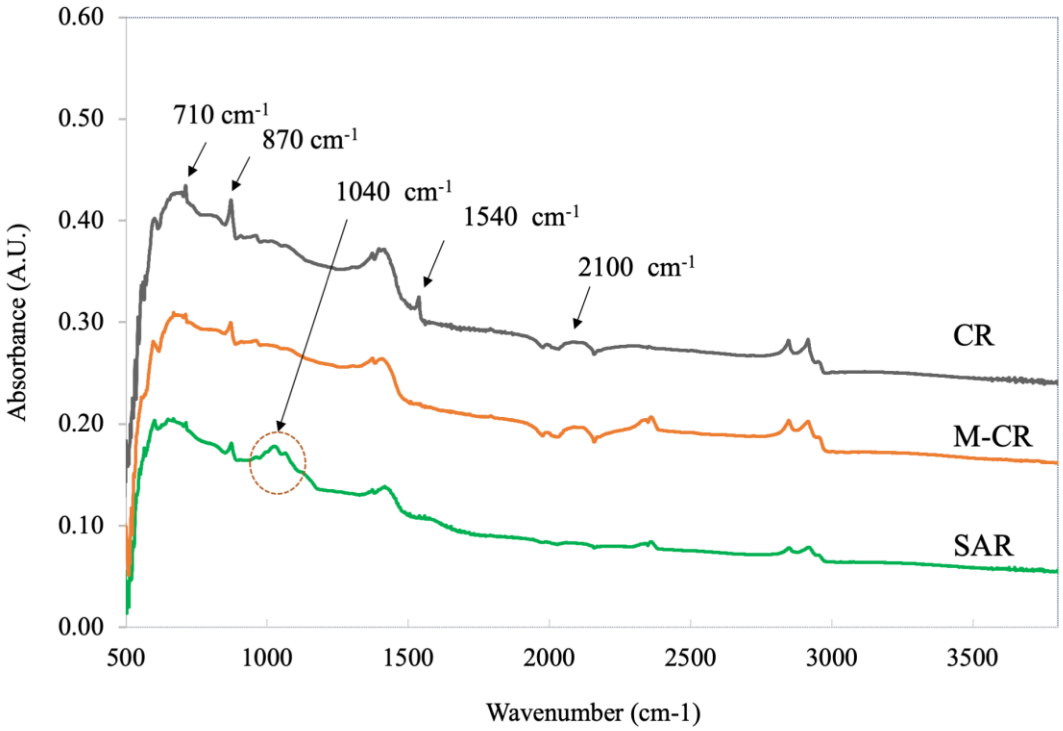

Figure 3-1. FTIR Spectra of Activated and Non-Activated Rubber.

The IGC results showed that surface energy of rubber particles significantly increased due to treatment of rubber; this was even more evident in the case of acid-base component of surface energy which was increased nearly five times after treatment. The observed increase in polarity can be attributed to the grafting of polar bio-molecules such as hexadecanamide onto the surface of the rubber particles due to the treatment. In

addition, in the case of treated rubber, the values of dispersive and acid-base surface energy increased as the surface coverages increased indicating energetically heterogeneous nature of the surface-activated rubber. The trend was nearly constant for non-treated scenarios indicating a more uniform composition on the surface of non-treated rubber.

Table 3-3. Surface Energy (mJ/m^2) of Control and Treated Rubber at 0.07 n/n_m Surface Coverage

	Dispersive	Acid-base	Total Surface Energy
Control rubber	43.3	2.9	46.2
Treated rubber	128.3	14.6	142.9

3.5.2 Thermo-mechanical Analysis

The viscosity results of SAR, M-CRM, CRM and neat binder at 120°C, 135°C, and 150°C can be seen in Figure 3-2. A substantial reduction in viscosity was observed in case of activated rubbers compared to non-activated scenarios in all measured temperatures. The observed reduction in the viscosity of the activated scenarios, which can be attributed to breakage of crosslinks and disulfide bonds leads to improved workability of crumb-rubber-modified asphalt after surface activation. It should be noted that among activated scenarios, SAR showed higher viscosity than the M-CRM binder, which can be attributed to the role of polar groups of bio-molecules grafted onto the rubber surface. Increased surface polarity in SAR can promote formation of a network among rubber particles and particles and asphalt molecules increasing overall viscosity of SAR compared to that of M-CRM. Authors believe that if a dual helical Impeller (DHI)

were used instead of SC-27 spindle the viscosity of crumb rubber modifier would be lower. This is due to the fact that, a vertical dragging of particles within a fluid of lower density by the inner screw is obtained, while the outer screw transports the suspended particles down. By this induced flow, heterogenous fluid system is confirmed and this in turns allows recording more stable viscosity measurements (Presti et al., 2017).

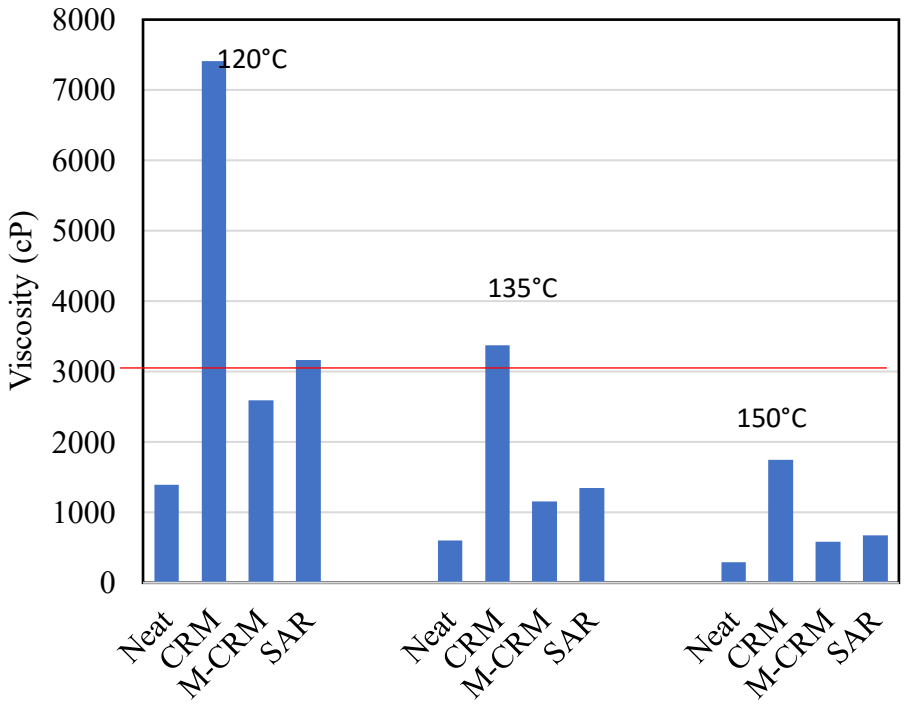

Figure 3-2. Viscosity of Activated and Non-Activated Rubber-Modified Asphalt Binder.

Figure 3-3 shows segregation index for activated and non-activated binder scenarios. As it can be seen the SI value of the activated scenarios are significantly lower than non-activated scenario indicating treatment approach was very effective to improve compatibility of rubber and asphalt matrix. Both modified scenarios (M-CRM and SAR)

have lower SI value, with SAR having 86.33% and M-CRM having 93% lower segregation than the non-activated scenario. The former is in-line with previous studies showing bio-modification was effective to enhance interaction between asphalt and rubber (Bocoum et al., 2014b). However, physisorption of bio-modifier onto the surface of the rubber via Van der Waals forces can be significantly enhanced by micro-wave irradiation giving rise to the bond formation and consuming energy of irradiation to create radicals. Such reallocation of energy of irradiation to bond formation reduced the extent of disintegration of rubber bulk structure in SAR compared to M-CRM and this could be the reason for higher segregation index of SAR binder comparing M-CRM.

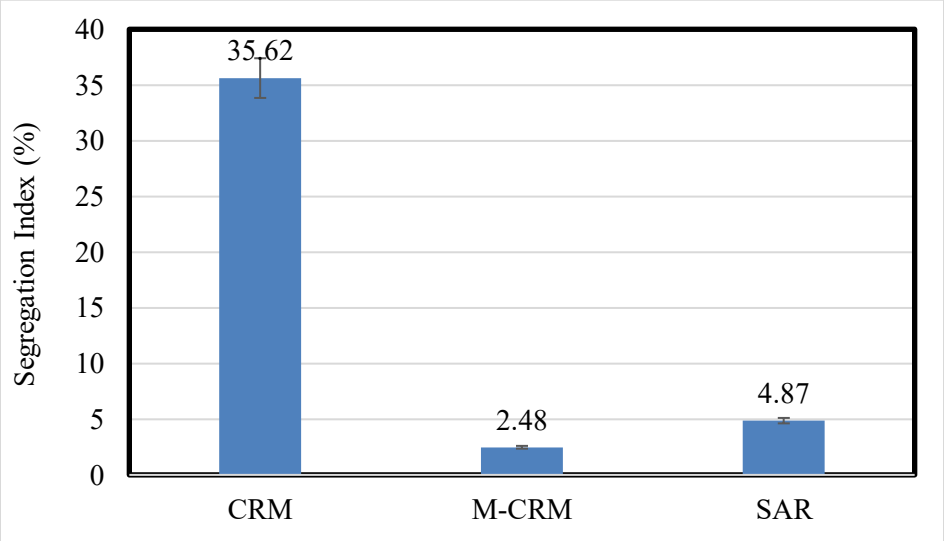

Figure 3-3. Segregation Indices for Activated and Non-Activated Rubber-Modified Asphalt Binder.

Figure 3-4 depicts the complex modulus and phase angle for temperatures ranging from 22 to 70°C for all rubber modified binders. The G* values of CRM and SAR are the same from 22 to 64°C, but beyond that CRM has a higher modulus than SAR. In

temperature range of 22 to 34°C CRM and SAR have the same trend in phase angle value, but above 34°C, phase angle(δ) does not change much as evidenced by a plateau for CRM, while for SAR, the rate of change in δ is higher. Through the measured temperatures of 22 to 70°C, M-CRM shows lower G* and higher phase angle value than SAR and CRM. A high asphalt complex modulus (G*) together with a low phase angle makes the asphalt pavement more resistant to rutting. As a result, SAR and CRM have both higher rutting resistance than M-CRM, while SAR has better workability and storage stability than CRM.

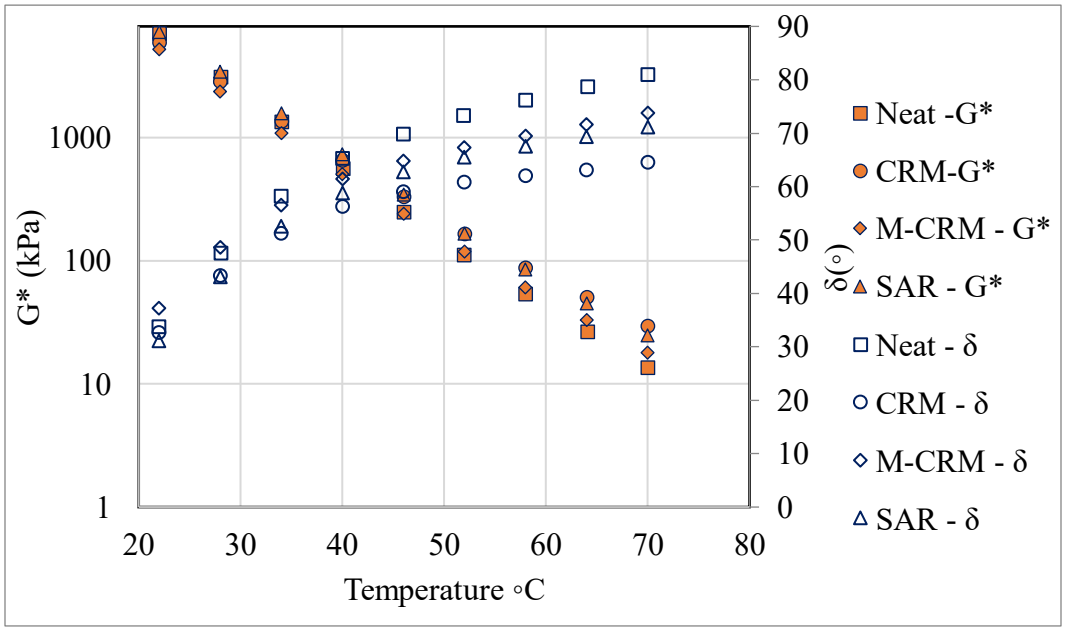

Figure 3-4. Temperature Dependency of G*, Δ for Activated and Non-Activated Rubber-Modified Asphalt Binder.

Figure 3-5 shows percent recovery and the Jnr values measured through MSCR test for activated and non-activated rubber at 3.2 kPa load and 58°C. Among the three

modified asphalt binders, CRM had the highest percent recovery which was expected due to intact structure of the rubber particle. Among the activated scenarios, SAR had a significantly higher percent recovery than M-CRM indicating a more elastic behavior. The latter can be attributed to the presence of bio-molecules, which in turn consumed energy of irradiation to create radicals and leading to formation of new bonds. Such reallocation of energy of irradiation to bond formation reduced the extent of disintegration of rubber bulk structure in SAR compared to M-CRM. The lower Jnr value indicates the resistance to rutting and it was shown between activated rubbers, SAR has lowest value and higher resistance to rutting.

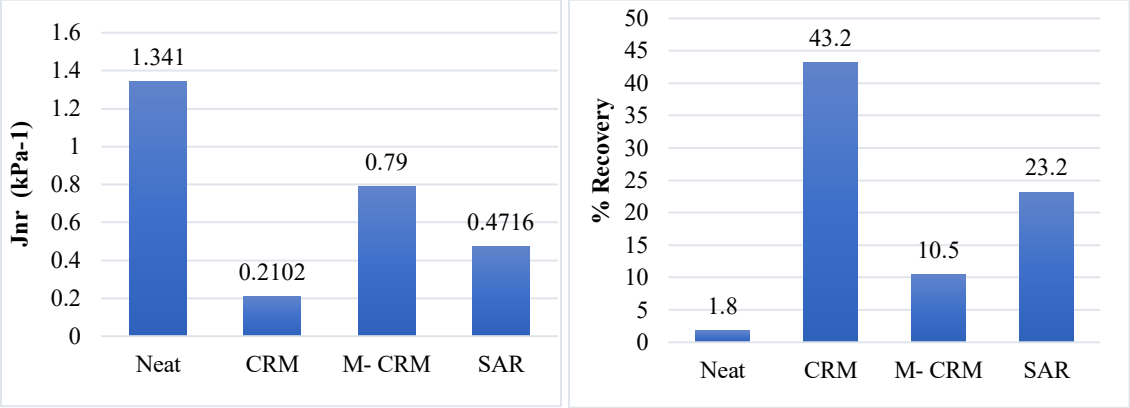

Figure 3-5. MSCR Results for Activated and Non-Activated Rubber Measured at 58°C: (a) Non-Recoverable Creep Compliance (Jnr), and (b) Percent Recovery

To analyze fracture energy and evaluate susceptibility of each specimen to low-temperature cracking, a fracture test was incorporated at low temperature using the direct tension test (DTT). Figure 3-6 shows CRM has a lower fracture energy than both activated scenarios mainly due to reduced strain at failure. The decrease in strain at failure due to the presence of crumb rubber has also been observed in mixture studies as

well (Bennert et al., 2004). In case of activated rubber scenarios, fracture energy of SAR found to be 34.68% more than that of M-CRM. This effect can be the result of interaction between the molecules of bio-modifier such as hexadecanamide, and n-butyl octadecanamide while one side is involved with carbon centered radicals of rubber, long tails of these molecules, can interact with asphalt molecules mainly through attractive-dispersion forces between carbon chains of fragments. Formation of such secondary network can enhance performance of asphalt containing surface activated rubber as evidenced in fracture energy of SAR being 34.6% higher than M-CRM.

Figure 3-7 shows further analysis of the fracture energy in terms of peak loads and ductility. The SAR peak load and strain at failure are 22% and 9.59% more than M-CRM. The latter improvements are attributed to the formation of secondary network in SAR mainly due to successful grafting of bio-molecules to rubber surface and interaction between activated rubber particles and binder structure.

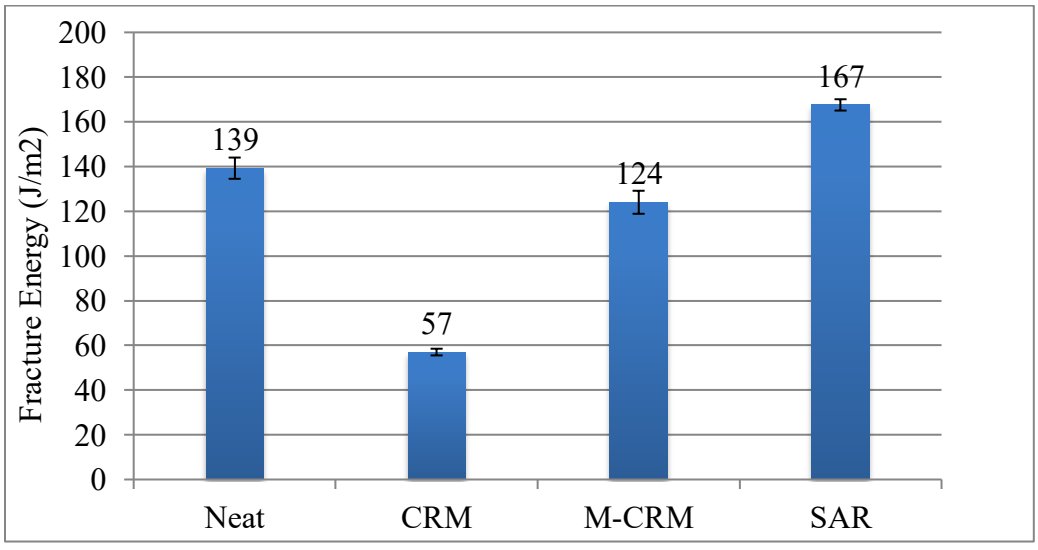

Figure 3-6. Fracture Energy Results for Samples at -12°C.

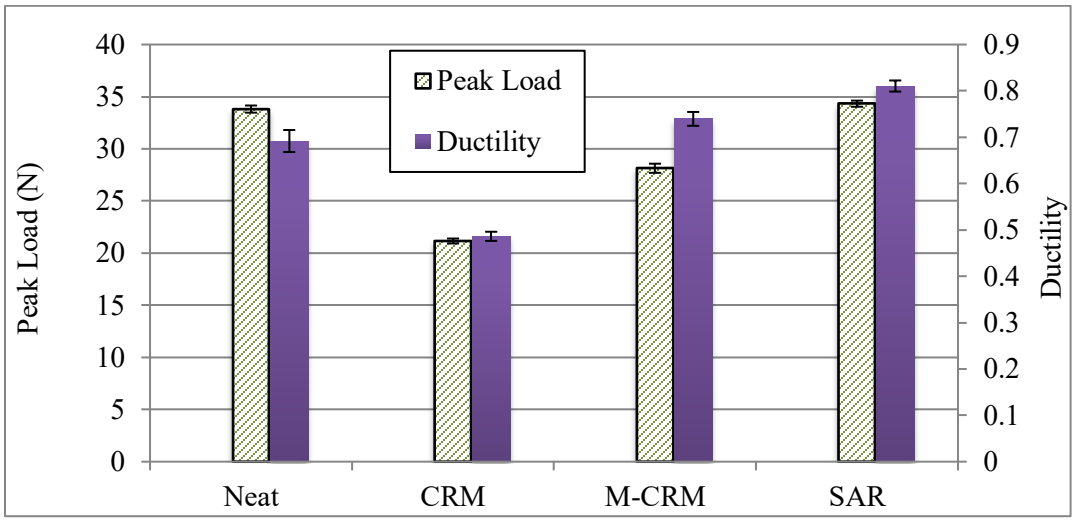

Figure 3-7. Peak Load and Ductility Results for Samples at -12°C.

Morphological Studies

Figure 3-8 shows SEM imaging of activated and non-activated rubber. SEM adequately differentiated among samples before and after radiation as well as bio-modification. Based on these images, the surfaces roughness of microwave untreated rubber (CR) was significantly reduced after microwave treatment which can be due to degradation of rubber. This in turn led to smoothing out surface features, however the sample treated with bio-modifier showed presence of new characteristic features after microwave irradiation, which was attributed to grafting bio-molecules onto the rubber surface. Approximate calculation of attached bio-molecules area to rubber area from figure 3-8 shows that 13.9% attachment of bio-oil to rubber after treatment and wash, instead of 50%-50% mixing at the time of preconditioning. The unattached bio-oils were washed away due to acetone wash and drying. From that estimation each 1g has 0.12g

bio-oil attached. Hence, each 15g rubber has 1.83g rubber attached, final rubber content was found to be approximately 13.17%.

As such while SEM images cannot speak to the bulk properties of any of rubber modified asphalt scenarios, the surface characteristics could be used to better explain observed enhancement in SAR performance compared to M-CRM, which both went through irradiation. The observed differences in surface features of M-CRM and SAR were reflected in reduced segregation index and enhanced fracture energy of SAR compared with M-CRM. SAR showed 86% reduction in segregation index compared to the other CRM scenarios. Such enhancement was also reflected in significant improvement in workability of SAR modified binder compared to the other CRM scenarios. Mechanical tests showed a high fracture energy (167 J/m^2) for SAR modified asphalt, which was approximately three times higher than that of convectional CRM asphalt (57 J/m^2).

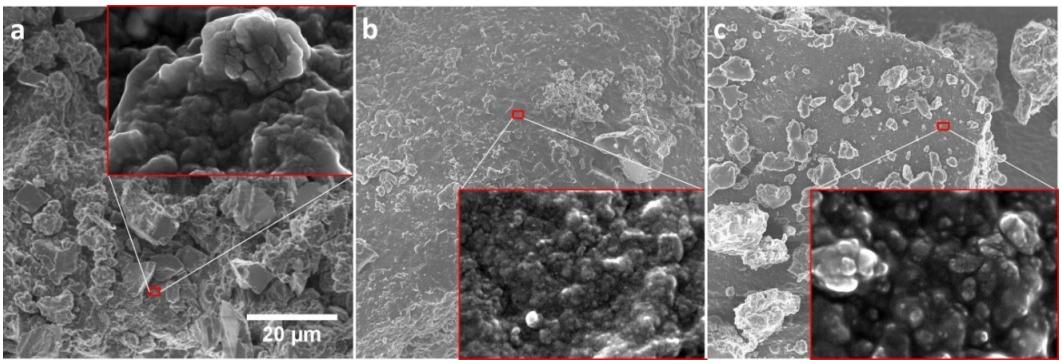

Figure 3-8. SEM Images of (a) CR, (b) M-CR, and (c) SAR

3.5.3 Density Functional Theory Analysis

3.5.3.1 DFT-Based Molecular Modeling

Microwave treatment has been introduced to devulcanize rubber though a uniform heat leading to partial devocalization of rubber by cleavage of disulfide bonds. Cleaving the cross-linked networks of sulfur leads to the activation of irradiated rubber. This activation is associated with the formation of a variety of free radicals including sulfur and carbon that can be the origin for the subsequent reactions of rubber with organic materials of asphalt or bio-modifiers added to asphalt. From computation point of view formation of radicals by irradiation is of crucial importance as the interaction of amide functional groups of modifiers with broken chains of rubber polymer containing carbon radicals and also monovalent/divalent sulfur radicals for the possible mechanism for interaction between two components needs to be investigated. The bio-modifier used in this study is an amide-rich product synthesized from molecular species extracted from swine manure that includes traces of oxime (–C=N–O–), amine (R–N–R'R") and amide (–CO–NRR′) functional groups, such as tetradecanal o-methyloxime, heptadecanenitrile, benzo[c]cinnolin-4-amine, N,N-dimethyl, hexadecanamide, and n-butyl octadecanamide.(Fini et al., 2011b) Hexadecanamide, and N-butyl octadecanamide are examples of the amide-type components identified in our bio-modifier. (Fini et al., 2011b)

It is documented that lighter components penetrate more readily into the internal matrix of rubber. (Gaweł et al., 2011), (Gawel et al., 2006) Hexadecanamide could be among the light nitrogen-carrier compounds which can be easily trapped into the matrix

of polymer. This is further supported by the appearance of the new FTIR peaks which are attributed to the C–N bonds.(Hosseinnezhad et al., 2018) Accordingly, DFT-based studies in this section is performed on truncated models of hexadecanamide as the appropriate representatives for nitrogen-carrying compounds available in the bio-modifier used in this study.

In addition to the representative components of bio-modifier, molecular models of devulcanized rubber are needed to fully model bio-modified rubber. Vulcanized rubber could be imagined as the network of polymer filaments which are strongly interconnected by covalent crosslinks of sulfur. (Klüppel et al., 2001),(Treloar, 1944) In a reverse process, devulcanization, as a reclaiming method for elastomers, is a process through which the three-dimensional network of elastomer is broken to restore the flexibility of polymer chains in the elastomer. Electromagnetic irradiation is among the efficient techniques for devulcanization and cleavage of the S–S and S–C bonds.

Figure 3-9-a presents the 3D and 2D molecular structure models for a cross-linked styrene-butadiene rubber (SBR) model before any treatment. **Figure 3-9-b** shows aforementioned structure after microwave irradiation and penetration of amide molecule into the space created after dross-link breaking. As shown in **Figure 3-9-b**, the backbone of hexadecanamide molecules has been reduced to ten carbon atoms, decanamide, $C_{10}H_{21}NO$, to reduce the computational cost. Each SBR chain in this figure contains three blocks of c-butadiene and one block of styrene.

Two structures in **Figures 3-9** have been fully optimized at the PBEPBE/6-31G(d) level using Gaussian 09 package. The unrestricted open-shell ground state (multiplicity 3) was considered for the structure in **Figure 3-9-b** to simulate one radical on each sulfur atom.

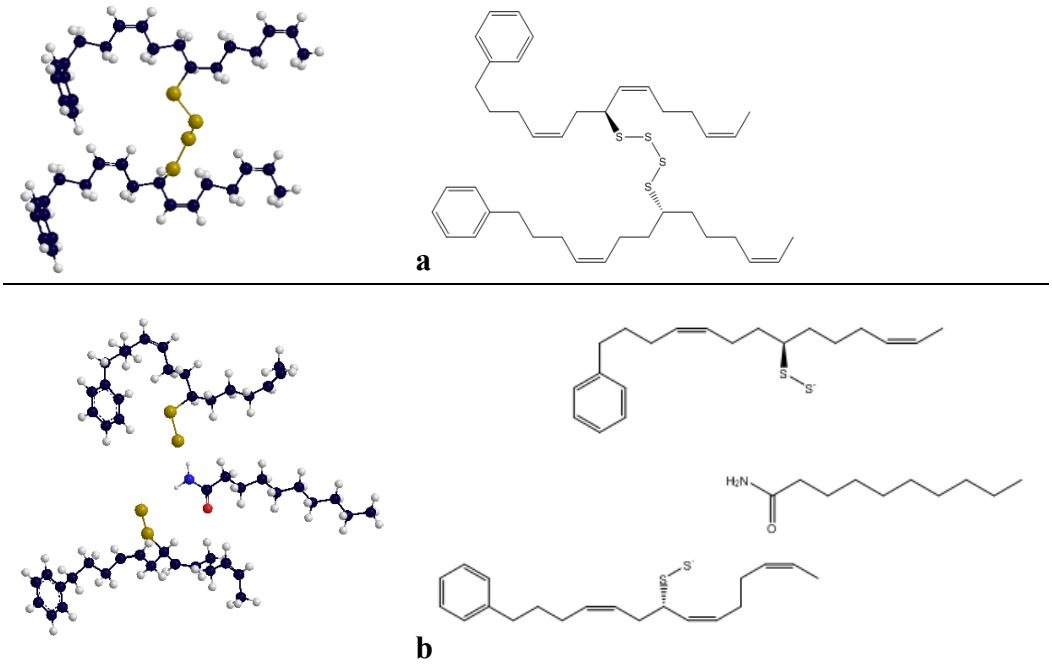

Figure 3-9. (a) Vulcanized Styrene-Butadiene-Rubber (SBR) Model Molecule, and (b) Penetration of Amide Molecule into The Polymeric Chains of Devulcanized SBR

Cleavage of polysulfide bonds and degradation of the main SBR backbone chain leads to formation of free radicals of carbon and sulfide. From the other side, if the rubber is pre-treated with the bio-modifier prior to microwave treatment, light molecules of bio-modifier are not only adsorbed onto the rubber surface via physisorption but also defuse into the void spaces of the rubber clusters; microwave irradiation leads to creation of

radicals such as amidyl. In the following sections, the nature of interactions between representative molecules of the bio-modifier (acetamide and decanamide) and small chains of disintegrated SBR carrying sulfur and carbon radicals is discussed.

Amidyl radical

Nitrogen-centered radicals, such as aminyl, amidyl, and iminyl are highly reactive intermediates that offer great opportunity for the assembly of C-N bonds and development of nitrogen carrying compounds. In the case of amidyl, conjugation of nitrogen lone pair with acyl substituents in the parent amide molecule provides the stabilization for the closed-shell structure, while in open-shell structure, delocalization of the unpaired electron into the π-system of carbonyl group disrupts the resonance interaction between lone pair of nitrogen and carbonyl group (Muchall et al., 1999). In **Figure 3-10**, three additional isomers are shown for a typical amidyl radical (formamidyl) reported by Hioe et al. who showed that all three isomers are energetically (based on radical stabilization energy) more stable than amidyl radical by -12.6, -81.0, and -19.9 kJ mol^{-1}, respectively. However, the calculated energy barriers ($\Delta G_{298}^{\neq}$) for their isomerization processes are notably high, 140.1, 134.8 and 133.7 kJ mol^{-1}, respectively, indicating that amidyl radical is kinetically quite stable and could be the only species existing under the experimental condition employed.(Hioe et al., 2015)

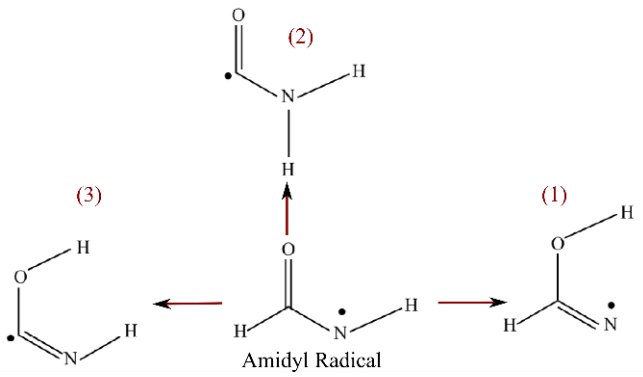

Figure 3-10. Three Isomers of Formamidyl Radical, Taken from Ref. (Hioe et al., 2015)

Considering that spectra indicate formation of new compounds containing N-C bonds and the fact that our bio-modifier has significant amount of amide-rich compounds, we hypothesize that amidyl radicals are formed during irradiation leading to covalent interactions with radicals of rubber. To examine the latter reactions, we first study plausible mechanisms for formation of the highly reactive amidyl via a) amide-H abstraction by the sulfur radicals, and b) microwave irradiation.

Amide-H abstraction by Monovalent Sulfur Radicals

Radicals of sulfur are of particular importance in regular function of rubber vulcanization or devulcanization, because they are assumed to be responsible for the formation of many intermediates.

One of the assumptions in proceeding of microwave irradiation of bio-modified rubber, in the present study, is the H abstraction of amide molecule by monovalent sulfur radicals, as illustrated in **Figure 3-11**. Amides are known for their participation in H-bonding in many solvents. In addition, it has been documented that heating a mixture of

H-donor species and disulfur results in a rapid formation of mercaptan (thiol), with a general formula of R-SH, as shown in Equations 3-4 and 3-5. (Walling and Rabinowitz, 1959),(Schaafsma et al., 1960),(Schmidt, 1964a)

$$R\text{-}S\text{-}S\text{-}R \xrightarrow{h\nu} 2\ R\text{-}\dot{S} \quad (3\text{-}4)$$

$$2\ R\text{-}\dot{S} + 2\ H\text{-donor} \rightarrow 2\ R\text{-}SH + Donor\dot{} \quad (3\text{-}5)$$

Accordingly, we tried to examine dehydrogenation of acetamide (as a simplest amide) and decanamide molecule by monovalent sulfur radicals and a free disulfur. **Figure 3-11** gives an overview of the possible radical fragments assumed to interact with amide molecules; monovalent radicals of –CHS•– , and –CHSS•–, and free disulfur S=S. DFT-based calculations, at the PBEPBE/6-31G(d) level, show that this reaction (H-transfer from amide to sulfur radicals) is thermodynamically unfavorable as the system is not in the lowest energy state and has the potential to reach another state. Thermodynamic stabilization energy, defined as the energy difference between the initial and final states is reported in **Equation 3-6** for the reaction of decanamide with monovalent sulfur radical.

$$R–CO–NH_2 + C_2H_5–CHS^{\bullet}–C_2H_5 \rightarrow R–CO–NH^{\bullet} + C_2H_5–CH_2S–C_2H_5 \quad (3\text{-}6)$$

for $R=C_9H_{19}$ $\Delta G=+25.01$ kcal/mol

The same trend was observed for interaction of acetamide molecule and monovalent radical of disulfur ($C_2H_5–CHS–S^{\bullet}–C_2H_5$) and also for free disulfur (S=S). To assess affinity of H atom transfer from amide molecules to sulfur radicals to form a highly reactive amidyl group (–CON•H), relaxed potential energy surface (Lopes and Constantinides) technique was performed along the –H…S•– bond. In **Figure 3-12**,

Potential Energy Surface (PES) is plotted for the bond formation between H and S˙ in a reaction coordinate through which the N–H bond is cleaved and H–S bond is formed. As shown in this figure, PES exhibits a pronounced ascending trend (decrease in absolute values in energy) without a minimum energy, indicating the system is not stabilized in this path.

Reluctance of H atom transfer clearly indicates that N–H bond of amide group is quite resistance to the attack by the sulfur radicals. Absence of any observation in support of the H atom transfer from amide molecules to sulfur radicals is indicative of the fact that amidyl groups are not readily generated within this reaction.

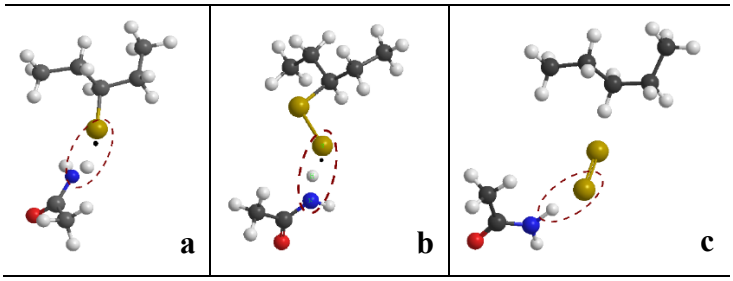

Figure 3-11. Three Possible Pathways for (a and b) Amide-H Abstraction by Sulfur Radicals, and (c) a Free Sulfur

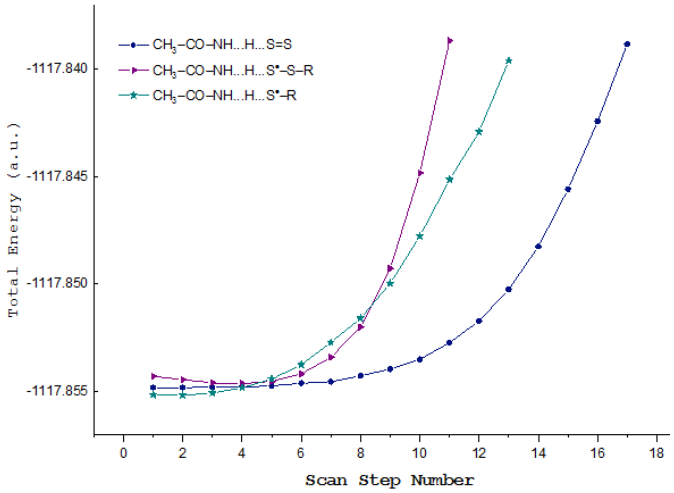

a) H-abstraction from acetamide

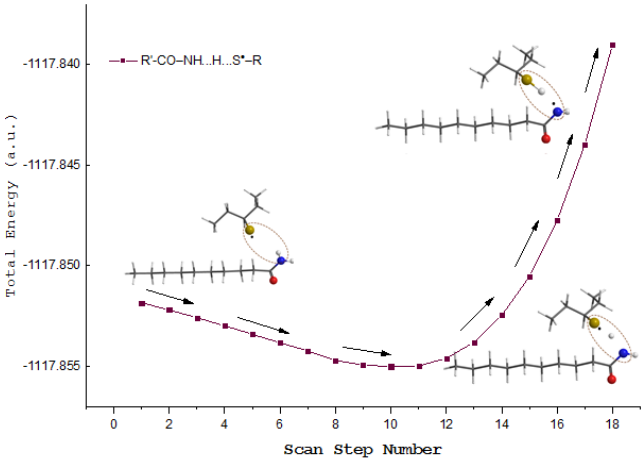

b) H-abstraction from decanamide

Figure 3-12. Relaxed Potential Energy Surface Scan for H-Abstraction from (a) Acetamide And (b) Decanamide by Monovalent Sulfur Radicals and Free Disulfur (The Scan Was Performed Along The –H…S– Bond from 3.0 Å to 1.3 Å by The Step Size of -0.1 Å).

Amidyl radical formation through microwave irradiation

Although amidyl formation (CO–N•H) via the H… S• coordination pathway found to be unlikely as evidenced by potential energy surface calculation, microwave irradiation can highly promote formation of amidyl radicals from amide molecules of bio-modifier. The higher temperatures associated with microwave irradiation are expected to increase

the rates of propagation steps in thermally initiated radical processes. Microwave heating significantly increases the rate of thermal dissociation of many initiators and thus increases the rate of initiation step.(McBurney et al., 2012) Accordingly, microwave-assisted radical formation has been extensively employed as a precursor for the production of N-centered radicals.(McBurney et al., 2012) In addition, elevated temperature (160-240 °C) under microwave irradiation has been shown to be a convenient procedures for generating iminyl radicals.(Cai et al., 2015),(Markey et al., 2013),(Portela-Cubillo et al., 2009),(Walton, 2014) The good record of the microwave heating in production of N-centered radicals and the fact that amidyl radical is kinetically quite stable justify the presence of amidyl radicals in the experimental conditions used for rubber treatment.

Interaction of amidyl radical with sulfur-centered radicals

In this section, we separately studied the interaction between amidyl radicals of both acetamide and decanamide with monovalent radical of sulfur as follows.

Acetamidyl and sulfur radicals

Upon formation of amidyl radicals, one possible reaction pathway for these highly reactive radicals is their interactions with sulfur radicals. Considering two free spins in the system (one for each amidyl and sulfur), two spin states including unrestricted open-shell triplet and unrestricted open-shell singlet were defined for approaching two radicals. The spin unrestricted SCF calculations at the PBEPBE/6-31G(d) level were carried out at each point along the reaction coordinate when amidyl radical of acetamide and decanamide are approaching the monovalent sulfur radicals. In this reaction path, all the

geometrical parameters are optimized in each point without imposing any constraint. **Figures 3-13-a and b** show the energy evolution for approaching the amidyl radical of acetamide to sulfur radical in two different spin sets leading to two distinguished products.

In the case of acetamidyl radical, shown in **Figure 3-13-a**, the energy evolution of triplet-state curve shows that the initial approach is associated with a continuous stabilization and decrease in energy, covering the coordinate path from about 3.0 Å to 2.41 Å (circles 1 to 2, in **Figure 3-13-a**). However, decreasing trend of energy does not hold beyond 2.41 Å. Beyond the –HN˙…˙S– distance of 2.41 Å (when the triplet energy stare is minimum), the curve ascends in energy up to 1.91 Å in which the N–S bond is being formed (circle 3, in **Figure 3-13-a**). This ascending trend of energy indicates that this path would not be energetically favorable and that a change of spin multiplicity is required to establish an energetically favorable reaction. The limit of spin-forbidden reaction, in which the reactants are in triplet state while the product should be in a singlet ground state, causes that the system tries to release itself from the extreme constraint available in this path. Accordingly, the activated complex in point 1.9 Å, circle 3 in **Figure 3-13-a**, surpasses the activation energy barrier, ΔE=12.62 kcal/mol, via cleavage of the –C–N– bond and formation of one carbon-centered radical and a new monovalent radical of sulfur.

Contrary to the energy evolution in triplet state curve, in which the reaction encounters the obstacle of "spin block" and activation barrier, no spin-forbidden transition is observed on the reaction path when the reactants and products are in their

singlet states. In this reaction path, as shown in **Figure 3-13-b**, the singlet curve descends in energy easily, indicating that this path will be energetically favorable. Accordingly, in the unrestricted singlet ground state, the reacting radicals easily form sulfur-nitrogen complexes, as shown in **Figure 3-13-b**. Comparing the potential energy surfaces for unrestricted singlet and triplet states shows that all the components are better stabilized in the singlet-state reaction path (**Figure 3-13)**. **Figure 3-14** schematically shows two mentioned products formed through interaction of the acetamidyl and sulfur radicals in two different spin states.

Decanamidyl and sulfur radicals

In addition to acetamide, the function of amidyl radical of decanamide towards monovalent radical of sulfur was investigated. The trend of energy evolution for decanamide, in triplet state curve was found to be quite similar to that of acetamide up to activation barrier, as indicated in **Figure 3-15**. While in acetamide curve, the unstable complex formed at top of the activation barrier releases its energy through C–S bond dissociation and formation of new radicals, in decanamide curve, the unstable complex does not follow the downward trend of energy. Longer chain of decanamide compared to acetamide prevents its facile motion to overcome the activation barrier (obstacle of spin block), and formation of new radicals, as what observed for acetamide in **Figure 3-13-a**. However, no barrier was observed for unrestricted singlet-state description of decanamidyl and sulfur radicals. The singlet curve for decanamide descends in energy

easily similar to that of acetamide (**Figure 3-13-b)**, indicating that this reaction path will be energetically favorable for two radicals.

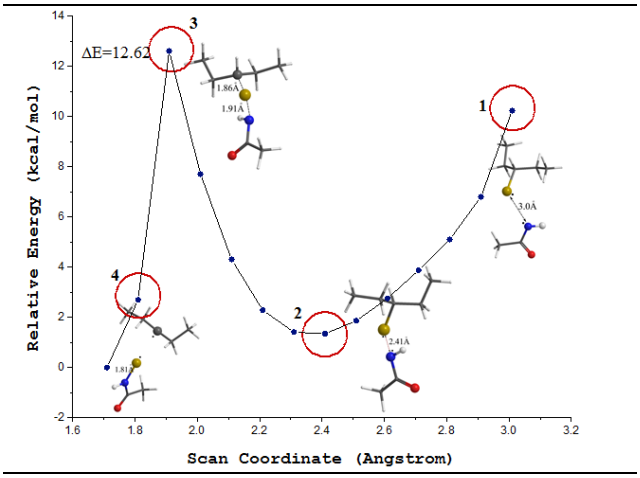

a) Energy evolution for open-shell triplet state

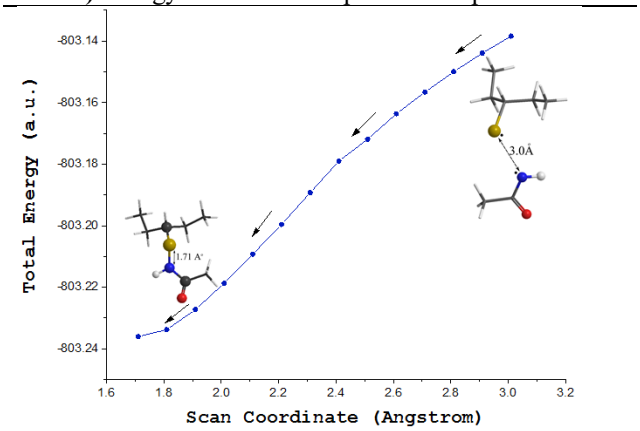

b) Energy evolution for open-shell singlet state

Figure 3-13. Unrestricted Description of Approaching Acetamidyl (CH_3–CO–N$^{\bullet}$H) to A Broken Chain of Rubber Containing Monovalent Sulfur Radical (R–S$^{\bullet}$–R); a) Open-Shell Triplet State Reaction Pathway, and b) Open-Shell Singlet State Reaction Pathway

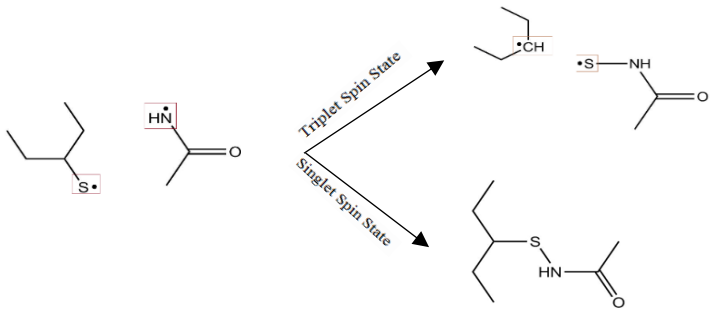

Figure 3-14. Two Distinct Products Resulting from Approaching Acetamidyl Radical to A Monovalent Sulfur Radical Regarding Two Different Spin-Sets (Unrestricted Open-Shell Triplet and Singlet States)

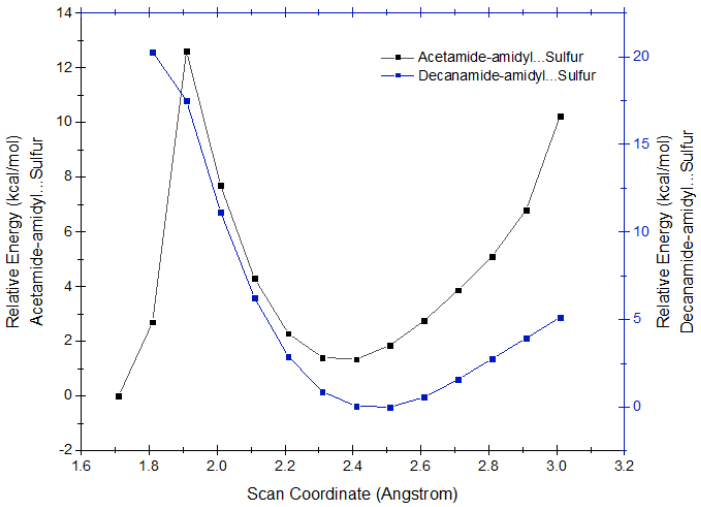

Figure 3-15. The Energy Evolution Diagrams for Interacting Radicals of Sulfur and Amidyl Originated from Decanamide and Acetamide, in Their Triplet States.

Interaction of amidyl radical with carbon-centered radical

Based on the FTIR spectra showing a reduced intensity in the peaks at 710 cm^{-1} and at 870 cm^{-1} pertaining to the C=C and C-H bonds, followed by an increase in C-N bond, we examine the plausible interactions between amidyl radicals and carbon-centered radicals of the polymeric chains of rubber.

Two spin states were defined for the approach of amidyl radical to carbon-centered radical, –N•…•C–. Similar to the –N•…•S– reaction pathway, shown in **Figures 3-13-b**, the singlet curve descends in energy easily, indicating that this path is energetically favorable. In triplet-spin state case, as shown in **Figure 3-16**, the energy of the triplet curve rises at the beginning of the coordination path, and starts descending after overcoming the energy barrier, eventually leading to an energy minimum at –N–C– distance of 1.71 Å. On the contrary to the –N•…•S– reaction pathway, no spin-forbidden transition is observed on the –N•…•C– reaction path; the energy curve descends after overcoming the energy barrier and a bound triplet state is achieved. The performance of the system on the triplet spin surface reinforces this idea that –N•…•C– reaction pathway is stabilized easier than that of –N•…•S– reaction pathway.

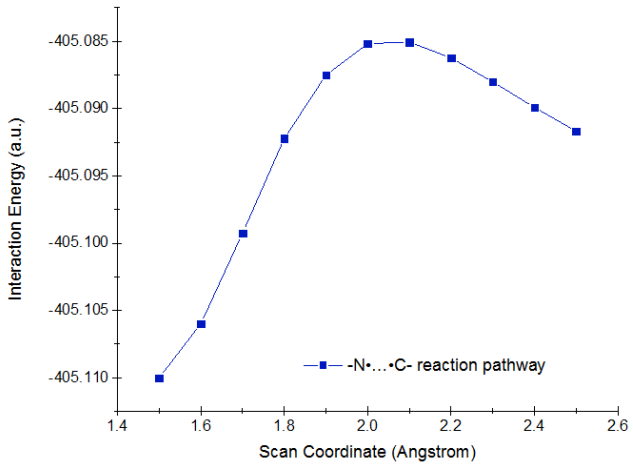

Figure 3-16. Unrestricted Description (Open-Shell Triplet State) of Approaching Acetamidyl to A Carbon-Centered Radical of an Irradiated Rubber Chain

Further support is provided by the comparison of interaction energies between the –N…C– and –N…S– reaction coordinates in singlet-spin state, which is indicative of the lower energies and more stabilization of –N…C– reaction pathway compared to that of –

N…S–, implying that the amidyl radicals bound to carbon radicals much easier than those to sulfur radicals. Comparison the values of interaction energy (ΔE_{int}) between two components in –N…C– reaction path (including $CH_3CO\text{-}HN^{\bullet}$ and R-C$^{\bullet}$H-R components) and those in –N…S– reaction path (including $CH_3CO\text{-}HN^{\bullet}$ and $^{\bullet}$S-R' components) are shown in **Figure 3-17**. In this figure, amidyl radical is derived from acetamide, and the reactants (nitrogen and sulfur radicals) and the corresponding product are at their singlet spin states. Similar trend was observed for decanamidyl; supporting that formation of N-C compounds is more probable than that of N-S compounds. This conclusion is also in line with the FTIR results showing formation of N-C bonds for the treated rubber. In parallel, the results of the optimization process show that the tendency of nitrogen-centered radicals to carbon-centered radicals is so high that their corresponding N-C compound is readily formed at one-step; without entering the step-by-step optimization process through relaxed potential energy surface (EPS) scan.

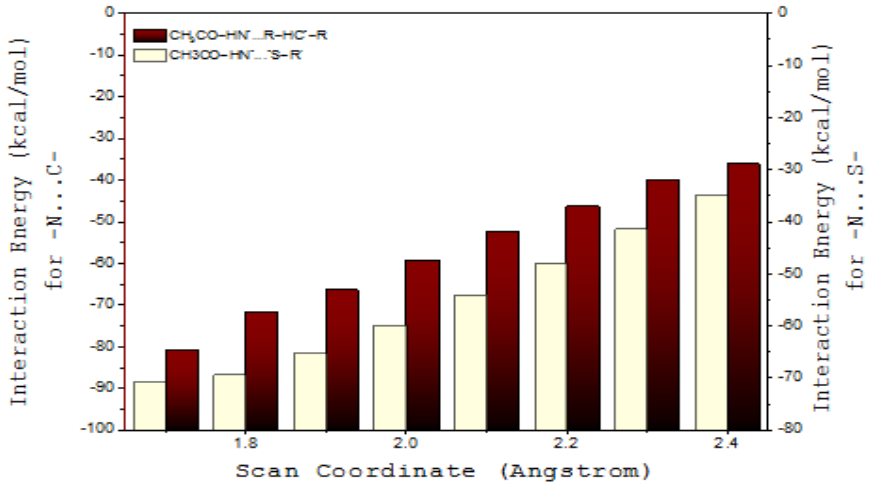

Figure 3-17. Comparison of The Interaction Energies for Two Reaction Pathways, –N…C– and –N…S–, for Singlet Spin States.

Another interesting conclusion drawn from the step-by-step optimization process of the reaction pathway (relaxed PES scan with geometry optimization at each point) is that if the nitrogen-centered radical cannot be easily tracked by carbon radical, possibility of formation of C=C bond within the broken chain of rubber is comparable to that of the C-N bond formation. In fact, in relaxed PES scan, the system is constrained to be fully optimized in each coordination step before it enters the next step. This constraint restricts the free motion of the system which in turn can allow carbon-centered radical shares its unpaired electron with neighboring carbon and balances its extra charge through formation of double bond. This scenario is prevailed for the decanamidyl radical because of its larger size and slower motion. The results show that before decanamidyl radical can reach the carbon-centered radical and form C-N compound (**Figure 3-18-a**) neighboring carbon provides another unpaired electron leading to formation of C=C bond (**Figure 3-18-b)**.

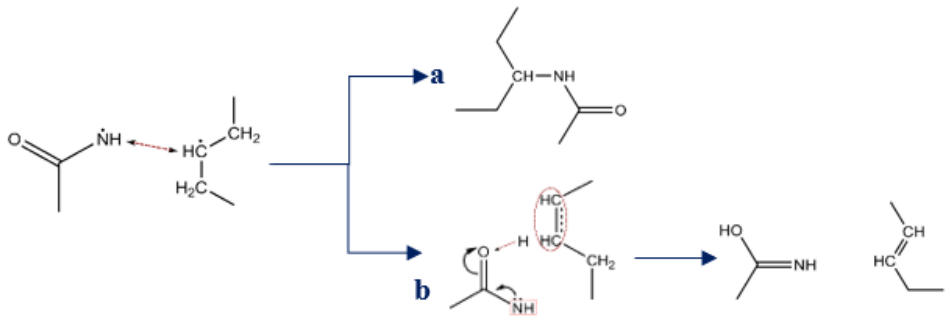

Figure 3-18. Two Plausible Products for Interaction of Nitrogen- and Carbon-Centered radicals (CH_3-CO-HN$^{\bullet}$ and R-C$^{\bullet}$H-R) at Their Unrestricted Open-Shell Singlet State

3.6 Summary and Conclusions

This study investigates efficacy of introducing sustainable surface-activated rubber particles into asphalt matrix to alleviate issues associated with rubber segregation and workability. The overall goal of the paper is to introduce a treatment method where partial devulcanization via irradiation is complemented by chemical grafting via bio-modification. The latter is specially found to be effective to alter surface polarity of rubber particles promoting formation of secondary network. To conduct the experiments, crumb rubber particles were surface activated via a hybrid processing involving microwave irradiation and bio-modification to produce surface activated rubber, which was then introduced to the asphalt binder. Efficacy of SAR to address rubber segregation and workability issues were investigated via a combined theoretical and experimental approach using Density Functional Theory and thermo-mechanical analysis. Characteristics of SAR was further compared with non-activated rubber scenario and a scenario where solely microwave irradiation was applied.

FTIR analysis indicated the breakage of the polymer chains of rubber due to the irradiation as well as subsequent crosslinking due to bio-modification. The latter was evidenced in appearance of a new peak at 1040 cm^{-1} of the FTIR spectra for SAR indicating formation of C-N group from an amine resulting from the interaction of bio-modifier and crumb rubber. Furthermore, DFT modeling indicate possible mechanism for breakage of N-H bond in bio-molecules followed by formation of C-N bond. Viscosity values showed a significant reduction of 59.95% from the viscosity value of CRM indicating an improvement in workability of asphalt containing SAR. In addition, the

segregation index of SAR showed to be 86.33% lower than CRM. The reduction of segregation was attributed to enhanced interaction between rubber and asphalt matrix mainly due to chemical grafting via bio-modification, which promotes enhanced interaction within asphalt-rubber matrix preventing segregation. Furthermore, effect of the network formation is reflected in asphalt containing SAR having 121 % higher percent recovery than M-CRM.

In addition, fracture energy of asphalt containing SAR (167 J/m^2) was nearly three times higher than that of non-activated rubber (57 J/m^2). Further analysis of the fracture energy in terms of peak loads and ductility showed M-CRM and SAR having 33% and 62.62% higher peak load than CRM. The strain at failure for M-CRM and SAR were found to be 52.12% and 66.71% higher than CRM.

The DFT results show that the reaction pathway of an amidyl radical (RCO-N•H) with a carbon-centered radical is energetically more favorable and stable than the pathway with a sulfur-centered radical. The increased acid-base component in the treated-rubber scenario indicates successful grafting of highly polar molecules of bio-modifier (such as hexadecanamide) onto the surface of rubber.

Based on the results of this study, the hybrid processing involving microwave irradiation and bio-modification to produce a sustainable surface activated rubber can alleviate both segregation and workability issues associated with the use of crumb rubber in asphalt while improving its thermo-mechanical properties.

3.7 Reference

AASHTO-T315, 2012. Standard method of test for determining the rheological properties of asphalt binder using a dynamic shear rheometer (DSR).

ASTM-D4402, 2015. Standard Test Method for Viscosity Determination of Asphalt at Elevated Temperatures Using a Rotational Viscometer. West Conshohocken, PA.

ASTM-D6723, 2012. Standard Test Method for Determining the Fracture Properties of Asphalt Binder in Direct Tension (DT). ASTM International.

ASTM-D7173, 2014. Standard Practice for Determining the Separation Tendency of Polymer from Polymer Modified Asphalt. ASTM.

Bennert, T., Maher, A., Smith, J., 2004. Evaluation of crumb rubber in hot mix asphalt. Rutgers University, Center for Advanced Infrastructure & Transportation, and Rutgers Asphalt/Pavement Laboratory.

Berry, J., 2017. Molecular Dynamics Simulations on Polymer-Modified Model Asphalts. Journal of Creative Inquiry 1(1).

Bocoum, A., Hosseinnezhad, S., Fini, E.H., 2014b. Investigating effect of amine based additives on asphalt rubber rheological properties. Asphalt Pavements 86, 921-931.

Cai, Y., Jalan, A., Kubosumi, A.R., Castle, S.L., 2015. Microwave-promoted tin-free iminyl radical cyclization with TEMPO trapping: A practical synthesis of 2-acylpyrroles. Organic letters 17(3), 488-491.

CalTrans, 2003. Asphalt Rubber Usage Guide. Division of Engineering Services, Sacramento, CA, 95819-94612.

Cao, X.-W., Luo, J., Cao, Y., Yin, X.-C., He, G.-J., Peng, X.-F., Xu, B.-P., 2014. Structure and properties of deeply oxidized waster rubber crumb through long time ozonization. Polymer degradation and stability 109, 1-6.

Colom, X., Marín-Genescà, M., Mujal, R., Formela, K., Cañavate, J., 2018. Structural and physico-mechanical properties of natural rubber/GTR composites devulcanized by microwaves: Influence of GTR source and irradiation time. J. Compos. Mater., 0021998318761554.

de Sousa, F.D., Scuracchio, C.H., Hu, G.-H., Hoppe, S., 2017. Devulcanization of waste tire rubber by microwaves. Polymer Degradation and Stability 138, 169-181.

Fini, E.H., Kalberer, E.W., Shahbazi, A., Basti, M., You, Z., Ozer, H., Aurangzeb, Q., 2011b. Chemical characterization of biobinder from swine manure: Sustainable modifier for asphalt binder. Journal of Materials in Civil Engineering 23(11), 1506-1513.

Gaweł, I., Piłat, J., Radziszewski, P., Kowalski, K., Król, J., 2011. Rubber modified bitumen, Polymer modified bitumen. Elsevier, pp. 72-97.

Gawel, I., Stepkowski, R., Czechowski, F., 2006. Molecular interactions between rubber and asphalt. Industrial & engineering chemistry research 45(9), 3044-3049.

Gehrke, S., Alznauer, H.T., Karimi-Varzaneh, H.A., Becker, J.A., 2017. Ab initio simulations of bond breaking in sulfur crosslinked isoprene oligomer units. The Journal of chemical physics 147(21), 214703.

Hanson, D.E., 2009. Numerical simulations of rubber networks at moderate to high tensile strains using a purely enthalpic force extension curve for individual chains. The Journal of chemical physics 131(22), 224904.

Hanson, D.E., 2011. The molecular kink paradigm for rubber elasticity: Numerical simulations of explicit polyisoprene networks at low to moderate tensile strains. The Journal of chemical physics 135(5), 054902.

Hanson, D.E., Barber, J.L., 2018. The bond rupture force for sulfur chains calculated from quantum chemistry simulations and its relevance to the tensile strength of vulcanized rubber. Physical Chemistry Chemical Physics 20(13), 8460-8465.

Hanson, D.E., Barber, J.L., Subramanian, G., 2013. The entropy of the rotational conformations of (poly) isoprene molecules and its relationship to rubber elasticity and temperature increase for moderate tensile or compressive strains. The Journal of chemical physics 139(22), 224906.

Hanson, D.E., Martin, R.L., 2009. How far can a rubber molecule stretch before breaking? Ab initio study of tensile elasticity and failure in single-molecule polyisoprene and polybutadiene. The Journal of chemical physics 130(6), 064903.

Hioe, J., Šakić, D., Vrček, V., Zipse, H., 2015. The stability of nitrogen-centered radicals. Organic & biomolecular chemistry 13(1), 157-169.

Hosseinnezhad, S., Bocoum, A., Martinez, F.M., Fini, E.H., 2015a. Biomodification of rubberized asphalt and its high temperature properties. Transportation Research Record: Journal of the Transportation Research Board(2506), 81-89.

Hosseinnezhad, S., Kabir, F., SK., Oldham, D.J., Mousavi, M., Fini, E.H., 2018. Sustainble Surface-Activated Rubber from Scrap Tire for Use in Construction. Journal of Cleaner Production Under Review.

Jana, G., Das, C., 2005. Recycling natural rubber vulcanizates through mechanochemical devulcanization. Macromolecular research 13(1), 30-38.

Klüppel, M., Menge, H., Schmidt, H., Schneider, H., Schuster, R., 2001. Influence of preparation conditions on network parameters of sulfur-cured natural rubber. Macromolecules 34(23), 8107-8116.

Kocevski, S., Yagneswaran, S., Xiao, F., Punith, V., Smith Jr, D.W., Amirkhanian, S., 2012. Surface modified ground rubber tire by grafting acrylic acid for paving applications. Construction and Building Materials 34, 83-90.

Leng, Z., Padhan, R.K., Sreeram, A., 2018. Production of a sustainable paving material through chemical recycling of waste PET into crumb rubber modified asphalt. Journal of Cleaner Production 180, 682-688.

Liang, H., 2015a. Characterization and Surface Modification of Rubber from Recycled Tires. Université Laval.

Liang, M., Xin, X., Fan, W., Ren, S., Shi, J., Luo, H., 2017b. Thermo-stability and aging performance of modified asphalt with crumb rubber activated by microwave and TOR. Materials & Design 127, 84-96.

Lopes, A.R., Constantinides, G.A., 2008. A high throughput FPGA-based floating point conjugate gradient implementation, International Workshop on Applied Reconfigurable Computing. Springer, pp. 75-86.

Manhart, J., Kramer, R., Schaller, R., Holzner, A., Kern, W., Schlögl, S., 2016. Surface Functionalization of Natural Rubber by UV-Induced Thiol-ene Chemistry, Macromolecular Symposia. Wiley Online Library, pp. 32-39.

Markey, S.J., Lewis, W., Moody, C.J., 2013. A new route to α-carbolines based on 6π-electrocyclization of indole-3-alkenyl oximes. Organic letters 15(24), 6306-6308.

McBurney, R.T., Portela-Cubillo, F., Walton, J.C., 2012. Microwave assisted radical organic syntheses. RSC Advances 2(4), 1264-1274.

Mohammadi-Jam, S., Waters, K., 2014. Inverse gas chromatography applications: A review. Advances in colloid and interface science 212, 21-44.

Muchall, H.M., Werstiuk, N.H., Lessard, J., 1999. Computational studies on acyclic amidyl radicals: Π and Σ states and conformations. Journal of Molecular Structure: THEOCHEM 469(1-3), 135-142.

Newell, H.E., Buckton, G., Butler, D.A., Thielmann, F., Williams, D.R., 2001. The use of inverse phase gas chromatography to measure the surface energy of crystalline, amorphous, and recently milled lactose. Pharm. Res. 18(5), 662-666.

Oliveira, J.R., Silva, H.M., Abreu, L.P., Fernandes, S.R., 2013. Use of a warm mix asphalt additive to reduce the production temperatures and to improve the performance of asphalt rubber mixtures. Journal of Cleaner Production 41, 15-22.

Perdew, J.P., Burke, K., Ernzerhof, M., 1996. Generalized gradient approximation made simple. Phys. Rev. Lett. 77(18), 3865.

Portela-Cubillo, F., Scott, J.S., Walton, J.C., 2009. Microwave-promoted syntheses of quinazolines and dihydroquinazolines from 2-aminoarylalkanone O-phenyl oximes. The Journal of organic chemistry 74(14), 4934-4942.

Presti, D.L., Giancontieri, G., Hargreaves, D., 2017. Improving the rheometry of rubberized bitumen: experimental and computation fluid dynamics studies. Construction and Building Materials 136, 286-297.

Presti, D.L., Izquierdo, M., del Barco Carrión, A.J., 2018. Towards storage-stable high-content recycled tyre rubber modified bitumen. Construction and Building Materials 172, 106-111.

Romero-Sánchez, M.a.D., Pastor-Blas, M.M., Martín-Martínez, J.M., 2003. Treatment of a styrene-butadiene-styrene rubber with corona discharge to improve the adhesion to polyurethane adhesive. International journal of adhesion and adhesives 23(1), 49-57.

Romero-Sánchez, M.D., Martín-Martínez, J.M., 2006. Surface modifications of vulcanized SBR rubber by treatment with atmospheric pressure plasma torch. International journal of adhesion and adhesives 26(5), 345-354.

Romero-Sánchez, M.D., Walzak, M.J., Torregrosa-Maciá, R., Martín-Martínez, J.M., 2007. Surface modifications and adhesion of SBS rubber containing calcium carbonate filler by treatment with UV radiation. International journal of adhesion and adhesives 27(6), 434-445.

Schaafsma, Y., Bickel, A., Kooyman, E., 1960. Photolysis of aromatic disulphides. Tetrahedron 10(1-2), 76-80.

Schmidt, U., 1964a. Free Radicals and Free-Radical Reactions of Monovalent and Divalent Sulfur. Angewandte Chemie International Edition 3(9), 602-608.

Shatanawi, K., Biro, S., Thodesen, C., Amirkhanian, S., 2009. Effects of water activation of crumb rubber on the properties of crumb rubber-modified binders. International Journal of Pavement Engineering 10(4), 289-297.

Shu, X., Huang, B., 2014. Recycling of waste tire rubber in asphalt and portland cement concrete: An overview. Construction and Building Materials 67, 217-224.

Treloar, L., 1944. Stress-strain data for vulcanised rubber under various types of deformation. Transactions of the Faraday Society 40, 59-70.

Tyczkowski, J., Krawczyk, I., Wożniak, B., 2003. Modification of styrene–butadiene rubber surfaces by plasma chlorination. Surface and coatings technology 174, 849-853.

Walling, C., Rabinowitz, R., 1959. The Photolysis of Isobutyl Disulfide in Cumene1. Journal of the American Chemical Society 81(5), 1137-1143.

Walton, J.C., 2014. The oxime portmanteau motif: Released heteroradicals undergo incisive EPR interrogation and deliver diverse heterocycles. Accounts of chemical research 47(4), 1406-1416.

Xiang, Y., Xie, Y., Long, G., Zeng, L., 2018. Ultraviolet irradiation of crumb rubber on mechanical performance and mechanism of rubberised asphalt. Road Materials and Pavement Design, 1-14.

Xiaowei, C., Sheng, H., Xiaoyang, G., Wenhui, D., 2017. Crumb waste tire rubber surface modification by plasma polymerization of ethanol and its application on oil-well cement. Applied Surface Science 409, 325-342.

Yu, G.-X., Li, Z.-M., Zhou, X.-L., Li, C.-L., 2011. Crumb rubber–modified asphalt: microwave treatment effects. Petroleum Science and Technology 29(4), 411-417.

Yu, H., Leng, Z., Zhou, Z., Shih, K., Xiao, F., Gao, Z., 2017. Optimization of preparation procedure of liquid warm mix additive modified asphalt rubber. Journal of cleaner production 141, 336-345.

Zhang, X., Lu, C., Liang, M., 2009. Properties of natural rubber vulcanizates containing mechanochemically devulcanized ground tire rubber. Journal of Polymer Research 16(4), 411-419.

Chapter 4 SELECTIVE ADSORPTION OF DIFFERENT BIO-OILS INTO RUBBER

4.1 Abstract

This study examines the merits of surface activation of rubber using various bio-oils to improve rubber-asphalt interaction. To do so a fusion method combining microwave irradiation and bio-chemical treatment was used to graft biomolecules on top of the exterior surface of the rubber. Five surface activated rubbers were prepared using waste vegetable oil, wood pellet, miscanthus, corn stover, and castor oil. The effectiveness of each oil was examined by measuring the chemisorption of the bio-oil and elastic recovery of bitumen containing rubber particles treated with each bio-oil. Our quantum-based density functional theory calculations showed presence of both physical and chemical interactions between polar aromatic components of bio-oils and rubber. Among studied bio-oils, wood-based bio-oil found to have the highest content of polar aromatics such as phenolic resins leading to its enhanced interaction with rubber. This was evidenced in percent recovery which was nearly doubled (from 13% to 24%) when wood-based bio-oil molecules were grafted onto the surface of rubber. Overall, wood-based bio-oil was shown to adsorb well to the rubber surface and reduce its tendency to separate from bitumen by 82%. The study results showed how composition of bio-oil affects its efficacy to activate rubber surface. It also proved the technical merits of using surface activated rubber to reduce segregation between rubber and bitumen which commonly occurs in rubberized asphalt. Therefore, the outcome of this study promotes recycling of waste tire to promote sustainability in pavement construction.

***Keywords*:** Bio-oils, Crumb rubber, surface activated rubber, segregation, adsorption, percent recovery

4.2 Introduction

Application of recycled rubber in pavement construction can significantly enhance its sustainability and long-term performance (Cong et al., 2013). However, it has been documented that rubber particles has tendency to segregate from asphalt binder matrix (Presti et al., 2018). There have been many attempts to reduce the segregation issue (Sienkiewicz et al., 2017). In one study it was shown that microwave-irradiation of crumb rubber can enhance interaction of rubber with asphalt binder leading to an improved storage stability. Researchers observed that the difference in softening point of the top and bottom parts of a cigar tube sample reduced from 8.6ºC to 1.2ºC when rubber was microwave treated (Yu et al., 2011). Another study showed application of hydrogen peroxide with $FeSO_4$ as a catalyst can enhance stability of rubber-modified asphalt binder regardless of rubber sources; both ambient and cryogenic rubber stability was improved after treatment (Shatanawi et al., 2013). Other studies reported role of furfural on activation on ambient and cryogenic rubber. The reduction in segregation for cryogenic rubber was more notable than that of the ambient rubber (Shatanawi et al., 2012). In a separate study a research group grafted acrylamide to the surface of crumb rubber and asphalt binder containing grafted-rubber showed 35% lower difference between softening point of the top and bottom parts of a cigar tube sample compared to asphalt binder containing conventional (non-grafted) rubber (Xie et al., 2019a). This study demonstrated that modifying asphalt binder with crumb rubber activated by trans-polyoctenamer

improves storage stability by lowering the segregation index to a value of 0.79 (Liang et al., 2017b). But study from this research group showed successful attachment of biomolecules from animal waste to external surface of rubber improved the storage stability by 86% compared to conventional crumb-rubber-modified asphalt (Hosseinnezhad et al., 2019a).

Many studies worldwide have incorporated bio-oils from various sources into asphalt. Among them are bio-oils from animal waste (Fini et al., 2011a), waste cooking oil (Dong et al., 2018; Wang et al., 2018), palm oil (Alamawi et al., 2019), microalgae (Chailleux et al., 2012), wood waste (Zhang, R. et al., 2018) , municipal solid waste (Yang et al., 2018), saw dust (Gao et al., 2018), and castor oil (Zeng, M. et al., 2018). Although rubber-modified asphalt binder and its application in pavement have been extensively studied, not many studies have been done on bio-modified rubber, where biomolecules help enhance the rubber-asphalt binder interaction to improve the asphalt binder's storage stability and rheological properties. Most studies have engrossed on the addition of bio-oil to existing rubberized asphalt binder; the bio-oil mainly acts as a modifier of the binder, with limited interaction with rubber (Fini et al., 2013). Some researchers used bio-oil for pre-swelling of rubber particles referred to as bio-modified rubber (BMR) (Dong et al., 2018; Lei et al., 2018; Peralta et al., 2012; Yu, J. et al., 2019). In another study, researchers used bio-modified rubber asphalt binder using castor oil and Styrene Butadiene Styrene (SBS); But no attempt was made to chemically bind the molecules of castor oil to the crumb rubber surface (Dong et al., 2019). Researchers from Duan’s group used biodiesel prepared from chemically modified microalgae oil to

modify an asphalt binder that was previously modified with pre-synthesized tire crumb rubber and Styrene Butadiene Styrene (SBS). The difference in softening point of top and bottom of Cigar tube test was reduced from 14.1^0C to 2.9^0C when 2% microalgae biodiesel was introduced to rubber-modified asphalt. (Duan et al., 2019).

However, none of the above studies attempt to chemically bind biomolecules on top the external surface of the rubber (Fini et al., 2013). They mainly added bio-oils to rubber-modified asphalt binder or first mix bio-oils with rubber particles and then add it to asphalt binder. Even though bio-oil helps with the swelling of rubber in above scenarios, when swollen particles of rubber are mixed into asphalt binder, the bio-oil may leach out of the rubber, increasing the extent of rubber segregation. Our prior studies on surface activated rubber using bio-molecules focused on a specific bio-oil derived from swine manure, where we used microwave radiation to graft bio-oils onto the rubber surface; the later process was found to be highly effective in reducing segregation of rubber in asphalt binder (Hosseinnezhad et al., 2019a; Mousavi et al., 2019b).

As a follow-up on the previous work, in this paper we compare efficacy of various bio-oils in terms of their adsorption and grafting onto the rubber surface. The study uses bio-oils of known chemical compounds derived from five different sources: waste vegetable oil, wood pellet, miscanthus, corn stover, and castor oil to compare their capacity for grafting and swelling rubber particles to create surface-activated rubber (SAR). The motivation of choosing these bio-oils over petroleum-based sources is due to their carbon-neutrality or carbon-negativity, which implies that the amount carbon dioxide released from them is less than or equal to the amount absorbed(Oldham, 2020).

It further examines effect of each surface activated rubber asphalt binder storage stability, the rheology, and the moisture susceptibility.

4.3 Experiment Plan

4.3.1 Materials

PG 64-22 asphalt binder used in this study was collected from Holy Frontier Corporation in Arizona **(Table 4-1)**. PG 64-22 stands for performance grade of asphalt where the highest pavement service temperature is 64 degree Celsius and lowest is -22 degree Celsius. The ground tire rubber which is also known as crumb rubber (60 mesh) was obtained from Crumb Rubber Manufacturers. Bio-oils used are derived from waste vegetable oil (WVO), wood pellet oil (WP), corn stover oil (CS), miscanthus oil (MS) and castor oil (CO), prepared using a fast pyrolysis technique. The details of the procedure can be found here (Hosseinnezhad et al., 2015b).

The physicochemical properties of these bio-oils are as follows:

Table 4-1. Physicochemical Properties of Bio-Oils Used

Bio-oil	pH	Density (g/ml)	Elemental Composition (wt%)				Ash Content (wt%)
			C	H	N	O	
Wood Pellet Oil (WP)	2.8	1.23	61.05	6.93	0.21	31.81	6.84
Corn Stover Oil (CS)	2.87	1.25	61.6	7.28	0.96	30.16	9.27
Miscanthus Oil (MS)	2.95	1.05	65.77	7.31	0.67	26.25	2.14

Table 4-2. General Asphalt Binder Properties Used in This Study

Specific Gravity @15.6 ºC	1.041
Cleveland Open Cup method Flash pointºC	335
Mass change after RTFO	-0.013
Absolute Viscosity @ 60 ºC, Pa.s	179
Stiffness (MPa) @-12ºC @ 60s	85.8

4.3.2 Treatment Methods

4.3.2.1 Microwave Treating

The microwave oven used operates at 2450 MHz frequency. For microwave treatment the microwave power was set to 400W. To prepare samples, 60 g of ground tire rubber was placed and exposed to microwave irradiation for 4 minutes in a microwavable beaker. The products are labeled as microwaved crumb rubber (M-CR).

Combined Treating with Bio-Modifier and Microwave

Crumb rubber particles were mixed in bio-modifiers at 1:1 ratio for 12 hours. The mixture was then kept in the same microwave oven at same wattage for 4 minutes, to boost the efficacy of combined treating. The resulting samples are labeled as surface-activated crumb rubber (SAR) from waste vegetable oil (WVO-SAR), wood pellet oil (WP-SAR), corn stover oil (CS-SAR), miscanthus oil (MS-SAR), and castor oil (CO-SAR).

Modification of Asphalt Binder

At the laboratory, all modified binders were prepared by introducing 15% (by the weight of PG 64-22 asphalt binder) of SAR samples by blending with 85% PG 64-22 asphalt binder. All materials were washed with acetone, dried, and grinded before incorporating them in asphalt binder. The modified binder with inactive crumb rubber is referred to as CRM, and microwave-treated CRM is referred to as M-CRM. Other binders modified with SAR are named as WVO-SARM, WP-SARM, MS-SARM, CS-SARM, and CO-SARM. The following Table 2 shows all the modification scenarios and their naming with acronyms:

Table 4-3. All Modification Scenarios Used in This Paper with Naming and Acronyms

Modification Scenario	Surface Activated Rubber (SAR)	Modifier Acronym
Crumb rubber (CR)	-	CRM
Waste Vegetable Oil (WVO)	WVO-SAR	WVO-SARM
Wood Pellet (WP)	WP-SAR	WP-SARM
Miscanthus (MS)	MS-SAR	MS-SARM
Corn Stover (CS)	CS-SAR	CS-SARM
Castor Oil (CO)	CO-SAR	CO-SARM

TLC-FID Thin-layer Chromatography with Flame Ionization Detection (TLC-FID)

The fractional composition of each bio-oil was investigated using an Iatroscan MK-6s model TLC Flame Ionization Detector (FID). The hydrogen flow rate and airflow rate were established at 160 mL/min and 2 L/min, respectively. The n-heptane-insoluble part specially the asphaltene content was isolated and evaluated using the difference in mass of the filter paper just before and subsequently after the filtration following standards (ASTM-D3279, 2019). Later, 20 mg of n-heptane soluble (maltene) was detected on the chromrods. To develop the solvent, Sigma Aldrich supplied solutions of pentane, toluene, and chloroform were used. In a pentane tank, the chromrods were developed for 35-40 minutes and dried in the air for about 2 to 5 minutes. The dried chromrods were then moved to a second chamber filled with toluene to chloroform solution ratio at 9:1 for 9 minutes. Finally, the rods were oven dried at 85 °C, and the prepared specimen was scanned for 30s using the Flame Ionization Detector.

Multiple Stress Creep Recovery (MSCR) Test

An Anton-Parr rheometer was used for the MSCR test. The oscillation rate was srt to 10 rad/s as this typically represents traffic speed at 90 km/hr. For the test, a set of 10 cycles of repetitive loading and unloading was measured by the instrument, with a loading time of 1 s and a relaxation time of 9 s. The measurements were taken for both stresses of 0.1 kPa and 3.2 kPa. The data is then utilized to calculate the percent recoverable strain in the specimens. In addition, the rutting performance of the binder was assessed using the MSCR test, as outlined in the standards (ASTM-D7405, 2015).

Segregation Test

Segregation test or cigar tube test separation was performed following ASTM D7173 to measure the degree of separation between rubber and asphalt binder. At first, the samples were heated to 163^0C to pour easily in aluminum tubes. Then they are placed in an upright position in a holder rack. Preventing air entrance into the tubes is important. So, tube tops were sealed and placed inside the oven at 163^0C for continuous 48 hours. After that, the rack was taken out and kept in a refrigerator for 4 hours at -10^0C. After 4 hours, while still cool the tubes cut into three equal sections at room temperature (ASTM-D7173, 2014). The mid-portion was thrown out, and the bottom and top sections were tested using a dynamic shear rheometer at 58^0C. The complex shear modulus (G*) and phase angle (δ) data from the test was used to find the Separation Index (SI) using Equation 4-1 (Shatanawi et al., 2009).

$$SI=\frac{\left(\frac{G^*}{sin\delta}\right)max-\left(\frac{G^*}{sin\delta}\right)avg}{\left(\frac{G^*}{sin\delta}\right)_{avg}} \quad (4\text{-}1)$$

Bitumen Bond Strength Test (BBS)

Bitumen bond strength (BBS) is significant parameter to assess a modified binder's ability to resist moisture susceptibility. The BBS testing device consists of a pressure hose, piston and reaction plate. The other components are a pneumatic adhesion tester (portable) and a metal pullout stub. To begin the test, the pullout stub is attached to a piston and stub is screwed on a reaction plate. Next, pressure is introduced via compressed air hose to the piston. Thus, the metal stub applies a pulling stress on the sample. When applied stress exceeds the cohesive strength of the binder or the adhesion

strength of the binder-substrate interface, failure occurs (Moraes et al., 2011). This test method measures the tensile force that is needed to remove a pullout stub attached to a solid glass substrate with modified asphalt binder. For dry conditioning, the specimen is prepared and kept in ambient temperature for 2 hours. For wet conditioning, the specimen is kept in a bath at 50^0C for two hours. After 2 hours of conditioning for the specimens, a pneumatic load is applied to the attached specimen pullout stub following standards until failure (ASTM-D4541, 2002). The pullout tensile strength and mode of failure are reported to describe the bonding properties of the modifiers. In this study, one type of substrate is used to evaluate the peak tensile strength of modified asphalt binder: a 3mm-thick sonicated glass plate substrate is used for BBS tests.

Attenuated Total Reflectance Fourier Transform Infrared Spectroscopy (ATR-FTIR)

A Bruker FT-IR Spectrometer situated in the Eyring Materials Center was used in absorbance mode to detect biomolecules covalently bonded to a rubber surface after irradiation of CR into SAR samples; a diamond ATR was used with mid-infrared range to detect any changes. A range of 4000 cm^{-1} to 400 cm^{-1} wavenumbers were attempted. All samples were washed in acetone and dried before detection.

4.3.3 Computational Simulation Methods

Quantum mechanical calculations were performed on the basis of dispersion-corrected density functional theory (DFT-D). The optimization of the model molecules were performed using $DMol^3$ module (Delley, 1990, 2000) of the Accelrys Materials Studio program package (version 6.0). At the generalized gradient approximation (GGA)

level, Perdew-Burke-Ernzerhof (PBE) (Perdew et al., 1996) was used as the exchange-correlation function, and DNP as the numerical basis for all-electron optimization process. The general quality for the numerical integrations was established to "fine" grid, and full optimization was achieved with the convergence criteria of 1.0×10^{-5} eV/atom, 3×10^{-2} eV/Å, 5×10^{-2} GPa, and 1×10^{-3} Å for energy, maximum force, stress, and displacement, respectively.

Interaction energy, E_{int}, between the model molecule of styrene-butadiene rubber and the model molecules of modifier was calculated by the energy difference between the total energy of the complex (rubber-modifier), $E_{complex}$, and sum of the energies of the interacting fragments, $E_{fragment}$, at their lowest state of energy;

$$E_{int} = E_{complex} - \left(\sum E_{fragment}\right) \quad (4\text{-}2)$$

Gaussian 09 program package (Frisch et al., 2009) was used to provide the r*elaxed potential energy surface (PES) scans; this technique is not implemented in DMol*^{3} module. *In relaxed PES technique, the* system is controlled to be fully optimized in every coordination step before entering the next step. During scanning the reaction paths, all interacting systems geometry was fully optimized at the gradient-corrected BPE density functional, the same as DMol^3 module, in conjunction with a standard 6-31g* basis set, comparable with DND numerical basis set in DMol^3 code.

4.4 Results and Discussion

Following sections delivers outcome of this research by means of a combination of chemical and laboratory experiment.

4.4.1 Chemical Analysis

Figure 4-1 shows the FTIR spectra of various surface activated and common rubber powders. The characteristic peak at 1012 cm^{-1} in WP-SAR is ether or alcohol C-O stretching (Hosseinnezhad et al., 2015b). As **Figure 4-1** shows, the peak between 1540 and 1580 cm^{-1} has disappeared for CS-SAR, MS-SAR, and WP-SAR. The peak in this zone is related to the stretching of methyl-assisted conjugated double bonds, which is common in vulcanized natural rubber. The vanishing of this peak for M-CR and corresponding SARs is indication of devulcanization and a reduction in conjugated double bonds in the rubber (Zhang et al., 2009). But this peak doesn't disappear in WVO-SAR and CO-SAR. A strong peak appears in WVO-SAR and CO-SAR at 1459 cm^{-1} that can be attributed to methyl-assisted C-H bending (Hosseinnezhad et al., 2015b). A strong peak at 1740 cm^{-1} can be seen for WVO-SAR and CO-SAR that can be attributed to strong C=O stretching; this peak is reduced in CS-SAR, MS-SAR, and WP-SAR, indicating a possible break in C=O bond (Hosseinnezhad et al., 2015b).

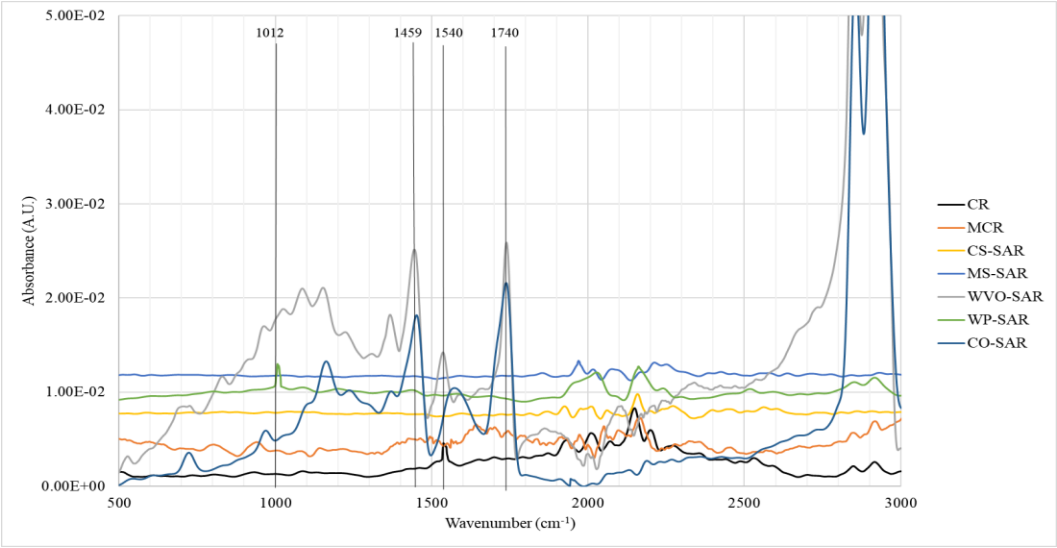

Figure 4-1. FTIR Spectra of Surface-Activated and Inactive Rubber

4.4.2 Rheological Analysis

Figure 4-2 shows the Separation Index (SI) for all surface-activated and inactive samples. It can be observed that the SI values of all activated samples are significantly inferior to the SI of the inactive CRM, indicating success of the treatment method to improve the compatibility of rubber and the asphalt binder matrix. Among the SARs, the wood pellet SAR and waste vegetable oil SAR reduce segregation the most, by 82% and 70%, respectively. This gives an idea that these two bio-oils performed better in being adsorbed while other bio-oils did not adsorb well. This is due to the underlying biomolecules that may have greater affinity to attach on the surface of crumb rubber particles, ensuring better dispersion in the asphalt binder matrix and better enhanced compatibility than their corn stover, miscanthus, and castor oil counterparts. CO-SAR activated rubber reduces separation tendency by 41% from CRM. So, it can be said that phenol-rich WP-SAR might have greater affinity to disperse in the asphalt binder matrix and thus reduce the separation tendency the most. To better examine effect of chemical composition TLC-FID was used to determine polar aromatics content of bio-oils (**Table 4-3**). Wood-based and castor oil has the highest polar aromatics (resin) content, which may explain their leading to better separation index compared to other bio-oils. To provide in-depth understanding of role of polar aromatics, we performed computational analysis in following sections of the paper.

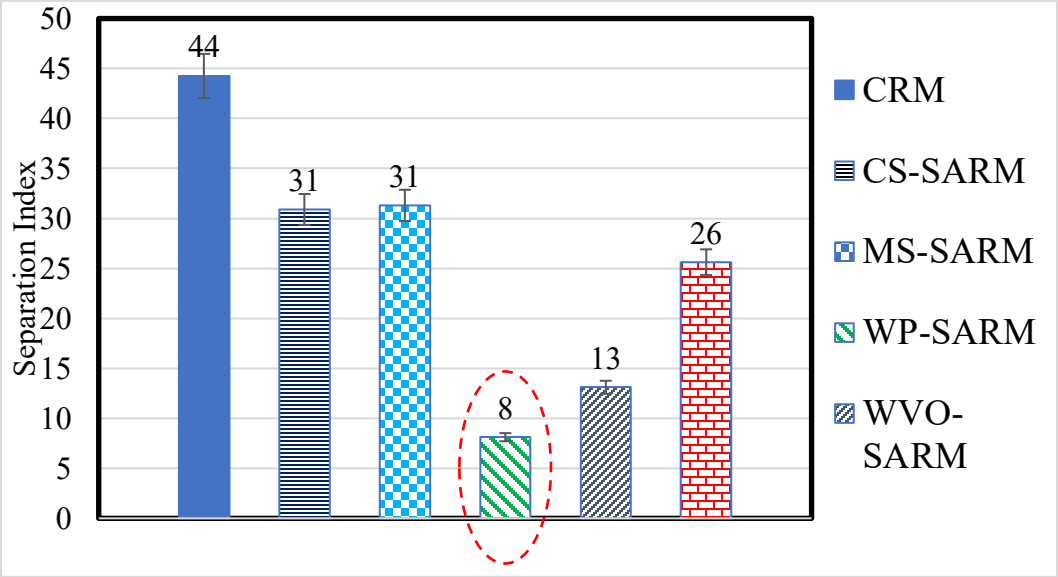

Figure 4-2. Separation Indices for Surface-Activated and Inactive Rubber-Modified Asphalt Binder.

Table 4-4. TLC-FID Results for Chemical Content (Asphaltene, Resin, Aromatics, and Saturates) of Bio-Oils

Bio-oil	*CS*	*MS*	*WP*	*WVO*	*CO*
Saturates	6.8	6.22	3.46	0.00	20.95
Naphthene Aromatics	3.73	8.56	2.93	87.19	0.00
Resins (Polar Aromatics)	67.49	60.47	76.21	12.80	78.17
Asphaltenes	21.96	24.47	17.38	0.00	0.87

4.4.3 DFT-based Modeling

This part of the study concentrates on the molecular aspects of the irradiated bio-modified rubber through density functional theory (DFT) calculations performed on the model systems. The modeling simulates characteristic interactions between molecules of microwaved rubber and biomodifier. The interactions become complicated due to the advent of many free radicals emerging from the irradiation. Considering the high

performance of the wood-based bio-oil in reducing the phase separation (82%) and enhancing the percent recovery (from 13% to 24%), intermolecular interactions between wood-pellet and styrene-butadiene rubber (SBR) model molecule are investigated.

Based on the GC-MS peak area % of the individual compounds detected by mass spectrometer, accounting for 60% of the total area, 17 molecules of wood pellet oil are shown in **Table 4-4**. The high contribution of phenolic compounds in chemical composition of wood pellet, shown in **Table 4-4**, is mainly due to the high content of lignin in wood and lignified elements of plants; wood is known as the main source of lignin, and lignin is the main source of phenolic compounds in the world. Presence of lignin, accompanied by cellulose and hemicellulose in plant's cell wall, is considered as a limiting factor in conversion of wood-based biomass into biofuels. Due to the variation in chemical composition, no precise structure is defined for lignin structure; however, it is widely known as a dendritic network of three phenylpropene (C_6H_5-CH_2CH=CH_2) basic units; coniferyl alcohol, sinapyl alcohol, and low amounts of p-coumaryl alcohol (**Figure 4-3**) (Kun and Pukánszky, 2017), (Vainio et al., 2004). As the phenolic content of wood pellet in **Table 4-4** and units of lignin in **Figure 4-3** show hydroxyl (OH) and methoxy (O-CH3) substituents and C=C double bond are the main potential active sites to interact with host species, such as rubber or bitumen. In this respect, strong self-interactions among lignin units are attributed to the high polarity and functionality of lignin (Kun and Pukánszky, 2017). It is worth noting that the nature and the amount of lignin functional groups (hydroxyl, methoxyl, carbonyl and carboxyl groups) vary depending on the genetic origin and applied extraction processes.

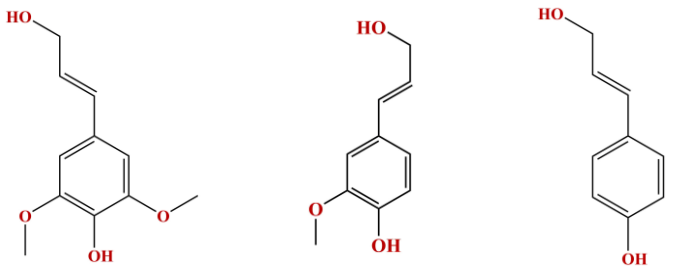

Sinapyl Coniferol Paracoumaryl

Figure 4-3. Three Monolignols Identified in Lignins.

Table 4-5. The Main Individual Compounds of Wood Pellet Identified by GC-MS

	Wood Pellet Oil	Formula	Area %
1	Phenol, 2,6-dimethoxy-	$C_8H_{10}O_3$	12.0
2	3,5-Dimethoxy-4- hydroxytoluene	$C_9H_{12}O_3$	9.9
3	5-tert-Butylpyrogallol	$C_{10}H_{14}O_3$	8.4
4	Phenol, 2-methoxy-	$C_7H_8O_2$	5.0
5	Creosol	$C_8H_{10}O_2$	4.8
6	Furfural	$C_5H_4O_2$	4.4
7	Phenol, 4-ethyl-2-methoxy-	$C_9H_{12}O_2$	4.4
8	Homosyringaldehyde	$C_{10}H_{12}O_4$	3.6
9	1,2-Cyclopentanedione, 3-methyl-	$C_6H_8O_2$	2.2
10	Phenol, 3-methyl-	C_7H_8O	1.9
11	Syringylacetone	$C_{11}H_{14}O_4$	1.7
12	trans-Isoeugenol	$C_{10}H_{12}O_2$	1.5
13	Phenol, 2-methoxy-4-propyl-	$C_{10}H_{14}O_2$	1.4
14	Phenol,2,6-dimethoxy-4-(2-propenyl)-	$C_{11}H_{14}O_3$	1.3
15	2-Furancarboxaldehyde, 5-methyl-	$C_6H_6O_2$	1.2
16	Ethanone, 1-(2-furanyl)-	$C_6H_6O_2$	1.2
17	2-Propanone,1-(4-hydroxy-3-methoxyphenyl)-	$C_{10}H_{12}O_3$	1.1
			60.0%

To gain an insight into the dispersion interactions between highly polar constituents of wood pellet and rubber, **Figure 4-4** represents the interaction a cross-linked model of styrenebutadiene rubber (SBR) molecule and 2,6-dimethoxyphenol molecule which has shown the largest contribution (12.0%, **Table 4-4**) into the chemical composition of wood pellet. The corresponding theoretical calculations have been performed using DMol^3 software module (Delley, 1990, 2000) at the PBE-D/DNP level which include dispersion corrected contribution into correlation energy.

Considering the high functionality of the representative wood pellet molecule, methoxyphenol, and the vulcanized rubber molecule, due to the presence of sulfur groups, the polar-polar interactions between two model molecules led to the -18.0 kcal/mol interaction energy, **Figure 4-4-a**. In another orientation, π-π interactions between aromatic rings of two molecules, as shown in **Figure 4-4-b**, is associated with the -15.3 kcal/mol interaction energy. Comparing two energy values highlights the electronic performance of aromatic rings in developing dispersive forces as effective as polar-polar interactions.

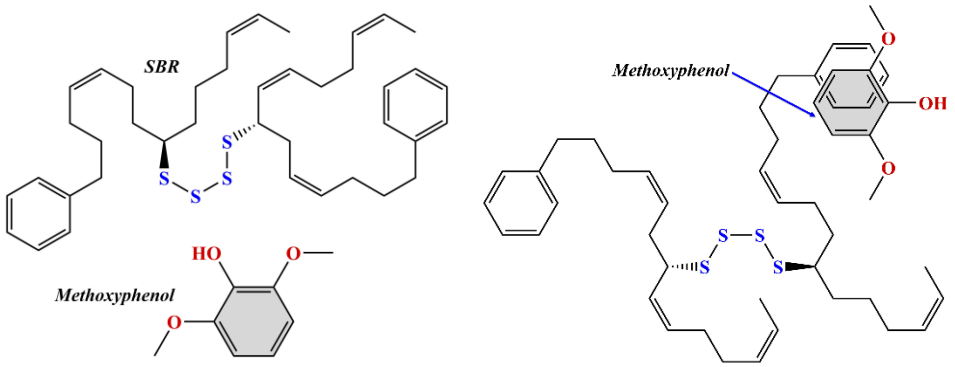

a ΔE= -18.0 kcl/mol **b** ΔE= -15.3 kcl/mol

Figure 4-4. Typical Dispersion Interactions, at The PBE-D/DNP Level of Theory, Between Vulcanized Styrene-Butadiene Rubber (SBR) Model Molecule and 2,6-Dimethoxyphenol Molecule of Wood Pellet.

Studies already reveal that both physical and chemical modification of rubber improves physio-chemical performance. Our recent evaluation on effectiveness of tire crumb rubber treatment via a fusion processing of microwaving and an animal-waste bio oil have shown the merits of devulcanization via microwaving followed by chemical treatment leading to decrement of phase separation in asphalt-rubber matrix (Hosseinnezhad et al., 2019a; Mousavi et al., 2019b). Electromagnetic radiation cleaves the cross-links in sulfur chains (S-S and S-C bonds) as well as increases the activated species in biomodifier. The infusible three-dimensional network of rubber is broken into the free chains of polymers that can interact with activate biomodifier molecules. In following, we will have a look at some possible reaction pathways through which radicals of irradiated rubber may involve in wood pellet chemical species. For doing so, DFT-based studies of this section are completed on truncated branches of styrene-butadiene rubber (SBR) model shown in **Figure 5**, and 2-methoxyphenol molecule as an appropriate representative molecule for lignin compounds identified in wood pellet. The theoretical calculations are performed using Gaussian program package (Frisch et al., 2009), at the PBEPBE/6-31G* level of theory. The technique of relaxed potential energy surface (ESP) is used to get close the target constituents; in relaxed ESP, the system is controlled to be completely optimized in every coordination step before entering into the next step.

Hydrogen Abstraction of Bio-modifier by Radicals of Sulfur

Considering the particular importance of sulfur radicals in regular function of devulcanized rubber, one of the assumptions in developing the reactions of irradiated rubber is the H-abstraction by sulfur-centered radicals (C_6H_5-OH + •S-S-R). This assumption is based on the available literature indicating dehydrogenation of aliphatic and hydroaromatic compounds by thermally or photolytically formed sulfur radicals (Schmidt, 1964b). Additionally it was seen that, that photolysis of a mixture containing a H-donor species and disulfur leads to the rapid formation of mercaptan (R-SH), (Walling and Rabinowitz, 1959), as the following Equations 3 and 4:

$$\text{R-S-S-R} \xrightarrow{h\nu} 2\ \text{R-}\dot{\text{S}} \tag{4-3}$$

$$2\ \text{R-}\dot{\text{S}} + 2\ \text{H-donor} \rightarrow 2\ \text{R-SH} + \text{Donor}\dot{} \tag{4-4}$$

However, based on the DFT results, shown by the scan of energy path in **Figure 4-5**, the H transfer from phenolic OHs is not thermodynamically favorable, and the energy values fall in an ascending trend, suggesting that the H transfer from phenolic hydroxyl to radicals of sulfur does not occur spontaneously. The same energy trend is observed when H is going to detach from the methoxy group of the ring (C_6H_5OH-O-CH_2….H….•S-S-R).

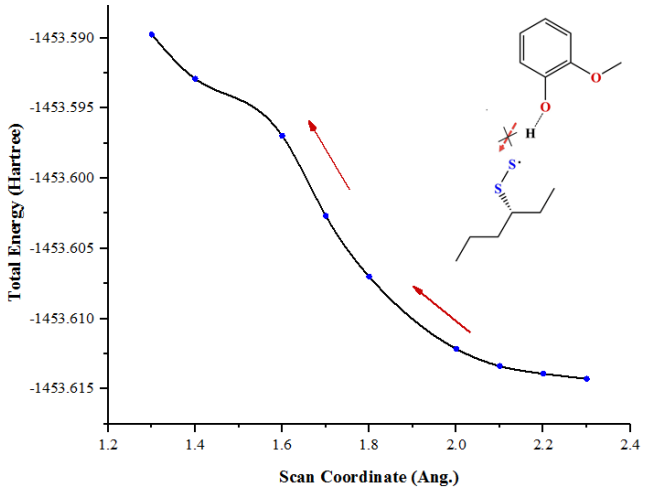

Figure 4-5. Relaxed Potential Energy Surface Scan for H-Abstraction From 2-Methoxyphenol to Sulfur Radical. The Scan Was Completed Along The –H…S– Bond From 2.3 Å to 1.3 Å by The Step Size of -0.1 Å.

Although DFT results do not validate the formation of radicals of methoxyphenol through attacking sulfur radicals, these radicals can be produced from other agents or magnetic radiation. This justification is based on the FTIR results indicating the presence of ether groups, and also increase in the content of C-O-C bond in SBR-phenolic nanocomposites (Liu et al., 2015). This is in-line with our DFT results showing the high reactivity of phenoxyl radical (C6H5-O•) with C=C double bonds of the SBR rubber and formation of C-O-C bonds; see the descending trend of energy in **Figure 4-6** while scanning the reaction path way when two constitutes are getting close to each other. This reaction is followed by the displacement of free radical on C-chain of rubber which propagates the chain or forms C=C bond in new positions.

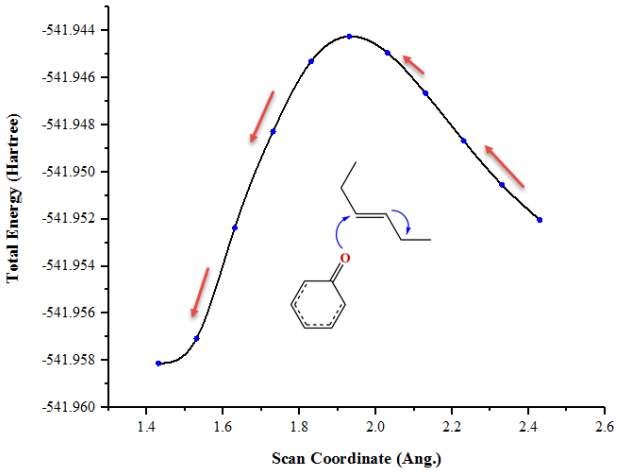

Figure 4-6. Relaxed Potential Energy Surface Scan for Phenoxyl Radical and C=C Double Bond of The C-Chain of Rubber. The Scan Was Completed Along The –O…C– Bond from 2.4 Å to 1.4 Å by The Step Size of -0.1 Å.

Another notable reaction pathway for effective interaction between irradiated wood pellet modifier and rubber could be performed through addition of sulfur to the double bonds of C=C or C=O, produced by the free radical former agents or radiation. As show in **Figure 4-7**, this reaction pathway goes forward without any activation barrier, indicating the high preference of sulfur radicals of rubber in co-operation with unsaturated bonds of the modifier.

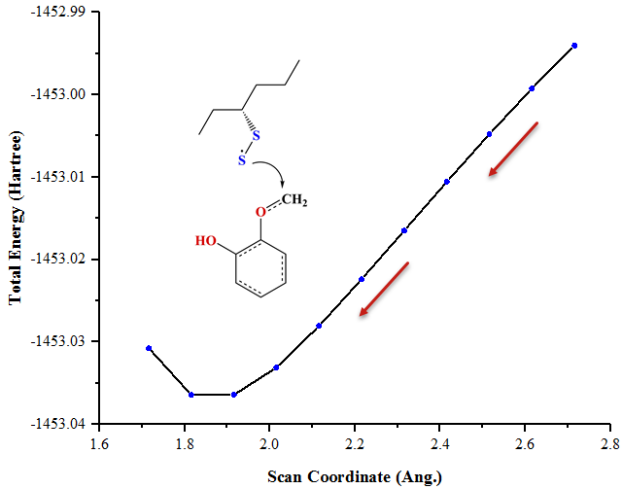

Figure 4-7. Relaxed Potential Energy Surface Scan for Reaction of Sulfur Radical and C=O Double Bond of The Modifier. The Scan Was Performed Along The –S…C– Bond from 2.7 Å To 1.7 Å by The Step Size of -0.1 Å

Given the high content of ortho and para substituted phenols in wood pellet (**Table 4-4**) and other terrestrial plant-based oils, as well as ability of phenolic resins (polar aromatics) in interacting with rubber (Lattimer et al., 1989) (Durairaj et al., 1989; Obrecht and Sumner, 2004) (Derakhshandeh et al., 2008), we conclude that amount of polar aromatics (resin) in each bio-oil affects its ultimate performance on efficient interaction with rubber and subsequently with asphalt binder.

It should be noted that based on the TLC-FID results (**Table 4-3)**, wood-based bio-oil has high content of polar aromatics (resin), around 76%. The high amounts of polar aromatics combined with our above computational analysis explains superior performance of wood-based bio-oils compared to the other counterparts.

To further evaluate interactions of above surface activated rubbers with asphalt, we examined rheological properties and adhesion characteristics of asphalt specimens

containing each surface activated rubber. **Figure 4-8** shows Jnr values and percentage of recovery obtained through an MSCR test at 3.2 kPa and 52^0C for different bio-oil-activated samples and the non-activated M-CRM. Among the six modified asphalt binders, M-CRM has the lower percent recovery than CS-SARM, MS-SARM and WP-SARM, which is expected as the degradation of the rubber particles occur. Interestingly among the activated samples, WVO-SARM and CO-SARM have approximately a 50% lower percentage recovery than M-CRM. This can be attributed to the fact that waste vegetable oil does not make a strong interaction with the bitumen matrix. On the other hand, CO-SARM neither did show any higher adsorption nor did show any strong interaction with bitumen matrix. WP-SARM, CS-SARM, and MS-SARM have 83%, 203%, and 92% higher percentage recovery than M-CRM indicating the latter bio-oils make strong interaction with bitumen matrix. WP-SARM showed nearly double recovery compared to M-CRM. **Figure 4-8** shows that CS-SARM and WP-SARM modified asphalt binders have lower Jnr value which indicates a higher resistance to rutting than other scenarios. WVO-SARM has the highest Jnr value and the lowest recovery followed by CO-SARM. This in turn indicates that these two bio-oils do not contribute to development of internal networks between treated rubber particles and asphalt. It should be noted that Caster oil showed good interaction with rubber surface but failed to adequately interact with asphalt matrix. This is a strong evidence that desirable bio-oils are the ones that interact with both rubber surface and asphalt matrix.

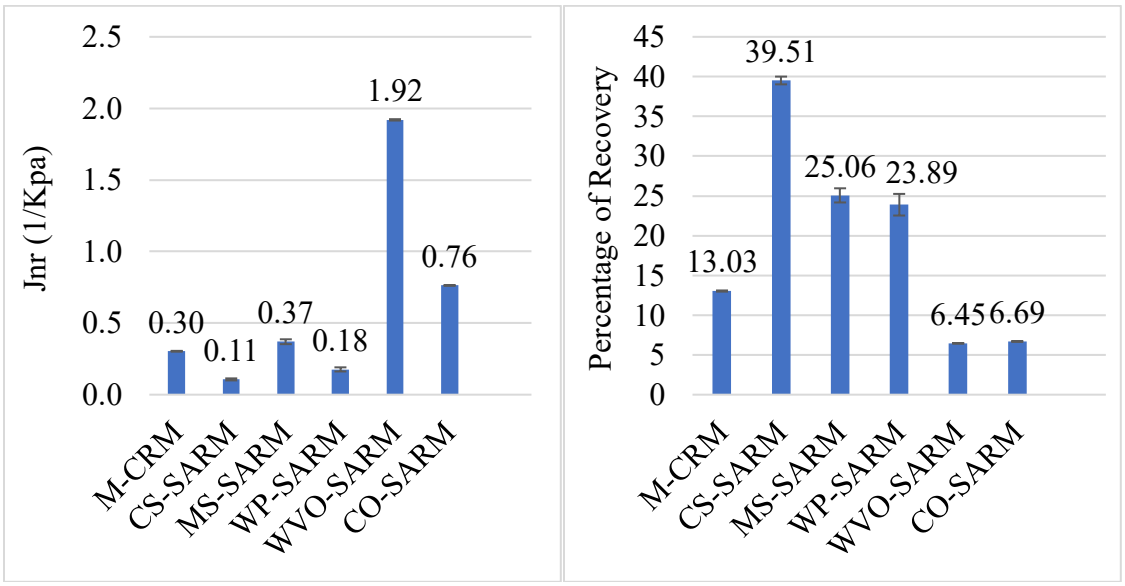

Figure 4-8. (left) Non-Recoverable Creep Compliance Value for Different SARMs; (Right) Percentage Recoverable Strain for Different SARMs.

To evaluate overall effect of each bio-oil on bitumen performance, a bitumen bond strength test was performed on all the modified asphalts following ASTM D4451. For both dry- and wet-conditioned specimens, the failure type was adhesion failure. An example of both dry- and wet-conditioned failure (Miscanthus-SARM) can be seen in **Figure 4-9**. According to the data analysis, Miscanthus-SARM showed the highest reduction in tensile strength after it was exposed to water.

(a) **(b)**

Figure 4-9. Examples of BBS adhesion failure on a glass plate substrate; (a) MS-SARM dry-conditioned, (b) MS-SARM wet-conditioned

Table 4-5 shows that the average tensile peak strength of all asphalt binder specimens is reduced after water conditioning. The ratios of wet-to-dry strength are all above 80%, except for Miscanthus-SARM which is 68%. WP-SARM showed only 12% reduction in strength showing the highest resistance to moisture damage compared to other scenarios.

Table 4-6. BBS Results of Modified Asphalt Binder After Dry and Wet Conditioning for 2 Hours on A Glass Plate Substrate

Sample name	Avg. Dry (kPa)	CV Dry	Avg. Wet (kPa)	CV Wet	Wet/Dry Ratio
WVO-SARM	732.95	3.15	640.46	5.17	87
CS-SARM	1302.48	7.5	1157.56	7.86	89
MS-SARM	1291.5	15.06	876.29	30.54	68
WP-SARM	1409.43	22.9	1259.07	2.19	89
CO-SARM	1604.31	1.29	1418.81	4.08	88
CRM	1369.65	6.86	1270.15	2.28	93

4.5 Conclusion

This study aimed at investigating the merits of surface activation of rubber with various bio-oils and examines the effect of each treatment on the performance of rubberized asphalt. The outcomes of the experiments are as follows:

Segregation Indices were found to be reduced for all surface-activated rubbers compared to non-activated rubber. The segregation index was reduced by 82% and 70% when rubber was treated by wood-based oil and waste vegetable oil, respectively. This can be credited to the successful attaching of biomolecules onto the surface of crumb rubber. The percent recovery was used as an indicator of extent of interaction between surface treated rubber and asphalt matrix. Active biomolecules grafted on the rubber surface are expected to form internal network with asphalt molecules giving rise to percent recovery. Accordingly, some of the surface-activated rubbers led to 83%-203% gain in percent recovery compared to the non-treated rubber scenario. Among surface-activated rubbers, corn stover had the highest percent recovery of 40% followed by miscanthus (25%), wood pellet (24%).

It should be noted that wood pellet and waste vegetable oil both showed the highest adsorption onto the surface of rubber, as evidenced by the notable peaks in the FTIR spectra. However, Waste vegetable oil, which showed good adsorption to rubber did not make a strong interaction with the bitumen matrix, leading to a very low percent recovery. It should be noted that Wood-based bio-oil had both a good adsorption and a good percent recovery leading to 82% reduction in segregation. The observed desirable performance of wood-based bio-oil was attributed to the high contribution of polar

aromatics (resin) content compared to its counterparts as evidenced in TLC-FID results wood-based bio-oil contains 76% resin. In addition to the physical interactions between polar aromatics of the bio-oil and rubber, our DFT results exhibit reaction pathways for effective interactions between radicals of sulfur with C=O and C=C bonds of bio-oils. An energetically favorable reaction pathway was also found for interaction of phenoxyl radicals of bio-oil with C=C double bonds of rubber.

In terms of moisture susceptibility, all the asphalt binders containing surface-activated rubber except the one treated with Miscanthus oil performed well showing wet-to-dry strength ratios above 80% as measured by bitumen bond strength tests (ASTM D4541). In case of Miscanthus, tensile strength dropped by 32% when samples were conditioned in water, indicating a high vulnerability to moisture damage. The outcome of this study shows how bio-oil's chemical composition affect its efficacy as a modifier. Desirable bio-oils should be able to both adsorb well onto the surface of rubber surface and form internal network with bitumen matrix. The study results promote sustainability in construction by facilitating resource conservation via effective treatment of waste rubber for reuse in new construction.

4.6 References

Alamawi, M.Y., Khairuddin, F.H., Yusoff, N.I.M., Badri, K., Ceylan, H., 2019. Investigation on physical, thermal and chemical properties of palm kernel oil polyol bio-based binder as a replacement for bituminous binder. Construction and Building Materials 204, 122-131.

ASTM-D3279, 2019. Standard Test Method for n-Heptane Insolubles ASTM International, West Conshohocken, PA.

ASTM-D4541, 2002. Standard Test Method for Pull-Off Strength of Coatings Using Portable Adhesion Testers. pp. 1-13.

ASTM-D7173, 2014. Standard Practice for Determining the Separation Tendency of Polymer from Polymer Modified Asphalt. ASTM.

ASTM-D7405, 2015. Standard Test Method for Multiple Stress Creep and Recovery (MSCR) of Asphalt Binder Using a Dynamic Shear Rheometer. ASTM International, West Conshohocken, PA.

Chailleux, E., Audo, M., Bujoli, B., Queffelec, C., Legrand, J., Lepine, O., 2012. Alternative binder from microalgae: Algoroute project, Workshop alternative binders for sustainable asphalt pavements. pp. pp 7-14.

Cong, P., Xun, P., Xing, M., Chen, S., 2013. Investigation of asphalt binder containing various crumb rubbers and asphalts. Construction and Building Materials 40, 632-641.

Delley, B., 1990. An all-electron numerical method for solving the local density functional for polyatomic molecules. Journal of chemical physics 92(1), 508-517.

Delley, B., 2000. From molecules to solids with the DMol3 approach. Journal of chemical physics 113(18), 7756-7764.

Derakhshandeh, B., Shojaei, A., Faghihi, M., 2008. Effects of rubber curing ingredients and phenolic-resin on mechanical, thermal, and morphological characteristics of rubber/phenolic-resin blends. Journal of applied polymer science 108(6), 3808-3821.

Dong, R., Zhao, M., Xia, W., Yi, X., Dai, P., Tang, N., 2018. Chemical and microscopic investigation of co-pyrolysis of crumb tire rubber with waste cooking oil at mild temperature. Waste Manage. (Oxford) 79, 516-525.

Dong, Z.-j., Zhou, T., Luan, H., Williams, R.C., Wang, P., Leng, Z., 2019. Composite modification mechanism of blended bio-asphalt combining styrene-butadiene-styrene with crumb rubber: A sustainable and environmental-friendly solution for wastes. Journal of cleaner production 214, 593-605.

Duan, S., Muhammad, Y., Li, J., Maria, S., Meng, F., Wei, Y., Su, Z., Yang, H., 2019. Enhancing effect of microalgae biodiesel incorporation on the performance of crumb Rubber/SBS modified asphalt. Journal of Cleaner Production, 117725.

Durairaj, B., Peterson Jr, A., Salee, G., 1989. Novel rubber compounding resorcinolic resins. Google Patents.

Fini, E.H., Kalberer, E.W., Shahbazi, A., 2011. Biobinder from swine manure: Sustainable alternative for asphalt binder.

Fini, E.H., Oldham, D.J., Abu-Lebdeh, T., 2013. Synthesis and characterization of biomodified rubber asphalt: Sustainable waste management solution for scrap tire and swine manure. Journal of Environmental Engineering 139(12), 1454-1461.

Frisch, M.J., Trucks, G.W., Schlegel, H.B., al., e., 2009. GAUSSIAN 09. revision A.1, Gaussian, Inc., Wallingford CT.

Gao, J., Wang, H., You, Z., Mohd Hasan, M., Lei, Y., Irfan, M., 2018. Rheological behavior and sensitivity of wood-derived bio-oil modified asphalt binders. Applied Sciences 8(6), 919.

Hosseinnezhad, S., Fini, E.H., Sharma, B.K., Basti, M., Kunwar, B., 2015. Physiochemical characterization of synthetic bio-oils produced from bio-mass: a sustainable source for construction bio-adhesives. RSC Advances 5(92), 75519-75527.

Hosseinnezhad, S., Kabir, S.F., Oldham, D., Mousavi, M., Fini, E.H., 2019. Surface functionalization of rubber particles to reduce phase separation in rubberized asphalt for sustainable construction. Journal of Cleaner Production 225, 82-89.

Kun, D., Pukánszky, B., 2017. Polymer/lignin blends: Interactions, properties, applications. European Polymer Journal 93, 618-641.

Lattimer, R.P., Kinsey, R.A., Layer, R.W., Rhee, C., 1989. The mechanism of phenolic resin vulcanization of unsaturated elastomers. Rubber chemistry and technology 62(1), 107-123.

Lei, Y., Wang, H., Fini, E.H., You, Z., Yang, X., Gao, J., Dong, S., Jiang, G., 2018. Evaluation of the effect of bio-oil on the high-temperature performance of rubber modified asphalt. Construction and Building Materials 191, 692-701.

Liang, M., Xin, X., Fan, W., Ren, S., Shi, J., Luo, H., 2017. Thermo-stability and aging performance of modified asphalt with crumb rubber activated by microwave and TOR. Materials & Design 127, 84-96.

Liu, W.W., Ma, J.J., Zhan, M.S., Wang, K., 2015. The toughening effect and mechanism of styrene-butadiene rubber nanoparticles for novolac resin. Journal of Applied Polymer Science 132(9).

Moraes, R., Velasquez, R., Bahia, H.U., 2011. Measuring the effect of moisture on asphalt–aggregate bond with the bitumen bond strength test. Transportation Research Record 2209(1), 70-81.

Mousavi, M., Hosseinnezhad, S., Kabir, S.F., Burnett, D.J., Fini, E.H., 2019. Reaction pathways for surface activated rubber particles. Resources, Conservation and Recycling 149, 292-300.

Obrecht, W., Sumner, A., 2004. Rubber gels and rubber compounds containing phenolic resin adducts. Google Patents.

Peralta, J., Williams, R.C., Rover, M., Silva, H.M.R.D.d., 2012. Development of a rubber-modified fractionated bio-oil for use as noncrude petroleum binder in flexible pavements. Transportation Research Circular(E-C165), 23-36.

Perdew, J.P., Burke, K., Ernzerhof, M., 1996. Generalized gradient approximation made simple. Phys. Rev. Lett. 77(18), 3865.

Presti, D.L., Izquierdo, M., del Barco Carrión, A.J., 2018. Towards storage-stable high-content recycled tyre rubber modified bitumen. Construction and Building Materials 172, 106-111.

Schmidt, U., 1964. Free radicals and free-radical reactions of monovalent and divalent sulfur. Angewandte Chemie International Edition in English 3(9), 602-608.

Shatanawi, K., Biro, S., Thodesen, C., Amirkhanian, S., 2009. Effects of water activation of crumb rubber on the properties of crumb rubber-modified binders. International Journal of Pavement Engineering 10(4), 289-297.

Shatanawi, K.M., Biro, S., Geiger, A., Amirkhanian, S.N., 2012. Effects of furfural activated crumb rubber on the properties of rubberized asphalt. Construction and Building Materials 28(1), 96-103.

Shatanawi, K.M., Biro, S., Naser, M., Amirkhanian, S.N., 2013. Improving the rheological properties of crumb rubber modified binder using hydrogen peroxide. Road Materials and Pavement Design 14(3), 723-734.

Sienkiewicz, M., Borzędowska-Labuda, K., Wojtkiewicz, A., Janik, H., 2017. Development of methods improving storage stability of bitumen modified with ground tire rubber: A review. Fuel Process. Technol. 159, 272-279.

Vainio, U., Maximova, N., Hortling, B., Laine, J., Stenius, P., Simola, L.K., Gravitis, J., Serimaa, R., 2004. Morphology of dry lignins and size and shape of dissolved kraft lignin particles by X-ray scattering. Langmuir 20(22), 9736-9744.

Walling, C., Rabinowitz, R., 1959. The Photolysis of Isobutyl Disulfide in Cumene1. Journal of the American Chemical Society 81(5), 1137-1143.

Wang, C., Xue, L., Xie, W., You, Z., Yang, X., 2018. Laboratory investigation on chemical and rheological properties of bio-asphalt binders incorporating waste cooking oil. Construction and Building Materials 167, 348-358.

Xie, J., Yang, Y., Lv, S., Peng, X., Zhang, Y., 2019. Investigation on Preparation Process and Storage Stability of Modified Asphalt Binder by Grafting Activated Crumb Rubber. Materials 12(12), 2014.

Yang, Y., Zhang, Y., Omairey, E., Cai, J., Gu, F., Bridgwater, A.V., 2018. Intermediate pyrolysis of organic fraction of municipal solid waste and rheological study of the pyrolysis oil for potential use as bio-bitumen. Journal of Cleaner Production 187, 390-399.

Yu, G.-X., Li, Z.-M., Zhou, X.-L., Li, C.-L., 2011. Crumb rubber–modified asphalt: microwave treatment effects. Petroleum Science and Technology 29(4), 411-417.

Yu, J., Ren, Z., Gao, Z., Wu, Q., Zhu, Z., Yu, H., 2019. Recycled Heavy Bio Oil as Performance Enhancer for Rubberized Bituminous Binders. Polymers 11(5), 800.

Zeng, M., Li, J., Zhu, W., Xia, Y., 2018. Laboratory evaluation on residue in castor oil production as rejuvenator for aged paving asphalt binder. Construction and Building Materials 193, 276-285.

Zhang, R., You, Z., Wang, H., Chen, X., Si, C., Peng, C., 2018. Using bio-based rejuvenator derived from waste wood to recycle old asphalt. Construction and Building Materials 189, 568-575.

Zhang, X., Lu, C., Liang, M., 2009. Properties of natural rubber vulcanizates containing mechanochemically devulcanized ground tire rubber. Journal of Polymer Research 16(4), 411-419.

Chapter 5 MICROBIAL DESULFURIZATION OF RUBBER

5.1 Abstract

This paper examines the merits of using microbially desulfurized rubber to enhance the performance of bituminous pavements and promote recycling of scrap tires. To prepare microbially desulfurized rubber, we incubated crumb rubber obtained from waste tires in medium with microbes from waste activated sludge. The concentration of sulfate was monitored during the treatment process and desulfurization was estimated to be about 34%. Microbially desulfurized crumb rubber (MDR) was then added to bitumen to produce rubberized bitumen. Performance of the rubberized bitumen was then compared with those of conventional crumb rubber modified (CRM) bitumen. To do so, Fourier transform infrared spectroscopy (FTIR), inverse gas chromatography (IGC), and rheometry were utilized. Chemical analysis of rubber particles after desulfurization showed a significant reduction of the peak at 500-540 cm^{-1}; this was attributed to the breakage of disulfide bonds after microbial desulfurization. Measurement of surface energy showed that the acid-base component of surface energy increased three times (increasing from 1.85 mJ/m^2 to 5.55 mJ/m^2) after desulfurization. Such enhancement could lead to increased interactions between rubber and bitumen reducing their separation. This was evidenced in a 68% reduction in separation index in bitumen containing microbially desulfurized rubber compared to bitumen having non-treated rubber. In addition, study results showed a 6% increase in elastic recovery, a 27% increase in resistance to moisture diffusion, a 12.5% decrease in viscosity, a 10% increase in stiffness, and a 5% increase in stress relaxation capacity compared to bitumen's having

non-treated rubber. The outcome of the study promotes resource conservation by offering a simultaneous solution for recycling of scrap tire and enhancing pavement performance.

5.2 Introduction

In 2018, almost 7% of the bitumen used worldwide was modified by polymers. According to an estimate, the valuation of the polymer-modified bitumen market in 2018 was USD 5.14 billion, and it is projected to reach USD 7.44 billion by 2026(Globenewswire, 2019). The pavement construction industry uses crumb rubber from scrap tires as an inexpensive source of polymer; In the US, the states of California, Arizona, Texas, and Florida have been among the first states implementing crumb-rubber-modified bitumen in highway pavements (Way et al., 2012). Studies have shown that adding crumb rubber in bitumen improves its thermo-mechanical properties and long-term performance (Huang et al., 2007; Liang et al., 2017b; Xiaowei et al., 2017). The use of crumb rubber in construction has increased by 15% from 2015 to 2017 (UTMA, 2017). Despite the benefits of adding rubber to bitumen, the separation of crumb rubber from bitumen at high temperatures remains a challenge (Zani et al., 2017). The size of the rubber particles, the difference in density between rubber and bitumen, and the swelling of rubber particles are factors contributing to the separation of rubber from bitumen (Shu and Huang, 2014).

Commonly used methods for applying crumb rubber to bitumen necessitate continuous agitation to prevent separation of rubber and bitumen, making this process costly. As a result, many road authorities and contractors are reluctant to incorporate crumb rubber in bitumen (Presti et al., 2018; Yu et al., 2017).

A variety of physical and/or chemical methods have been tried in efforts to address crumb rubber's inadequate dispersion and phase separation in bitumen (Liu et al., 2020; Xiang et al., 2019; Xie et al., 2019b). For example, microwave-irradiated crumb rubber in combination with bio-oil resulted in partial surface devulcanization, which enhanced the rubber-bitumen interaction and reduced the rubber-bitumen separation tendency (Hosseinnezhad et al., 2019a; Kabir et al., 2019). Previous studies have shown surface activation or partial desulfurization of rubber improves the interaction between rubber and bitumen (Hosseinnezhad et al., 2019a; Li et al., 2020; Liang et al., 2017b). However, the cost and scalability of those approaches remain an issue (Kabir et al., 2019).

A potentially low-cost approach could be microbial desulfurization of rubber. A variety of naturally occurring aerobic or anerobic microorganisms at neutral or acidic pH have been shown to desulfurize tire rubber (Cui et al., 2016; Ghavipanjeh et al., 2018; Kim and Park, 1999; Tatangelo et al., 2019). Different *Thiobacillus sp.* have been used by researchers for desulfurization of tire rubber and shown to successfully desulfurize tire rubber. It has even been reported that *Thiobacillus* desulfurization is more effective than chemical treatment (Kim and Park, 1999). Studies performed using *sphingomonous sp.* reported successful desulfurization of crumb rubber (Jiang et al., 2011). Among many

microbial treatments, *alicyclobacillus sp.* was found to be most successful in reduction of sulfur content (Yao et al., 2013). Table 1 summarizes the pertinent studies on microbial desulfurization.

Table 5-1. Microbial Desulfurization Studies Using Ground Tire Rubber

Microorganism	Amount of rubber/size	Medium	Outcome	Reference
Acidithiobacillus ferrooxidans *DSM 583*	7.5 g, <0.4 mm	DSM-medium 71, 150 ml, pH 2.1	8% (w/w) of sulfur to sulfate conversion	(Chritiansson et al., 1998)
Thiobacillus perometabolis	10 g, 0.1 mm	Mineral salt medium with yeast extract, 500 ml	0.45 % decrease in sulfur content	(Kim and Park, 1999)
S*phingomonas* sp.	2.5% (w/v), <0.4 mm	Mineral salt medium	Gel fraction of desulfurized crumb rubber increased from 4.3% to 7.3%	(Jiang et al., 2011)
S*phingomonas* sp.	2.5% (w/v), <0.1 mm	Mineral salt medium	An increase in soluble fraction of crumb rubber from 4.69% to 8.7% in 20 days	(Li et al., 2012b)
Thiobacillus sp.	<0.1 mm	Mineral salt medium	The soluble fraction of crumb rubber increased from 4.69 % to 7.63 %	(Li et al., 2012a)
Thiobacillus ferroxidans	0.355 mm and 0.18-0.25 mm, 0.5% w/v	DSMZ medium 70 without ferrous sulfate at pH 1.4, 40 ml	Sulfur content decrease by 27%	(Ghavipanjeh et al., 2018)
Alicyclobacillus sp.	5% w/v	Mineral salt medium with glucose and yeast extract; pH 2.5	Sulfur content decreased by 62.5% and the oxygen content increased by 34.9% on the surface of latex	(Yao et al., 2013)
Sphingomonas sp. and Gordonia sp	0.12 mm	Mineral salt medium with glucose, peptone and yeast extract; pH 6.5 Mineral salt medium with glucose; pH 7	Sulfur content on the surface decreased by 32.4%	(Cui et al., 2016)
Gordonia desulfuricans and Rhodococcus sp	150g	Mineral salt medium with glucose, 1.5 L	*G. desulfuricans* increased gel fraction from 2.3 to 3.3 and *Rhodococcus sp.* increased gel fraction from 2.3 to 2.9	(Tatangelo et al., 2019)
Bacillus cereus TISTR 2651	2.5 g, 2.88-2 mm	Mineral medium with beef extract and glucose; pH 7.0, 100 ml	26.44% removal of sulfur	(Kaewpetch et al., 2019)

We hypothesize that microbial treatment of scrap tire rubber by a desulfurization process enhances bitumen-rubber interaction and reduces separation. It is expected that the broken crosslinked di-sulfide bond become more flexible due to the availability of unreacted and unsaturated bonds in rubber. This in turn can enhance interaction with bitumen molecules, reducing phase separation and thereby reducing the energy needed for continuous agitation. While multiple studies have investigated the efficacy of microbial treatment for desulfurization of rubber, to the best of our knowledge, the application of desulfurized crumb rubber in bitumen has not been examined. This is the first attempt to use desulfurized crumb rubber in bitumen to improve the properties of rubberized asphalt while facilitating the use of recycled rubber.

5.3 Materials and Methods

5.3.1 Materials and preparation of bitumen containing crumb rubber

The bitumen used in this study was PG 64-22 (Table 2), obtained from Holy Frontier Company in Phoenix, Arizona. Crumb rubber of <0.25 mm was acquired from Crumb Rubber Manufacturers, Mesa, Arizona. Bitumen samples were prepared by introducing 15% treated (MDR) or un-treated (CR) rubber to 85% bitumen using a bench top high shear mixer at 3000 rpm at 165 °C. and named microbially desulfurized rubber modifier (MDRM) and crumb rubber modifier (CRM) respectively. A crumb rubber (CR) sample with mineral medium without microbiome was also added for comparison; this sample is referred to as CRM plus medium. The mineral medium used for microbial growth was left in place, and it was not centrifuged.

Table 5-2. General Properties of The PG 64-22 Bitumen

Specific Gravity @15.6 ºC	1.041
Cleveland Open Cup method Flash point	335 ºC
Mass change after RTFO	-0.013
Absolute Viscosity @ 60 ºC	179 Pa.s
Stiffness @-12ºC @ 60s	71.67 MPa

5.3.2 Experiment Setup for Microbial Desulfurization of Crumb Rubber

Microbial desulfurization was performed in 500 mL Erlenmeyer flasks (Corning, Corning City, NY, USA) containing 200 mL mineral medium. The initial experiment conditions were as follows: 50 g crumb rubber (CR), 50 g CR + 10 g soil, and 50 g CR + 10 mL waste activated sludge. It should be noted that the CR used was not sterilized before the experiments. The soil and the waste activated sludge served as an added source of desulfurizing microorganisms. Bitumen was prepared using microbially desulfurized crumb rubber (MDR) from the experiment condition with activated sludge after 36 days of incubation. Further detail on the composition of the mineral medium can be found in the work by (Delgado et al., 2014); however, we also added 0.2 mM $FeSO_4$, 25 mM sodium acetate, and 6.3 mM $Na_2S_2O_3 \bullet 5H_2O$. The medium was buffered with 10 mM potassium phosphate and had an initial pH of 7. The soil was collected from a residential area near Arizona State University, Tempe, AZ. The waste activated sludge was obtained from The Mesa Northwest Water Reclamation Plant, Mesa, AZ. All conditions were tested in duplicates. The flasks were agitated on a rotary shaker at 170 RPM and incubated at 34°C. The pH was monitored and adjusted to ~ 7 when it decreased below 6.

A solution containing NaCl, KH_2PO_4, and NH_4Cl was added every 10 days to ensure the availability of nutrients. Medium was re-added to replace the liquid taken during sampling. Samples for sulfate analyses were prepared from 1 mL of liquid contents from the incubating flasks. The liquid samples were centrifuged at 4°C and 156000 rcf for 6.5 min and filtered through 0.2 µm SY13VF syringe filters (Advanced Microdevices PVT. LTD., Ind Area, India. The sulfate concentration was analyzed using a Metrohm 930 Compact IC Flex instrument with a Metrosep A Supp 5-150/4.0 column and A Supp 5 100X carbonate-based eluent. The eluent flow rate was 0.7 mL/min, the temperature was 30°C, and the total analysis time was 19 min. Calibration curves in the range of 0.1-100 mg/L sulfate were made with the Custom Anion Mix: 3 (Cat. No. REAIC1035, Metrohm, Riverview, FL, USA). The samples were diluted 1:10 or 1:20 as appropriate.

5.3.3 Attenuated Total Reflectance Fourier Transform Infrared Spectroscopy (ATR-FTIR)

FT-IR Spectroscopy was performed using a Bruker FT-IR instrument. The instrument was used in absorbance mode to track breakage of disulfide bonds and the formation of new covalent bonds during the microbial desulfurization of rubber. For detection of any change, a mid-infrared-range diamond ATR was used. A range of 4000 cm^{-1} to 400 cm^{-1} wavenumbers were selected. Samples were splashed in acetone and dried before detection.

5.3.4 Surface Energy Measurement

Surface energy was measured using inverse gas chromatography (IGC). This technique was conducted using an IGC-Surface Energy Analyzer, IGC-SEA (Surface Measurement Systems Ltd., Allentown, PA, USA). Before surface energy analysis, samples were preconditioned for 120 min using helium passing the chamber at the rate of 10 scc/m at zero humidity, to remove any impurities from the surface of rubber. The specifics of determining the IGC surface energy components can be found elsewhere (Mohammadi-Jam and Waters, 2014). To begin the procedure of determining the surface energy, the samples were placed in silanized glass columns with an inner diameter of 4 mm. Next, silanized glass wool was used to fix each sample's position. Throughout the experiment, the temperature of the columns was kept stable at 30°C. Four alkane probes (nonane, octane, heptane, and hexane) were used for dispersive energy. Acid-base energy was determined using two polar probes: dichloromethane for Lewis acid, and ethyl acetate for Lewis base. All probes were run across the column, along with helium as a carrier gas, permitting enough time for the entire probe to elute through the column. Data analysis was performed using IGC-SEA Advanced Analysis Software version 1.4.4.1.

5.3.5 Rotational Viscosity

Viscosity of the rubber samples was measured using a Brookfield rotational viscometer, DVII-Ultra, according to the standard (ASTM-D-4402, 2015). A standard smooth spindle (SC4-27) was used for 10 minutes to apply a continuous shear to measure

viscosity. Four viscosity measurements were completed at four temperatures (135°C, 150°C, 165°C, and 180°C), using a shearing speed of 20 rpm.

5.3.6 Bending Beam Rheometer (BBR)

To determine the subzero temperature behavior of bitumen, a BBR is widely used (Marasteanu and Basu, 2004). The test is a three-point bending test of a bitumen beam with fixed length, width, and height performed under a cold bath of ethanol. The test measures flexural creep stiffness (S) and stress relaxation capacity (m-value) by applying a load of 980 ± 50 mN for the duration of 240s at the midpoint of the beam. The beam deflection (d) is measured at the center with respect to loading time using a linear variable differential transducer (LVDT) following the Superpave™ specification (AASHTO-T-313, 2019a). The stress relaxation value tells us the bitumen's ability to prevent thermal cracking triggered by a sudden drop of temperature in a cold climate environment. A testing temperature of -12°C was selected for this experiment. Using the deformation data during the loading period, the stiffness was determined using Equation 5-1:

$$S(t) = \frac{PL^3}{4bh^3\partial(t)} \quad (5\text{-}1)$$

where:

P = applied constant load (100 g or 0.98 N)

L = distance between beam supports (102 mm)

b = beam width (12.5 mm)

h = beam thickness (6.25 mm)

S(t) = bitumen stiffness at a specific time, MPa

∂(t) = deflection at a specific time, mm

5.3.7 Dynamic Shear Rheometer (DSR)

An Anton-Paar DSR was used to obtain a specified oscillation rate of 10 rad/s, which is relevant to realistic traffic conditions with a speed of 90 km/hr (AASHTO-T-315, 2019). The acquired data were then applied to calculate the complex shear modulus (G*) and phase angle (δ) to determine the separation index. In addition, the rutting performance of the modified bitumen was evaluated using the method of multiple stress creep recovery (MSCR) at 52°C, as outlined in the AASHTO-T-315 standard. In all cases, an 8-mm plate with 2-mm gap was used.

5.3.8 Separation Tendency Test

The separation tendency of rubber particles from the bitumen is an issue that needs attention for wet-mixing of bitumen. To determine the separation tendency, the samples were heated to 163°C to make them sufficiently fluid to pour in aluminum tubes and then tube tops were sealed to bar air from entering. Then, they were placed vertically in a sample holder rack. Tubes were then placed inside an oven at 163°C for 48 hours. After 48 hours, the rack was put in a freezer for 4 hours at -18°C. Upon cooling the tubes were taken out and cut into three equal segments ((ASTM-D7173, 2014)). The middle section was discarded, and the bottom and top sections were stored for tests with the dynamic shear rheometer at 58°C. After calculating the complex modulus and phase

angle, these data were applied to obtain the segregation index (SI) according to Equation 2 ((Shatanawi et al., 2009)).

$$SI=\frac{\left(\frac{G^*}{sin\delta}\right)max-\left(\frac{G^*}{sin\delta}\right)avg}{\left(\frac{G^*}{sin\delta}\right)_{avg}} \quad (5\text{-}2)$$

where:

G* = complex shear modulus and

δ = phase angle

5.3.9 Softening Point Difference

Another method to test separation behavior is to test the softening point difference between the top and bottom portions of cigar tube test samples. The softening point is a temperature at which bituminous sample fails to support the weight of a 3.5-g steel ball. Widely used in Europe and Asia, this method can be used to compare the top and bottom parts of cigar tube test samples. To perform this test, two horizontal disks of poured bitumen supporting two steel balls in brass rings are heated at a controlled rate in a liquid bath. The softening point is reported as the mean of the temperatures at which the steel balls are allowed to fall a distance of 25 mm (1.0 inch) (ASTM-D36, 2014).

5.3.10 Moisture-Induced Shear-Thinning Index (MISTI)

An Anton-Paar dynamic shear rheometer was used at a ramping shear rate of 0.1 to 420 1/s to determine the change in viscosity of the samples, especially the shear thinning slope using an 8-mm spindle. To prepare a sample, modified bitumen was blended with glass beads of 100-micron diameter by 50% weight of binder. The glass

bead diameter was chosen to be several orders of magnitude smaller than the sample thickness. Ten samples each weighing 0.30 grams were prepared. Five of the samples were tested in dry condition (unconditioned) and the other five were conditioned in distilled water at 60°C for 24 hours. After taking the conditioned samples out of water, the samples were surface dried and placed for trimming in the DSR at 25°C. The test temperature was set to 64°C, as the optimal initial viscosity for observing the shear-thinning slope was approximately 1 Pa.s for the samples at that temperature. This was done to observe the effect of moisture damage between aggregate and binder. The average of three replicates was used to determine the MISTI, which is defined as the ratio of thinning slopes of the unconditioned to moisture-conditioned samples.

5.4 Results and Discussion

5.4.1 Microbial desulfurization of crumb rubber

Sulfate concentrations were measured at regular intervals to monitor the rates and extent of microbial desulfurization. Figure 5-1A shows the time-course sulfate concentrations in the flasks containing 50 g crumb rubber (CR). Note that some spent medium still remained on the rubber as we did not centrifuge or dry out the rubber. As seen in Figure 1A, sulfate concentrations substantially increased during incubation in all three conditions. The rates of sulfate release were fastest in the flasks with 50 g CR + waste activated sludge; this condition also reached the highest final concentration of ~2000 mg/L sulfate after 36 days of incubation. The amount of sulfate released in CR with waste activated sludge was 35% higher than in the condition with soil and 37% higher than in the condition with medium only. These data strongly indicate that

microorganisms capable of breaking the di-sulfide bonds in the rubber are easily enriched from aerobic environmental samples (e.g., soils, wastewater sludge) and can be effectively stimulated to desulfurize CR by providing them with nutrients and a source of carbon.

The sulfate concentrations were measured immediately after re-adding the medium and 7 days later. Figure 5-1 B is an analysis of the amount of sulfur released per gram of crumb rubber from the experiments in Figure 1A. It can be seen that the highest release in sulfur per gram crumb rubber was achieved in the samples with 50 g CR+ sludge (Figure 5-1B).

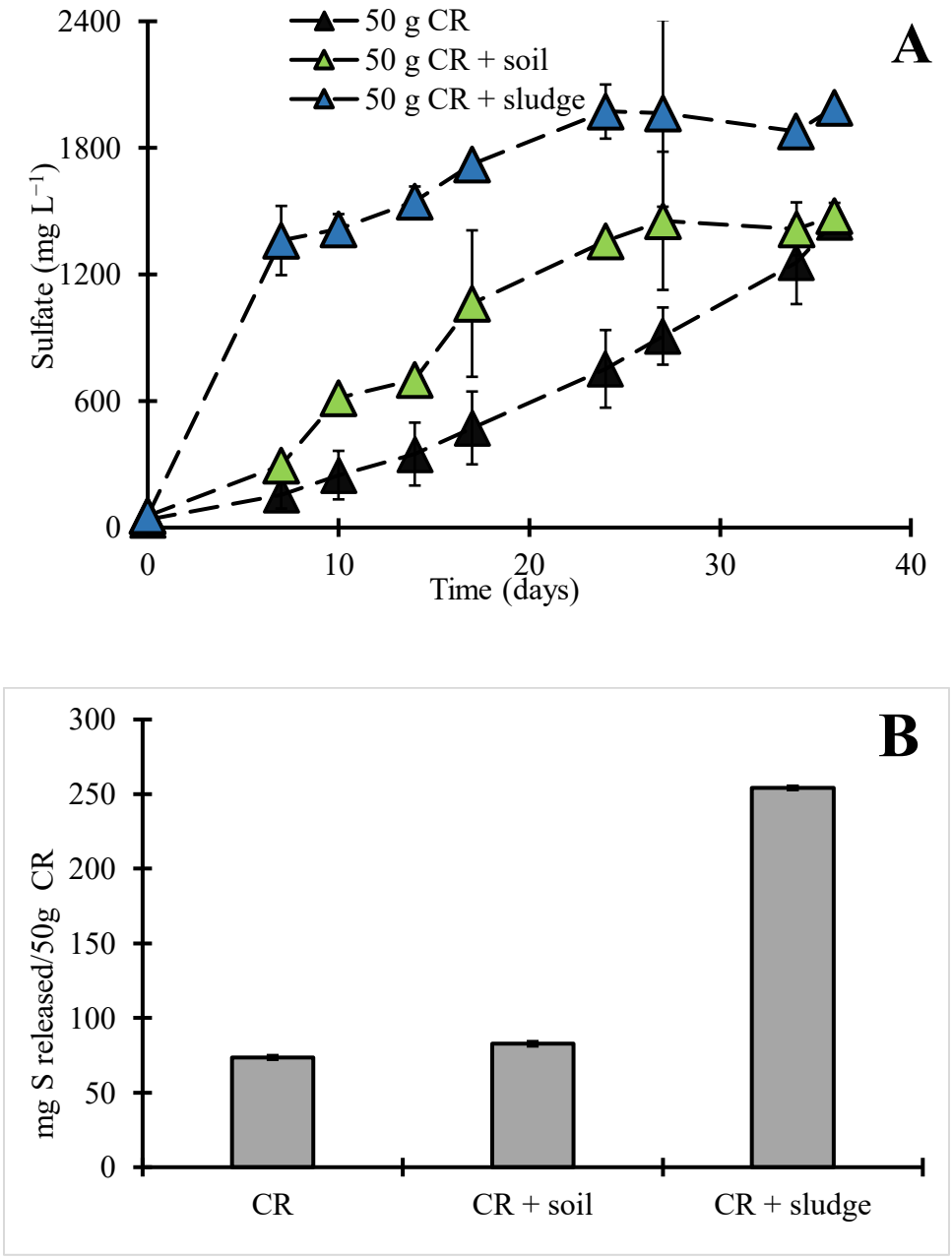

Figure 5-1 A) Sulfate Concentrations Released During Microbial Desulfurization of 50 g, and (B) Sulfur Released Per 50 Gram Crumb Rubber (CR).

In panel A, the inoculum were the microbes from the crumb rubber and/or microbes from soil and wastewater activated sludge. The data area in A shows average

with standard deviation of sample replicates. In panel B, the inoculum of sulfate release per 50 gram of crumb rubber is shown.

Sulfur content in tires is found to be 1.5~1.6 wt.% of crumb rubber ((de Marco Rodriguez et al., 2001; Susa and Haydary, 2013)). Table 3 shows an estimate of sulfur release and percentage of desulfurization in crumb rubber, assuming 1.5 wt.% of sulfur content is present in rubber. Table 3 shows that the percent of desulfurization in the samples with only crumb rubber and medium is almost 10%. This indicates limited activity of microorganisms, as the crumb rubber samples were not washed before the experiment started. Crumb rubber samples with soil microbes did not show much improvement in desulfurization in comparison to crumb rubber samples in medium only, whereas crumb rubber samples with activated sludge showed almost 34 percent of desulfurization, which was a significant indicator of the success of microbial activity on rubber.

Table 5-3. Sulfur Release and Estimated Percent of Desulfurization

Sample Name	Sample weight (g)	Sulfur content (mg)	Sulfur Release (Fig 1)	% desulfurization
CR	50	750	73.62	9.82
CR + soil	50	750	82.71	11.03
CR + sludge	50	750	254.17	33.89

5.4.2 Chemical Characterization

FTIR spectra of changes in microbially desulfurized rubber (MDR) in comparison to non-desulfurized crumb rubber (CR) can be seen in Figure 2. Spectral analysis of microbially desulfurized rubber showed a significant reduction of weak di-sulfide bonds (S-S) in the range 500-540 cm^{-1} in comparison to crumb rubber. This weak di-sulfide bond appears in vulcanized rubber as a crosslinking agent (Segneanu et al., 2012). The reduction in peak can be credited to partial desulfurization at the rubber's surface due to microbial activity. In CR, the characteristic peak of butadiene is visible in the range of 1000-1015 cm^{-1} (NIST, 2019). This peak is weaker in the spectra for MDR (NIST, 2019). A significant reduction in a medium peak in the range of 1350-1470 cm^{-1} is observed in microbially desulfurized rubber in comparison to crumb rubber. This reduction can be attributed to the bending vibration due to methyl group deformation (Bacher, 2001). C-H stretching vibration in the range of 2800-3100 cm^{-1} is lower in MDR than in CR, indicating that there has also been some partial devulcanization taking place due to microbial activity on the surface of crumb rubber.

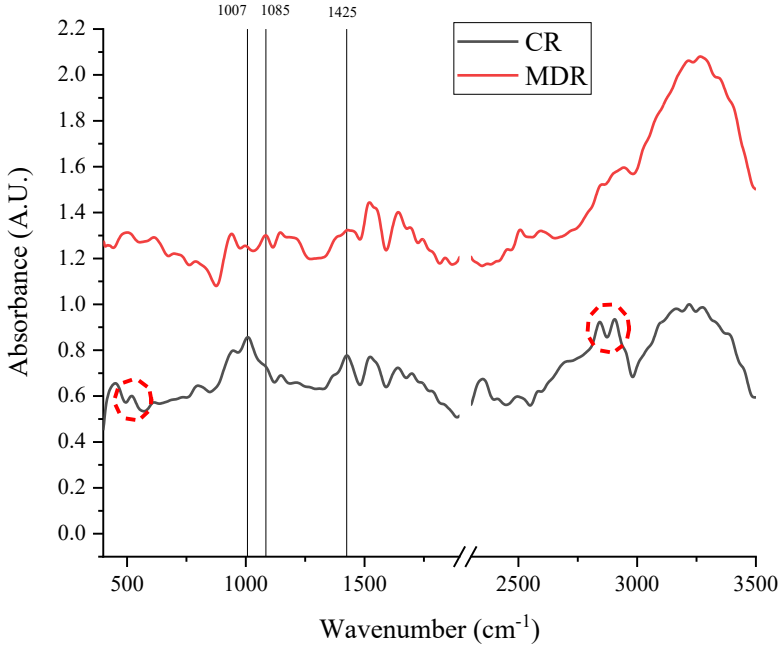

Figure 5-2. FTIR Spectra of Control Crumb Rubber (CR) and Microbially Desulfurized Rubber (MDR) Using Microbes from Wastewater Sludge.

5.4.3 Surface energy measurement

The surface energy of samples was measured using inverse gas chromatography (IGC). The IGC results demonstrated that the total surface energy of rubber particles increased by 3.18% due to desulfurizing of rubber. This was more clearly apparent for the acid-base part of surface energy, which was 3.7 mJ/m^2 higher after desulfurizing. The observed increase in surface energy profile could be due to partial devulcanization from breakage of disulfide bonds via microbial treatment. At 0.02 n/nm coverage, the acid-base component was 1.85 mJ/m^2 for control rubber; this value was increased by 3.7 mJ/m^2 (197%) to 5.5 mJ/m^2 for desulfurized rubber (Table 5-4). This improvement is

significant, as it has been documented that activation of rubber leads to an increase in the acid-base component of surface energy (Hosseinnezhad et al., 2019a). Such an increase in the acid-base component can promote interactions with bitumen molecules, reducing the phase separation (segregation of rubber particles) in the bituminous matrix (Hosseinnezhad et al., 2019).

Table 5-4. Surface Energy (mJ/m^2) of Control (CR) and Desulfurized (MDR) Rubber at 0.02 n/nm Surface Coverage

Sample	Dispersive	Acid-base	Total Surface Energy
CR	62.89	1.85	64.74
MDR	61.25	5.55	66.80

5.4.4 Viscosity Measurements

Figure 5-3 shows the viscosity results for crumb rubber modifier (CRM), CRM+medium, and microbially desulfurized rubber modifier (MDRM) at 135°C, 150°C, 165°C and 180°C. A considerable reduction in viscosity was observed in the case of desulfurized rubber compared to non-desulfurized rubber, at all testing temperatures. For instance, the viscosity at 135°C at 20 rpm in microbially desulfurized rubber modifier was 12.5% lower compared to crumb rubber modifier. The lower viscosity and consequent improved flowability of the microbially desulfurized rubber modifier are probably due to partial breaking of crosslinks and disulfide bonds in the crumb-rubber-modified bitumen.

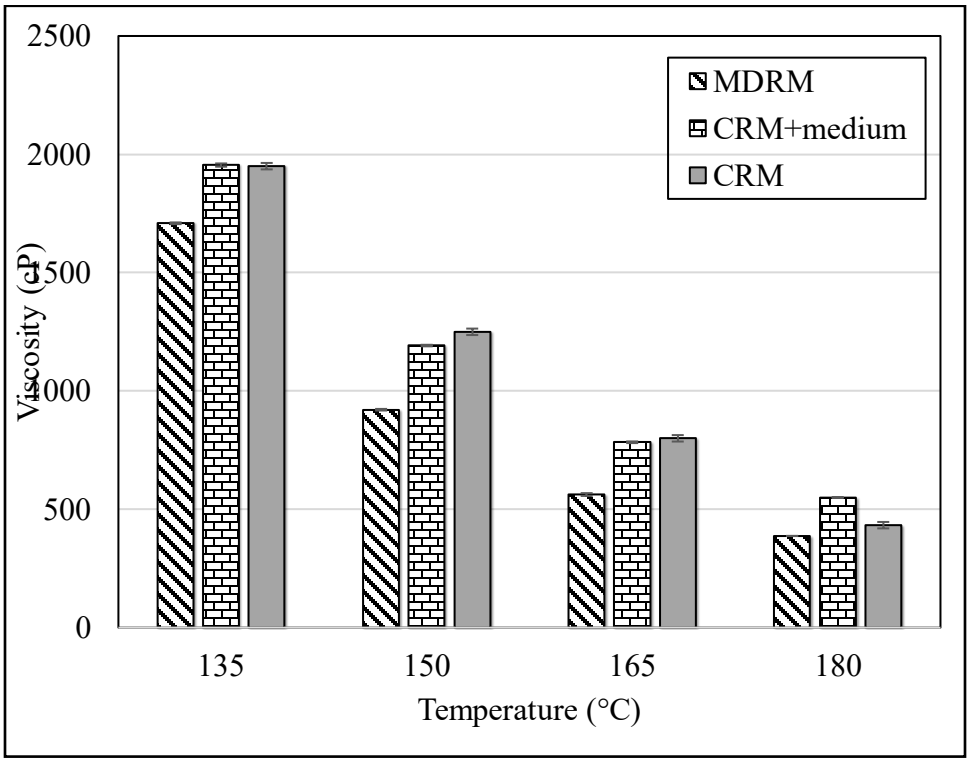

Figure 5-3. Viscosity of Desulfurized and Non-Desulfurized Rubber-Modified Bitumen

5.4.5 Thermal Cracking Properties (Low Temperature)

Traditional blending with rubber has shown to have decreased stiffness and increased m-value with increasing crumb-rubber percentage (Lee et al., 2008). Figure5- 4 shows that due to the presence of traditionally blended crumb rubber, stiffness and m value both decreased in crumb rubber modifier (CRM) in comparison to neat bitumen. However, with microbially desulfurized rubber-modified bitumen, stiffness increased up to 10% and the stress relaxation value increased by 5% compared to the traditional blend of crumb rubber modifier. This increase in stress relaxation capacity indicates that

surface desulfurization of rubber using microbial treatment successfully enhanced the binder's ability to resist thermal cracking at low temperatures.

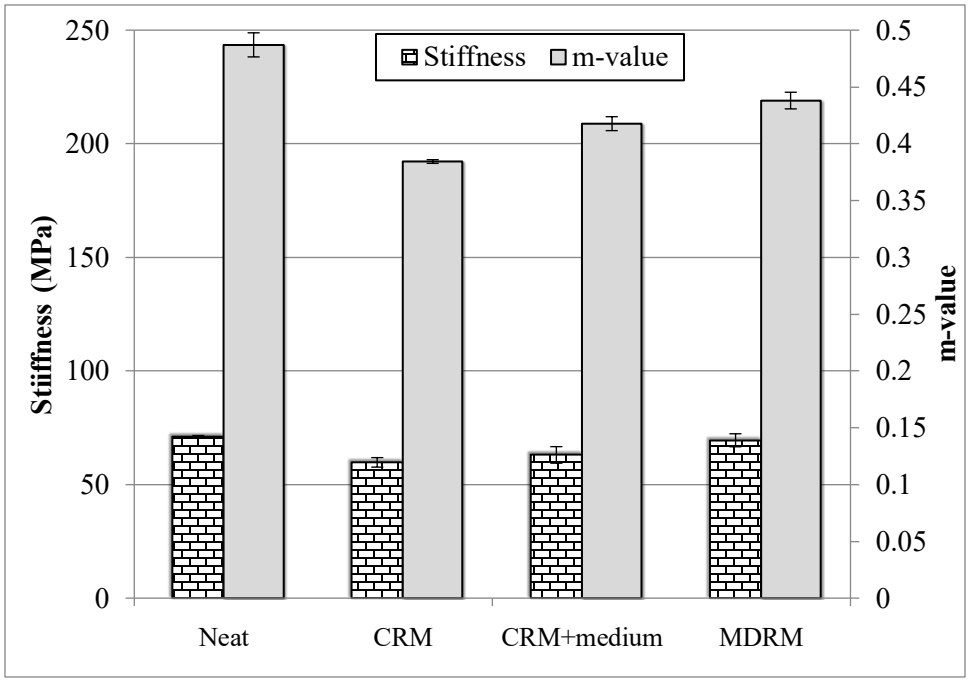

Figure 5-4. Stiffness and m-Value Results for Samples At -12°C Using The BBR

5.4.6 Separation Tendency

The separation index (SI) for all desulfurized and non-desulfurized samples was calculated using data from the cigar tube test, as shown in Figure 5-5. Figure 5-5 shows that the SI value of desulfurized sample (MDRM) is substantially lower than the SI of the traditional blend of crumb rubber modifier (CRM). Figure 5-5 also shows that there was no substantial reduction in segregation in the sample that added only medium without any microorganisms to crumb rubber. This indicates success of the desulfurizing method to enhance the compatibility of rubber and the bitumen. Microbially desulfurized rubber-modified bitumen has a separation index 68% lower than CRM. This indicates better absorption and dispersion of rubber particles in the bitumen matrix. A previous study that

surface-activated rubber using a bio-modifier and a microwave treatment improved the separation index by 86% compared to CRM (Hosseinnezhad et al., 2019a).

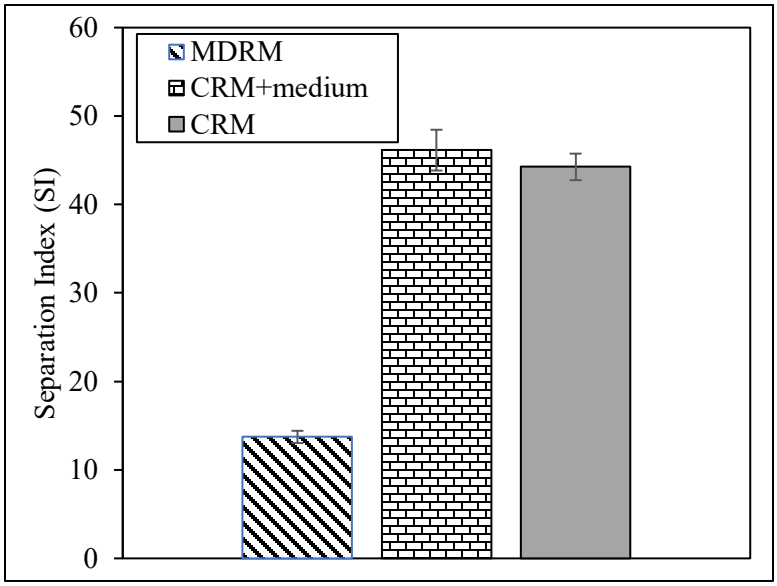

Figure 5-5. Separation Index from Cigar Tube Test Data for Desulfurized and Non-Desulfurized Rubber Modifiers

Separation tendency was also measured by the widely used softening point test. In this case, the difference in the softening point between the top and bottom portions of the cigar tube was measured. Figure 5-6 shows the difference between the softening points of the top and bottom sections. The microbially desulfurized crumb rubber modifier has an average 1.75°C difference between its top and bottom segments, which is within the acceptable range of 5°C, whereas crumb rubber modifier + medium has a softening point difference between top and bottom sections of 6.75°C, and crumb rubber modifier has a softening point difference between top and bottom sections of 7.5°C. This is another

indication of the successful partial breaking of the three-dimensional network in rubber using microbial desulfurization.

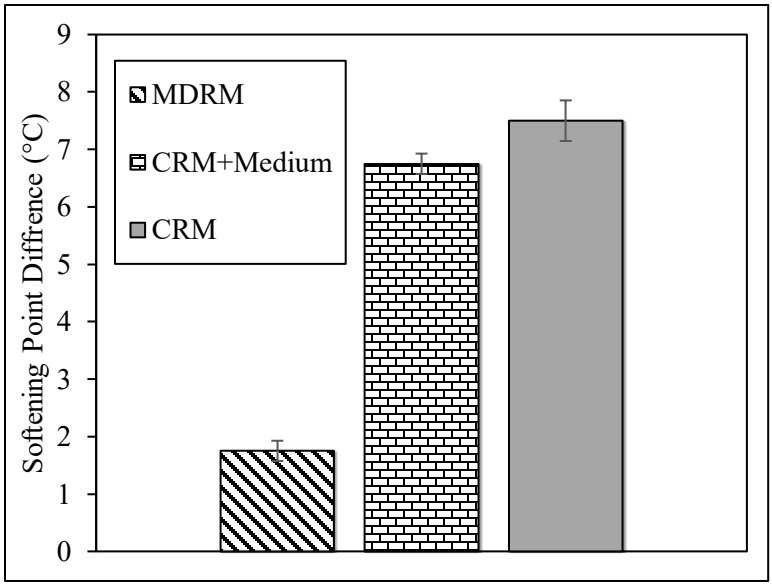

Figure 5-6. Softening Point Difference Between Top and Bottom Portions of Cigar Tube Test, for All Modifiers

5.4.7 Multiple Stress Creep Recovery (MSCR)

MSCR data from Figure 5-7 shows that the strain accumulation with time is 28% lower in microbially desulfurized rubber modifier (MDRM) compared to crumb rubber modifier (CRM). Lower strain accumulation means higher elasticity, which indicates microbial activity not only partially desulfurized the particles, the dangling bonds must have re-vulcanized and been better adsorbed in the bitumen. This indicates that microbially desulfurized rubber is less susceptible to rutting than crumb rubber.

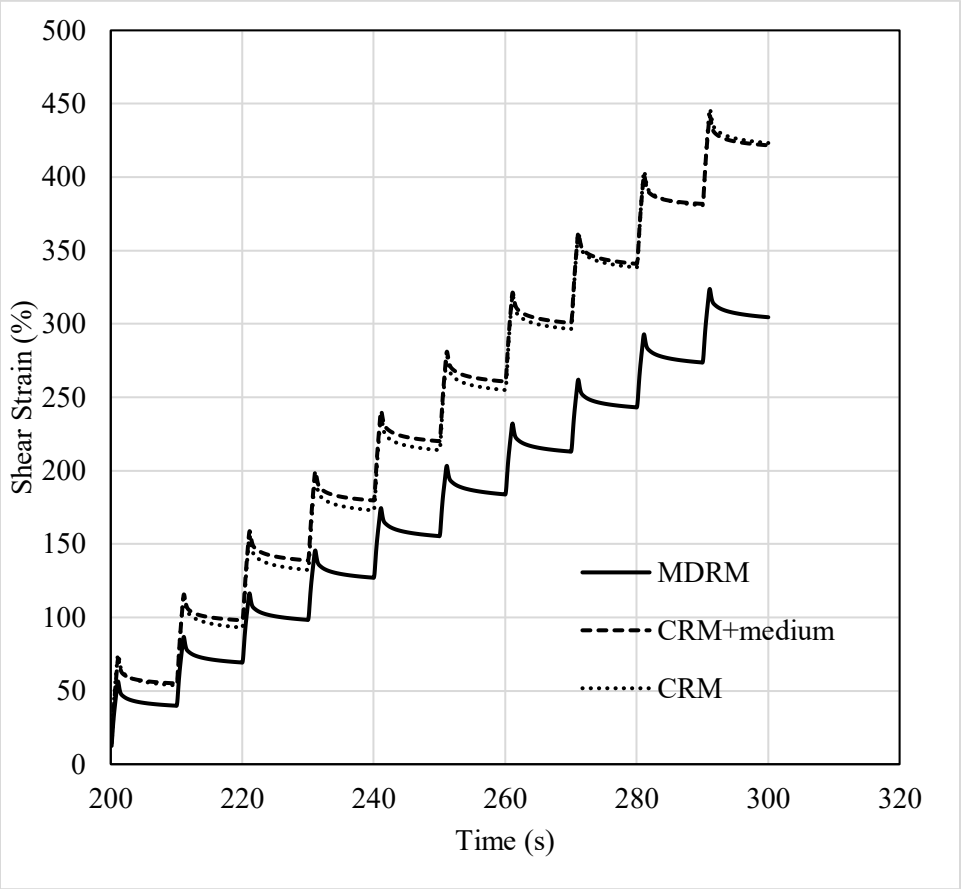

Figure 5-7. Strain Accumulation Data from MSCR Test for Desulfurized and Non-Desulfurized Rubber Modifiers

Figure 5-8 shows the Jnr values and percent recovery obtained in an MSCR test. It is clear that the Jnr values of crumb rubber modifier (CRM) and CRM+medium are almost equal. In terms of percent recovery at 3.2kPa, it was found that CRM has an average percent recovery of 31%, whereas microbially desulfurized rubber modifier has an average percent recovery of 37%. Considering the other benefits, this increase in percent recovery is significant at the bitumen level and proves the efficacy of microbial desulfurizing.

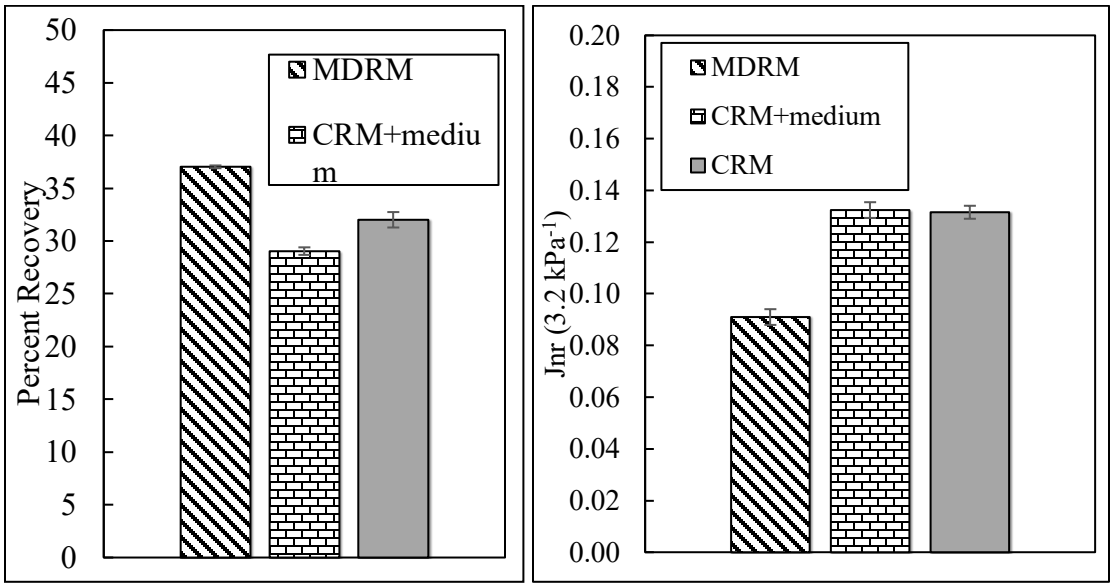

Figure 5-8. Percent Recovery and Jnr Data from MSCR Test for Non-Desulfurized Rubber and Desulfurized Rubber Modifiers

5.4.8 Moisture-Induced Shear-Thinning Index

To evaluate the effect of moisture on binder-aggregate interactions in the crumb rubber modifier (CRM) and microbially desulfurized rubber modifier (MDRM) samples, a MISTI test was performed. Figure 5-9 shows the data for the unconditioned and moisture-conditioned shear-thinning behavior of all rubber-modified bitumen samples.

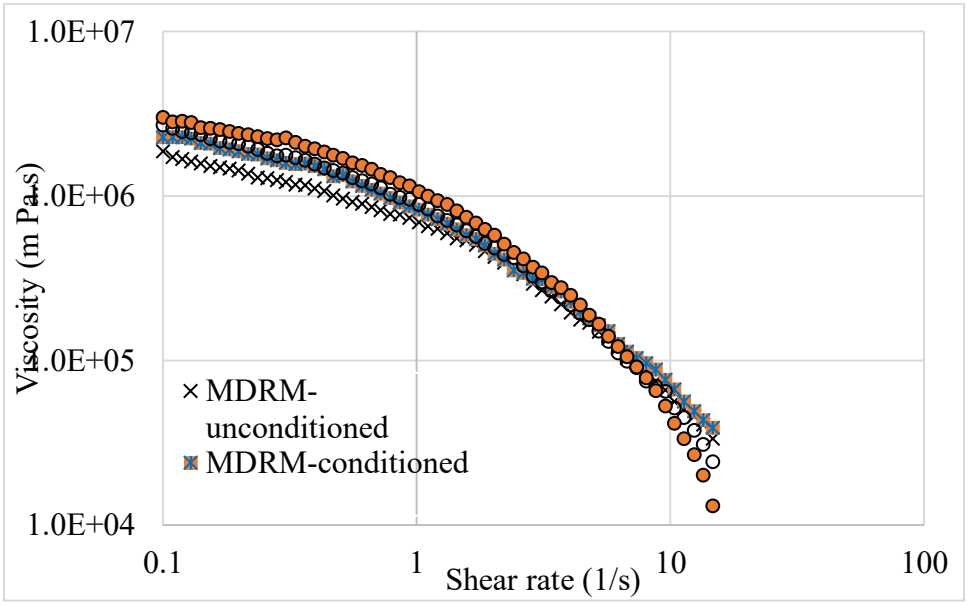

Figure 5-9. A Plot of Unconditioned and Moisture-Conditioned Shear-Thinning Behavior for All Rubber Modifiers

Table 5-5 shows the moisture-induced shear-thinning index for crumb rubber modifier (CRM) and for microbially desulfurized rubber modifier (MDRM). Both samples showed a steeper slope after moisture conditioning, with the changes being more evident in the microbially devulcanized sulfurized samples. The latter could be attributed to the presence of freed-up sulfur due to the microbes' activity and breakage of disulfide bonds in microbially desulfurized rubber; upon exposure to water, this freed-up sulfur could give rise to the formation of acidic compounds. Acidic compounds have been implicated in moisture damage (Fini et al., 2019b; Hung et al., 2019b). Ensuring the complete removal of sulfur from microbially desulfurized rubber before introducing it to bitumen could alleviate the issue.

Table 5-5. Absolute Value of Power-Law Slopes and MISTI Values for Control Crumb Rubber Modifier (CRM) and Microbially Desulfurized Rubber Modifier (MDRM)

		Unconditioned	Conditioned
CRM	Power-Law Slope	1.896	1.93
	COV (3 samples)	4.62%	3.85%
	MISTI (Unconditioned/Conditioned)		**98%**
MDRM	Power-Law Slope	1.05	1.48
	COV (3 samples)	6.6%	3.69%
	MISTI (Unconditioned/Conditioned)		**71%**

5.5 Conclusion

This paper investigates the merits of using microbially desulfurized rubber in bitumen to reduce the rubber-bitumen separation. Microbes from a wastewater treatment sludge were collected and used to treat crumb rubber particles made from scrap tire. The microbial exposure continued for 36 days; during the exposure period, the sulfate concentration was regularly measured. It was found that microbially desulfurized rubber reached an average concentration of ~2000 mg/L of sulfur. The percent of desulfurization in crumb rubber using activated sludge was found to be ~34%. Chemical analysis of rubber particles showed a significant reduction of the peak between 500-540 cm-1, associated to disulfide bonds (S-S) of vulcanized rubber. The reduction in the above-mentioned peak was attributed to breakage of disulfide bonds leading to activation of the rubber's surface, as evidenced by an increase in the acid-base component of the rubber's surface energy by 3.7 mJ/m2. The increase in surface energy promoted the interaction of rubber particles with bitumen, which reduced the segregation of rubber and bitumen by

68%. The reduction in the extent of segregation was also measured based on the difference in softening point of samples taken from the top and bottom sections of the cigar tube test and was found to be less than 2°C. Overall, the bitumen containing microbially treated rubber showed enhanced rheological properties. For instance, the stiffness and stress relaxation capacity of bitumen containing desulfurized rubber was found to be 10% and 5% higher than those of the control sample, respectively. Also, the elastic recovery of bitumen containing desulfurized rubber was found to be 6% higher than control, and the viscosity of bitumen containing desulfurized rubber was found to be 12.5% lower than that of the control sample. Based on the study results, microbially desulfurized rubber (MDR) can be a promising candidate for use in asphalt to improve pavement performance and facilitate recycling and resource conservation.

5.6 References

AASHTO-T-313, 2019a. Standard Method of Test for Determining the Flexural Creep Stiffness of Asphalt Binder Using the Bending Beam Rheometer (BBR).

AASHTO-T-315, 2019. Standard Method of Test for Determining the Rheological Properties of Asphalt Binder Using a Dynamic Shear Rheometer (DSR).

ASTM-D36, 2014. Standard test method for softening point of bitumen (ring-and-ball apparatus). ASTM International West Conshohocken, PA.

ASTM-D7173, 2014. Standard Practice for Determining the Separation Tendency of Polymer from Polymer Modified Asphalt. ASTM.

ASTM-D-4402, 2015. Standard test method for viscosity determination of asphalt at elevated temperatures using a rotational viscometer, American Society for Testing and Materials.

Bacher, A.D., 2001. Infrared Spectroscopy Table. https://www.chem.ucla.edu/~bacher/General/30BL/IR/ir.html.

Chritiansson, M., Stenberg, B., Wallenberg, L., Holst, O., 1998. Reduction of surface sulphur upon microbial devulcanization of rubber materials. Biotechnology letters 20(7), 637-642.

Cui, X., Zhao, S., Wang, B., 2016. Microbial desulfurization for ground tire rubber by mixed consortium-Sphingomonas sp. and Gordonia sp. Polymer degradation and stability 128, 165-171.

de Marco Rodriguez, I., Laresgoiti, M., Cabrero, M., Torres, A., Chomon, M., Caballero, B., 2001. Pyrolysis of scrap tyres. Fuel processing technology 72(1), 9-22.

Delgado, A.G., Fajardo-Williams, D., Popat, S.C., Torres, C.I., Krajmalnik-Brown, R., 2014. Successful operation of continuous reactors at short retention times results in high-density, fast-rate Dehalococcoides dechlorinating cultures. Applied microbiology and biotechnology 98(6), 2729-2737.

Fini, E.H., Hung, A.M., Roy, A., 2019b. Active Mineral Fillers Arrest Migrations of Alkane Acids to the Interface of Bitumen and Siliceous Surfaces. ACS Sustainable Chemistry & Engineering 7(12), 10340-10348.

Ghavipanjeh, F., Rad, Z.Z., Pazouki, M., 2018. Devulcanization of ground tires by different strains of bacteria: optimization of culture condition by taguchi method. Journal of Polymers and the Environment 26(8), 3168-3175.

Globenewswire, 2019. Bitumen Market To Reach USD 112.01 Billion By 2026: Reports And Data. https://www.globenewswire.com/news-release/2019/04/11/1802979/0/en/Bitumen-Market-To-Reach-USD-112-01-Billion-By-2026-Reports-And-Data.html. (Accessed 11 April, 2020 2020).

Hosseinnezhad, S., Kabir, S.F., Oldham, D., Mousavi, M., Fini, E.H., 2019a. Surface functionalization of rubber particles to reduce phase separation in rubberized asphalt for sustainable construction. Journal of Cleaner Production 225, 82-89.

Huang, Y., Bird, R.N., Heidrich, O., 2007. A review of the use of recycled solid waste materials in asphalt pavements. Resources, conservation and recycling 52(1), 58-73.

Hung, A.M., Pahlavan, F., Shakiba, S., Chang, S.L., Louie, S.M., Fini, E.H., 2019b. Preventing Assembly and Crystallization of Alkane Acids at the Silica–Bitumen Interface To Enhance Interfacial Resistance to Moisture Damage. Industrial & Engineering Chemistry Research 58(47), 21542-21552.

Jiang, G., Zhao, S., Li, W., Luo, J., Wang, Y., Zhou, Q., Zhang, C., 2011. Microbial desulfurization of SBR ground rubber by Sphingomonas sp. and its utilization as filler in NR compounds. Polymers for Advanced Technologies 22(12), 2344-2351.

Kabir, S.F., Mousavi, M., Fini, E.H., 2019. Selective adsorption of bio-oils' molecules onto rubber surface and its effects on stability of rubberized asphalt. Journal of Cleaner Production, 119856.

Kaewpetch, B., Prasongsuk, S., Poompradub, S., 2019. Devulcanization of natural rubber vulcanizates by Bacillus cereus TISTR 2651. Express Polymer Letters 13(10), 877-888.

Kim, J.K., Park, J.W., 1999. The biological and chemical desulfurization of crumb rubber for the rubber compounding. Journal of applied polymer science 72(12), 1543-1549.

Lee, S.-J., Akisetty, C.K., Amirkhanian, S.N., 2008. The effect of crumb rubber modifier (CRM) on the performance properties of rubberized binders in HMA pavements. Construction and Building Materials 22(7), 1368-1376.

Li, B., Zhu, X., Zhang, X., Yang, X., Su, X., 2020. Surface area and microstructure of microwave activated crumb rubber modifier and its influence on high temperature properties of crumb rubber modifier binders. Materials Express 10(2), 272-277.

Li, Y., Zhao, S., Wang, Y., 2012a. Improvement of the properties of natural rubber/ground tire rubber composites through biological desulfurization of GTR. Journal of Polymer Research 19(5), 9864.

Li, Y., Zhao, S., Wang, Y., 2012b. Microbial desulfurization of ground tire rubber by Sphingomonas sp.: a novel technology for crumb rubber composites. Journal of Polymers and the Environment 20(2), 372-380.

Liang, M., Xin, X., Fan, W., Ren, S., Shi, J., Luo, H., 2017b. Thermo-stability and aging performance of modified asphalt with crumb rubber activated by microwave and TOR. Materials & Design 127, 84-96.

Liu, B., Li, J., Han, M., Zhang, Z., Jiang, X., 2020. Properties of polystyrene grafted activated waste rubber powder (PS-ARP) composite SBS modified asphalt. Construction and Building Materials 238, 117737.

Marasteanu, M.O., Basu, A., 2004. Stiffness m-value and the Low Temperature Relaxation Properties of Asphalt Binders. Road Materials and Pavement Design 5(1), 121-131.

Mohammadi-Jam, S., Waters, K., 2014. Inverse gas chromatography applications: A review. Advances in colloid and interface science 212, 21-44.

NIST, 2019. NIST Chemistry WebBook, SRD 69. https://webbook.nist.gov/cgi/cbook.cgi?Value=1015&VType=Vibe&Formula=&AllowExtra=on&Units=SI&cIR=on. 2019).

Presti, D.L., Izquierdo, M., del Barco Carrión, A.J., 2018. Towards storage-stable high-content recycled tyre rubber modified bitumen. Construction and Building Materials 172, 106-111.

Segneanu, A.E., Gozescu, I., Dabici, A., Sfirloaga, P., Szabadai, Z., 2012. Organic compounds FT-IR spectroscopy. InTech Romania.

Shatanawi, K., Biro, S., Thodesen, C., Amirkhanian, S., 2009. Effects of water activation of crumb rubber on the properties of crumb rubber-modified binders. International Journal of Pavement Engineering 10(4), 289-297.

Shu, X., Huang, B., 2014. Recycling of waste tire rubber in asphalt and portland cement concrete: An overview. Construction and Building Materials 67, 217-224.

Susa, D., Haydary, J., 2013. Sulphur distribution in the products of waste tire pyrolysis. Chemical Papers 67(12), 1521-1526.

Tatangelo, V., Mangili, I., Caracino, P., Bestetti, G., Collina, E., Anzano, M., Branduardi, P., Posteri, R., Porro, D., Lasagni, M., 2019. Microbial desulfurization of ground tire rubber (GTR): Characterization of microbial communities and rheological and mechanical properties of GTR and natural rubber composites (GTR/NR). Polymer degradation and stability 160, 102-109.

UTMA, 2017. SCRAP TIRE MARKETS. https://www.ustires.org/scrap-tire-markets. 2019).

Way, G.B., Kaloush, K.E., Biligiri, K.P., 2012. Asphalt-rubber standard practice guide. Rubber Pavements Association, Tempe.

Xiang, Y., Xie, Y., Long, G., Zeng, L., 2019. Ultraviolet irradiation of crumb rubber on mechanical performance and mechanism of rubberised asphalt. Road Materials and Pavement Design 20(7), 1624-1637.

Xiaowei, C., Sheng, H., Xiaoyang, G., Wenhui, D., 2017. Crumb waste tire rubber surface modification by plasma polymerization of ethanol and its application on oil-well cement. Applied Surface Science 409, 325-342.

Xie, J., Yang, Y., Lv, S., Zhang, Y., Zhu, X., Zheng, C., 2019b. Investigation on Rheological Properties and Storage Stability of Modified Asphalt Based on the Grafting Activation of Crumb Rubber. Polymers 11(10), 1563.

Yao, C., Zhao, S., Wang, Y., Wang, B., Wei, M., Hu, M., 2013. Microbial desulfurization of waste latex rubber with Alicyclobacillus sp. Polymer degradation and stability 98(9), 1724-1730.

Yu, H., Leng, Z., Zhou, Z., Shih, K., Xiao, F., Gao, Z., 2017. Optimization of preparation procedure of liquid warm mix additive modified asphalt rubber. Journal of cleaner production 141, 336-345.

Zani, L., Giustozzi, F., Harvey, J., 2017. Effect of storage stability on chemical and rheological properties of polymer-modified asphalt binders for road pavement construction. Construction and Building Materials 145, 326-335.

Chapter 6 INTERPLAY BETWEEN RUBBERIZED ASPHALT AND MODIFIERS

6.1 Abstract

This study examines the synergistic effects of using bio-modifiers and polyphosphoric acid (PPA) in bitumen as a means of promoting the durability and sustainability of bituminous composites. PPA has commonly been used to increase bitumen's elasticity, however, PPA's efficacy varies widely depending on the bitumen's composition. Typically, a low dosage of PPA is preferred, due to its plausible negative side effects on other properties of bitumen. The use of bio-modifiers that have been shown to be promising to enhance bitumen's properties can change the bitumen's composition and consequently affect PPA's efficacy. Here, we hypothesize that there is a synergistic effect between PPA and certain bio-modifiers that amplifies PPA's effect on bitumen's elasticity, enhancing the efficiency of a PPA dosage. To test this hypothesis, we use laboratory experiments and computational modeling using density functional theory to compare the efficacy of PPA on bitumen with various bio-modifiers. The study results showed that a bio-modifier made from wood pellets had the highest synergy with PPA (leading to the best dosage efficiency for PPA), followed by bio-modifiers made from miscanthus, castor oil, and corn stover, with the bio-modifier made from waste vegetable oil having the least synergy with PPA. The results of density functional theory showed that there is strong non-covalent interaction between PPA oligomers and the lignin units of the wood-based bio-modifier; this interaction could be responsible for the observed strong synergy. In addition, due to the higher polarity of the wood-based bio-

modifier compared to the bio-modifier from waste vegetable oil, a higher phosphorylation is expected to occur in the wood-based bio-modifier when exposed to PPA. Our results show that alcoholic OHs (alkanols) of the wood-based bio-modifier can chemically interact with PPA; aliphatic OHs are readily phosphorylated in the presence of PPA. However, phenolic OHs (Ar-OH) and alkoxy (-OR) groups do not undergo a chemical reaction with PPA. In the case of the bio-modifier made from waste vegetable oil, the head group of fatty acids and polar groups in triglycerides interact with PPA; however, the latter interactions are not as strong as those between the wood-based bio-modifier and PPA. The results of this study show that PPA has a strong interaction with a wood-based bio-modifier that leads to superior performance in bitumen containing both PPA and the wood-based bio-modifier.

Keywords: Bitumen, Bio-modifiers; Polyphosphoric acid; Phenolic compounds; Fatty acids

6.2 Introduction

In recent years, a variety of organic and inorganic substances extracted from biomass or petroleum have been introduced to bitumen, aiming to upgrade bitumen's performance characteristics and, depending on their origin, to promote sustainable practices geared toward resource conservation. Polyphosphoric acid (PPA), dating back to 1973, (Alexander, 1973) is among a few chemical reagents practically used in the asphalt industry to increase bitumen's stiffness and performance grade and/or widen bitumen's operative temperature. (Baumgardner et al., 2005)·(Falkiewicz and

Grzybowski, 2004),(Maldonaldo et al., 2006),(Kodrat et al., 2007),(Edwards et al., 2006),(Orange et al., 2004) PPA has been a favored modifier in the asphalt industry for several reasons: an appropriate compatibility between PPA and bitumen's constituents (no phase separation during long-term storage), facilitated processing, and relatively low cost.

Despite the popularity of PPA compared to other polymeric modifiers, the use of PPA is usually accompanied by several concerns of the asphalt community: (1) PPA has strong hydrophilicity that makes PPA-modified bitumen more susceptible to moisture than virgin bitumen. (2) PPA has undesirable reactions with other bituminous additives such as hydrated lime, phosphate esters, and amines, which are mainly used to improve the moisture resistance of bitumen. (3) There remain some unknown aspects of the long-term performance of PPA-modified asphalt. (D'Angelo, 2012),(Hossain et al., 2018),(Al-Qadi et al., 2014) While PPA is well-known for its good performance at high temperatures without compromising the bitumen's properties at low temperatures, there are scattered reports of impaired low-temperature rheology of PPA-modified bitumen, particularly in the case of high-wax bitumen. (Liu et al., 2016), (Liu et al., 2018)

In the last twenty years, attention has been directed toward the use of PPA in conjunction with other synthetic polymers such as rubber (Martin, 2011),(Xiao et al., 2014),(Li et al., 2011) or ethylene-vinyl acetate,(Zhang, F. et al., 2018b),(Loza et al., 2000) to provide asphalt additives with improved performance. The major benefit of this combination can be the synergistic effects of two modifiers to amplify the effect of PPA or the polymer on bitumen's properties. These typically mutual effects are not limited to

PPA and polymers; our recent studies show that synergy between silica nanoparticles and PPA can increase the effectiveness of PPA as a modifier for bitumen. (Mousavi et al., 2019c) We also examined the plausible antagonistic effects of bitumen's wax content on the synergistic features of silica-PPA, where the synergy between modifiers diminishes in high-wax bitumen to a point that introduction of silica-supported PPA could not improve the complex viscosity of high-wax bitumen as much as it did in the case of low-wax bitumen. (Mousavi et al., 2019c)·(Mousavi and Fini, 2019)

Considering the importance of accounting for such antagonistic or synergistic interactions among various modifiers intended to enhance efficiency in sustainable construction, this study investigates the performance of PPA with each of five bio-based modifiers that have recently been introduced to upgrade bitumen performance, rejuvenate aged asphalt, or partially replace asphalt binder. The five bio-based modifiers are derived from these sources: wood pellets, waste vegetable oil, miscanthus, corn stover, and castor oil.

Replacing chemical materials with renewable resources has become a major contemporary challenge for both environmental and economic reasons. The primary sources (biomass) of bio-based materials include a wide range of biodegradable substances with animal or vegetal origin, such as wood-based materials,(Yang et al., 2013), (Yang et al., 2014) microalgae,(Chailleux et al., 2012) waste vegetable oil,(Sun et al., 2016), (Chen et al., 2014), (Wen et al., 2012) corn stover,(Raouf and Williams, 2010) and swine waste.(Fini et al., 2011b), (You et al., 2011), (Xiu et al., 2011) Compatibility of a bio-modifier with virgin binder and the quantity required for optimum blending are

among the concerns that are mostly addressed in laboratory experiments and ultimately in field investigations. Use of incompatible bio-modifiers could be associated with phase separation in long-range storage or loss of adhesion of the modified bitumen to aggregates, leading to raveling and moisture damage.(Zaumanis et al., 2014)

Among the bio-modifiers being studied here, wood-based bio-modifiers, from sources such as aspen wood or wood pellets, have the highest content of polar aromatics and have shown the most effective interaction with other bitumen additives such as high-impact polystyrene polymer (Mousavi et al., 2019a) and rubber polymer, (Kabir et al., 2020) as evidenced by reducing the tendency of phase separation by 82% and a doubled percent recovery (Kabir et al., 2020).

In contrast to wood-based bio-modifiers, the bio-modifiers with the lowest content of polar groups are bio-modifiers of vegetal origin. Natural vegetable oils such as castor oil (Zeng, M. et al., 2018), (Zeng et al., 2016) are among the most important class of renewable sources that have recently been introduced to the asphalt industry. Saturated and unsaturated fatty acids are the main components of the triglyceride vegetable oils that provide reactive sites for coatings. Waste vegetable oil, referring mainly to the end product of oils used for frying at high temperatures, is also a glycerol ester containing different types of long-chain fatty acids. Despite its reputation, waste vegetable oil does not seem to pass all criteria, including moisture susceptibility,(Zaumanis et al., 2014) required to be verified as an ideal rejuvenator/modifier. (Ahmed and Hossain, 2020)

This study uses a bottom-up approach using energy analysis in the framework of dispersion-corrected density functional theory (DFT-D) along with laboratory

experiments to investigate the synergistic or antagonistic pairwise interactions between PPA and a group of renewable bio-based modifiers from five sources: wood pellets, waste vegetable oil, miscanthus, corn stover, and castor oil. The phenolic (polar aromatic) nature of the wood-based bio-modifier and the esteric nature of vegetal-based oil are two ends of a spectrum in terms of chemical structure. We study the possible interactions between PPA and a series of phenolic and esteric compounds identified in these two bio-modifiers, using a DFT-D approach. Our theoretical findings at the micro level are verified by experiment data obtained from rheology-based descriptors of elastic recovery based on a multiple-stress creep-recovery (MSCR) test and the resistance to permanent deformation using an oscillation test.

6.3 Materials and Methods

6.3.1 Materials

The crumb rubber used in this experiment has particle size less than 0.25 mm and was supplied by Crumb Rubber Manufacturers. Five types of bio-modifiers were used, derived from these sources: castor oil (CO), corn stover oil (CS), miscanthus oil (MS), wood-pellet oil (WP), and waste vegetable oil (WVO). Polyphosphoric acid (83.3% P_2O_5, so-called 115% H_3PO_4) was acquired from Sigma-Aldrich. Bitumen (Table 1) was obtained from Holly Frontier Corporation in Arizona.

Table 6-1. General Properties of The PG64-22 Asphalt Binder

Specific Gravity @15.6ºC	1.041
Cleveland Open Cup method flash point	335 ºC
Mass change after RTFO	-0.013
Absolute Viscosity @ 60ºC	179 Pa.s
Stiffness @-12ºC @ 60s	71.67 MPa

6.3.2 Sample preparation

At first, all bitumen in this study contained 15% crumb rubber treated with the five types of modifiers. The details of the procedure can be found elsewhere (Kabir et al., 2020). Then, to produce modified bitumen, PPA was added to each of the bio-modified bitumens at 1% by weight of the base bitumen containing 15% bio-modified rubber. [32] The mixing was done at 155°C for 30 minutes to achieve a homogeneous blend.

6.3.3 Attenuated Total Reflectance Fourier Transform Infrared Spectroscopy (ATR-FTIR)

For ATR analysis, a built-in ATR with diamond crystal was used in a Bruker IFS 66V/S Vacuum FT-IR spectrometer equipped with a DLATGS detector. Individual particles were placed on the ATR crystal to completely cover the 1-mm crystal surface. Uniform pressure was applied on all samples using the built-in pressure clamp. Data were collected from 4800 to 400 cm^{-1} at 32 scans per second with a resolution of 4 cm^{-1}. Analysis of the spectra was carried out with OMNIC and Origin software.

6.3.4 TLC-FID Thin-layer Chromatography with Flame Ionization Detection (TLC-FID)

The fractional composition of each bio-oil was investigated using an Iatroscan MK-6s model TLC Flame Ionization Detector. The hydrogen flow rate and airflow rate

were set at 160 mL/min and 2 L/min, respectively. The n-heptane-insoluble part, especially the asphaltene content, was isolated and evaluated using the difference in mass of the filter paper just before and after the filtration, following standard ASTM-D3279 (2019)(D3279-19, 2019). Later, 20 mg of n-heptane soluble (maltene) was detected on the chromrods. To develop the solvent, solutions of pentane, toluene, and chloroform (all supplied by Sigma Aldrich) were used. In a pentane tank, the chromrods were developed for 35-40 minutes and dried in air for about 2 to 5 minutes. The dried chromrods were then moved to a second chamber filled with a 9:1 toluene:chloroform solution for 9 minutes. Finally, the rods were oven dried at 85 °C, and the prepared specimen was scanned for 30s using the flame ionization detector.

6.3.5 Dynamic Shear Rheometer (DSR)

An Anton Parr MCR 302 dynamic shear rheometer was used in accordance with standard ASTM-D7175(2015)(ASTMD7175-15, 2015) to determine the elastic modulus (G´), the viscous modulus (G´´), and the phase angle (δ) at a temperature of 52°C. To do so, an oscillation test was performed using a parallel-plate setup (8-mm spindle) at 0.1 strain and frequency ranging from 0.1-100 rad/sec. The data was used to calculate G*/sin(δ) as a measure of the material's elasticity and strain recovery. The latter parameter has commonly been used as an indicator of resistance to permanent deformation (rutting) in bituminous composites used in asphalt pavements under repeated load.

Another indicator is percent recovery under repeated load, which is usually evaluated using an MSCR test following the AASHTO-T315 standard. (AASHTO-T315,

2012) In this test, the binder is subjected to 10 cycles, where each cycle is a 1-second loading followed by a 9-second rest period, at a shear stress of 0.1 kPa or 3.2 kPa. The recoverable strains and non-recoverable strain in each cycle are then calculated and summed up through the ten cycles to report percent recovery.

6.4 Computation Methods

Quantum calculations were performed in the framework of dispersion-corrected density functional theory (DFT-D), using the DMol^3 module (Delley, 1990),(Delley, 2000) of the Accelrys Materials Studio program package. The Perdew-Burke-Ernzerhof (PBE) functional (Perdew et al., 1996) was used to apply the generalized gradient approximation (GGA) for the exchange and correlation energy of electrons. There are different gradient optimization techniques available (Naher et al., 2020a; Naher et al., 2020b; Naher et al., 2020c; Naher et al., 2019). The PBE type of GGA has been widely used for solids as well as molecules. A major benefit of PBE could be a "systematic" tendency in errors of the PBE results, (Rappoport et al., 2008),(Ernzerhof and Scuseria, 1999) making it easier to estimate the properties under study. In addition, PBE typical functionals provide a high accuracy for relative quantities such as bond length changes, frequency shifts, and energy differences. (Rappoport et al., 2008),(Ernzerhof and Scuseria, 1999) Grimme's correction was included in calculations to account for the long-range dispersion corrections. (Grimme, 2011) In an all-electron optimization, without imposing any constraints, the numerical DNP basis set was used for all atoms: PBE-D/DNP.

The interaction energy between two compounds expresses the thermodynamic stability of the complex formed. This term is calculated as the energy difference (ΔE) between the complex formed and its constituents when they are in their lowest energy state, as shown in Equation 6-1.

$$\Delta E = E_{complex} - (E_{PPA} - E_{modifier'smolecule}) \quad (6\text{-}1)$$

Due to the complexity, our computational model focused only on PPA's interaction with two bio-modifiers (from wood pellets and from waste vegetable oil); the model did not attempt to include the crumb rubber and bitumen.

6.4.1 Polyphosphoric Acid (PPA) Model

As a short-chain polymeric product, PPA is produced either by dehydration (thermal dehydration and condensation of a series of phosphoric acid (H_3PO_4) molecules) or by dispersion (heating phosphorus pentoxide (P_2O_5) dispersed in H_3PO_4). Commercially available PPA is a mixture of oligomer chains of H_3PO_4 with a general formula of $HO[PO_2OH]_nH$, where $n \geq 2$. Oligomers of PPA produced from heating the dispersed P_2O_5 in H_3PO_4 include longer chains of PPA. PPA is commercially provided in different grades; their percentage often exceeds 100%, due to the calculation of H_3PO_4 concentration on the base of P_2O_5 content in the medium.(Masson, 2008) The commonly used grades of PPA in asphalt are 105%, 110%, and 114% H_3PO_4 including P_2O_5 contents of 75.9%, 79.8%, and 82.6% P_2O_5, respectively. The PPA used in this study contains 83.3% P_2O_5, equivalent to 115% H_3PO_4. The number of repeating units of a

high-grade PPA (>114%) does not exceed 14. Therefore, in the present study, a short-chain PPA containing 5 monomer units was used to represent the PPA structure (**Figure 6-1)**.

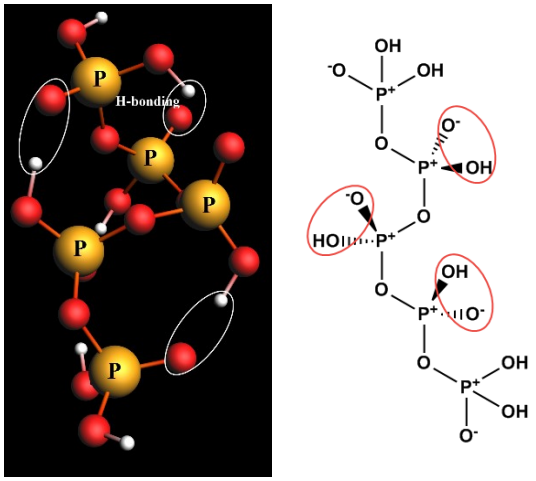

Figure 6-1. Chemical Structure of Polyphosphoric Acid (PPA) Containing 5 Repeating Units. The Intramolecular H-Bonding Interactions Within The Internal OHs Are Circled.

6.5 Results and Discussion

6.5.1 Chemical Analysis

To better understand the influence of the chemical composition of the bio-modifiers used to prepare bio-modified rubberized bitumen, TLC-FID was performed. The test is used to determine the content of saturates, polar aromatics, resins, and asphaltenes in each bio-modifier (**Table 6-2**). Phenol-rich wood-based oil has a higher polar aromatics (resin) content along with amounts of asphaltenes and naphthene aromatics comparable to other bio-oils. Aromatics contribute to viscous behavior, and

resins help to stabilize the asphaltenes in bitumen and can contribute to increased stiffness. (Eberhardsteiner et al., 2015) The highest percentage of naphthene aromatics occurs in the bio-modifier made from waste vegetable oil; they are expected to reduce the elasticity.

Table 6-2. TLC-FID Results for Chemical Content (Asphaltene, Resin, Aromatics, and Saturates) of Bio-Oils

Bio-oil	CO	CS	MS	WP	WVO
Saturates	20.95	6.8	6.22	3.46	0.00
Naphthene Aromatics	0.00	3.73	8.56	2.93	87.19
Resins (Polar Aromatics)	78.17	67.49	60.47	76.21	12.80
Asphaltenes	0.87	21.96	24.47	17.38	0.00

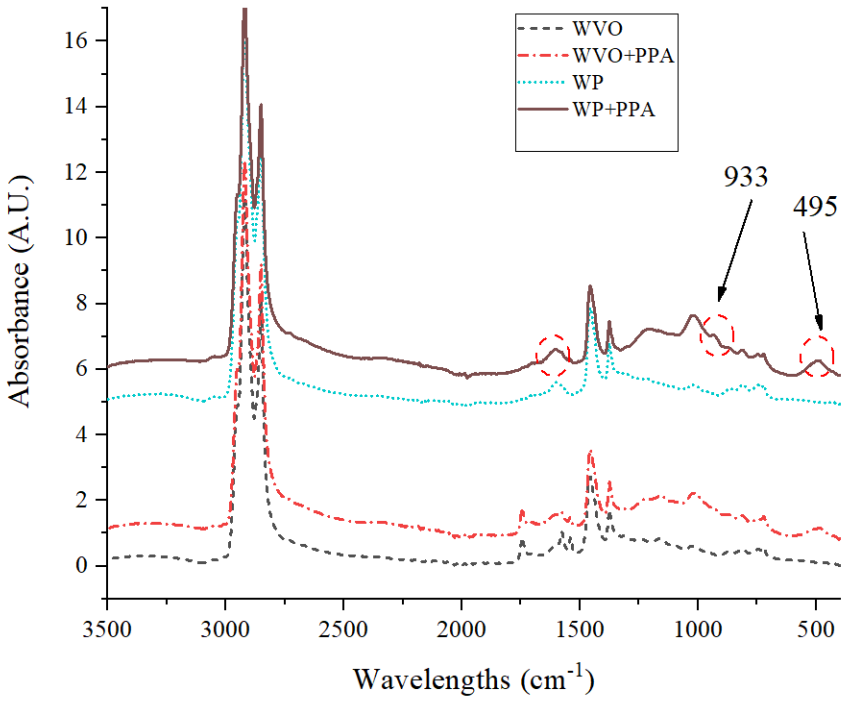

Figure 6-2. FT-IR Spectroscopy of Bitumen with Bio-Modifier from Waste Vegetable Oil or Wood-Pellet Oil, Before and After Adding PPA to It.

To observe the effect of any bond formation, ATR-FTIR was performed. In **Figure 6-2**, fingerprint regions of PPA-modified bitumen can be seen. PPAs give characteristic peaks around 495 cm^{-1} that correspond to bending vibration of P-O-P. (Zhang, F. et al., 2018a) These peaks can be seen in both bitumen modified by wood-pellet oil and bitumen modified by waste vegetable oil. A new absorption peak appears at 933 cm^{-1} after PPA is added; the new peak corresponds to asymmetric vibrations of P-O-P in that region. (Zhang and Yu, 2010) Investigation around this region shows phosphorus functions can give this new peak as well in the 900-1050 cm^{-1} region, indicating PPA reaction with the aliphatic OH functional group and formation of phosphoric bonds (P-O-R). Although it is highly likely for bitumen modified with phenol-rich wood-pellet oil to react with PPA, which may have created new complexes, this is hard to distinguish due to the overlapping of peaks. (Zhang and Yu, 2010) This overlapping can be seen at the broad peak spreading from 1577-1650 cm^{-1}, which overlaps with the O-H deformation vibration at 1645 cm^{-1}. (Zhang and Yu, 2010)

6.5.2 Rheological analysis

Figure 6-3 shows the elastic modulus (G´) versus the frequency for bitumen modified with wood-pellet oil and bitumen modified with waste vegetable oil before and after adding 1% PPA. The bitumen modified with wood-pellet oil had an elastic modulus of nearly 5.7 kPa at 10 rad/s before adding PPA; after adding 1% PPA, the elastic modulus was 18 times that value at 102.5 kPa. The bitumen modified with waste vegetable oil had an elastic modulus of 1.8 kPa before adding PPA; after 1% PPA was

added, the elastic modulus was nearly 6 times that value at 11 kPa. The results clearly show that bitumen modified with wood-pellet oil benefits more from adding 1% PPA.

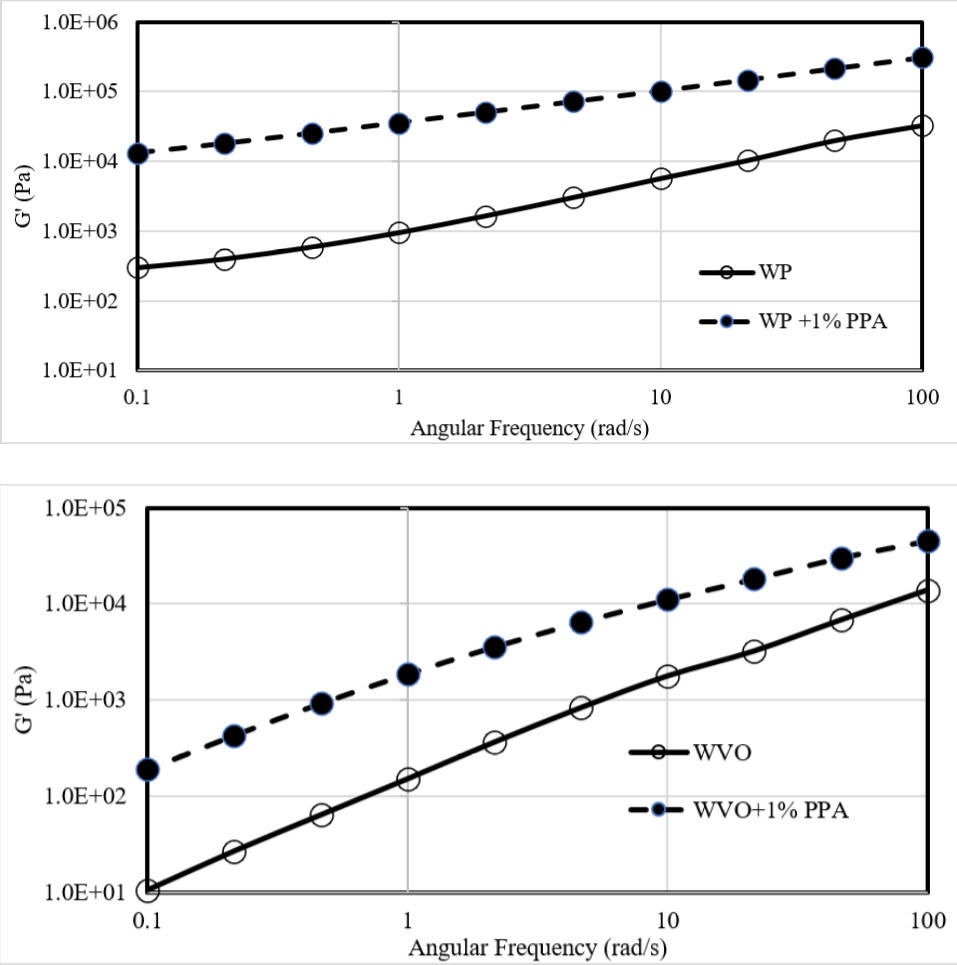

Figure 6-3. Behavior of Elastic Modulus (G´) of Bitumen Modified with Wood-Pellet Oil and Bitumen Modified with Waste Vegetable Oil Before and After Adding 1% PPA.

Figure 6-4 shows the complex modulus (G*) versus angular frequency for bitumen modified with wood-pellet oil and bitumen modified with waste vegetable oil, before and after adding PPA.

The complex modulus for bitumen modified with wood-pellet oil was 18 kPa; after PPA was added, the complex modulus was 151 kPa, eight times the earlier value. The complex modulus of bitumen modified with waste vegetable oil was three times the earlier value after adding 1% PPA. This shows that PPA has a different level of synergy with different bio-modifiers, with the synergy between PPA and the bio-modifier being higher for wood-pellet oil and lower for waste vegetable oil.

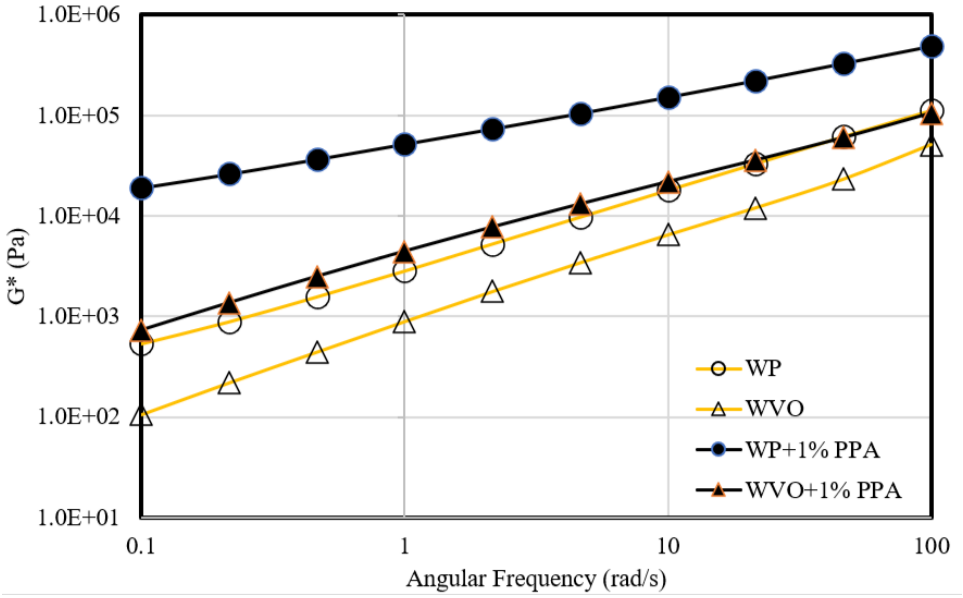

Figure 6-4. Complex Modulus (G*) Vs. Angular Frequency for Bitumen Modified with Wood-Pellet Oil and Bitumen Modified with Waste Vegetable Oil.

Figure 6-5 shows the changes in percentage recovery before and after adding PPA, obtained at 52°C from MSCR test data. Bitumen modified with wood-pellet oil had a 56% increase in recovery after adding 1% PPA, followed by bitumen modified by miscanthus oil and bitumen modified by castor oil. Bitumen modified by waste vegetable

oil and bitumen modified by corn stover oil had an equal increase of 36% in recovery after adding PPA. This finding aligns with the TLC-FID results, where we saw that the wood-pellet oil was highest in polar aromatics and waste vegetable oil had the lowest amount of resins.

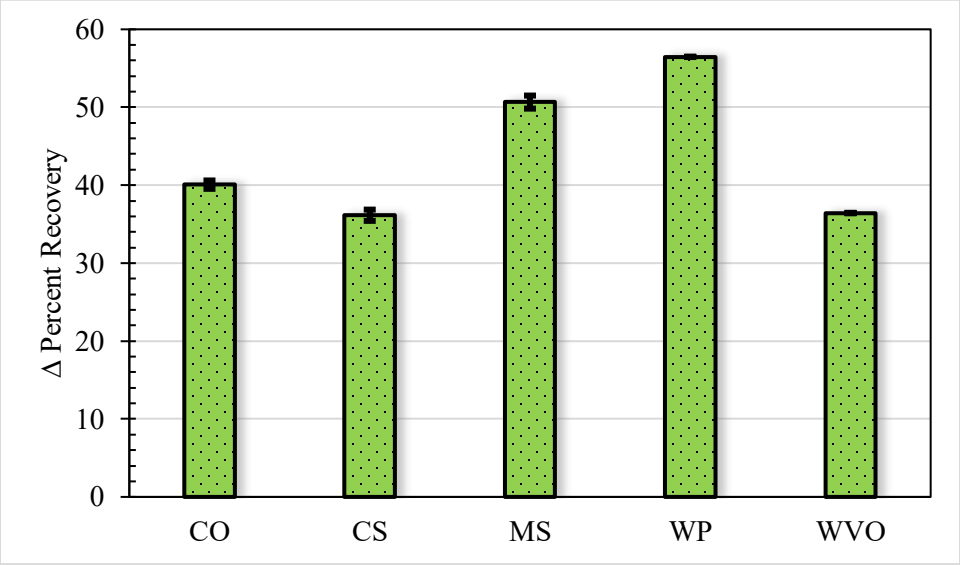

Figure 6-5. Changes in Percent Recovery Due to Addition of PPA, from A Multiple-Stress Creep-Recovery Test

Figure 6-6 shows changes in the G*/sinδ parameter at 10 rad/s at 52°C for all bio-modified bitumens. A higher value of G*/sinδ is desirable to enhance resistance to permanent deformation. After adding PPA, the bitumen with the bio-modifier from wood pellets showed a 187 kPa increase in G*/sinδ, followed by the bitumens with bio-modifiers from miscanthus, corn stover, castor oil, and waste vegetable oil. The bitumen with bio-modifier from waste vegetable oil had an increase of only 19kPa.

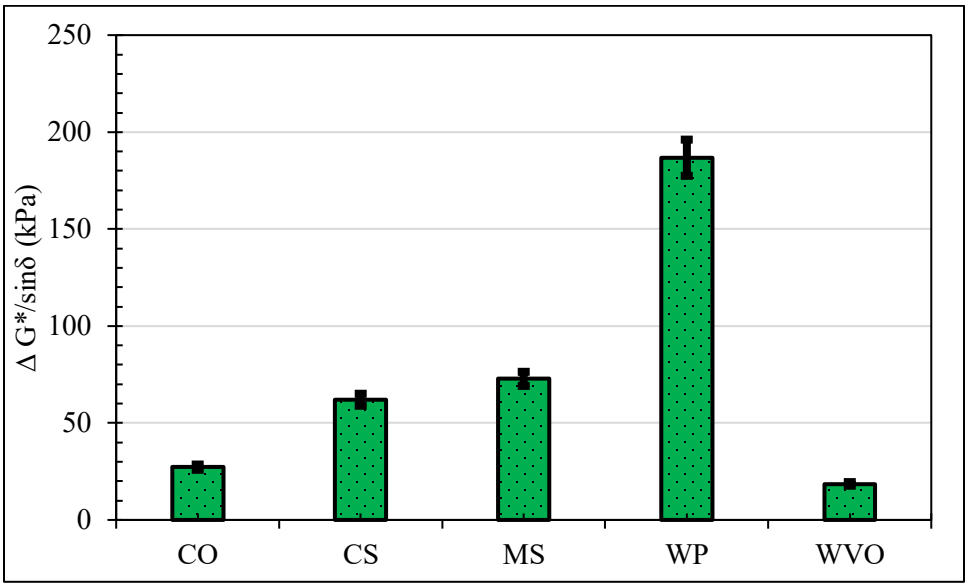

Figure 6-6. Changes in G*/sinδ After Adding PPA, for All Bio-Modified Bitumens

Considering that PPA is typically used to enhance the elastic behavior of bitumen, **Table 6-3** shows the minimum dosage of PPA that is required to achieve a recovery of 80% and a G*/sin δ of 200kPa. Assuming a linear relationship between the PPA dosage and percent recovery and between PPA dosage and G*/sin δ, the required dosage was calculated in each bio-modified bitumen scenario. As shown in Table 3, bitumen modified with wood-pellet oil needs less than 1% PPA to achieve the target elasticity. This is followed by bitumen with bio-modifiers from miscanthus, corn stover, castor oil, and waste vegetable oil; the bitumen with bio-modifier from waste vegetable oil needs more than 10% PPA to achieve the target elasticity. This relative comparison clearly shows that the efficacy of PPA to enhance the elasticity of bio-modified bitumen varies significantly with the composition of the bio-modifier.

Table 6-3. Dosage of PPA Required to Reach Specified Elastic Properties

Bio-Modifier	CO	CS	MS	WP	WVO
PPA dosage to reach Percent Recovery=80%	1.83	1.12	1.08	0.99	2.02
PPA dosage to reach G*/sin δ =200kPa	6.71	2.90	2.47	0.97	10.40

Phosphorylation of lignin units through chemical reactions

The mechanism of PPA action in bitumen is not well understood. The same scenario is expected concerning the reactions of PPA with wood components. According to the literature, the evaluation of lignin phosphorylation is not an easy task, because phosphorylation depends on the phosphorus-containing precursor used and the chemical structure of a lignin, which varies with its natural origin. Wood is known as the main source of lignin, and lignin is the main source of phenolic compounds in the world. Due to the variation in chemical composition, no precise structure is defined for lignin. However, lignin's structure is widely known as a dendritic network of three phenylpropene (C_6H_5-$CH_2CH=CH_2$) basic units: coniferyl alcohol, sinapyl alcohol, and low amounts of p-coumaryl alcohol. (Kun and Pukánszky, 2017), (Vainio et al., 2004) **Figure 6-7** shows the chemical structures of three monolignols identified in lignin. The hydroxyl (OH) and methoxy (O-CH_3) substituents and C=C double bond in the chemical structure of lignols act as potential active sites to interact with guest molecules. The strong self-interaction between building units of lignin is also attributed to the function of polar groups in these chemical entities.(Kun and Pukánszky, 2017)

There are some reports of phosphorylation of OH groups in lignin using H_3PO_4, indicating a good phosphorus content after modification. (Bykov and Ershov, 2010) Aside from the specific nature of lignin in reaction with H_3PO_4, the direct catalytic

reaction of H_3PO_4 and alcohol is a pathway introduced for the production of phosphoric acid monoesters.(Sakakura et al., 2005)

In the specific case of PPA, upon the reaction of PPA with alkanols, the hydroxyl group is often readily phosphorylated, leading to a phosphate ester. This will be shown in the following DFT results. However, the reaction of PPA with aromatic alkanols (phenolic OHs) could be totally different. In general, two types of hydroxyl groups are found in bio-based products: the aliphatic OHs, such as those available in cellulose, and aromatic OHs, such as those available in phenols (lignin derivatives). Considering the dominant contribution of phenolic OHs in wood-based modifiers, the main focus of the theoretical section would be on probing the reaction mechanism and possible interactions between PPA and phenolic compounds.

Phosphorylation of monolignols using phosphorus pentoxide (P_4O_{10})

Figure 6-7 shows the chemical reaction between sinapyl alcohol, a dominant monomer of hardwood lignin, and phosphorus pentoxide, P_4O_{10}, which commonly gets its name from its empirical formula. P_4O_{10} is a strong dehydrating agent used as a desiccant to keep places dry and free from airborne moisture. As shown in **Figure 6-7**, P_4O_{10} readily reacts with the phenolic OH of sinapyl to form a phosphate esteric bond, C-O-P, accompanied by -17.5 kcal/mol stabilization energy. This reaction can be continued to phosphate esterification of other P=O groups of P_4O_{10}, indicating the strong affinity of P_4O_{10} to aromatic OHs. This result is in accordance with the experiment demonstrating

the ability of P_4O_{10} in phosphorylation of the hydroxyl group of salicylic acid, $C_6H_4(OH)COOH$, and the formation of Ar-O-P bonds (WO9804567A1, 1998).

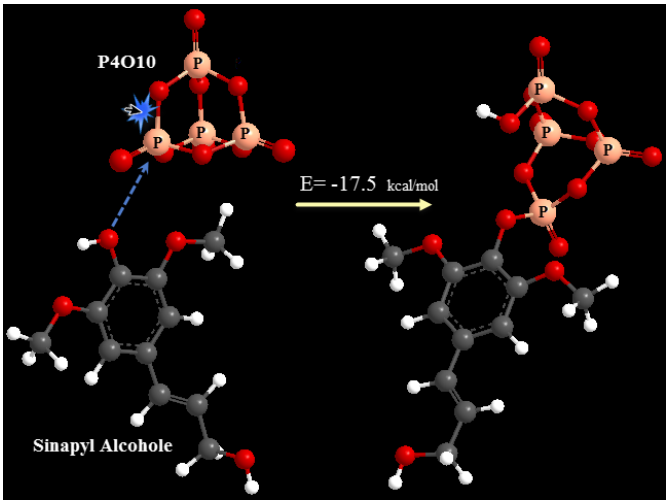

Figure 6-7. Phosphorylation of The Hydroxyl Function (OH) of Sinapyl Alcohol (One of The Building Blocks of Hardwood Lignin) with Phosphorus Pentoxide (P_4O_{10}). Similarly, All Four Phosphorous Atoms of P_4O_{10} Can React with Other OH Groups.

Phosphorylation of the phenolic and benzylic OHs (Ar-OH and Ar-CH_2OH) using PPA

Although not as strong as P_4O_{10}, PPA is another dehydrating agent expected to have a good reaction with OH groups. Aligning with experiments, our DFT analysis verifies the ability of PPA to phosphorylate OH groups not directly attached to the benzene ring. As shown in **Figure 6-8**, phosphorylation of benzyl alcohol (phenylmethanol, C_6H_5-CH_2OH) is associated with -4.6 kcal/mol.

Since PPA is a weak acid, it needs a medium with sufficiently high dielectric constant (ε) to be dissociated to PPA^- and H^+. The dielectric constant of a material is a measure of its ability to stabilize a charge under an applied electric field resulting from other neighboring species. Taken as a measure of solvent polarity, higher ε means higher polarity, and greater ability to stabilize charges. Water has a large and temperature-

dependent dielectric constant (ε= 79) due to its permanent dipole moment and its H-bonding effects. Upon dissociation of PPA in water, its equilibrium shifts back to the formation of H_3PO_4.(Masson, 2008) The bitumen medium, with its hydrocarbonic non-polar nature, does not provide a sufficiently high dielectric constant to promote PPA for chemical reactions; the dielectric constant of virgin bitumen is about 2.8.(Adamu et al., 2019) Considering the role of heteroatoms in raising the polarizability and ultimately ε, (Bonardd et al., 2019) an increase in the polarity of bitumen by highly polar modifiers such as wood-based components can be a driving force for limited chemical interactions of PPA in the matrix of bitumen.(Masson and Gagné, 2008)

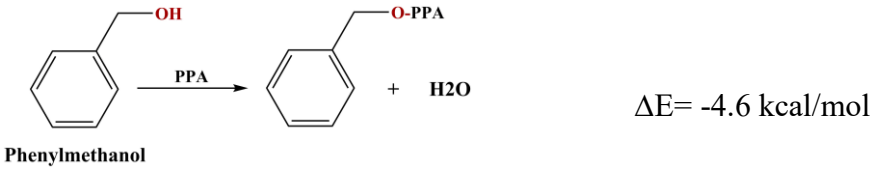

Figure 6-8. Phosphorylation of Benzyl Alcohol (Phenylmethanol) at The PBE-D/DNP Level of Theory.

In **Table 6-4**, the phosphorylation of OH and OR groups directly bound to the aromatic ring is investigated for three model molecules available in a wood-based bio-modifier: phenol, alkoxy benzene, and 2-6-dimethoxy-4-alkylphenol. In this table, the reaction energies are provided for R=CH_3. The results of this simulation are of particular interest to verify the ability of PPA for chemical reactions with phenolic OHs or ether (alkoxy benzene) groups to produce aromatic phosphate esters.

Based on the DFT results, in contrast to aliphatic OHs (which are readily phosphorylated with PPA), phenolic OHs do not undergo the chemical reaction to

produce aromatic phosphate esters; see **Table 6-4-a** with ΔE= +13.3 kcal/mol. This result aligns with the FTIR findings by Masson et al. demonstrating that no phosphorylation occurs on phenolic OHs of bisphenol A(Masson et al., 2008). Considering the dehydrating nature of PPA, dehydration of hydroxyl groups could always be a first estimation on PPA function; however, the OH-containing compounds used in **Table 6-4** are not alkanols but phenols, so the dehydration mechanism is most unlikely in these cases.

Phosphorylation of alkyl aromatic ethers (OR containing groups)

Considering the available reports on ether cleavage reactions in the presence of PPA,(Orlando Jr et al., 1970) the acidolysis of alkyl aromatic ethers (Ar-O-R) and nucleophilic displacement of PPA could be a potential mechanism to explain the performance of PPA in virgin or bio-modified bitumen. Alkoxy groups (-OR) are among the functionals identified in bitumen as well as in wood-based biomass, though the contribution of alkoxy groups could be much more significant in wood-based biomass, due to its lignin-based origin. In the context of a PPA mechanism in bitumen, Baumgardner et al.(Baumgardner et al., 2005) proposed the nucleophilic attack of PPA, detachment of a –OR group, and the formation of PPA-adduct to explain the reduced molecular weight of bitumen's components under PPA modification.

In **Table 6-4-b**, one possible reaction pathway for phosphorylation of alkyl aromatic ether is investigated. To avoid the interfering effects of other ring substituents, a mono-substituted aromatic is used here. The nucleophilic attack of PPA in this postulated mechanism leads to the cleavage of an alkoxy group and the formation of a less-polar

alcohol. As shown, this reaction is not energetically stabilized, $\Delta E = +5.2$ kcal/mol, indicating the inability of PPA to displace an OR group bound to the aromatic ring. Our DFT result is supported by FTIR and TLC records that indicate butyl phenyl ether (Ar-O-C_4H_9) is immune to the effect of PPA.(Masson et al., 2008) In this experiment, the strong characteristic IR peak of Ar-O-CH_2 near 1240 cm^{-1} was unaffected by the reaction with PPA, and no new products were detected by TLC.(Masson et al., 2008)

Direct phosphorylation of the phenolic ring through dealkylation

Based on the GC-MS results performed in our group(Hosseinnezhad et al., 2015b), derivatives of dimethoxy phenol are among the main compounds detected in the bio-modifier from wood pellets. These derivatives directly originate from the sinapyl alcohols of hardwood lignin. We used this substituted phenol to examine another probable mechanism for the interaction of PPA with the phenolic compounds of the bio-modifier or bio-modified bitumen. As shown in **Table 6-4-c**, direct dealkylation of the phenolic ring using PPA is investigated, whereupon a protonated intermediate is subject to a nucleophilic displacement by an anion of PPA to produce a non-aromatic phosphorylated byproduct. As indicated by the energy value, $\Delta E = +11.3$ kcal/mol, this reaction mechanism does not provide enough stabilization energy either.

Table 6-4. Some Possible Reaction Pathways For Phosphorylation of Dominant Organic Compounds of Wood-Based Bio-Modifier and Their Unsuccessful Function: a) Phosphorylation of Phenolic Hydroxyl Group, b) Phosphorylation by Displacement of An Alkoxy Group to Produce An Alcohol (R-OH) or Phenol (Ar-OH), c) Dealkylation of A Para-Substituted Aromatic and Production of A Non-Aromatic Phosphorylated Product.

a	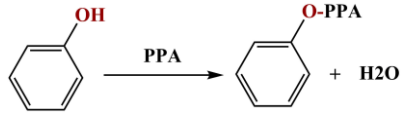	ΔE= +13.3 kcal/mol
b	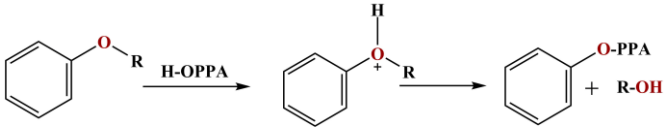 Alkoxy benzene	for R=CH_3 ΔE= +5.2 kcal/mol
c	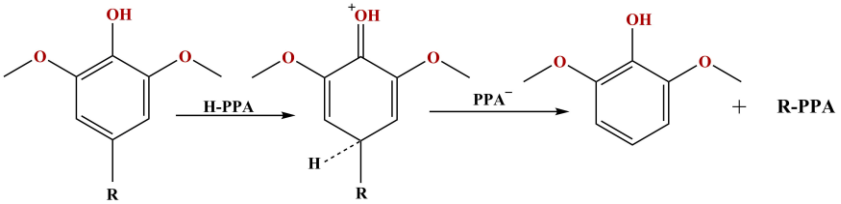 2-6-Dimethoxy-4-alkylphenol 2,6-Dimethoxyphenol	for R=CH_3 ΔE= +11.3 kcal/mol

Phosphorylation of lignin units through non-covalent interactions

DFT calculations were performed on a series of isolated model compounds containing oxygen functional groups, compounds that are representative derivatives of phenol available in wood-based bio-modifier and bio-modified binder. The DFT calculations showed that phenolic OHs are not directly phosphorylated by PPA, implying that aromatic phosphate esters (Ar-O-P-) cannot be responsible for the enhanced performance of bitumen under modification of PPA and wood-based bio-modifier.(Masson et al., 2008) Phenolic OHs or ORs are the main functionals in wood-based bio-modifier, but they are not the only functionals. As shown in **Figure 6-9**, the building blocks of hardwood lignin (sinapyl, coniferyl, and paracoumaryl) are alcohols

containing the same number of aliphatic OHs and phenolic OHs in each unit. Thus, what was shown so far is the rejection of the common belief that attributes improved performance of the bitumen containing phenolic compounds to the formation of phosphate esters in the presence of PPA. In addition, our recent study on PPA interactions with the components of virgin bitumen shows that there are other active sites that can establish strong interactions with PPA, such as basic components of bitumen including quinoline-resin and pyridine-resin.(Mousavi and Fini, 2019)

In addition to the probable chemical reactions of PPA with active compounds of bio-modifiers, our DFT calculations provide evidence for strong physical interactions between PPA oligomers and the lignin units. **Figure 6-9** shows the range of interaction energies, ΔE, for the non-covalent physical interactions of PPA with three lignols: sinapyl, coniferyl, and paracoumaryl alcohols. To achieve the (locally) lowest energy states, different orientations were examined for adsorption complexes shown in **Figure 6-9**. For the maximum overlap between two components, the ΔE average of three adsorption complexes is -(21.2-34.6) kcal/mol. As stated before, the repeating units of a high-grade PPA (>114%) do not exceed more than 14, so the typical PPA oligomer used here contains 5 repeating units, which provides an appropriate overlap with target alcohols.

Based on our recent findings, terminal OHs of PPA are responsible for the acid-base reactions occurring between PPA and basic compounds of bitumen, leading to the formation of ion-pair compounds stabilized through oppositely charged ions held together by coulombic attractions. Ionic interactions are not covalent in nature, since electrons are

not shared between two interacting units; however, these typical interactions are associated with a significant energy stabilization. Accordingly, $\Delta E = -(82.5 - 85.5)$ kcal/mol was found for the ion-pair interaction between PPA and two basic compounds of bitumen: pyridine-resin and quinoline-resin. Comparison of the range of energy values for PPA-lignols (-(21.2-34.6) kcal/mol in average, **Figure 6-9** with strong acid-base interactions of PPA (-(82.5-85.5) kcal/mol) implies that the contribution of non-covalent interactions of PPA with phenolic compounds is considerable and should be taken into account.

It was expected that lignols with more heteroatoms, such as sinapyl alcohol, exhibit higher interaction energy. However, based on the outcomes, the interaction energy is strongly correlated with the orientation of PPA's terminal OHs toward active sites of the target alcohol, to establish H-bonding interactions. As shown previously in **Figure 6-1**, internal OHs of PPA are strongly involved in H-bonding interactions within the molecule, so they are not available for interaction with guest molecules. PPA is not a straight-chain oligomer, mainly due to intramolecular H-bonding interactions within PPA. This result aligns with the resistance of high-grade PPA to hydrolytic degradation, suggesting that the backbone of PPA is not disintegrated under hydrolysis, but the terminal $-O_2P(OH)_2$ group containing two OH groups is separated from the polymer. (Platonov, 2000)

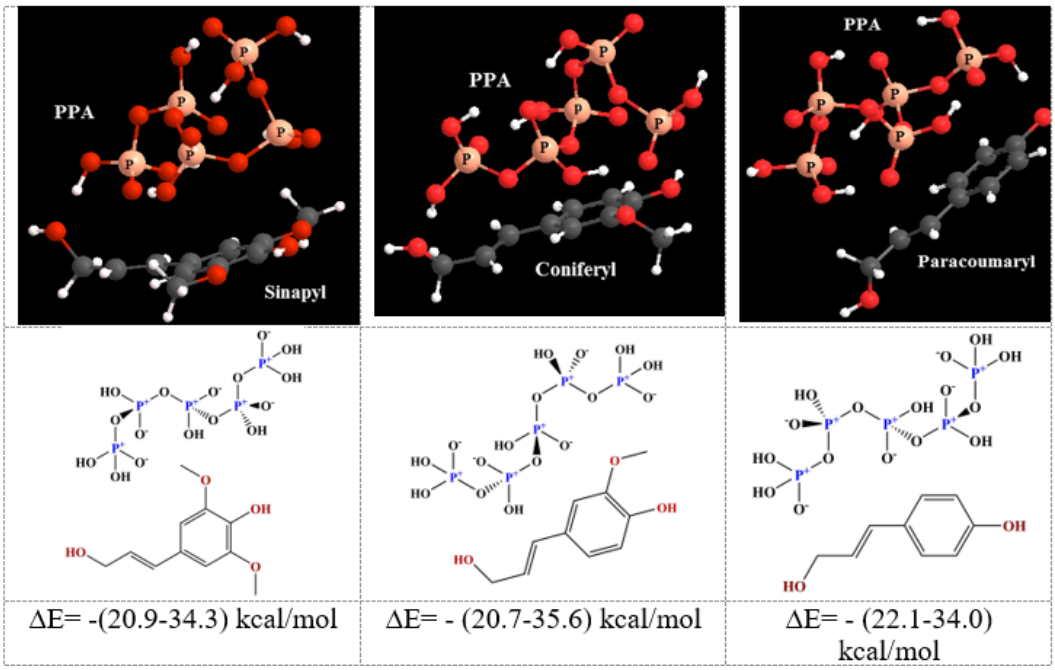

Figure 6-9. Non-Covalent Physical Interactions of Polyphosphoric Acid (PPA) with The Building Blocks of Hardwood Lignin: Sinapyl, Coniferyl, and Paracoumaryl Alcohols.

Phosphorylation of Triglycerides

Triglycerides are esteric compounds derived from glycerol (CH_2OH-$CHOH$-CH_2OH) and three fatty acids with animal or vegetal origin. A typical triglyceride structure is schematically shown in **Figure 6-10**. Vegetable oils from various oilseeds are among the cheapest and most abundant, annually renewable natural resources available. Vegetable oils are all triglycerides that differ greatly in their fatty acid composition. Fatty acids of triglycerides are categorized as short-chain (C6–8), medium-chain (C10–12), and long-chain (C14–18).(Dupont, 2003) They could be highly saturated or less unsaturated, containing few C=C double bonds in a cis configuration. Depending on the oil source and the synthesis processes, triglycerides contain degrees of functional groups such as double bonds, hydroxyl, carboxylic, or epoxy functions. The waste vegetable oil used as an

asphalt rejuvenator or replacement is indeed a mixture of different vegetable oils with other nonvegetable oils produced after cooking and frying activities, with higher percentages of oxidative agents such as carbonyl (C=O) or sulfoxide (S=O).

Given the phenolic nature of wood-based bio-modifiers (containing aromatic rings) and the esteric nature of waste vegetable oils (containing alkane chains), here, we study the phosphorylation of a triglyceride and a free fatty acid and then compare the results with those of lignols. Apart from the contribution of chemical reactions that may exist between the building blocks of waste cooking oil and PPA, which is highly probable due to the aliphatic OHs and COOH functionals, the comparison performed here focuses on the range of non-covalent interactions.

To have an estimation of the range of interactions, PPA was placed on the three different zones of the castor-oil triglyceride, as shown in **Figure 6-11-a**. The central zone of the triglyceride contains three esters (R-COO-R') able to set up electrostatic and H-bonding interactions with PPA active sites (**Figure 6-11-b**) associated with ΔE= -(19.3-23.9) kcal/mol stabilization energy. The presence of an aliphatic OH in the second zone and its direct interaction with the terminal OHs of PPA (**Figure 6-11-c**), has led to a considerable interaction energy for this region: ΔE= -(26.4-28.6) kcal/mol. The third zone is an alkane chain without any potential active site, showing the least interaction with PPA (**Figure 6-11-d**), ΔE= -(11.4-11.7) kcal/mol. The range of energies reported here is based on different orientations of two components when they are in the best arrangement for non-covalent interactions.

Our recent GC-MS analysis of waste vegetable oil confirms the presence of free fatty acids (medium- to long-chain) that are responsible for the hydrophilic characteristic. It is worth noting that elimination of the acid content is among the techniques proposed to treat waste vegetable oils to be used as an appropriate asphalt modifier.(Ahmed and Hossain, 2020) cis-Vaccenic acid ($C_{18}H_{34}O_2$) (**Figure 6-12**) is one of the main long-chain fatty acids (with 44% area) detected in our GC-MS analysis of a sample of waste vegetable oil. The interaction energy of cis-Vaccenic acid with PPA can reach to about 29 kcal/mol, indicating the strong interaction between the acidic head and PPA's terminal OHs.

In the context of comparison, although PPA non-covalent interactions with fatty acids or triglycerides are not very much behind those with lignols, the probability of a successful interaction, in terms of the energy value and stability of the newly formed complex, is higher for PPA-lignols. As seen in **Figure 6-11-a**, the number of potentially active sites, those carrying polar groups, is noticeably less than in carbon chains in the building blocks of waste vegetable oil, resulting in reduced phosphorylation. In lignols, the number of active sites in each unit is obviously more than those in a fatty acid, providing more appropriate conditions for PPA function. This hypothesis is further supported by our recent studies (Kabir et al., 2019) performed on a series of bio-modifiers, using thin-layer chromatography with flame ionization detection (TLC-FID), indicating that the chemical content of the bio-modifier from wood pellets contains a considerable percentage of polar compounds, 76.2%, whereas polar compounds do not exceed 12.8% in the bio-modifier from waste vegetable oil. Given the higher polarity in

the content of the wood-based bio-modifier compared to the bio-modifier from waste vegetable oil, a higher phosphorylation is expected for the wood-based bio-modifier.

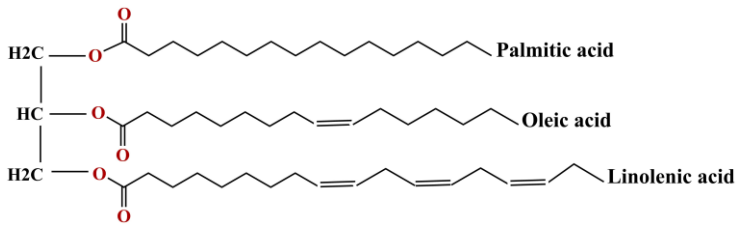

Figure 6-10. A Typical Triglyceride Structure ($C_{55}H_{98}O_6$) Originated from Glycerol and Three Fatty Acids: Palmitic Acid, Oleic Acid, and Linolenic Acid.

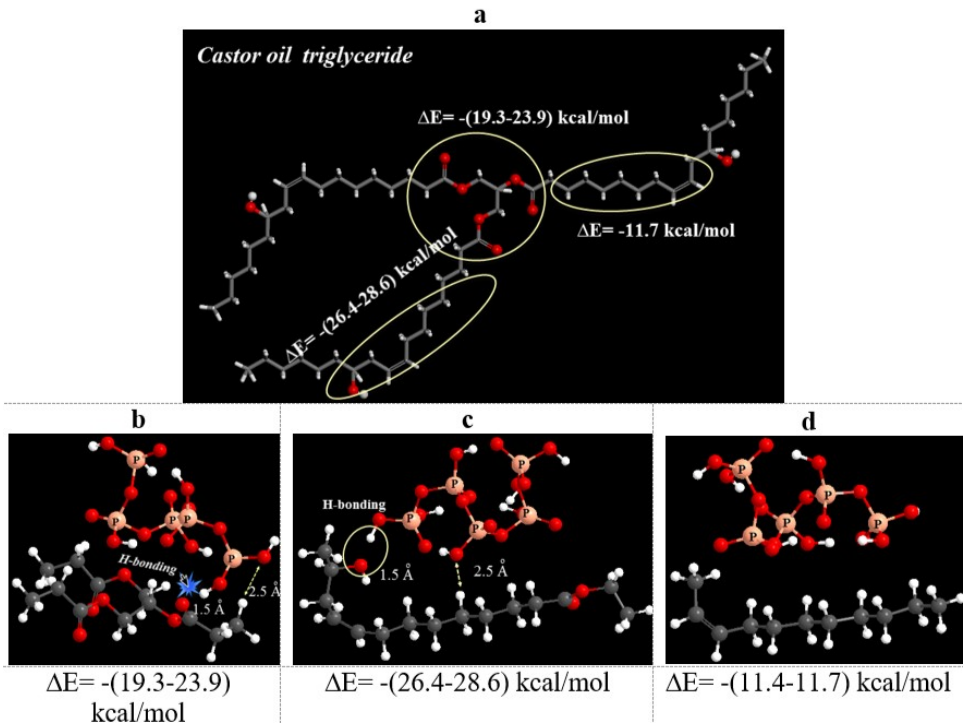

Figure 6-11 a) The Range of Non-Covalent Interaction Energies of A PPA Oligomer (Containing Five Repeating Units) with Different Zones of A Castor Oil Triglyceride Molecule. B) PPA Interaction with The Central Zone of The Triglyceride Molecule, Containing Three Ester Groups. C) PPA Interaction with The Zone of The Triglyceride Molecule Containing OH and C=C Groups. D) PPA Interaction with The Alkane Chain of The Triglyceride Molecule That Does Not Include Any Active Site.

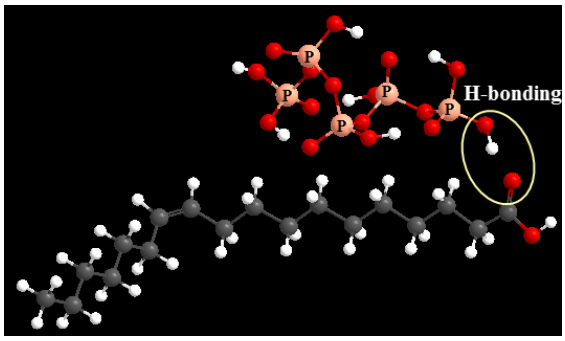

ΔE= -(26.4-28.6) kcal/mol

Figure 6-12. Non- Covalent Interaction of Cis-Vaccenic Acid ($C_{18}H_{34}O_2$) With PPA Oligomer.

6.6 Conclusion

The study examines the synergistic interactions between polyphosphoric acid (PPA) and a group of renewable bio-modifiers used to upgrade bitumen's properties. The target bio-modifiers are derived from five different sources of biomass: waste vegetable oil, wood pellet, miscanthus, corn stover, and castor oil. In a macro-scale evaluation, we evaluated the efficacy of the PPA to increase the elasticity and stiffness of bitumen containing each bio-modifier. It was found that bio-modifiers made from wood pellets had the highest synergy with PPA, and bio-modifiers made from waste vegetable oil had the least synergy with PPA. This was evidenced by an increase of almost 10% in G*/Sin (δ) and 56% in the percent recovery when PPA was introduced to the bitumen containing wood-based modifier, while only approximately 3% and 36% respective increases were observed when PPA was introduced to the bitumen containing the bio-modifier from waste vegetable oil. The wood-based bio-modifier has 76.2% polar compounds, whereas

the bio-modifier from waste vegetable oil has only 12.8% polar compounds. Given the higher polarity in the content of the wood-based bio-modifier compared to the bio-modifier from waste vegetable oil, a higher phosphorylation is expected for the wood-based bio-modifier when exposed to PPA compared to that of the bio-modifier from waste vegetable oil. To further understand the mechanisms underlying the abovementioned synergy, we computationally modeled the molecular interactions of PPA with building blocks of the bio-modifier from wood pellets (lignin units and phenolic compounds) and building blocks of the bio-modifier from waste vegetable oil (triglycerides and fatty acids). Due to the complexity, our computational model focused only on PPA's interaction with the two bio-modifiers; the model did not attempt to include the crumb rubber and bitumen.

In the case of the bio-modifier from wood pellets, our results using density functional theory showed that the alkanols (alcoholic OHs) of wood pellets can chemically interact with PPA. In addition, it was found that there are strong interactions between PPA oligomers and the lignin units of wood pellets that can explain the strong synergy found in the experiments between PPA and the bio-modifier from wood pellets.

It was also found that while aliphatic OHs of wood pellets are readily phosphorylated with PPA, phenolic OHs are not directly phosphorylated, implying that aromatic phosphate esters (Ar-O-P-) cannot be responsible for the observed synergy. A similar trend was observed for the alkoxy benzenes (Ar-OR), in which –OR groups do not undergo the chemical reaction with PPA to form phosphate esters, indicating the inability of PPA to displace -OR groups bound to the aromatic ring.

However, phenolic OHs or ORs are not the only functionals in the bio-modifier from wood pellets. The building blocks of hardwood lignin (sinapyl, coniferyl, and paracoumaryl) are alcohols containing the same number of aliphatic OHs and phenolic OHs in each unit. While DFT calculations do not predict the formation of phosphate esters through phenolic OHs, alkanols (alcoholic OHs) can chemically interact with PPA.

In the case of the bio-modifier from waste vegetable oil, alcoholic OHs are relatively low. The head group of fatty acids and the polar groups of triglycerides interact with PPA; however, such interactions are not as strong as those between the wood-based bio-modifier and PPA. The study outcome shows that PPA has a high synergy with the bio-modifier from wood pellets, amplifying the effect of PPA and leading to a bio-modified bitumen with superior performance

6.7 References

AASHTO-T315, 2012. Standard method of test for determining the rheological properties of asphalt binder using a dynamic shear rheometer (DSR).

Adamu, I., Aziz, M., Yeow, Y., Jakarmi, F.M., 2019. Dielectric measurement of bitumen: A review, IOP Conference Series: Materials Science and Engineering. IOP Publishing, p. 012056.

Ahmed, R.B., Hossain, K., 2020. Waste cooking oil as an asphalt rejuvenator: A state-of-the-art review. Construction and Building Materials 230, 116985.

Al-Qadi, I.L., Abauwad, I.M., Dhasmana, H., Coenen, A.R., 2014. Effects of various asphalt binder additives/modifiers on moisture-susceptible asphaltic mixtures. Illinois Center for Transportation.

Alexander, S., 1973. Method of treating asphalt. Google Patents.

ASTMD7175-15, 2015. Standard Test Method for Determining the Rheological Properties of Asphalt Binder Using a Dynamic Shear Rheometer. ASTM International, West Conshohocken, PA, 2015, www.astm.org.

Baumgardner, G.L., Masson, J., Hardee, J.R., Menapace, A.M., Williams, A.G., 2005. Polyphosphoric acid modified asphalt: proposed mechanisms. Journal of the Association of Asphalt Paving Technologists 74, 283-305.

Bonardd, S., Moreno-Serna, V., Kortaberria, G., Díaz Díaz, D., Leiva, A., Saldías, C., 2019. Dipolar glass polymers containing polarizable groups as dielectric materials for energy storage applications. A Minireview. Polymers 11(2), 317.

Bykov, G., Ershov, B., 2010. A sorbent based on phosphorylated lignin. Russian Journal of Applied Chemistry 83(2), 316-319.

Chailleux, E., Audo, M., Bujoli, B., Queffelec, C., Legrand, J., Lepine, O., 2012. Alternative Binder from microalgae: Algoroute project, Workshop alternative binders for sustainable asphalt pavements. pp. pp 7-14.

Chen, M., Leng, B., Wu, S., Sang, Y., 2014. Physical, chemical and rheological properties of waste edible vegetable oil rejuvenated asphalt binders. Construction and Building materials 66, 286-298.

D3279-19, A., 2019. Standard Test Method for n-Heptane Insolubles. ASTM International, www.astm.org, West Conshohocken, PA.

D'Angelo, J.A., 2012. Polyphosphoric Acid Modification of Asphalt Binders: A Workshop. Workshop Summary. Transportation Research E-Circular(E-C160).

Delley, B., 1990. An all-electron numerical method for solving the local density functional for polyatomic molecules. Journal of chemical physics 92(1), 508-517.

Delley, B., 2000. From molecules to solids with the DMol3 approach. Journal of chemical physics 113(18), 7756-7764.

Dupont, J., 2003. VEGETABLE OILS| Dietary Importance.

Eberhardsteiner, L., Füssl, J., Hofko, B., Handle, F., Hospodka, M., Blab, R., Grothe, H., 2015. Influence of asphaltene content on mechanical bitumen behavior: experimental investigation and micromechanical modeling. Materials and Structures 48(10), 3099-3112.

Edwards, Y., Tasdemir, Y., Isacsson, U., 2006. Rheological effects of commercial waxes and polyphosphoric acid in bitumen 160/220—low temperature performance. Fuel 85(7-8), 989-997.

Ernzerhof, M., Scuseria, G.E., 1999. Assessment of the Perdew–Burke–Ernzerhof exchange-correlation functional. The Journal of chemical physics 110(11), 5029-5036.

Falkiewicz, M., Grzybowski, K., 2004. Polyphosphoric Acid in Asphalt Modification, Western Research Institute Symposium on Pavement Performance Prediction, Laramie, Wyo.

Fini, E.H., Kalberer, E.W., Shahbazi, A., Basti, M., You, Z., Ozer, H., Aurangzeb, Q., 2011b. Chemical characterization of biobinder from swine manure: Sustainable modifier for asphalt binder. Journal of Materials in Civil Engineering 23(11), 1506-1513.

Grimme, S., 2011. Density functional theory with London dispersion corrections. Wiley Interdisciplinary Reviews: Computational Molecular Science 1(2), 211-228.

Hossain, Z., Alam, M.S., Baumgardner, G., 2018. Evaluation of rheological performance and moisture susceptibility of polyphosphoric acid modified asphalt binders. Road Materials and Pavement Design, 1-16.

Hosseinnezhad, S., Fini, E.H., Sharma, B.K., Basti, M., Kunwar, B., 2015b. Physiochemical characterization of synthetic bio-oils produced from bio-mass: a sustainable source for construction bio-adhesives. RSC Advances 5(92), 75519-75527.

Kabir, S.F., Mousavi, M., Fini, E.H., 2019. Selective adsorption of bio-oils' molecules onto rubber surface and its effects on stability of rubberized asphalt. Journal of Cleaner Production, 119856.

Kabir, S.F., Mousavi, M., Fini, E.H., 2020. Selective adsorption of bio-oils' molecules onto rubber surface and its effects on stability of rubberized asphalt. Journal of Cleaner Production 252, 119856.

Kodrat, I., Sohn, D., Hesp, S., 2007. Comparison of polyphosphoric acid-modified asphalt binders with straight and polymer-modified materials. Transportation Research Record: Journal of the Transportation Research Board(1998), 47-55.

Kun, D., Pukánszky, B., 2017. Polymer/lignin blends: Interactions, properties, applications. European Polymer Journal 93, 618-641.

Li, X., Clyne, T., Reinke, G., Johnson, E.N., Gibson, N., Kutay, M.E., 2011. Laboratory evaluation of asphalt binders and mixtures containing polyphosphoric acid. Transportation research record 2210(1), 47-56.

Liu, J., Yan, K., Liu, J., 2018. Rheological properties of warm mix asphalt binders and warm mix asphalt binders containing polyphosphoric acid. International Journal of Pavement Research and Technology 11(5), 481-487.

Liu, J., Yan, K., You, L., Ge, D., Wang, Z., 2016. Laboratory performance of warm mix asphalt binder containing polyphosphoric acid. Construction and Building Materials 106, 218-227.

Loza, R., Dammann, L.G., Hayner, R.E., Doolin, P.K., 2000. Unblown ethylene-vinyl acetate copolymer treated asphalt and its method of preparation. Google Patents.

Maldonaldo, R., Falkiewicz, M., Bazi, G., Grzybowski, K., 2006. Asphalt modification with polyphosphoric acid, PROCEEDINGS OF THE FIFTY-FIRST ANNUAL CONFERENCE OF THE CANADIAN TECHNICAL ASPHALT ASSOCIATION (CTAA): CHARLOTTETOWN, PRINCE EDWARD ISLAND, NOVEMBER 2006.

Martin, J.-V., 2011. Asphalt additive with improved performance. Google Patents.

Masson, J., 2008. Brief review of the chemistry of polyphosphoric acid (PPA) and bitumen. Energy & Fuels 22(4), 2637-2640.

Masson, J., Gagné, M., 2008. Ionic pairs in polyphosphoric acid (PPA)-modified bitumen: insights from model compounds. Energy & fuels 22(5), 3390-3394.

Masson, J., Gagné, M., Robertson, G., Collins, P., 2008. Reactions of polyphosphoric acid and bitumen model compounds with oxygenated functional groups: where is the phosphorylation? Energy & fuels 22(6), 4151-4157.

Mousavi, M., Fini, E.H., 2019. Moderating Effects of Paraffin Wax on Interactions between Polyphosphoric Acid and Bitumen Constituents. ACS Sustainable Chemistry & Engineering 7(24), 19739-19749.

Mousavi, M., Høgsaa, B., Fini, E.H., 2019a. Intermolecular interactions of bio-modified halloysite nanotube within high-impact polystyrene and linear low-density polyethylene. Applied Surface Science 473, 750-760.

Mousavi, M., Oldham, D.J., Hosseinnezhad, S., Fini, E.H., 2019c. Multiscale Evaluation of Synergistic and Antagonistic Interactions between Bitumen Modifiers. ACS Sustainable Chemistry & Engineering 7(18), 15568-15577.

Naher, J., Gloster, C., Doss, C.C., Jadhav, S.S., 2020a. An Automated Tool for Design Space Exploration of Matrix Vector Multiplication (MVM) Kernels Using OpenCL Based Implementation on FPGAs, 2020 IEEE 28th Annual International Symposium on Field-Programmable Custom Computing Machines (FCCM). IEEE, pp. 205-205.

Naher, J., Gloster, C., Doss, C.C., Jadhav, S.S., 2020b. Using Machine Learning to Estimate Utilization and Throughput for OpenCL-Based Matrix-Vector Multiplication (MVM), 2020 10th Annual Computing and Communication Workshop and Conference (CCWC). IEEE, pp. 0365-0372.

Naher, J., Gloster, C., Jadhav, S.S., Doss, C.C., 2020c. Design Space Exploration of an OpenCL Based SAXPY Kernel Implementation on FPGAs.

Naher, J., Sakib, A.S., Jadhav, S.S., Gloster, C., Doss, C.C., 2019. An FPGA based implementation of the Conjugate Gradient Kernels, 2019 4th International Conference on Electrical Information and Communication Technology (EICT). IEEE, pp. 1-6.

Orange, G., Dupuis, D., Martin, J., Farcas, F., Such, C., Marcant, B., 2004. Chemical modification of bitumen through polyphosphoric acid: properties-micro-structure relationship, PROCEEDINGS OF THE 3RD EURASPHALT AND EUROBITUME CONGRESS HELD VIENNA, MAY 2004.

Orlando Jr, C.M., Wirth, J., Heath, D., 1970. Methyl aryl ether cleavage in benzazole syntheses in polyphosphoric acid. The Journal of Organic Chemistry 35(9), 3147-3149.

Perdew, J.P., Burke, K., Ernzerhof, M., 1996. Generalized gradient approximation made simple. Phys. Rev. Lett. 77(18), 3865.

Platonov, V., 2000. Properties of polyphosphoric acid. Fibre Chemistry 32(5), 325-329.

Raouf, M.A., Williams, R.C., 2010. Rheology of fractionated cornstover bio-oil as a pavement material. International Journal of Pavements 9(1-2-3).

Rappoport, D., Crawford, N.R., Furche, F., Burke, K., Wiley, C., 2008. Which functional should I choose? Computational Inorganic and Bioinorganic Chemistry, 594.

Sakakura, A., Katsukawa, M., Ishihara, K., 2005. Selective synthesis of phosphate monoesters by dehydrative condensation of phosphoric acid and alcohols promoted by nucleophilic bases. Organic letters 7(10), 1999-2002.

Sun, Z., Yi, J., Huang, Y., Feng, D., Guo, C., 2016. Properties of asphalt binder modified by bio-oil derived from waste cooking oil. Construction and Building Materials 102, 496-504.

Vainio, U., Maximova, N., Hortling, B., Laine, J., Stenius, P., Simola, L.K., Gravitis, J., Serimaa, R., 2004. Morphology of dry lignins and size and shape of dissolved kraft lignin particles by X-ray scattering. Langmuir 20(22), 9736-9744.

Wen, H., Bhusal, S., Wen, B., 2012. Laboratory evaluation of waste cooking oil-based bioasphalt as an alternative binder for hot mix asphalt. Journal of Materials in Civil Engineering 25(10), 1432-1437.

Xiao, F., Amirkhanian, S., Wang, H., Hao, P., 2014. Rheological property investigations for polymer and polyphosphoric acid modified asphalt binders at high temperatures. Construction and Building Materials 64, 316-323.

Xiu, S., Rojanala, H., Shahbazi, A., Fini, E., Wang, L., 2011. Pyrolysis and combustion characteristics of Bio-oil from swine manure. Journal of thermal analysis and calorimetry 107(2), 823-829.

Yang, X., You, Z.-P., Dai, Q.-L., 2013. Performance evaluation of asphalt binder modified by bio-oil generated from waste wood resources. International Journal of Pavement Research and Technology 6(4), 431-439.

Yang, X., You, Z., Dai, Q., Mills-Beale, J., 2014. Mechanical performance of asphalt mixtures modified by bio-oils derived from waste wood resources. Construction and Building Materials 51, 424-431.

You, Z., Mills-Beale, J., Fini, E., Goh, S.W., Colbert, B., 2011. Evaluation of low-temperature binder properties of warm-mix asphalt, extracted and recovered RAP and RAS, and bioasphalt. Journal of materials in Civil Engineering 23(11), 1569-1574.

Zaumanis, M., Mallick, R.B., Poulikakos, L., Frank, R., 2014. Influence of six rejuvenators on the performance properties of Reclaimed Asphalt Pavement (RAP) binder and 100% recycled asphalt mixtures. Construction and Building Materials 71, 538-550.

Zeng, M., Li, J., Zhu, W., Xia, Y., 2018. Laboratory evaluation on residue in castor oil production as rejuvenator for aged paving asphalt binder. Construction and Building Materials 193, 276-285.

Zeng, M., Pan, H., Zhao, Y., Tian, W., 2016. Evaluation of asphalt binder containing castor oil-based bioasphalt using conventional tests. Construction and Building Materials 126, 537-543.

Zhang, F., Hu, C., Zhang, Y., 2018a. The effect of PPA on performances and structures of high-viscosity modified asphalt. Journal of Thermal Analysis and Calorimetry 134(3), 1729-1738.

Zhang, F., Hu, C., Zhang, Y., 2018b. Influence of poly (phosphoric acid) on the properties and structure of ethylene–vinyl acetate-modified bitumen. Journal of Applied Polymer Science 135(29), 46553.

Zhang, F., Yu, J., 2010. The research for high-performance SBR compound modified asphalt. Construction and Building Materials 24(3), 410-418.

Chapter 7 RECYCLING OF RUBBERIZED ASPHALT

7.1 Abstract

This study examines the effects of five bio-modifiers on the aging and rejuvenation of bio-modified rubberized bitumen. It further discusses the challenges associated with restoration and re-use of aged bitumen, especially bitumen located in a geographic area with high ultraviolet intensity. Exposing bitumen to oxidation changes its colloidal stability, while the content of asphaltene increases and the content of aromatics decreases as aging progresses. In addition to that, bitumen's evolution during aging includes oxidation, aromatization, chain scission, and carbonization, which alters bitumen's molecular structure and subsequently its restoration capacity. To revitalize aged bitumen, there is a need to restore bitumen's molecular conformation. The latter becomes more complex when rubber molecules are involved, since the presence of polymeric structures and carbon black in tire could have counteracting effects on bitumen's aging. The polymer structure can degrade and act as a sacrificing agent, while carbon black may work as a ultraviolet blocker and free radical scavenger. In addition, the presence of other modifiers such as bio-oils could alter the evolution of aging. To study the interplay of modifiers on the aging evolution of rubberized bitumen, this study compares the resistance to ultraviolet aging of various bio-modified rubberized bitumens. It further examines the efficacy of a rejuvenator to restore each aged bitumen. It was found that not all bio-modified rubberized bitumens had similar restoration capacity. The

results showed that bitumen containing wood-based modifier has the least signs of aging among all scenarios studied. This can be attributed to the presence of a significant content of furfural in wood-based modifier that helped reduce molecular-level changes. After aging, each specimen was rejuvenated using a bio-based rejuvenator. The success of rejuvenation was tracked using rejuvenating index calculated based on the extent of changes in the chemical and rheological properties of rejuvenated bitumen comparing with unaged bitumen due to the introduction of the rejuvenator. It was found that introducing 10% rejuvenator restored aged rubberized bitumen having waste vegetable oil the most, followed by bio-modifiers derived from castor oil, wood oil miscanthus and corn stover. The study results show that the composition of bio-modified rubberized bitumen not only affects its evolution during aging but also its rejuvenation capacity.

Keywords: rubberized bitumen, rejuvenation, oxidation, aging, UV aging

7.2 Introduction

The service life of bitumen is greatly reduced due to aging. As bitumen ages, it becomes stiffer and loses its stress-relaxation capability, becoming more prone to thermal cracking and fatigue cracking (Oldham et al., 2019; Zhang, H. et al., 2018). The underlying factors of aging are heat, oxygen, and ultraviolet (UV) radiation, which cause irreversible changes in the rheological and physicochemical properties of bitumen by

oxidation, aromatization, chain scission, and carbonization (Sirin et al., 2018; Xiang et al., 2015). The aging process of bitumen is a complex phenomenon; when the bitumen has been modified with rubber, the aging mechanism becomes even more complex, due to the dependence on time and temperature of the swelling nature of rubber in bitumen (Bahia et al., 1998; Lu and Isacsson, 1998). It has been proven that polymeric chains like the ones in styrene butadiene rubber (SBR) can delay the aging mechanism by hampering the oxygen molecules from penetrating into bitumen and by thermal degradation of polymers in bitumen working as sacrificing agents. These in term reduce the oxidation rate of the main functional groups in bitumen (Lu and Isacsson, 1998; Zadshir et al., 2020). Other modifiers such as various polymers, wax, polyphosphoric acid, and bio-modifiers each affect the aging evolution of bitumen (Samieadel, 2020). In addition, aging caused by oxidation affects bitumen differently from aging caused by UV radiation (Hung and Fini, 2019; Hung et al., 2019a).

Accelerated laboratory aging of bitumen is performed in standard instruments like a rolling thin-film oven and a pressure aging vessel (PAV); Qin et al. (2014) showed that bottom slice (~75 mm from pavement surface) of the 8-year old ambient field aged core has similar aging severity to the rolling thin film oven (RTFO) followed by pressure aging vessel (PAV) aging on the control binder. This implies that laboratory-based aging though not as severe as field aging still can be closely correlated and attributed to the compositional changes within asphalts (Qin et al., 2014). However, that laboratory aging does not account for the effect of ultraviolet radiation. Currently, there is no standard

method to simulate other types of environmental factors like UV radiation, which can lead to significant aging in bitumen located in regions with high UV intensity (Hung et al., 2019a). For instance, the average monthly solar radiation level in Phoenix, Arizona, is 6.57 kilowatt hours per square meter per day (kWh/m^2/day) which is one of the highest in the United States (NREL, 2020; Sengupta et al., 2018). In such a sunny place, UV irradiation of bitumen tends to produce oxidation products like carbonyls and sulfoxides at a faster rate than thermal aging (He et al., 2018; Li et al., 2019). The effects of UV exposure vary through the depth of a film of bitumen; in just 20 hours of UV exposure, a film of bitumen 600nm thick became stiff and fully lost its viscoelastic property (Hung et al., 2019a). UV exposure can also be harmful for the thermomechanical properties of bitumen (Wu et al., 2017). In just 10 days of UV exposure, UV-generated compounds can reach a depth of 2200 μm (Zeng, W. et al., 2018).

Researchers investigated both PAV aging and UV aging of bitumen modified with Styrene Butadiene Styrene (SBS) and showed that UV aging is more detrimental to SBS copolymers than PAV aging (Yu, H. et al., 2019; Zhang, D. et al., 2017). UV aging can also cause rapid structural change in bitumen, as evidenced by an increase of carbonyl content and a loss of saturated hydrocarbons (Hung et al., 2019a). A comparative study found that the resistance to UV of SBS-modified bitumen was much lower than that of rubber-modified bitumen (Wang et al., 2016). The result was attributed to the presence of carbon black in rubberized bitumen (Wang et al., 2016). Carbon black is a common component in crumb rubber coming from waste tire rubber. It works as a

free-radical scavenger and combines with organic free radicals to delay the photodegradation process (Apeagyei, 2011; Ghasemi-Kahrizsangi et al., 2015).

In another study, researchers exposed bitumens modified with two percentages of crumb rubber to UV aging; they found that UV exposure caused oxidation in all samples, with a decrease in the carbonyl index and an increase in the sulfoxide index (Zadshir et al., 2020). Research conducted by Zhu et al. involved the addition of a bio-rejuvenator to PAV-aged base bitumen and SBS-modified bitumen. The FTIR results showed that the carbonyl and sulfoxide indexes of the PAV-aged bitumen were reduced after the modification (Zhu et al., 2017).

To recycle aged rubberized bitumen, Alavi et al. in their preliminary study used reclaimed rubberized asphalt pavement (R-RAP) materials for partial aggregate and bitumen replacement in conventional dense-graded mixture. Their laboratory outcome showed that at 64°C, recycled asphalt pavement (RAP) binder and R-RAP binder had approximately the same stiffness. But adding R-RAP binder to virgin binder caused an increase in viscosity at 135° C that was 10 times greater than the increase from adding RAP binder, making it less workable and more difficult to compact (Alavi et al., 2016).

There has been considerable research on finding proper recycling agents for aged bitumen. Bio-based rejuvenators produced either from animal or plant materials are very different from additives, apart from their value-added benefits such as low cost and sustainable sources (Fini et al., 2011b; Fini et al., 2020; Pahlavan et al., 2020; Samieadel et al., 2020; Xiu et al., 2012; Yang et al., 2014; You et al., 2011; Zhu et al., 2017).

Recycling reagents like additives only soften stiff bitumen by adding shorter molecules (Pahlavan et al., 2018). A comprehensive rejuvenator should restore the rheological properties of oxidized bitumen through reducing the intensified molecular agglomeration that occurs during aging (Pahlavan et al., 2018; Pahlavan et al., 2019).

Among the research conducted to delay UV aging, Zadshir et al. worked on applying a bio-based fog sealant. The researchers showed that spraying the fog sealant reduced the oxidation of bitumen subjected to UV aging (Zadshir et al., 2018). A byproduct of the attempt to make bio-fuel from wood is furfural, which can act to delay oxidative aging. Research conducted on furfural found that a 2% furfural modification by weight of bitumen had the lowest aging index compared to the aged bitumen, indicating an improvement in resisting oxidative aging (Fini et al., 2016). Experiment results from another study showed that the anti-aging performance of bitumen can be improved by the addition of carbon black with high oil-absorption capability and high surface area (Cong et al., 2014). In more recent research, it has been shown that the chemical composition of bio-modifiers changes bitumen's resistance to aging (Hosseinnezhad et al., 2020; Hosseinnezhad et al., 2019c).

This study examines the effect of a combination of rubber and each of several bio-modifiers on bitumen's resistance to aging and subsequent rejuvenation capacity. To do so, the evolution of the chemical and rheological properties of rubberized bitumen with each bio-modifier was studied during the aging process and the rejuvenation process.

7.3 Materials and Methods

Materials

The bitumen used for this study is a PG 64-22 supplied by HollyFrontier Corporation in Arizona, USA (Table 7-1). Crumb rubber was supplied by Crumb Rubber Manufacturers in Mesa, Arizona and had particle size less than 0.25 mm. The rubberized bitumen binder was made by introducing 15% crumb rubber to base bitumen by weight of the bitumen using a bench top high shear mixer for 30 minutes at 165°C. Surface-activated rubberized bitumen (referred to as SAR) was prepared from rubberized bitumen by using each of the bio-modifiers from castor oil (CO), corn stover (CS) oil, miscanthus (MS) oil, wood pellets (WP) oil, and waste vegetable oil (WVO), resulting in five types of SARs named CO-SAR, CS- SAR, MS- SAR, WP- SAR, and WVO- SAR. Details of the preparation of bio-modified rubberized bitumen can be found elsewhere (Hosseinnezhad et al., 2015c; Kabir et al., 2019).

Table 7-1. General Properties of The PG 64-22 Bitumen

Specific Gravity @15.6 ºC	**1.041**
Cleveland Open Cup method Flash point	335 ºC
Absolute Viscosity @ 60 ºC	179 Pa.s
Stiffness @-12ºC @ 60s	71.67 MPa

UV aging of Bitumen

To mimic exposure to sunlight, a QUV Accelerated Weathering Tester (The Q-Panel Company, Cleveland, Ohio, USA) was used to expose samples to UV radiation.

For UV aging, each sample was prepared by preheating it and spreading it over a silicon rubber pan to form a uniform film of bitumen. The average thickness of each specimen was 1 mm (Figure 7-1). All SAR specimens were placed in the UV chamber with an exposure time of 200 hours and a radiation intensity of 0.71 W/m^2 at 65 °C, following a method in (Yu et al., 2009).

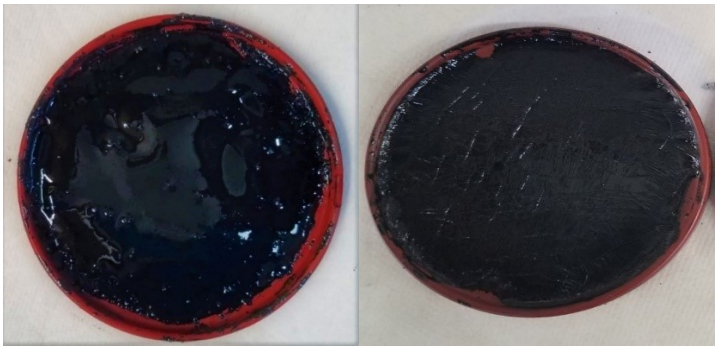

(a) (b)

Figure 7-1. Visual Comparison (a) Before and (b) After 200-Hour UV Aging for Wood-Based Bio-Modified Rubber Bitumen

Rejuvenator

The rejuvenator, referred to as the hybrid rejuvenator (HY), is made by co-liquefaction of a blend (1:1 ratio) of swine manure and algae (Rajib et al., 2020). The rejuvenator was added to aged bitumen at 10% dosage by weight of the aged bitumen.

Fourier Transform-Infrared (FTIR) Spectroscopy

A Bruker IFS 66V/S Vacuum FT-IR spectrometer with diamond ATR and pyroelectric DLaTGS detector was used to characterize the functional groups of unaged

and UV-aged SAR samples. An FT-IR spectrum range from 400 to 4000 cm^{-1} wavenumbers was collected with a resolution of 4 cm^{-1} with 32 scans per second. OMNIC software was used to calculate the area under the peak in each spectrum.

Chemical Indexing

The above-mentioned FT-IR spectrum data were used to trace the changes in the chemical structure of rubberized bitumen during UV-aging. Changes in the carboxyl functional groups and the sulfoxide functional groups were calculated for all samples using Equation 7-1 and Equation 7-2 using the method shown in (Hosseinnezhad et al., 2019b). These indices were used to track the evolution of samples through aging and restoring.

$$Carbonyl\ Index\ = \frac{Area\ under\ curve\ from\ 1680-1800\ \mathrm{cm^{-1}}}{Area\ under\ curve\ from\ 600-4000\ \mathrm{cm^{-1}}} x1000 \quad (7\text{-}1)$$

$$Sulfoxide\ Index\ = \frac{Area\ under\ curve\ from\ 960-1050\ \mathrm{cm^{-1}}}{Area\ under\ curve\ from\ 600-4000\ \mathrm{cm^{-1}}} x1000 \quad (7\text{-}2)$$

Then the chemical aging index was calculated using Equation 7-3

Chemical aging index =

$$\frac{aged\ (Carbonyl+Sulfoxide)Index - unaged\ (Carbonyl+Sulfoxide)Index}{unaged\ (Carbonyl+Sulfoxide)\ Index} x100 \quad (7\text{-}3)$$

Similarly, a chemical rejuvenating index was calculated which is defined as the ratio of the change in (carbonyl index + sulfoxide index) between rejuvenated and unaged samples divided by unaged (carbonyl index + sulfoxide index). By comparing the rejuvenated conditions to the unaged conditions, rejuvenating index provides a

comprehensive picture of the restoration towards unaged properties. The latter indexes were used to track evolution of samples through aging and rejuvenating.

Rheology-based Indexing

An Anton Paar MCR 302 dynamic shear rheometer was used to determine the elastic and viscous properties of each specimen. The test was performed using a parallel plate setup with an 8-mm spindle. An oscillation test was performed at 0.1% strain rate at frequencies ranging from 0.1-100 rad/s. The complex modulus (G*), elastic modulus (G'), viscous modulus (G''), and phase angle (δ) were calculated based on Equation 7-4(AASHTO-T-315, 2019). The complex shear modulus (G*) is a measurement of a material's resistance to deformation when repeatedly sheared, and δ is the time lag between stress and strain. A rheological aging index was calculated based on crossover modulus value, which is the value where the elastic modulus (G') and viscous modulus (G") are equal. The values of the rheological aging index were used to track the evolution of samples through aging and restoring.

$$G^* = \frac{\tau_{max}}{\gamma_{max}} \tag{7-4}$$

in which $\gamma = \left(\frac{\theta r}{h}\right)_{max}$ and $\tau = \frac{2T}{\pi r^3 max}$

where:

γ_{max} = maximum strain

τ_{max} = maximum stress

T = maximum applied torque

r = radius of the sample

θ = deflection (rotational) angle

h = height of the sample

$$\text{Rheological aging index} = \frac{|\text{aged crossover modulus - unaged crossover modulus}|}{\text{unaged crossover modulus}} x100 \quad (7\text{-}5)$$

Similarly, the rheological rejuvenating index was calculated which is defined as the ratio of the change in crossover modulus between rejuvenated and unaged samples divided by unaged crossover modulus. the values of the rheological aging and rejuvenating index were used to track the evolution of samples through aging and rejuvenating.

Activation-Energy based Indexing

Activation energy was calculated based on the zero-shear viscosity of each sample. To measure zero-shear viscosity, a shear rate sweep test was performed using an 8-mm parallel plate setup at 50, 60, and 70 °C. The viscosity values at different temperatures were used to plot viscosity versus reverse of temperature (1/T) (Equation 7-6), where the slope ($\frac{E_f}{R}$) of the resulting line was used to calculate E_f. Activation energy was used to track the evolution of samples through aging and restoring.

$$ln\,\eta = ln\,A + \frac{E_f}{R}\frac{1}{T} \quad (7\text{-}6)$$

where:

η = viscosity of bitumen in Pa·s

E_f = flow activation energy (KJ. mol^{-1})

R = universal gas constant (8.314×10^{-3} KJ.mol^{-1}. K^{-1})

T = the temperature in kelvin

A is constant.

$$\text{Activation energy based aging index} = \frac{|\text{aged activation energy - unaged activation energy}|}{\text{unaged activation energy}} x100 \quad (7\text{-}7)$$

7.4 Results and Discussion

Table 7-2 shows the mean values of the carbonyl index and sulfoxide index for the unaged, aged, and rejuvenated states of all modified samples and neat bitumen. An increase in the carbonyl index and sulfoxide index was observed after aging in all modified samples as well as neat. Increase in carbonyl and sulfoxide bands in the mid infrared spectrum is an indication of oxygen uptake which causes oxidation reactions in bitumen (Farrar et al., 2013). After equal amounts of rejuvenator (10% by weight of each sample) were added to the aged samples, the reduced carbonyl and sulfoxide index is shown in the "rejuvenated" column of Table 7-2. It is noteworthy that if the rejuvenator added were high in carbonyl and sulfoxide index reduction would not be possible. This reduction in both carbonyl and sulfoxide index establishes the fact that the added rejuvenator can effectively reduce the chemical aging of modified and neat bitumen.

Table 7-2 Carbonyl index and Sulfoxide index in all unaged, aged and rejuvenated bio-modified rubber bitumen

Sample Name	Carbonyl Index			Sulfoxide Index		
	Unaged	Aged	Rejuvenated	Unaged	Aged	Rejuvenated
CO-SAR	7.92	9.57	5.42	2.08	6.19	3.01
WVO-SAR	10.44	12.65	6.84	2.49	11.72	3.92
CS-SAR	3.31	4.89	1.55	2.82	4.39	3.85
MS-SAR	3.77	4.97	2.19	2.57	4.22	3.93
WP-SAR	3.62	4.55	2.66	3.21	4.69	3.67
CRM	1.76	5.33	2.94	3.32	6.21	3.95
Neat	2.90	9.30	6.23	3.61	9.29	5.87

Figure 7-2(a) and Figure 7-2(b) show the Aging Index (AI) and the Rejuvenating Index (RI) for chemical changes given in the Methods section. In Figure 7-2(a), WP-SAR was lowest in the chemical aging index with a value of 35.35% (highest resistance to UV aging). It was followed in increasing order of chemical aging index (decreasing resistance to UV aging) by MS-SAR (44.78%), CS-SAR (51.45%), CO-SAR (88.51%), and WVO-SAR (57.60%). The result that lignin-rich WP-SAR was most resistive to UV aging may be due to the presence of a high amount of furfural in wood-pellet oil; furfural has been shown to resist aging (Fini et al., 2016; Kabir et al., 2019). Figure 7-2(b) shows the proposed chemical rejuvenating index. Chemical rejuvenating index clearly shows how rejuvenation varies greatly based on the chemical composition of the bio-modifier. It was found to be lowest in MS-SAR (3.61%), followed by WP-SAR (7.30%), CS-SAR (12.01%), CO-SAR (15.75%) and WVO-SAR (16.83%). A lower value of the

rejuvenating index indicates the result of the applied dosage was closer to restoring the unaged properties whereas a higher value indicates a higher dose may be required to fully restore.

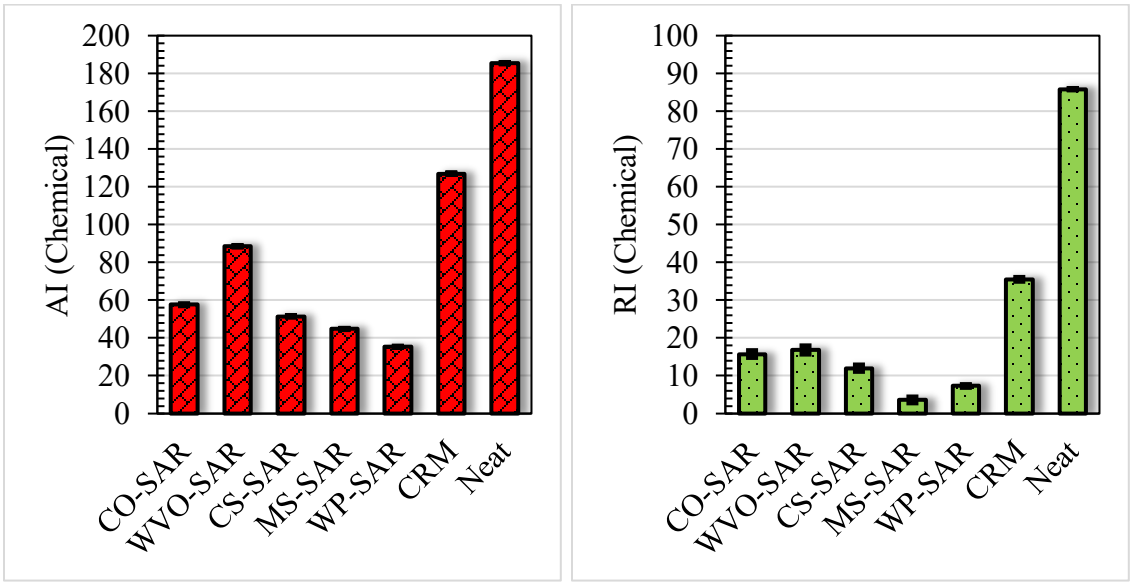

(a) (b)

Figure 7-2. Chemical (a) Aging Index (AI) and(b) Rejuvenating Index (RI) For All Modifications and Neat Bitumen

Table 7-3 shows mean crossover modulus and frequency at -2°C for all modifiers and neat bitumen for unaged, aged, and rejuvenated states. The crossover modulus and crossover frequency both decreased after aging. The lowest decrease from unaged to aged (smallest change due to UV aging) in WP-SAR (2.50 MPa), followed by MS-SAR (3.61 MPa), CS-SAR (3.66 MPa), WVO-SAR (10.89 MPa). and CO-SAR (13 MPa). In rejuvenated samples, all samples had higher crossover modulus and crossover frequency than their aged counterparts. The largest increase occurred in CO-SAR (11.66 MPa),

followed by WVO-SAR (11.25 MPa), WP-SAR (10.26 MPa), MS-SAR (6.16 MPa), and CS-SAR (5.95 MPa).

Table 7-3. Crossover Modulus and Crossover Frequency in All Unaged, Aged and Rejuvenated Modifications and Neat

Sample Name	Unaged		Aged		Rejuvenated	
	Crossover Modulus (MPa)	Crossover frequency (rad/s)	Crossover Modulus (MPa)	Crossover frequency (rad/s)	Crossover Modulus (MPa)	Crossover frequency (rad/s)
CO-SAR	16.74	2.59	3.74	0.11	15.40	3.75
WVO-SAR	18.70	2.29	7.81	0.17	19.06	3.24
CS-SAR	11.21	0.50	7.55	0.09	13.50	0.63
MS-SAR	8.51	0.21	4.90	0.11	11.06	0.25
WP-SAR	10.28	0.15	7.78	0.08	18.04	0.28
CRM	6.11	1.93	3.10	0.05	13.14	2.13
Neat	23.65	3.62	11.41	0.32	18.35	3.87

Figure 7-3(a) and **Figure 7-3(b)** show the rheology-based Aging Index (AI) and the Rejuvenating Index (RI), respectively. In **Figure 3(a)**, the highest aging index (worst resistance to UV aging) occurred in aged CO-SAR (78%), and the lowest aging index (best resistance to UV aging) occurred in WP-SAR (24%), followed by CS-SAR (32.63%). WP-SAR's resistance to UV aging may be due to the presence of higher amounts of furfural in wood-pellet oil; furfural has been shown to resist aging (Fini et al., 2016; Kabir et al., 2019). This finding implies that resistance to UV aging greatly depends on the source of the bio-modifier.

Figure 7-3(b) shows a good demonstration of how a bio-modifier's composition can influence the rejuvenation effect. It shows that after rejuvenation, the two highly aged

samples, WVO-SAR and CO-SAR, were found to be lowest in the rejuvenating index, which indicates the 10% dosage of rejuvenator was close to the optimum dose required to rejuvenate them, with index values of 2% and 8%, respectively.

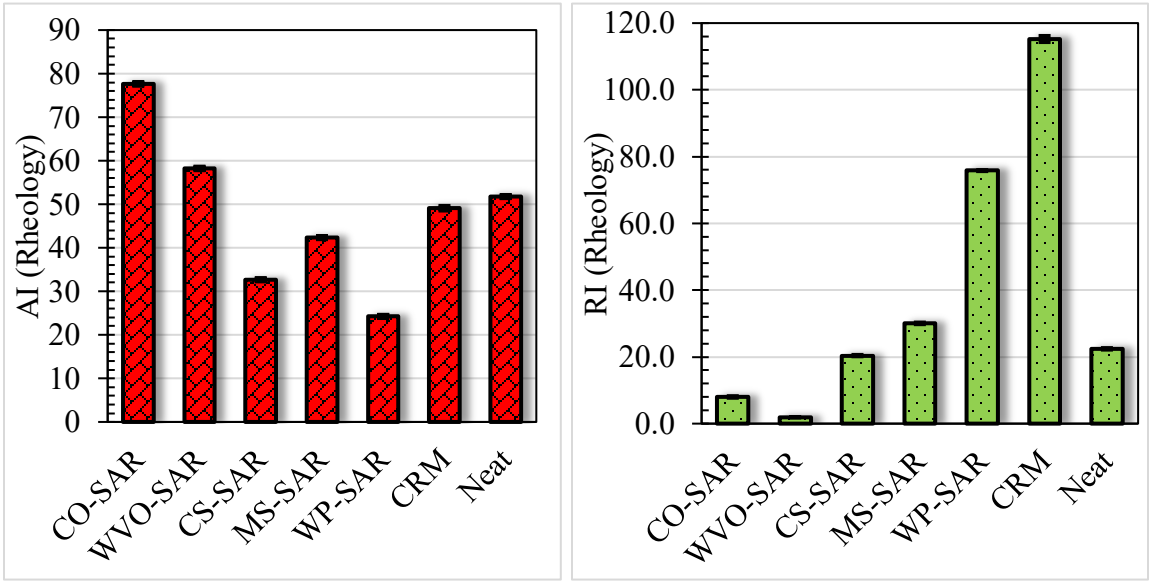

(a) (b)

Figure 7-3. Rheology-Based (a) Aging Index (AI) and (b) Rejuvenating Index (RI) For All Modifications and Neat Bitumen

Table 7-4 shows the mean activation energy of unaged, aged, and rejuvenated samples. Polymer-blended bitumen can have wide variations in activation energy depending on the polymeric effect, the polymer type, and variation in polymeric content; variations in activation energy can also be due to the effect of treating the rubber with different bio-modifiers (Kabir et al., 2019; Salomon and Zhai, 2002). It can be seen that the activation energy increased in all cases after aging. The flow activation energy is the energy required to change the resistance to flow. This is due to the fact of asphaltene

agglomeration caused by their increase in polarity during aging(Oldham et al., 2019). Which in turn increases resistance to flow and as a consequence higher activation energy is observed. WP-SAR had the lowest increase in comparison to others: 2.43 kJ/mol. Adding rejuvenator to the aged samples has reduced activation energy indicating a reduction to the agglomeration (Oldham et al., 2019).

Table 7-4. Activation Energy in All Unaged, Aged and Rejuvenated Modifications and Neat

Sample Name	Unaged	Aged	Rejuvenated
	Activation Energy (Kj/Mol)	Activation Energy (Kj/Mol)	Activation Energy (Kj/Mol)
Co-Sar	95.53	133.45	96.5
Wvo-Sar	115.63	134.19	116.5
Cs-Sar	112.17	126.42	120.1
Ms-Sar	135.30	156.62	120.8
Wp-Sar	134.74	137.17	131.4
Crm	131.64	136.46	133.5
Neat	135.60	143.18	122.1

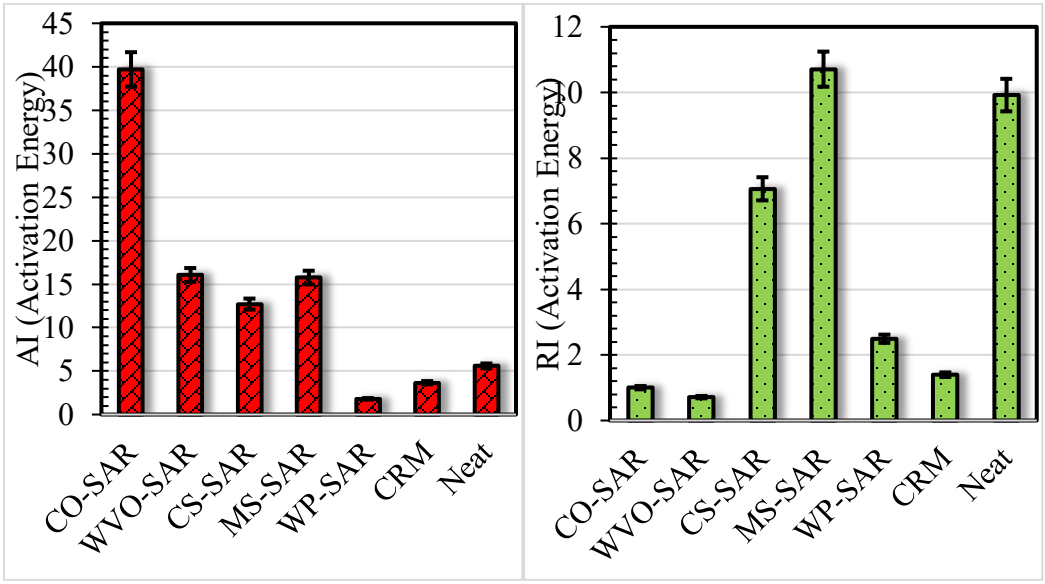

(a) (b)

Figure 7-4. Activation Energy Based (a) Aging Index (AI) and (b) Rejuvenating Index (RI) for All Modifications and Neat Bitumen

Figure 7-4(a) and **Figure 7-4(b)** show the activation-energy-based Aging Index (AI) and Rejuvenation Index (RI), respectively. WP-SAR had the lowest aging index (1.80%), whereas CO-SAR had the highest (39.7%) aging index. Wood-pellet oil is high in lignin content and includes furfural in its composition, which can hinder an increase in activation energy during the aging process.

Figure 7-4(b) shows WVO-SAR, CO-SAR, and WP-SAR were found to have the lowest rejuvenating index based on activation energy, with index values of 0.71%, 1%, and 2.49%, respectively. This indicates that the applied dosage were very close to optimally deagglomerate the asphaltene in these samples. The rejuvenating index was

high in CS-SAR (7.06%) and MS-SAR (10.71%), indicating a deviation in activation energy restoration.

Finally, an optimum dose of rejuvenator was calculated based on the unaged crossover modulus and crossover frequency for the rubberized bitumens used with a purpose to restore the unaged condition. Based on the optimum dose of rejuvenator required for full restoration, WP-SAR needed the lowest dosage (5.7%), followed by MS-SAR (8.1%), CS-SAR (8.3%), WVO-SAR (9.81%), and CO-SAR (10.87%). It should be noted that the maximum rejuvenator dose was required for neat bitumen (12.88%). The applied dosage of rejuvenator was enough to restore the crossover modulus and frequency in WP-SAR, CS-SAR, and WVO-SAR. Also, it was very close to restoring the unaged crossover modulus and frequency in CO-SAR. However, that dose did not rejuvenate enough to restore the unaged properties in neat. This shows that each aged bitumen varies in terms of its rejuvenation requirement.

Table 7-5. Optimum Rejuvenation Dosage Based on Crossover Modulus and Crossover Frequency for All Samples.

Samples	Optimum Dosage based on crossover modulus	Optimum dosage based on crossover frequency	Optimum Rej. dose= maximum of the two
CO-SAR	10.87	6.90	10.87
WVO-SAR	9.81	7.05	9.81
CS-SAR	8.30	8.00	8.30
MS-SAR	7.69	8.10	8.10
WP-SAR	5.70	5.28	5.70
CRM	4.62	9.08	9.08
Neat	12.88	9.37	12.88

7.5 Conclusion

The aim of this study was to evaluate the effect of UV aging on rubberized bitumen treated with each of five types of bio-modifiers (waste vegetable oil, corn stover, miscanthus, wood pellet, and castor oil). To do so, the samples were exposed to 200-hour continuous UV aging and then rejuvenated by adding 10% (by weight of bitumen) rejuvenator to them. During the aging process, chemical, rheological, and activation energy changes occurred, which were captured via aging and rejuvenating indexes. Based on these indices, it was found that aging of bio-modified rubberized bitumen varies greatly due to the chemical composition of the bio-modifier used to treat it. WVO-SAR and CO-SAR are mostly composed of fatty acids, which are very susceptible to UV aging underwent the most physicochemical changes during the aging period. WP-SAR being rich in hard wood lignins which contains large phenolic groups are found to be effective for their anti-oxidative performance. Besides being high in polar aromatics it also contains furfural, which may have helped to hinder UV aging. In addition, the presence of carbon black coming from crumb rubber and brown carbonaceous particles of bio-modifiers act as free-radical scavengers and UV blockers. The results obtained after adding 10% rejuvenator showed a decrease in the carbonyl index and the sulfoxide index, a reduction in crossover modulus and crossover frequency, and a reduction in activation energy. The newly proposed rejuvenating index was able to distinguish well between

these bio-modifiers. The rejuvenation of WVO-SAR based on chemical, rheological and activation energy based rejuvenating index was closest to its unaged state. The study of finding optimum dosage based on crossover modulus and crossover frequency for each modifier shows that the rejuvenation capacity of bio-modified rubberized bitumen depends on the composition of the bio-modifiers, even though all of them were exposed to the same amount of UV radiation. While the applied dosage was almost optimum for WVO-SAR (9.81%) The most resistant to UV aging, WP-SAR and MS-SAR, required only 5.7% and 8.1% of rejuvenator by weight of bitumen, respectively. Both contain furfural, which plays a role requiring a relatively smaller dosage than others. These combined results from various aging indices and their required rejuvenator dosage to restore unaged properties indicate that not every bio-modifier is good against UV aging. This findings can be helpful for choosing the best performing bio-modifier for rubberized bitumen to enhance UV resistance in highly solar-irradiated regions as well as for choosing the optimum dosage of a bio-based rejuvenator to restore the physical properties as closely as possible to the molecular level of the unaged condition.

7.6 References

AASHTO-T315, 2012. Standard method of test for determining the rheological properties of asphalt binder using a dynamic shear rheometer (DSR).
AASHTO-T-313, 2019a. Standard Method of Test for Determining the Flexural Creep Stiffness of Asphalt Binder Using the Bending Beam Rheometer (BBR).
AASHTO-T-313, 2019b. Standard method of test for determining the flexural creep stiffness of asphalt binder using the bending beam rheometer (BBR). American Association of State Highway and Transportation Officials.

AASHTO-T-315, 2019. Standard Method of Test for Determining the Rheological Properties of Asphalt Binder Using a Dynamic Shear Rheometer (DSR).
Adamu, I., Aziz, M., Yeow, Y., Jakarmi, F.M., 2019. Dielectric measurement of bitumen: A review, IOP Conference Series: Materials Science and Engineering. IOP Publishing, p. 012056.
Adhikari, B., De, D., Maiti, S., 2000. Reclamation and recycling of waste rubber. Progress in Polymer Science 25(7), 909-948.
Ahmed, R.B., Hossain, K., 2020. Waste cooking oil as an asphalt rejuvenator: A state-of-the-art review. Construction and Building Materials 230, 116985.
Al-Qadi, I.L., Abauwad, I.M., Dhasmana, H., Coenen, A.R., 2014. Effects of various asphalt binder additives/modifiers on moisture-susceptible asphaltic mixtures. Illinois Center for Transportation.
Alamawi, M.Y., Khairuddin, F.H., Yusoff, N.I.M., Badri, K., Ceylan, H., 2019. Investigation on physical, thermal and chemical properties of palm kernel oil polyol bio-based binder as a replacement for bituminous binder. Construction and Building Materials 204, 122-131.
Alavi, Z., Hung, S., Jones, D., Harvey, J., 2016. Preliminary Investigation into the Use of Reclaimed Asphalt Pavement in Gap-Graded Asphalt Rubber Mixes, and Use of Reclaimed Asphalt Rubber Pavement in Conventional Asphalt Concrete Mixes.
Alexander, S., 1973. Method of treating asphalt. Google Patents.
Alturk, S., Avci, D., Tamer, O., Atalay, Y., 2017. Comparison of different hybrid DFT methods on structural, spectroscopic, electronic and NLO parameters for a potential NLO material. Computational and Theoretical Chemistry 1100, 34-45.
Apeagyei, A.K., 2011. Laboratory evaluation of antioxidants for asphalt binders. Construction and Building Materials 25(1), 47-53.
ASTM-D36, 2014. Standard test method for softening point of bitumen (ring-and-ball apparatus). ASTM International West Conshohocken, PA.
ASTM-D2872, 2019. Standard Test Method for Effect of Heat and Air on a Moving Film of Asphalt (Rolling Thin-Film Oven Test), ASTM International, West Conshohocken, PA.
ASTM-D2872, 2019a. Standard practice for accelerated aging of asphalt binder using a pressurized aging vessel (PAV), USA: Annual Book of ASTM Standards.
ASTM-D3279, 2019. Standard Test Method for n-Heptane Insolubles ASTM International, West Conshohocken, PA.
ASTM-D4402, 2015. Standard Test Method for Viscosity Determination of Asphalt at Elevated Temperatures Using a Rotational Viscometer. West Conshohocken, PA.
ASTM-D4541, 2002. Standard Test Method for Pull-Off Strength of Coatings Using Portable Adhesion Testers. pp. 1-13.
ASTM-D6373-16, 2016. Standard Specification for Performance Graded Asphalt Binder. ASTM International, West Conshohocken, PA, 2016, www.astm.org, ASTM International, West Conshohocken, PA, 2016, www.astm.org.

ASTM-D6723, 2012. Standard Test Method for Determining the Fracture Properties of Asphalt Binder in Direct Tension (DT). ASTM International.
ASTM-D7173, 2014. Standard Practice for Determining the Separation Tendency of Polymer from Polymer Modified Asphalt. ASTM.
ASTM-D7405, 2015. Standard Test Method for Multiple Stress Creep and Recovery (MSCR) of Asphalt Binder Using a Dynamic Shear Rheometer. ASTM International, West Conshohocken, PA.
ASTM-D-4402, 2015. Standard test method for viscosity determination of asphalt at elevated temperatures using a rotational viscometer, American Society for Testing and Materials.
ASTMD7175-15, 2015. Standard Test Method for Determining the Rheological Properties of Asphalt Binder Using a Dynamic Shear Rheometer. ASTM International, West Conshohocken, PA, 2015, www.astm.org.
Bacher, A.D., 2001. Infrared Spectroscopy Table. https://www.chem.ucla.edu/~bacher/General/30BL/IR/ir.html.
Bader, R.F.W., 1990. Atoms in Molecules: A Quantum Theory. Wiley Online Library, Ontario, Canada.
Bahia, H.U., Zhai, H., Rangel, A., 1998. Evaluation of stability, nature of modifier, and short-term aging of modified binders using new tests: LAST, PAT, and modified RTFO. Transportation Research Record 1638(1), 64-71.
Baumgardner, G.L., Masson, J., Hardee, J.R., Menapace, A.M., Williams, A.G., 2005. Polyphosphoric acid modified asphalt: proposed mechanisms. Journal of the Association of Asphalt Paving Technologists 74, 283-305.
Bennert, T., Maher, A., Smith, J., 2004. Evaluation of crumb rubber in hot mix asphalt. Rutgers University, Center for Advanced Infrastructure & Transportation, and Rutgers Asphalt/Pavement Laboratory.
Berry, J., 2017. Molecular Dynamics Simulations on Polymer-Modified Model Asphalts. Journal of Creative Inquiry 1(1).
Biegler-Konig, F., Bader, R.F., 2002. AIM 2000, Version 2
Bocoum, A., Hosseinnezhad, S., Fini, E.H., 2014a. Investigating effect of amine based additives on asphalt rubber rheological properties, Asphalt Pavements. CRC Press, pp. 945-956.
Bocoum, A., Hosseinnezhad, S., Fini, E.H., 2014b. Investigating effect of amine based additives on asphalt rubber rheological properties. Asphalt Pavements 86, 921-931.
Bonardd, S., Moreno-Serna, V., Kortaberria, G., Díaz Díaz, D., Leiva, A., Saldías, C., 2019. Dipolar glass polymers containing polarizable groups as dielectric materials for energy storage applications. A Minireview. Polymers 11(2), 317.
Brandenburg, J.G., Alessio, M., Civalleri, B., Peintinger, M.F., Bredow, T., Grimme, S., 2013. Geometrical Correction for the Inter- and Intramolecular Basis Set Superposition Error in Periodic Density Functional Theory Calculations. Journal of Physical Chemistry A 117(38), 9282-9292.

Bressi, S., Fiorentini, N., Huang, J., Losa, M., 2019. Crumb rubber modifier in road asphalt pavements: state of the art and statistics. Coatings 9(6), 384.
Brown, R., 1993. Historical Development Crumb rubber modifier workshop notes: Design procedures and construction practices. Federal Highway Administration Washington, DC.
Buckingham, A.D., Fowler, P.W., Hutson, J.M., 1988. THEORETICAL-STUDIES OF VANDERWAALS MOLECULES AND INTERMOLECULAR FORCES. Chemical Reviews 88(6), 963-988.
Burns, L.A., Vazquez-Mayagoitia, A., Sumpter, B.G., Sherrill, C.D., 2011. Density-functional approaches to noncovalent interactions: A comparison of dispersion corrections (DFT-D), exchange-hole dipole moment (XDM) theory, and specialized functionals. Journal of Chemical Physics 134(8).
Bykov, G., Ershov, B., 2010. A sorbent based on phosphorylated lignin. Russian Journal of Applied Chemistry 83(2), 316-319.
Cai, Y., Jalan, A., Kubosumi, A.R., Castle, S.L., 2015. Microwave-promoted tin-free iminyl radical cyclization with TEMPO trapping: A practical synthesis of 2-acylpyrroles. Organic letters 17(3), 488-491.
CalTrans, 2003. Asphalt Rubber Usage Guide. Division of Engineering Services, Sacramento, CA, 95819-94612.
Caltrans, 2019. Cost Differential Analysis Between Asphalt Containing Crumb Rubber and Conventional Asphalt, Public Resources Code Section 42703. Caltrans.
Cao, X.-W., Luo, J., Cao, Y., Yin, X.-C., He, G.-J., Peng, X.-F., Xu, B.-P., 2014. Structure and properties of deeply oxidized waster rubber crumb through long time ozonization. Polymer degradation and stability 109, 1-6.
Cardenas, C., Ayers, P., De Proft, F., Tozer, D.J., Geerlings, P., 2011. Should negative electron affinities be used for evaluating the chemical hardness? Physical Chemistry Chemical Physics 13(6), 2285-2293.
Chai, J.D., Head-Gordon, M., 2008. Long-range corrected hybrid density functionals with damped atom-atom dispersion corrections. Physical Chemistry Chemical Physics 10(44), 6615-6620.
Chailleux, E., Audo, M., Bujoli, B., Queffelec, C., Legrand, J., Lepine, O., 2012. Alternative Binder from microalgae: Algoroute project, Workshop alternative binders for sustainable asphalt pavements. pp. pp 7-14.
Chen, M., Leng, B., Wu, S., Sang, Y., 2014. Physical, chemical and rheological properties of waste edible vegetable oil rejuvenated asphalt binders. Construction and Building materials 66, 286-298.
Chritiansson, M., Stenberg, B., Wallenberg, L., Holst, O., 1998. Reduction of surface sulphur upon microbial devulcanization of rubber materials. Biotechnology letters 20(7), 637-642.
Colom, X., Marín-Genescà, M., Mujal, R., Formela, K., Cañavate, J., 2018. Structural and physico-mechanical properties of natural rubber/GTR composites devulcanized by

microwaves: Influence of GTR source and irradiation time. J. Compos. Mater., 0021998318761554.
Cong, P., Xu, P., Chen, S., 2014. Effects of carbon black on the anti aging, rheological and conductive properties of SBS/asphalt/carbon black composites. Construction and Building Materials 52, 306-313.
Cong, P., Xun, P., Xing, M., Chen, S., 2013. Investigation of asphalt binder containing various crumb rubbers and asphalts. Construction and Building Materials 40, 632-641.
Coropceanu, V., Malagoli, M., da Silva Filho, D., Gruhn, N., Bill, T., Brédas, J., 2002. Hole-and electron-vibrational couplings in oligoacene crystals: intramolecular contributions. Physical review letters 89(27), 275503.
Cui, X., Zhao, S., Wang, B., 2016. Microbial desulfurization for ground tire rubber by mixed consortium-Sphingomonas sp. and Gordonia sp. Polymer degradation and stability 128, 165-171.
D3279-19, A., 2019. Standard Test Method for n-Heptane Insolubles. ASTM International, www.astm.org, West Conshohocken, PA.
D'Angelo, J.A., 2012. Polyphosphoric Acid Modification of Asphalt Binders: A Workshop. Workshop Summary. Transportation Research E-Circular(E-C160).
De, D., Das, A., De, D., Dey, B., Debnath, S.C., Roy, B.C., 2006. Reclaiming of ground rubber tire (GRT) by a novel reclaiming agent. European Polymer Journal 42(4), 917-927.
de Marco Rodriguez, I., Laresgoiti, M., Cabrero, M., Torres, A., Chomon, M., Caballero, B., 2001. Pyrolysis of scrap tyres. Fuel processing technology 72(1), 9-22.
de Sousa, F.D., Scuracchio, C.H., Hu, G.-H., Hoppe, S., 2017. Devulcanization of waste tire rubber by microwaves. Polymer Degradation and Stability 138, 169-181.
Delgado, A.G., Fajardo-Williams, D., Popat, S.C., Torres, C.I., Krajmalnik-Brown, R., 2014. Successful operation of continuous reactors at short retention times results in high-density, fast-rate Dehalococcoides dechlorinating cultures. Applied microbiology and biotechnology 98(6), 2729-2737.
Delley, B., 1990. An all-electron numerical method for solving the local density functional for polyatomic molecules. Journal of chemical physics 92(1), 508-517.
Delley, B., 2000. From molecules to solids with the DMol3 approach. Journal of chemical physics 113(18), 7756-7764.
Derakhshandeh, B., Shojaei, A., Faghihi, M., 2008. Effects of rubber curing ingredients and phenolic-resin on mechanical, thermal, and morphological characteristics of rubber/phenolic-resin blends. Journal of applied polymer science 108(6), 3808-3821.
Diener, M.D., Alford, J.M., 1998. Isolation and properties of small-bandgap fullerenes. Nature 393(6686), 668-671.
Dong, R., Zhao, M., Xia, W., Yi, X., Dai, P., Tang, N., 2018. Chemical and microscopic investigation of co-pyrolysis of crumb tire rubber with waste cooking oil at mild temperature. Waste Manage. (Oxford) 79, 516-525.

Dong, Z.-j., Zhou, T., Luan, H., Williams, R.C., Wang, P., Leng, Z., 2019. Composite modification mechanism of blended bio-asphalt combining styrene-butadiene-styrene with crumb rubber: A sustainable and environmental-friendly solution for wastes. Journal of cleaner production 214, 593-605.
Duan, S., Muhammad, Y., Li, J., Maria, S., Meng, F., Wei, Y., Su, Z., Yang, H., 2019. Enhancing effect of microalgae biodiesel incorporation on the performance of crumb Rubber/SBS modified asphalt. Journal of Cleaner Production, 117725.
Dubkov, K.A., Semikolenov, S.V., Ivanov, D.P., Babushkin, D.E., Voronchikhin, V.D., 2014. Scrap tyre rubber depolymerization by nitrous oxide: products and mechanism of reaction. Iranian Polymer Journal 23(11), 881-890.
Dumont, R.S., 2014. Effects of charging and polarization on molecular conduction via the source-sink potential method. Canadian Journal of Chemistry-Revue Canadienne De Chimie 92(2), 100-111.
Dupont, J., 2003. VEGETABLE OILS| Dietary Importance.
Durairaj, B., Peterson Jr, A., Salee, G., 1989. Novel rubber compounding resorcinolic resins. Google Patents.
EAPA, 2020. Warm Mix Asphalt. https://eapa.org/warm-mix-asphalt/. (Accessed July 17 2020).
Eberhardsteiner, L., Füssl, J., Hofko, B., Handle, F., Hospodka, M., Blab, R., Grothe, H., 2015. Influence of asphaltene content on mechanical bitumen behavior: experimental investigation and micromechanical modeling. Materials and Structures 48(10), 3099-3112.
Edwards, Y., Tasdemir, Y., Isacsson, U., 2006. Rheological effects of commercial waxes and polyphosphoric acid in bitumen 160/220—low temperature performance. Fuel 85(7-8), 989-997.
EIA, 2019. Energy Expplained-Biomass Independent Statistics and Analysis. www.eia.gov/energyexplained/biomass/. 2020).
EPA, 2013. Coking is a refinery process that produces 19% of finished petroleum product exports. https://www.eia.gov/todayinenergy/detail.php?id=9731.
EPA, 2019. “Rubber and Leather: Material-Specific Data.”.
Ernzerhof, M., Scuseria, G.E., 1999. Assessment of the Perdew–Burke–Ernzerhof exchange-correlation functional. The Journal of chemical physics 110(11), 5029-5036.
Falkiewicz, M., Grzybowski, K., 2004. Polyphosphoric Acid in Asphalt Modification, Western Research Institute Symposium on Pavement Performance Prediction, Laramie, Wyo.
Fan, L.-T., Shafie, M.R., Tollas, J.M., Lee, W.A.F., 2013. Extraction of hydrocarbons from hydrocarbon-containing materials and/or processing of hydrocarbon-containing materials. Google Patents.
FHWA, 2014. The Use of Recycled Tire Rubber to Modify Asphalt Binder and Mixtures in: Office of Asset Management, P., and Construction (Ed.).

FHWA, 2020. Average Monthly Asphalt Price. highways.dot.gov/federal-lands/business/escalation-factors-wfl/2020-average-monthly-asphalt-prices. (Accessed 20 June 2020).
Fini, E., Hajikarimi, P., Rahi, M., and Moghadas Nejad, F., 2015. Physiochemical, Rheological, and Oxidative Aging Characteristics of Asphalt Binder in the Presence of Mesoporous Silica Nanoparticles. J. Mater. Civ. Eng. 28(2), 1-9.
Fini, E.H., Al-Qadi, I.L., You, Z., Zada, B., Mills-Beale, J., 2012. Partial replacement of asphalt binder with bio-binder: characterisation and modification. International Journal of Pavement Engineering 13(6), 515-522.
Fini, E.H., Bocoum, A., Hosseinnezhad, S., Martinez, F.M., 2015. Bio-Modification of Rubberized Asphalt and Its High Temperature Properties.
Fini, E.H., Buabeng, F.S., Abu-Lebdeh, T., Awadallah, F., 2016. Effect of introduction of furfural on asphalt binder ageing characteristics. Road Materials and Pavement Design 17(3), 638-657.
Fini, E.H., Hosseinnezhad, S., Oldham, D., Mclaughlin, Z., Alavi, Z., Harvey, J., 2019a. Bio-modification of rubberised asphalt binder to enhance its performance. International Journal of Pavement Engineering 20(10), 1216-1225.
Fini, E.H., Hung, A.M., Roy, A., 2019b. Active Mineral Fillers Arrest Migrations of Alkane Acids to the Interface of Bitumen and Siliceous Surfaces. ACS Sustainable Chemistry & Engineering 7(12), 10340-10348.
Fini, E.H., Kalberer, E.W., Shahbazi, A., 2011a. Biobinder from swine manure: Sustainable alternative for asphalt binder.
Fini, E.H., Kalberer, E.W., Shahbazi, A., Basti, M., You, Z., Ozer, H., Aurangzeb, Q., 2011b. Chemical characterization of biobinder from swine manure: Sustainable modifier for asphalt binder. Journal of Materials in Civil Engineering 23(11), 1506-1513.
Fini, E.H., Oldham, D.J., Abu-Lebdeh, T., 2013. Synthesis and characterization of biomodified rubber asphalt: Sustainable waste management solution for scrap tire and swine manure. Journal of Environmental Engineering 139(12), 1454-1461.
Fini, E.H., Samieadel, A., Rajib, A., 2020. Moisture Damage and Its Relation to Surface Adsorption/Desorption of Rejuvenators. Industrial & Engineering Chemistry Research.
Fini, E.H., Yang, S.-H., Xiu, S., 2010. Characterization and application of manure-based bio-binder in asphalt industry.
Fletcher, R., 1980. Unconstrained optimization. Practical methods of optimization 1.
Fominykh, O.D., Sharipova, A.V., Balakina, M.Y., 2016. The Choice of Appropriate Density Functional for the Calculation of Static First Hyperpolarizability of Azochromophores and Stacking Dimers. International Journal of Quantum Chemistry 116(2), 103-112.
Frisch, M.J., Trucks, G.W., Schlegel, H.B., al., e., 2009. GAUSSIAN 09. revision A.1, Gaussian, Inc., Wallingford CT.
Froese, R.D.J., Hustad, P.D., Kuhlman, R.L., Wenzel, T.T., 2007. Mechanism of activation of a hafnium pyridyl-amide olefin polymerization catalyst: Ligand

modification by monomer. Journal of the American Chemical Society 129(25), 7831-7840.
Fukumori, K., Matsushita, M., Okamoto, H., Sato, N., Suzuki, Y., Takeuchi, K., 2002. Recycling technology of tire rubber. Jsae Review 23(2), 259-264.
Gao, J., Wang, H., You, Z., Mohd Hasan, M., Lei, Y., Irfan, M., 2018. Rheological behavior and sensitivity of wood-derived bio-oil modified asphalt binders. Applied Sciences 8(6), 919.
Garcia-Hernandez, Z., Flores-Parra, A., Grevy, J.M., Ramos-Organillo, A., Contreras, R., 2006. 2-Aminobenzothiazole phosphorus amides: Molecular and supramolecular structures, hydrogen bonds and sulfur donor-acceptor interactions. Polyhedron 25(7), 1662-1672.
Garza, A.J., Osman, O.I., Asiri, A.M., Scuseria, G.E., 2015. Can Gap Tuning Schemes of Long-Range Corrected Hybrid Functionals Improve the Description of Hyperpolarizabilities? Journal of Physical Chemistry B 119(3), 1202-1212.
Gaussian09, 2020. Optimization
Gaweł, I., Piłat, J., Radziszewski, P., Kowalski, K., Król, J., 2011. Rubber modified bitumen, Polymer modified bitumen. Elsevier, pp. 72-97.
Gawel, I., Stepkowski, R., Czechowski, F., 2006. Molecular interactions between rubber and asphalt. Industrial & engineering chemistry research 45(9), 3044-3049.
Geerlings, P., De Proft, F., Langenaeker, W., 2003. Conceptual density functional theory. Chemical Reviews 103(5), 1793-1873.
Gehrke, S., Alznauer, H.T., Karimi-Varzaneh, H.A., Becker, J.A., 2017. Ab initio simulations of bond breaking in sulfur crosslinked isoprene oligomer units. The Journal of chemical physics 147(21), 214703.
Ghasemi-Kahrizsangi, A., Neshati, J., Shariatpanahi, H., Akbarinezhad, E., 2015. Improving the UV degradation resistance of epoxy coatings using modified carbon black nanoparticles. Progress in Organic Coatings 85, 199-207.
Ghavipanjeh, F., Rad, Z.Z., Pazouki, M., 2018. Devulcanization of ground tires by different strains of bacteria: optimization of culture condition by taguchi method. Journal of Polymers and the Environment 26(8), 3168-3175.
Globenewswire, 2019. Bitumen Market To Reach USD 112.01 Billion By 2026: Reports And Data. https://www.globenewswire.com/news-release/2019/04/11/1802979/0/en/Bitumen-Market-To-Reach-USD-112-01-Billion-By-2026-Reports-And-Data.html. (Accessed 11 April, 2020 2020).
Goldshtein, V., 2002. US Patent, 6 387: 966
Goldshtein, V., 2003. US Patent 6, 541: 526.
Grimme, S., 2006. Semiempirical GGA-type density functional constructed with a long-range dispersion correction. Journal of Computational Chemistry 27(15), 1787-1799.
Grimme, S., 2011. Density functional theory with London dispersion corrections. Wiley Interdisciplinary Reviews: Computational Molecular Science 1(2), 211-228.

Hansen, K.R., Copeland, A., 2015. Asphalt pavement industry survey on recycled materials and warm-mix asphalt usage: 2014.
Hanson, D.E., 2009. Numerical simulations of rubber networks at moderate to high tensile strains using a purely enthalpic force extension curve for individual chains. The Journal of chemical physics 131(22), 224904.
Hanson, D.E., 2011. The molecular kink paradigm for rubber elasticity: Numerical simulations of explicit polyisoprene networks at low to moderate tensile strains. The Journal of chemical physics 135(5), 054902.
Hanson, D.E., Barber, J.L., 2018. The bond rupture force for sulfur chains calculated from quantum chemistry simulations and its relevance to the tensile strength of vulcanized rubber. Physical Chemistry Chemical Physics 20(13), 8460-8465.
Hanson, D.E., Barber, J.L., Subramanian, G., 2013. The entropy of the rotational conformations of (poly) isoprene molecules and its relationship to rubber elasticity and temperature increase for moderate tensile or compressive strains. The Journal of chemical physics 139(22), 224906.
Hanson, D.E., Martin, R.L., 2009. How far can a rubber molecule stretch before breaking? Ab initio study of tensile elasticity and failure in single-molecule polyisoprene and polybutadiene. The Journal of chemical physics 130(6), 064903.
He, X., Hochstein, D., Ge, Q., Ali, A.W., Chen, F., Yin, H., 2018. Accelerated aging of asphalt by UV photo-oxidation considering moisture and condensation effects. Journal of Materials in Civil Engineering 30(1), 04017261.
Hinchliffe, A., 2005. Molecular modelling for beginners. John Wiley & Sons.
Hioe, J., Šakić, D., Vrček, V., Zipse, H., 2015. The stability of nitrogen-centered radicals. Organic & biomolecular chemistry 13(1), 157-169.
Hohenberg, P., Kohn, W., 1964. Inhomogeneous Electron Gas. Physical Review 136(3B), B864-B871.
Honarparvar, B., Pawar, S.A., Alves, C. N., Lameira, J., Maguire, G. E., Silva, J. R., Govender, T, Kruger, H. G., Pentacycloundecane lactam vs lactone norstatine type protease HIV inhibitors: binding energy calculations and DFT study. Journal of Biomedical Science 22(15), 1-15.
Hossain, Z., Alam, M.S., Baumgardner, G., 2018. Evaluation of rheological performance and moisture susceptibility of polyphosphoric acid modified asphalt binders. Road Materials and Pavement Design, 1-16.
Hosseinnezhad, S., Bocoum, A., Martinez, F.M., Fini, E.H., 2015a. Biomodification of rubberized asphalt and its high temperature properties. Transportation Research Record: Journal of the Transportation Research Board(2506), 81-89.
Hosseinnezhad, S., Fini, E.H., Sharma, B.K., Basti, M., Kunwar, B., 2015b. Physiochemical characterization of synthetic bio-oils produced from bio-mass: a sustainable source for construction bio-adhesives. RSC Advances 5(92), 75519-75527.
Hosseinnezhad, S., Holmes, D., Fini, E.H., 2014. Decoupling the physical filler effect and the time dependent dissolution effect of crumb rubber on asphalt matrix Rheology.

Hosseinnezhad, S., Hung, A.M., Mousavi, M., Sharma, B.K., Fini, E., 2020. Resistance Mechanisms of Biomodified Binders against Ultraviolet Exposure. ACS Sustainable Chemistry & Engineering 8(6), 2390-2398.
Hosseinnezhad, S., Kabir, F., SK., Oldham, D.J., Mousavi, M., Fini, E.H., 2018. Sustainble Surface-Activated Rubber from Scrap Tire for Use in Construction. Journal of Cleaner Production Under Review.
Hosseinnezhad, S., Kabir, S.F., Oldham, D., Mousavi, M., Fini, E.H., 2019a. Surface functionalization of rubber particles to reduce phase separation in rubberized asphalt for sustainable construction. Journal of Cleaner Production 225, 82-89.
Hosseinnezhad, S., Oldham, D., Fini, E.H., Sharma, B.K., Kunwar, B., 2015c. Investigation of effectiveness of liquid rubber as a modifier for asphalt binder.
Hosseinnezhad, S., Shakiba, S., Mousavi, M., Louie, S.M., Karnati, S.R., Fini, E.H., 2019b. Multi-scale Evaluation of Moisture Susceptibility of Bio-Modified Bitumen. ACS Applied Bio Materials.
Hosseinnezhad, S., Zadshir, M., Yu, X., Yin, H., Sharma, B.K., Fini, E., 2019c. Differential effects of ultraviolet radiation and oxidative aging on bio-modified binders. Fuel 251, 45-56.
Huang, Y., Bird, R.N., Heidrich, O., 2007. A review of the use of recycled solid waste materials in asphalt pavements. Resources, conservation and recycling 52(1), 58-73.
Hung, A.M., Fini, E.H., 2019. Absorption spectroscopy to determine the extent and mechanisms of aging in bitumen and asphaltenes. Fuel 242, 408-415.
Hung, A.M., Kazembeyki, M., Hoover, C.G., Fini, E.H., 2019a. Evolution of Morphological and Nanomechanical Properties of Bitumen Thin Films as a Result of Compositional Changes Due to Ultraviolet Radiation. ACS Sustainable Chemistry & Engineering 7(21), 18005-18014.
Hung, A.M., Pahlavan, F., Shakiba, S., Chang, S.L., Louie, S.M., Fini, E.H., 2019b. Preventing Assembly and Crystallization of Alkane Acids at the Silica–Bitumen Interface To Enhance Interfacial Resistance to Moisture Damage. Industrial & Engineering Chemistry Research 58(47), 21542-21552.
Isayev, A.I., 2005. Recycling of rubbers. In: Mark JE, Erman B, Eirich FR. editors Science and technology of rubber. 3rd ed Elsevier Inc, p. 663e701.
Isayev AI, 2005. Recycling of rubbers.Science and technology of rubber, Chapter 15,. Elsevier, USA.
Jana, G., Das, C., 2005. Recycling natural rubber vulcanizates through mechanochemical devulcanization. Macromolecular research 13(1), 30-38.
Jeong, K.-D., Lee, S.-J., Amirkhanian, S.N., Kim, K.W., 2010. Interaction effects of crumb rubber modified asphalt binders. Construction and Building Materials 24(5), 824-831.
Jiang, G., Zhao, S., Li, W., Luo, J., Wang, Y., Zhou, Q., Zhang, C., 2011. Microbial desulfurization of SBR ground rubber by Sphingomonas sp. and its utilization as filler in NR compounds. Polymers for Advanced Technologies 22(12), 2344-2351.

John B. Macleod, M.E.M., Ronald D. Myers, Peter Nicholson, 1995. Rubber devulcanization process, in: Company, E.R.A.E. (Ed.). USA.
Jorgensen, W.L., Madura, J.D., Swenson, C.J., 1984. OPTIMIZED INTERMOLECULAR POTENTIAL FUNCTIONS FOR LIQUID HYDROCARBONS. Journal of the American Chemical Society 106(22), 6638-6646.
Jung, I.H., Lo, W.-Y., Jang, J., Chen, W., Zhao, D., Landry, E.S., Lu, L., Talapin, D.V., Yu, L., 2014. Synthesis and Search for Design Principles of New Electron Accepting Polymers for All-Polymer Solar Cells. Chemistry of Materials 26(11), 3450-3459.
Kabir, S.F., Mousavi, M., Fini, E.H., 2019. Selective adsorption of bio-oils' molecules onto rubber surface and its effects on stability of rubberized asphalt. Journal of Cleaner Production, 119856.
Kabir, S.F., Mousavi, M., Fini, E.H., 2020. Selective adsorption of bio-oils' molecules onto rubber surface and its effects on stability of rubberized asphalt. Journal of Cleaner Production 252, 119856.
Kaewpetch, B., Prasongsuk, S., Poompradub, S., 2019. Devulcanization of natural rubber vulcanizates by Bacillus cereus TISTR 2651. Express Polymer Letters 13(10), 877-888.
Kanazawa, H., Higuchi, M., Yamamoto, K., 2006. Synthesis and chemical degradation of thermostable polyamide with imine bond for chemical recycling. Macromolecules 39(1), 138–144.
Kemnitz, C.R., Loewen, M.J., 2007. "Amide resonance" correlates with a breadth of C-N rotation barriers. Journal of the American Chemical Society 129(9), 2521-2528.
Kim, J.K., Park, J.W., 1999. The biological and chemical desulfurization of crumb rubber for the rubber compounding. Journal of applied polymer science 72(12), 1543-1549.
Kim, K.S., Tarakeshwar, P., Lee, J.Y., 2000. Molecular clusters of pi-systems: Theoretical studies of structures, spectra, and origin of interaction energies. Chemical Reviews 100(11), 4145-4185.
Kleps, T., Piaskiewicz, M., Parasiewicz, W., 2000. The use of thermogravimetry in the study of rubber devulcanization. Journal of Thermal Analysis and Calorimetry 60(1), 271-277.
Klüppel, M., Menge, H., Schmidt, H., Schneider, H., Schuster, R., 2001. Influence of preparation conditions on network parameters of sulfur-cured natural rubber. Macromolecules 34(23), 8107-8116.
Knorr, K., 1994. RECLAIM FROM NATURAL AND SYNTHETIC RUBBER SCRAP FOR TECHNICAL RUBBER GOODS. Kautschuk Gummi Kunststoffe 47(1), 54-57.
Kobko, N., Dannenberg, J.J., 2001. Effect of basis set superposition error (BSSE) upon ab initio calculations of organic transition states. Journal of Physical Chemistry A 105(10), 1944-1950.
Kocevski, S., Yagneswaran, S., Xiao, F., Punith, V., Smith Jr, D.W., Amirkhanian, S., 2012. Surface modified ground rubber tire by grafting acrylic acid for paving applications. Construction and Building Materials 34, 83-90.

Kodrat, I., Sohn, D., Hesp, S., 2007. Comparison of polyphosphoric acid-modified asphalt binders with straight and polymer-modified materials. Transportation Research Record: Journal of the Transportation Research Board(1998), 47-55.
Kojima, M., Tosaka, M., Ikeda, Y., Kohjiya, S, 2005. Devulcanization of carbon black filled natural rubber using supercritical carbon dioxide. Applied Polymer 95(1), 137–143.
Kojima, M., Tosakaa, M., Ikedab, Y. , 2004. Chemical recycling of sulfur-cured natural rubber using supercritical carbon dioxide. Green Chemistry(6), 84-89.
Kojimaa, M., Kohjiyaa, S., Ikedab,Y. , , 2005. Role of supercritical carbon dioxide for selective impregnation of decrosslinking reagent into isoprene rubber vulcanizate. Polymer 46(7), 2016–2019.
Kun, D., Pukánszky, B., 2017. Polymer/lignin blends: Interactions, properties, applications. European Polymer Journal 93, 618-641.
Laidig, K.E., Cameron, L.M., 1996. Barrier to rotation in thioformamide: Implications for amide resonance. Journal of the American Chemical Society 118(7), 1737-1742.
Lameira, J., Alves, C.N., Moliner, V., Silla, E., 2006a. A density functional study of flavonoid compounds with anti-HIV activity. Eur J Med Chem 41(5), 616-623.
Lameira, J., Medeiros, I.G., Reis, M., Santos, A.S., Alves, C.N., 2006b. Structure-activity relationship study of flavone compounds with anti-HIV-1 integrase activity: A density functional theory study. Bioorg Med Chem 14(21), 7105-7112.
Lattimer, R.P., Kinsey, R.A., Layer, R.W., Rhee, C., 1989. The mechanism of phenolic resin vulcanization of unsaturated elastomers. Rubber chemistry and technology 62(1), 107-123.
Lee, S.-J., Akisetty, C.K., Amirkhanian, S.N., 2008. The effect of crumb rubber modifier (CRM) on the performance properties of rubberized binders in HMA pavements. Construction and Building Materials 22(7), 1368-1376.
Lei, Y., Wang, H., Fini, E.H., You, Z., Yang, X., Gao, J., Dong, S., Jiang, G., 2018. Evaluation of the effect of bio-oil on the high-temperature performance of rubber modified asphalt. Construction and Building Materials 191, 692-701.
Lei, Z., Bahia, H., Yi-qiu, T., 2015. Effect of bio-based and refined waste oil modifiers on low temperature performance of asphalt binders. Construction and Building Materials 86, 95-100.
Leng, Z., Padhan, R.K., Sreeram, A., 2018. Production of a sustainable paving material through chemical recycling of waste PET into crumb rubber modified asphalt. Journal of Cleaner Production 180, 682-688.
Levin, V.Y., Kim, S.H., Isayev, A.I., 1997. Vulcanization of ultrasonically devulcanized SBR elastomers. Rubber Chemistry and Technology 70(1), 120-128.
Li, B., Zhu, X., Zhang, X., Yang, X., Su, X., 2020. Surface area and microstructure of microwave activated crumb rubber modifier and its influence on high temperature properties of crumb rubber modifier binders. Materials Express 10(2), 272-277.

Li, F., Yan, B., Zhang, Y.P., Zhang, L.H., Lei, T., 2014. Effect of activator on the structure and desulphurization efficiency of sludge-activated carbon. Environmental Technology 35(20), 2575-2581.
Li Feng-Yu, Zhao Ji-Jun 2010. Quantum chemistry PM3 calculations of sixteen mEGF molecules. 1(1), 68-77.
Li, P., Ding, Z., Zou, P., Sun, A., 2017. Analysis of physico-chemical properties for crumb rubber in process of asphalt modification. Construction and Building Materials 138, 418-426.
Li, X., Clyne, T., Reinke, G., Johnson, E.N., Gibson, N., Kutay, M.E., 2011. Laboratory evaluation of asphalt binders and mixtures containing polyphosphoric acid. Transportation research record 2210(1), 47-56.
Li, Y., Wu, S., Liu, Q., Xie, J., Li, H., Dai, Y., Li, C., Nie, S., Song, W., 2019. Aging effects of ultraviolet lights with same dominant wavelength and different wavelength ranges on a hydrocarbon-based polymer (asphalt). Polymer Testing 75, 64-75.
Li, Y., Zhao, S., Wang, Y., 2012a. Improvement of the properties of natural rubber/ground tire rubber composites through biological desulfurization of GTR. Journal of Polymer Research 19(5), 9864.
Li, Y., Zhao, S., Wang, Y., 2012b. Microbial desulfurization of ground tire rubber by Sphingomonas sp.: a novel technology for crumb rubber composites. Journal of Polymers and the Environment 20(2), 372-380.
Liang, H., 2015a. Characterization and Surface Modification of Rubber from Recycled Tires. Université Laval.
Liang, H., 2015b. Characterization and surface modification of rubber from recycled tires.
Liang, M., Ren, S., Fan, W., Wang, H., Cui, W., Zhao, P., 2017a. Characterization of fume composition and rheological properties of asphalt with crumb rubber activated by microwave and TOR. Construction and Building Materials 154, 310-322.
Liang, M., Xin, X., Fan, W., Ren, S., Shi, J., Luo, H., 2017b. Thermo-stability and aging performance of modified asphalt with crumb rubber activated by microwave and TOR. Materials & Design 127, 84-96.
Liu, B., Li, J., Han, M., Zhang, Z., Jiang, X., 2020. Properties of polystyrene grafted activated waste rubber powder (PS-ARP) composite SBS modified asphalt. Construction and Building Materials 238, 117737.
Liu, J., Yan, K., Liu, J., 2018. Rheological properties of warm mix asphalt binders and warm mix asphalt binders containing polyphosphoric acid. International Journal of Pavement Research and Technology 11(5), 481-487.
Liu, J., Yan, K., You, L., Ge, D., Wang, Z., 2016. Laboratory performance of warm mix asphalt binder containing polyphosphoric acid. Construction and Building Materials 106, 218-227.

Liu, W.W., Ma, J.J., Zhan, M.S., Wang, K., 2015. The toughening effect and mechanism of styrene-butadiene rubber nanoparticles for novolac resin. Journal of Applied Polymer Science 132(9).
Lo Presti, D., 2013. Recycled Tyre Rubber Modified Bitumens for road asphalt mixtures: A literature review. Construction and Building Materials 49, 863-881.
Lopes, A.R., Constantinides, G.A., 2008. A high throughput FPGA-based floating point conjugate gradient implementation, International Workshop on Applied Reconfigurable Computing. Springer, pp. 75-86.
Loza, R., Dammann, L.G., Hayner, R.E., Doolin, P.K., 2000. Unblown ethylene-vinyl acetate copolymer treated asphalt and its method of preparation. Google Patents.
Lu, X., Isacsson, U., 1998. Chemical and rheological evaluation of ageing properties of SBS polymer modified bitumens. Fuel 77(9-10), 961-972.
MacLeod, D., Ho, S., Wirth, R., Zanzotto, L., 2007. Study of crumb rubber materials as paving asphalt modifiers. Canadian Journal of Civil Engineering 34(10), 1276-1288.
Maldonaldo, R., Falkiewicz, M., Bazi, G., Grzybowski, K., 2006. Asphalt modification with polyphosphoric acid, PROCEEDINGS OF THE FIFTY-FIRST ANNUAL CONFERENCE OF THE CANADIAN TECHNICAL ASPHALT ASSOCIATION (CTAA): CHARLOTTETOWN, PRINCE EDWARD ISLAND, NOVEMBER 2006.
Manhart, J., Kramer, R., Schaller, R., Holzner, A., Kern, W., Schlögl, S., 2016. Surface Functionalization of Natural Rubber by UV-Induced Thiol-ene Chemistry, Macromolecular Symposia. Wiley Online Library, pp. 32-39.
Marasteanu, M.O., Basu, A., 2004. Stiffness m-value and the Low Temperature Relaxation Properties of Asphalt Binders. Road Materials and Pavement Design 5(1), 121-131.
Markey, S.J., Lewis, W., Moody, C.J., 2013. A new route to α-carbolines based on 6π-electrocyclization of indole-3-alkenyl oximes. Organic letters 15(24), 6306-6308.
Martin, J.-V., 2011. Asphalt additive with improved performance. Google Patents.
Maseras, F., Morokuma, K., 1995. IMOMM - A NEW INTEGRATED AB-INITIO PLUS MOLECULAR MECHANICS GEOMETRY OPTIMIZATION SCHEME OF EQUILIBRIUM STRUCTURES AND TRANSITION-STATES. Journal of Computational Chemistry 16(9), 1170-1179.
Masson, J., 2008. Brief review of the chemistry of polyphosphoric acid (PPA) and bitumen. Energy & Fuels 22(4), 2637-2640.
Masson, J., Gagné, M., 2008. Ionic pairs in polyphosphoric acid (PPA)-modified bitumen: insights from model compounds. Energy & fuels 22(5), 3390-3394.
Masson, J., Gagné, M., Robertson, G., Collins, P., 2008. Reactions of polyphosphoric acid and bitumen model compounds with oxygenated functional groups: where is the phosphorylation? Energy & fuels 22(6), 4151-4157.
McBurney, R.T., Portela-Cubillo, F., Walton, J.C., 2012. Microwave assisted radical organic syntheses. RSC Advances 2(4), 1264-1274.

Md Abdur Rauf S, A.P.I.A., F., Govender T., Maguire G. E. M., Kruger, H. G., Honarparvar, B., 2015. The effect of N-methylation of amino acids (Ac-X-OMe) on solubility and conformation: a DFT study. Organic & Biomolecular Chemistry 13(39), 9885-10076.
Mohammadi-Jam, S., Waters, K., 2014. Inverse gas chromatography applications: A review. Advances in colloid and interface science 212, 21-44.
Mohaved, S.O., Ansarifar, A., Nezhad, S.K., Atharyfar, S., 2015. A novel industrial technique for recycling ethylene-propylene-diene waste rubber. Polymer Degradation and Stability 111, 114-123.
Monajjemi, M., Honarparvar, B., Hadad, B.K., Ilkhani, A.R., and Mollaamin, F., 2010. Thermo-chemical investigation and NBO analysis ofsome anxileotic as Nano-drugs. African Journal of Pharmacy and Pharmacology 4 (8), 521-529.
Monajjemi, M., Lee, V.S., Khaleghian, M., Honarparvar, B., Mollaamin, F., 2010. Theoretical Description of Electromagnetic Nonbonded Interactions of Radical, Cationic, and Anionic NH2BHNBHNH2 Inside of the B18N18 Nanoring. Journal of Physical Chemistry C 114(36), 15315-15330.
Moraes, R., Velasquez, R., Bahia, H.U., 2011. Measuring the effect of moisture on asphalt–aggregate bond with the bitumen bond strength test. Transportation Research Record 2209(1), 70-81.
Morgado, C.A., McNamara, J.P., Hillier, I.H., Burton, N.A., 2007. Density functional and semiempirical molecular orbital methods including dispersion corrections for the accurate description of noncovalent interactions involving sulfur-containing molecules. Journal of Chemical Theory and Computation 3(5), 1656-1664.
Mosapour Kotena Z, B.A.R., Hashim R., 2014. AIM and NBO analyses on hydrogen bonds formation in sugar-based surfactants (α/β-d-mannose and n-octyl-α/β-d-mannopyranoside): a density functional theory study. Liquid Crystals 41(6), 784-792.
Mosapour Kotena ZB-A, R., Hashim, R., Manickam Achari, V., 2013. Hydrogen bonds in galactopyranoside and glucopyranoside: a density functional theory study. Journal of Molecular Modeling 19(2), 589-599.
Mousavi, M., Fini, E.H., 2019. Moderating Effects of Paraffin Wax on Interactions between Polyphosphoric Acid and Bitumen Constituents. ACS Sustainable Chemistry & Engineering 7(24), 19739-19749.
Mousavi, M., Høgsaa, B., Fini, E.H., 2019a. Intermolecular interactions of bio-modified halloysite nanotube within high-impact polystyrene and linear low-density polyethylene. Applied Surface Science 473, 750-760.
Mousavi, M., Hosseinnezhad, S., Kabir, S.F., Burnett, D.J., Fini, E.H., 2019b. Reaction pathways for surface activated rubber particles. Resources, Conservation and Recycling 149, 292-300.
Mousavi, M., Oldham, D.J., Hosseinnezhad, S., Fini, E.H., 2019c. Multiscale Evaluation of Synergistic and Antagonistic Interactions between Bitumen Modifiers. ACS Sustainable Chemistry & Engineering 7(18), 15568-15577.

Mousavi, M., Pahlavan, F., Oldham, D., Abdollahi, T., Fini, E.H., 2016. Alteration of intermolecular interactions between units of asphaltene dimers exposed to an amide-enriched modifier. RSC Advances 6(58), 53477-53492.
Muchall, H.M., Werstiuk, N.H., Lessard, J., 1999. Computational studies on acyclic amidyl radicals: Π and Σ states and conformations. Journal of Molecular Structure: THEOCHEM 469(1-3), 135-142.
Mujika, J.I., Matxain, J.M., Eriksson, L.A., Lopez, X., 2006. Resonance structures of the amide bond: The advantages of planarity. Chemistry-a European Journal 12(27), 7215-7224.
Naher, J., Gloster, C., Doss, C.C., Jadhav, S.S., 2020a. An Automated Tool for Design Space Exploration of Matrix Vector Multiplication (MVM) Kernels Using OpenCL Based Implementation on FPGAs, 2020 IEEE 28th Annual International Symposium on Field-Programmable Custom Computing Machines (FCCM). IEEE, pp. 205-205.
Naher, J., Gloster, C., Doss, C.C., Jadhav, S.S., 2020b. Using Machine Learning to Estimate Utilization and Throughput for OpenCL-Based Matrix-Vector Multiplication (MVM), 2020 10th Annual Computing and Communication Workshop and Conference (CCWC). IEEE, pp. 0365-0372.
Naher, J., Gloster, C., Jadhav, S.S., Doss, C.C., 2020c. Design Space Exploration of an OpenCL Based SAXPY Kernel Implementation on FPGAs.
Naher, J., Sakib, A.S., Jadhav, S.S., Gloster, C., Doss, C.C., 2019. An FPGA based implementation of the Conjugate Gradient Kernels, 2019 4th International Conference on Electrical Information and Communication Technology (EICT). IEEE, pp. 1-6.
Newell, H.E., Buckton, G., Butler, D.A., Thielmann, F., Williams, D.R., 2001. The use of inverse phase gas chromatography to measure the surface energy of crystalline, amorphous, and recently milled lactose. Pharm. Res. 18(5), 662-666.
NIST, 2019. NIST Chemistry WebBook, SRD 69. https://webbook.nist.gov/cgi/cbook.cgi?Value=1015&VType=Vibe&Formula=&AllowExtra=on&Units=SI&cIR=on. 2019).
NRC, 1994. Microwave processing of materials. National Academies Press.
NREL, N.R.E.L., 2020. “Solar Energy and Solar Power in Arizona.”. (Accessed 8 june 2020).
Obrecht, W., Sumner, A., 2004. Rubber gels and rubber compounds containing phenolic resin adducts. Google Patents.
Oldham, D., 2020. Implications of Bio-Modification on Moisture Damage Mechanisms in Asphalt Binder Matrix. Arizona State University.
Oldham, D.J., Rajib, A.I., Onochie, A., Fini, E.H., 2019. Durability of bio-modified recycled asphalt shingles exposed to oxidation aging and extended sub-zero conditioning. Construction and Building Materials 208, 543-553.
Oliveira, J.R., Silva, H.M., Abreu, L.P., Fernandes, S.R., 2013. Use of a warm mix asphalt additive to reduce the production temperatures and to improve the performance of asphalt rubber mixtures. Journal of Cleaner Production 41, 15-22.

Olmsted III, J., Williams, G.M., 1997. Chemistry: the Molecular Science, 2nd Edition ed. Wm.C. Brown.
Orange, G., Dupuis, D., Martin, J., Farcas, F., Such, C., Marcant, B., 2004. Chemical modification of bitumen through polyphosphoric acid: properties-micro-structure relationship, PROCEEDINGS OF THE 3RD EURASPHALT AND EUROBITUME CONGRESS HELD VIENNA, MAY 2004.
Orlando Jr, C.M., Wirth, J., Heath, D., 1970. Methyl aryl ether cleavage in benzazole syntheses in polyphosphoric acid. The Journal of Organic Chemistry 35(9), 3147-3149.
Pahlavan, F., Mousavi, M., Hung, A.M., Fini, E.H., 2018. Characterization of oxidized asphaltenes and the restorative effect of a bio-modifier. Fuel 212, 593-604.
Pahlavan, F., Mousavi, M., Hungb, A., Fini, E. H. , 2016. Investigating molecular interactions and surface morphology of wax-doped asphaltenes Physical Chemistry Chemical Physics
Pahlavan, F., Rajib, A., Deng, S., Lammers, P., Fini, E.H., 2020. Investigation of Balanced Feedstocks of Lipids and Proteins To Synthesize Highly Effective Rejuvenators for Oxidized Asphalt. ACS Sustainable Chemistry & Engineering.
Pahlavan, F., Samieadel, A., Deng, S., Fini, E., 2019. Exploiting Synergistic Effects of Intermolecular Interactions To Synthesize Hybrid Rejuvenators To Revitalize Aged Asphalt. ACS Sustainable Chemistry & Engineering 7(18), 15514-15525.
Paizs, B., Suhai, S., 1998. Comparative study of BSSE correction methods at DFT and MP2 levels of theory. Journal of Computational Chemistry 19(6), 575-584.
Parr, R., Zhou, Z., 1993. Absolute hardness: unifying concept for identifying shells and subshells in nuclei, atoms, molecules, and metallic clusters. Accounts of Chemical Research 26(5), 256-258.
Pearson, R., 1987. Recent advances in the concept of hard and soft acids and bases. Journal of Chemical Education 64(7), 561.
Pearson, R., 1988. Absolute electronegativity and hardness: application to inorganic chemistry. Inorganic Chemistry 27(4), 734-740.
Pearson, R.G., 1989. Absolute electronegativity and hardness: applications to organic chemistry. The Journal of Organic Chemistry 54(6), 1423-1430.
Pearson, R.P., 1997. Chemical hardness: applications from molecules to solids. Wiley-VCH, Weinheim.
Peralta, J., Williams, R.C., Rover, M., Silva, H.M.R.D.d., 2012. Development of a rubber-modified fractionated bio-oil for use as noncrude petroleum binder in flexible pavements. Transportation Research Circular(E-C165), 23-36.
Perdew, J.P., Burke, K., Ernzerhof, M., 1996. Generalized gradient approximation made simple. Phys. Rev. Lett. 77(18), 3865.
Platonov, V., 2000. Properties of polyphosphoric acid. Fibre Chemistry 32(5), 325-329.
Platts, J.A., Maarof, H., Harris, K.D.M., Lim, G.K., Willock, D.J., 2012. The effect of intermolecular hydrogen bonding on the planarity of amides. Physical Chemistry Chemical Physics 14(34), 11944-11952.

Portela-Cubillo, F., Scott, J.S., Walton, J.C., 2009. Microwave-promoted syntheses of quinazolines and dihydroquinazolines from 2-aminoarylalkanone O-phenyl oximes. The Journal of organic chemistry 74(14), 4934-4942.
Presti, D.L., Giancontieri, G., Hargreaves, D., 2017. Improving the rheometry of rubberized bitumen: experimental and computation fluid dynamics studies. Construction and Building Materials 136, 286-297.
Presti, D.L., Izquierdo, M., del Barco Carrión, A.J., 2018. Towards storage-stable high-content recycled tyre rubber modified bitumen. Construction and Building Materials 172, 106-111.
Qin, Q., Schabron, J.F., Boysen, R.B., Farrar, M.J., 2014. Field aging effect on chemistry and rheology of asphalt binders and rheological predictions for field aging. Fuel 121, 86-94.
Rajib, A.I., Pahlavan, F., Fini, E.H., 2020. Investigating Molecular-Level Factors That Affect the Durability of Restored Aged Asphalt Binder. Journal of Cleaner Production, 122501.
Ralph G. Pearson, 1963. Hard and Soft Acids and Bases. J. Am. Chem. Soc. 85(22), 3533–3539.
Raouf, M.A., Williams, R.C., 2010. Rheology of fractionated cornstover bio-oil as a pavement material. International Journal of Pavements 9(1-2-3).
Rappoport, D., Crawford, N.R., Furche, F., Burke, K., Wiley, C., 2008. Which functional should I choose? Computational Inorganic and Bioinorganic Chemistry, 594.
Rauf, M.A., Arvidsson, P., Albericio, F., Govender, T., Maguire, G. E., Kruger, H. G., Honarparvar, B., 2015. The effect of N-methylation of amino acids (Ac-X-OMe) on solubility and conformation: a DFT study. Organic & biomolecular chemistry 13(39), 9993-10006.
Reed, A.E., Curtiss, L.A., Weinhold, F., 1988. INTERMOLECULAR INTERACTIONS FROM A NATURAL BOND ORBITAL, DONOR-ACCEPTOR VIEWPOINT. Chemical Reviews 88(6), 899-926.
Reed, A.E., Weinhold, F., 1985. Natural localized molecular orbitals. Chemical Physics 83(4), 1736-1740.
Robert G. Parr , Ralph G. Pearson, 1983. Absolute hardness: companion parameter to absolute electronegativity. J. Am. Chem. Soc., 105(26), 7512–7516.
Romero-Sánchez, M.a.D., Pastor-Blas, M.M., Martín-Martínez, J.M., 2003. Treatment of a styrene-butadiene-styrene rubber with corona discharge to improve the adhesion to polyurethane adhesive. International journal of adhesion and adhesives 23(1), 49-57.
Romero-Sánchez, M.D., Martín-Martínez, J.M., 2006. Surface modifications of vulcanized SBR rubber by treatment with atmospheric pressure plasma torch. International journal of adhesion and adhesives 26(5), 345-354.
Romero-Sánchez, M.D., Walzak, M.J., Torregrosa-Maciá, R., Martín-Martínez, J.M., 2007. Surface modifications and adhesion of SBS rubber containing calcium carbonate

filler by treatment with UV radiation. International journal of adhesion and adhesives 27(6), 434-445.
Rooj, S., Basak,G. C., Maji, P. K., Bhowmick, A. K., 2011. New Route for Devulcanization of Natural Rubber and the Properties of Devulcanized Rubber. Journal of Polymers and the Environment 19(2), 382-390.
Sakakura, A., Katsukawa, M., Ishihara, K., 2005. Selective synthesis of phosphate monoesters by dehydrative condensation of phosphoric acid and alcohols promoted by nucleophilic bases. Organic letters 7(10), 1999-2002.
Salomon, D., Zhai, H., 2002. Ranking asphalt binders by activation energy for flow. Journal of Applied Asphalt Binder Technology 2(2), 52-60.
Samieadel, A., 2020. Multi-Scale Characterization of Bitumen Doped with Sustainable Modifiers. Arizona State University.
Samieadel, A., Rajib, A.I., Dandamudi, K.P.R., Deng, S., Fini, E.H., 2020. Improving recycled asphalt using sustainable hybrid rejuvenators with enhanced intercalation into oxidized asphaltenes nanoaggregates. Construction and Building Materials 262, 120090.
Sarasia, E.M., Soliman, M.E.S., Honarparvar, B., 2012. Theoretical study on the molecular electronic properties of salicylic acid derivatives as anti-inflammatory drugs. Journal of Structural Chemistry 53(3), 574-581.
Schaafsma, Y., Bickel, A., Kooyman, E., 1960. Photolysis of aromatic disulphides. Tetrahedron 10(1-2), 76-80.
Schlegel, H.B., 1984. Estimating the Hessian for gradient-type geometry optimizations. Theoretica chimica acta 66(5), 333-340.
Schlegel, H.B., Binkley, J., Pople, J., 1982. Chent Phys. 1984, 80, 1976-1981. Schlegel, HBJ. Comput. Chem 3, 214-218.
Schmidt, U., 1964a. Free Radicals and Free-Radical Reactions of Monovalent and Divalent Sulfur. Angewandte Chemie International Edition 3(9), 602-608.
Schmidt, U., 1964b. Free radicals and free-radical reactions of monovalent and divalent sulfur. Angewandte Chemie International Edition in English 3(9), 602-608.
Segneanu, A.E., Gozescu, I., Dabici, A., Sfirloaga, P., Szabadai, Z., 2012. Organic compounds FT-IR spectroscopy. InTech Romania.
Sengupta, M., Xie, Y., Lopez, A., Habte, A., Maclaurin, G., Shelby, J., 2018. The national solar radiation data base (NSRDB). Renewable and Sustainable Energy Reviews 89, 51-60.
Shatanawi, K., Biro, S., Thodesen, C., Amirkhanian, S., 2009. Effects of water activation of crumb rubber on the properties of crumb rubber-modified binders. International Journal of Pavement Engineering 10(4), 289-297.
Shatanawi, K.M., Biro, S., Geiger, A., Amirkhanian, S.N., 2012. Effects of furfural activated crumb rubber on the properties of rubberized asphalt. Construction and Building Materials 28(1), 96-103.

Shatanawi, K.M., Biro, S., Naser, M., Amirkhanian, S.N., 2013. Improving the rheological properties of crumb rubber modified binder using hydrogen peroxide. Road materials and pavement design 14(3), 723-734.
Shen, J., Amirkhanian, S., Xiao, F., Tang, B., 2009. Influence of surface area and size of crumb rubber on high temperature properties of crumb rubber modified binders. Construction and Building Materials 23(1), 304-310.
Shu, X., Huang, B., 2014. Recycling of waste tire rubber in asphalt and portland cement concrete: An overview. Construction and Building Materials 67, 217-224.
Shulman, V.L., 2019. Tire recycling, Waste. Elsevier, pp. 489-515.
Sienkiewicz, M., Borzędowska-Labuda, K., Wojtkiewicz, A., Janik, H., 2017. Development of methods improving storage stability of bitumen modified with ground tire rubber: A review. Fuel Process. Technol. 159, 272-279.
Sirin, O., Paul, D.K., Kassem, E., 2018. State of the art study on aging of asphalt mixtures and use of antioxidant additives. Advances in Civil Engineering 2018.
Sun, Z., Yi, J., Huang, Y., Feng, D., Guo, C., 2016. Properties of asphalt binder modified by bio-oil derived from waste cooking oil. Construction and Building Materials 102, 496-504.
Susa, D., Haydary, J., 2013. Sulphur distribution in the products of waste tire pyrolysis. Chemical Papers 67(12), 1521-1526.
Sutanto, P., Laksmana, F.L., Picchioni, E., Janssen, L.P.B.M., 2006. Modeling on the kinetics of an EPDM devulcanization in an internal batch mixer using an amine as the devulcanizing agent. Chemical Engineering Science 61(19), 6442-6453.
Sutanto, P., Laksmana, F.L. ,Picchioni, F. , Janssen, L.P.B.M., 2006. Modeling on the kinetics of an EPDM devulcanization in an internal batch mixer using an amine as the devulcanizing agent. Chemical Engineering Science 61(19), 6442 – 6453.
Svensson, M., Humbel, S., Morokuma, K., 1996. Energetics using the single point IMOMO (integrated molecular orbital plus molecular orbital) calculations: Choices of computational levels and model system. Journal of Chemical Physics 105(9), 3654-3661.
Szabo Attila. , Ostlund Neil.S., 1989. Modern Quantum Chemistry: Introduction to Advanced Electronic Structure Theory. McGraw Hill, Mineola, New York.
Tatangelo, V., Mangili, I., Caracino, P., Bestetti, G., Collina, E., Anzano, M., Branduardi, P., Posteri, R., Porro, D., Lasagni, M., 2019. Microbial desulfurization of ground tire rubber (GTR): Characterization of microbial communities and rheological and mechanical properties of GTR and natural rubber composites (GTR/NR). Polymer degradation and stability 160, 102-109.
Teixeira, J., 2015. Industrial Devulcanization of Rubber. Kgk-Kautschuk Gummi Kunststoffe 68(1-2), 6-9.
Thodesen, C., Xiao, F., Amirkhanian, S.N., 2009. Modeling viscosity behavior of crumb rubber modified binders. Construction and Building Materials 23(9), 3053-3062.
Treloar, L., 1944. Stress-strain data for vulcanised rubber under various types of deformation. Transactions of the Faraday Society 40, 59-70.

Tsoskounoglou, M., Ayerides, G., Tritopoulou, E., 2008. The end of cheap oil: Current status and prospects. Energy Policy 36(10), 3797-3806.
Tsuzuki, S., Uchimaru, T., Tanabe, K., Kuwajima, S., 1994. REFINEMENT OF NONBONDING INTERACTION POTENTIAL PARAMETERS FOR METHANE ON THE BASIS OF THE PAIR POTENTIAL OBTAINED BY MP3/6-311G(3D,3P)-LEVEL AB-INITIO MOLECULAR-ORBITAL CALCULATIONS - THE ANISOTROPY OF H/H INTERACTION. Journal of Physical Chemistry 98(7), 1830-1833.
Tyczkowski, J., Krawczyk, I., Wożniak, B., 2003. Modification of styrene–butadiene rubber surfaces by plasma chlorination. Surface and coatings technology 174, 849-853.
Udhayakalaa, P., Rajendiranb, T. V., Gunasekaranc, S. , 2012. Theoretical approach to the corrosion inhibition efficiency of some pyrimidine derivatives using DFT method. Journal of Computational Methods in Molecular Design 2(1), 1-15.
USTMA, 2017. 2017 U.S. Scrap Tire Management Summary. www.ustires.org/system/files/USTMA_scraptire_summ_2017_072018.pdf. (Accessed 6/19 2020).
UTMA, 2017. SCRAP TIRE MARKETS. https://www.ustires.org/scrap-tire-markets. 2019).
Vainio, U., Maximova, N., Hortling, B., Laine, J., Stenius, P., Simola, L.K., Gravitis, J., Serimaa, R., 2004. Morphology of dry lignins and size and shape of dissolved kraft lignin particles by X-ray scattering. Langmuir 20(22), 9736-9744.
Walling, C., Rabinowitz, R., 1959. The Photolysis of Isobutyl Disulfide in Cumene1. Journal of the American Chemical Society 81(5), 1137-1143.
Walters, R., Fini, E. H., Abu-Lebdeh, T., 2014. Introducing Combination of Nano-clay and Bio-char to Enhance Asphalt Binder's Rheological and Aging Characteristics. International Journal of Pavement Research and Technology 7(6), 451-455.
Walton, J.C., 2014. The oxime portmanteau motif: Released heteroradicals undergo incisive EPR interrogation and deliver diverse heterocycles. Accounts of chemical research 47(4), 1406-1416.
Wang, C., Xue, L., Xie, W., You, Z., Yang, X., 2018. Laboratory investigation on chemical and rheological properties of bio-asphalt binders incorporating waste cooking oil. Construction and Building Materials 167, 348-358.
Wang, Q., Li, S., Wu, X., Wang, S., Ouyang, C., 2016. Weather aging resistance of different rubber modified asphalts. Construction and Building Materials 106, 443-448.
Warner, W.C., 1994. METHODS OF DEVULCANIZATION. Rubber Chemistry and Technology 67(3), 559-566.
Way, G.B., Kaloush, K.E., Biligiri, K.P., 2012. Asphalt-rubber standard practice guide. Rubber Pavements Association, Tempe.
Weinhold F, Carpenter J.E., 1988. The Structure of Small Molecules and Ions, Plenum, New York.

Wen, H., Bhusal, S., Wen, B., 2012. Laboratory evaluation of waste cooking oil-based bioasphalt as an alternative binder for hot mix asphalt. Journal of Materials in Civil Engineering 25(10), 1432-1437.
Wen, Y., Liu, Q., Chen, L., Pei, J., Zhang, J., Li, R., 2020. Review and comparison of methods to assess the storage stability of terminal blend rubberized asphalt binders. Construction and Building Materials 258, 119586.
Williams, B.A., Willis, J.R., Ross, T.C., 2019. Asphalt Pavement Industry Survey on Recycled Materials and Warm-Mix Asphalt Usage: 2018.
Wong, K.Y., -Mercader, A.G., Saavedra, L. M., Honarparvar, B., Romanelli, G.P., Duchowicz, P. R., 2014. QSAR analysis on tacrine-related acetylcholinesterase inhibitors. Journal of Biomedical Science 21(84), 1-8.
Wright, M.M., Daugaard, D.E., Satrio, J.A., Brown, R.C., 2010. Techno-economic analysis of biomass fast pyrolysis to transportation fuels. Fuel 89, S2-S10.
Wu, S., Zhao, Z., Li, Y., Pang, L., Amirkhanian, S., Riara, M., 2017. Evaluation of aging resistance of graphene oxide modified asphalt. Applied Sciences 7(7), 702.
Xantheas, S.S., 1996. On the importance of the fragment relaxation energy terms in the estimation of the basis set superposition error correction to the intermolecular interaction energy. Journal of Chemical Physics 104(21), 8821-8824.
Xiang, L., Cheng, J., Kang, S., 2015. Thermal oxidative aging mechanism of crumb rubber/SBS composite modified asphalt. Construction and Building Materials 75, 169-175.
Xiang, Y., Xie, Y., Long, G., Zeng, L., 2018. Ultraviolet irradiation of crumb rubber on mechanical performance and mechanism of rubberised asphalt. Road Materials and Pavement Design, 1-14.
Xiang, Y., Xie, Y., Long, G., Zeng, L., 2019. Ultraviolet irradiation of crumb rubber on mechanical performance and mechanism of rubberised asphalt. Road Materials and Pavement Design 20(7), 1624-1637.
Xiao, F., Amirkhanian, S., Wang, H., Hao, P., 2014. Rheological property investigations for polymer and polyphosphoric acid modified asphalt binders at high temperatures. Construction and Building Materials 64, 316-323.
Xiaowei, C., Sheng, H., Xiaoyang, G., Wenhui, D., 2017. Crumb waste tire rubber surface modification by plasma polymerization of ethanol and its application on oil-well cement. Applied Surface Science 409, 325-342.
Xie, J., Yang, Y., Lv, S., Peng, X., Zhang, Y., 2019a. Investigation on Preparation Process and Storage Stability of Modified Asphalt Binder by Grafting Activated Crumb Rubber. Materials 12(12), 2014.
Xie, J., Yang, Y., Lv, S., Zhang, Y., Zhu, X., Zheng, C., 2019b. Investigation on Rheological Properties and Storage Stability of Modified Asphalt Based on the Grafting Activation of Crumb Rubber. Polymers 11(10), 1563.

Xiu, S., Rojanala, H., Shahbazi, A., Fini, E., Wang, L., 2011. Pyrolysis and combustion characteristics of Bio-oil from swine manure. Journal of thermal analysis and calorimetry 107(2), 823-829.
Xiu, S., Rojanala, H., Shahbazi, A., Fini, E., Wang, L., 2012. Pyrolysis and combustion characteristics of Bio-oil from swine manure. Journal of thermal analysis and calorimetry 107(2), 823-829.
Yang, X., You, Z.-P., Dai, Q.-L., 2013. Performance evaluation of asphalt binder modified by bio-oil generated from waste wood resources. International Journal of Pavement Research and Technology 6(4), 431-439.
Yang, X., You, Z., Dai, Q., Mills-Beale, J., 2014. Mechanical performance of asphalt mixtures modified by bio-oils derived from waste wood resources. Construction and Building Materials 51, 424-431.
Yang, Y., Zhang, Y., Omairey, E., Cai, J., Gu, F., Bridgwater, A.V., 2018. Intermediate pyrolysis of organic fraction of municipal solid waste and rheological study of the pyrolysis oil for potential use as bio-bitumen. Journal of Cleaner Production 187, 390-399.
Yao, C., Zhao, S., Wang, Y., Wang, B., Wei, M., Hu, M., 2013. Microbial desulfurization of waste latex rubber with Alicyclobacillus sp. Polymer degradation and stability 98(9), 1724-1730.
You, Z., Mills-Beale, J., Fini, E., Goh, S.W., Colbert, B., 2011. Evaluation of low-temperature binder properties of warm-mix asphalt, extracted and recovered RAP and RAS, and bioasphalt. Journal of materials in Civil Engineering 23(11), 1569-1574.
Yu, G.-X., Li, Z.-M., Zhou, X.-L., Li, C.-L., 2011. Crumb rubber–modified asphalt: microwave treatment effects. Petroleum Science and Technology 29(4), 411-417.
Yu, H., Bai, X., Qian, G., Wei, H., Gong, X., Jin, J., Li, Z., 2019. Impact of ultraviolet radiation on the aging properties of SBS-modified asphalt binders. Polymers 11(7), 1111.
Yu, H., Leng, Z., Zhou, Z., Shih, K., Xiao, F., Gao, Z., 2017. Optimization of preparation procedure of liquid warm mix additive modified asphalt rubber. Journal of cleaner production 141, 336-345.
Yu, J.-Y., Feng, P.-C., Zhang, H.-L., Wu, S.-P., 2009. Effect of organo-montmorillonite on aging properties of asphalt. Construction and Building Materials 23(7), 2636-2640.
Yu, J., Ren, Z., Gao, Z., Wu, Q., Zhu, Z., Yu, H., 2019. Recycled Heavy Bio Oil as Performance Enhancer for Rubberized Bituminous Binders. Polymers 11(5), 800.
Zadshir, M., Hosseinnezhad, S., Ortega, R., Chen, F., Hochstein, D., Xie, J., Yin, H., Parast, M.M., Fini, E.H., 2018. Application of a Biomodifier as Fog Sealants to Delay Ultraviolet Aging of Bituminous Materials. J. Mater. Civ. Eng. 30(12), 04018310.
Zadshir, M., Ploger, D., Yu, X., Sangiorgi, C., Yin, H., 2020. Chemical, thermophysical, rheological, and microscopic characterisation of rubber modified asphalt binder exposed to UV radiation. Road Materials and Pavement Design, 1-17.

Zanchet, A., Carli, L.N., Giovanela, M., Crespo, J.S., Scuracchio, C.H., Nunes, R.C.R., 2009. Characterization of Microwave-Devulcanized Composites of Ground SBR Scraps. Journal of Elastomers and Plastics 41(6), 497-507.
Zani, L., Giustozzi, F., Harvey, J., 2017. Effect of storage stability on chemical and rheological properties of polymer-modified asphalt binders for road pavement construction. Construction and Building Materials 145, 326-335.
Zaumanis, M., Mallick, R.B., Poulikakos, L., Frank, R., 2014. Influence of six rejuvenators on the performance properties of Reclaimed Asphalt Pavement (RAP) binder and 100% recycled asphalt mixtures. Construction and Building Materials 71, 538-550.
Zeng, M., Li, J., Zhu, W., Xia, Y., 2018. Laboratory evaluation on residue in castor oil production as rejuvenator for aged paving asphalt binder. Construction and Building Materials 193, 276-285.
Zeng, M., Pan, H., Zhao, Y., Tian, W., 2016. Evaluation of asphalt binder containing castor oil-based bioasphalt using conventional tests. Construction and Building Materials 126, 537-543.
Zeng, W., Wu, S., Pang, L., Chen, H., Hu, J., Sun, Y., Chen, Z., 2018. Research on Ultra Violet (UV) aging depth of asphalts. Construction and Building Materials 160, 620-627.
Zhang, D., Zhang, H., Shi, C., 2017. Investigation of aging performance of SBS modified asphalt with various aging methods. Construction and Building Materials 145, 445-451.
Zhang, F., Hu, C., Zhang, Y., 2018a. The effect of PPA on performances and structures of high-viscosity modified asphalt. Journal of Thermal Analysis and Calorimetry 134(3), 1729-1738.
Zhang, F., Hu, C., Zhang, Y., 2018b. Influence of poly (phosphoric acid) on the properties and structure of ethylene–vinyl acetate-modified bitumen. Journal of Applied Polymer Science 135(29), 46553.
Zhang, F., Yu, J., 2010. The research for high-performance SBR compound modified asphalt. Construction and Building Materials 24(3), 410-418.
Zhang, H., Chen, Z., Xu, G., Shi, C., 2018. Evaluation of aging behaviors of asphalt binders through different rheological indices. Fuel 221, 78-88.
Zhang, R., Wang, H., Gao, J., Yang, X., You, Z., 2017. Comprehensive performance evaluation and cost analysis of SBS-modified bioasphalt binders and mixtures. Journal of Materials in Civil Engineering 29(12), 04017232.
Zhang, R., You, Z., Wang, H., Chen, X., Si, C., Peng, C., 2018. Using bio-based rejuvenator derived from waste wood to recycle old asphalt. Construction and Building Materials 189, 568-575.
Zhang, X., Lu, C., Liang, M., 2009. Properties of natural rubber vulcanizates containing mechanochemically devulcanized ground tire rubber. Journal of Polymer Research 16(4), 411-419.

Zhao, Y., Gu, F., Xu, J., Jin, J., 2010. Analysis of Aging Mechanism of SBS Polymer Modified Asphalt based on Fourier Transform Infrared Spectrum. Journal of Wuhan University of Technology-Materials Science Edition 25(6), 1047-1052.
Zhu, H., Xu, G., Gong, M., Yang, J., 2017. Recycling long-term-aged asphalts using bio-binder/plasticizer-based rejuvenator. Construction and Building Materials 147, 117-129.
Zielinski, T.J., Harvey, E., Sweeney, R., Hanson, D.M., 2005. Quantum states of atoms and molecules. ACS Publications.

Chapter 8 CONCLUSION

This chapter has two subsections. The first subsection discusses the economic viability and market analysis of bio-modified rubber for use either as a modifier or as a partial replacement for bitumen. The second subsection summarizes the research outcomes and makes recommendations for future research.

8.1 Economic Viability and Market Analysis

8.1.1 Current market situation

The quality of crude-oil inputs in refineries is declining, and demand for transportation fuels is increasing. Similar to secondary processing units in other industries, thermal cracking combined with coking plays an important role in refinery economics (EPA, 2013). Thermal cracking uses heat to break chemical bonds. Increasing implementation of this coking technology breaks down the asphalt residual material to other products and coke, while the amount of asphalt being produced has been decreasing (Oldham, 2020). This entirely depends on the quality and cost of the crude oil run at a refinery (EPA, 2013). All these factors have recently increased the price of asphalt binder. Figure 8-1 shows the price of asphalt binder per U.S. ton for the past 4 years depicting that the price of asphalt binder has had an increasing trend since 2016, except for the 2020 pandemic situation (FHWA, 2020).

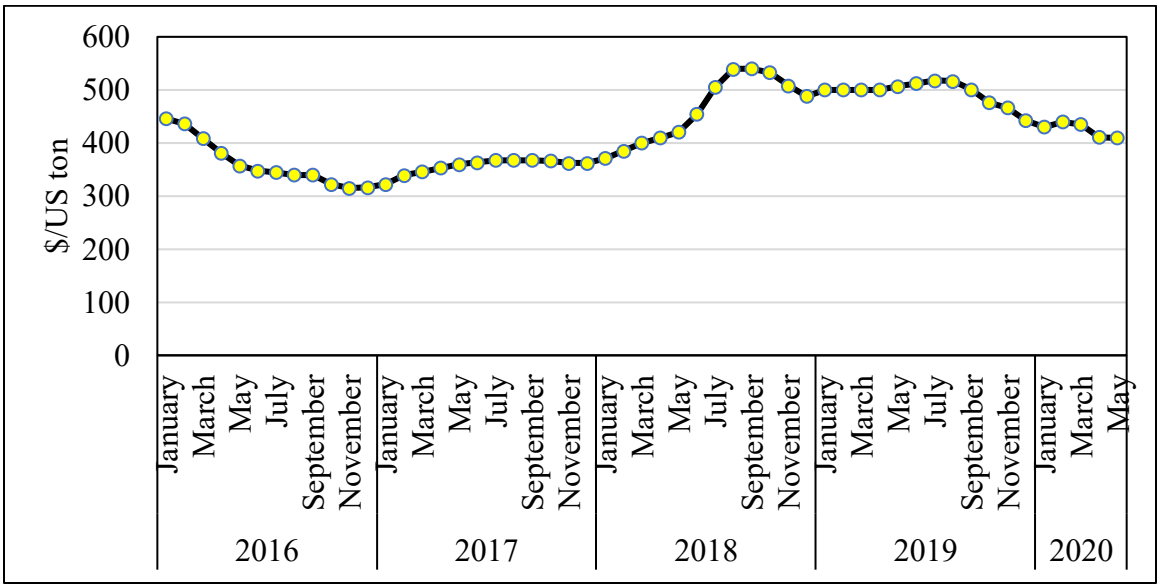

Figure 8-1. Price of Asphalt Binder on The West Coast of The U.S. Since 2016

The price per U.S. ton of asphalt binder increased from $315 to $540 (71%) in less than two years. The global bitumen market in 2017 was $71.9 billion and is forecast to reach $112.01 billion by 2026 (Globenewswire, 2019). The asphalt binder market is projected to grow at a 4.6% compound annual growth rate till 2026.

8.1.2 Economic Viability

The previous section discussed that due to the increasing demand for transportation fuels and the advancement of solid-to-gas conversion technologies, the bitumen price is on the rise. It is estimated that the peak in conventional crude oil production will start before 2040 and will irreversibly start to decline after that(Tsoskounoglou et al., 2008). So, finding an alternative to bitumen has received increased interest. From this perspective, bio-oils derived from animal wastes or

botanical residuals can be promising, mainly due to their inexpensive, eco-friendly sources (Fini et al., 2010; Lei et al., 2015). Figure 8-2 shows data from the U.S. Energy Information Administration that indicates increasing use of biomass in energy sourcing. Currently, 5% of total energy is coming from biomass. Unlike fossil fuels, bio-based oils are renewable. However, not all biomass fuel production is suitable for energy production; heavier bio-oils are less interesting to energy sectors. This is where alternative uses of this residual bio-oil enter the picture, and there is increasing research on testing and trials for modifying asphalt binder. An increasing number of researchers are optimistic about the application prospects of bio-oils in the paving industry. There are already several test projects of bio-oils as rejuvenators (EIA, 2019).

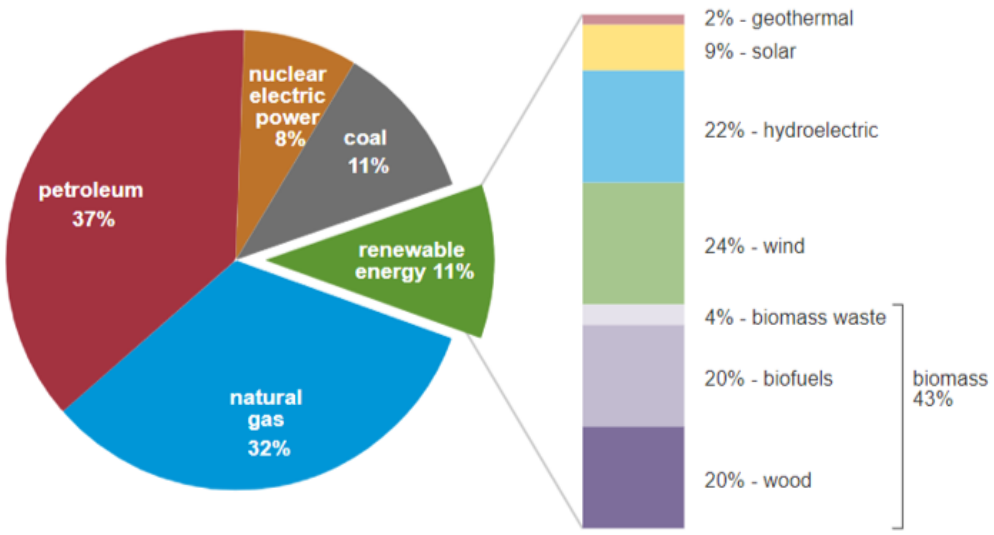

Figure 8-2. 20% of Renewable Energy Comes from Biofuels (EIA, 2019)

EIA also has forecast that U.S. crude oil production will average 11.6 million barrels per day in 2020 and 10.8 million barrels per day in 2021. Due to the nonrenewable nature of the resource, it is expected that U.S. crude oil production will further decrease in coming years.

On the other hand, with technological advancements and sustainable sources, it is expected that the price of bio-oils will further decrease until the price reaches a plateau. In 2011, the (0.54/gal) estimated cost of producing bio-binder from swine manure was approximately 1/4 of the cost of asphalt binder production (Fini et al., 2011b). In 2017, wood-based bio-oil had a price of $300/ unit, whereas base bitumen had a price of $750/unit (Zhang, R. et al., 2017). National Renewable Energy Laboratory research showed that if the cost of wood bio-mass can be kept below $75 per ton, the process is profitable (Wright et al., 2010). Since asphalt binder modified by 15%-20% crumb rubber is already in practice, asphalt binder with bio-modified rubber has more feasibility to be implemented in the market than directly using bio-oils as a partial replacement for bitumen.

8.1.3 Market Analysis

Due to the durability and improved properties of polymer-modified asphalt, the demand for it is increasing globally. The polymer-modified-bitumen industry is valued at USD 5.14 Billion in 2018 and is estimated to reach USD 7.44 Billion by 2026, at a current annual growth rate of 4.6% during the forecast period (Globenewswire, 2019).

The latest Caltrans published report is based on 2017 data. According to the regulations, on an annual average, Caltrans had to use not less than 11.58 pounds of CRM per metric ton of the total amount of asphalt paving materials used. Their calculations were based on 10% by weight for terminal-blended bitumen (Caltrans, 2019). Figure 8-4 shows the gradual increase in use of crumb-rubber modifier in the state of California.

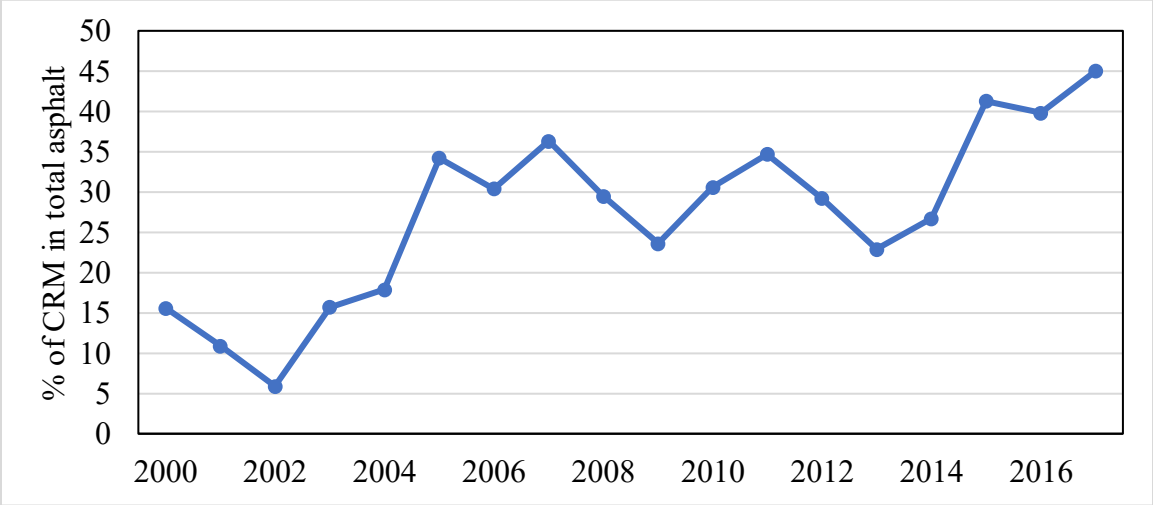

Figure 8-3. Percentage of Crumb Rubber Modifier Applied Among Total Asphalt in Roads in The State Of California (Caltrans, 2019).

Nearly 50% of asphalt used in the entire state of California state now has CRM in it, within just 18 years. Based on the assumptions Caltrans made, the cost difference between using CRM in asphalt and using conventional asphalt is shown in Figure 8-5. The graph shows the initialization cost of using rubberized asphalt binder minus the cost of using conventional asphalt binder on different types of projects. Green indicates the types of projects where use of CRM asphalt binder was less expensive (Caltrans, 2019). Using CRM in pavement preservation and maintenance saved $7.26 per metric ton; using

CRM in capital preventive maintenance (CAPM) projects saved $0.75 per metric ton (Caltrans, 2019).

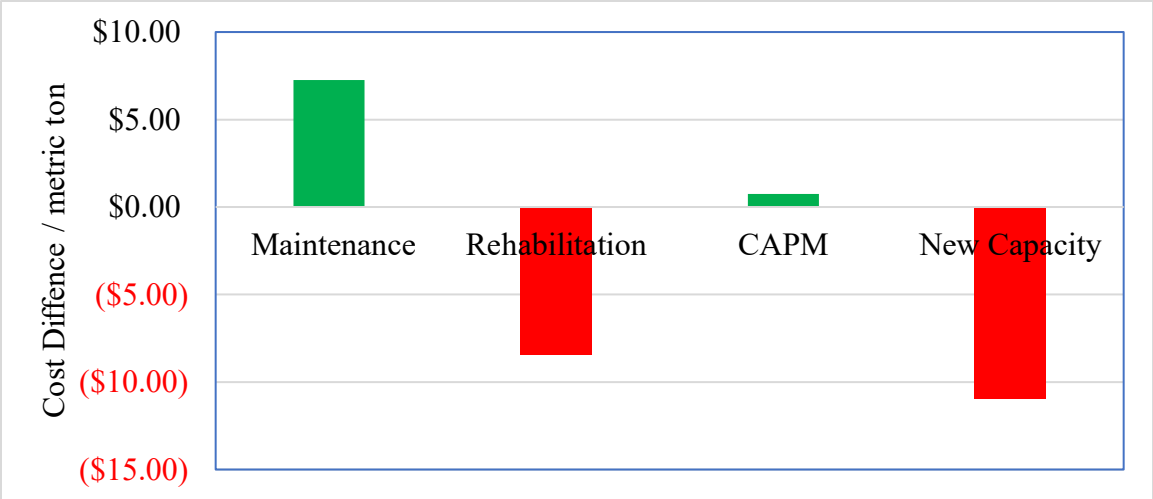

Figure 8-4. The Cost of Using Rubberized Asphalt Binder Minus The Cost of Using Conventional Asphalt Binder Per Metric Ton on Different Types of Projects.

With the surface functionalization of rubber using a hybrid method, more rubber can be introduced into asphalt without raising the storage stability issues currently faced in terminal-blended asphalt. This can further reduce the cost of materials and also reduce the cost related to storage stability issues, as well as the reduced elasticity faced when there is complete degradation of the elastic property of rubber in asphalt. Moreover, bio-oils from wood pellet can further reduce the extent of aging in crumb-rubber modifier, making it economically viable. The alternative approach of microbial desulfurization of rubber can also attain economic viability if it can be performed in a continuous process.

Table 8.1 shows a list of commercially available devulcanized rubber along with surface-activated rubber and microbially desulfurized rubber, providing the blending

temperature, viscosity, and estimated cost of one metric ton of modified bitumen containing 15% of each product.

Table 8-1. Commercially Available Devulcanized Rubber Products for Paving, Showing The Mechanism, Blending Temperature, Viscosity, and Estimated Energy Cost of One Metric Ton of Modified Bitumen Containing 15% of That Product

Product	**Mechanism**	**Viscosity (cP) (135°C)**	**Bitumen Production time (hour)**	**Temp. required (C)**	**Energy cost ($)/ 1 ton**	**Company**
RARX	Pre-swelling with mineral stabilizer	4900	0.775	180	126	Consulpav
ECORPHALT	Chemical mechanical	1600	1	173	165.32	Full Circle Technologies
Elastiko™ 100	Liquid surface treatment on rubber	N/A	1	180	165.73	Asphalt Plus LLC
PRISM™ TR	Chemical and physical	N/A	N/A	N/A	N/A	Prism Worldwide
SAR	Biochemical modification with heat treatment	1350	0.5	170	87	-
MDR	Microbial desulfurization	1709	0.5	165	86	-

8.2 Applicability and Scalability of SAR and MDR

Both SAR and MDR can be easily adapted for use in a wet process or a dry process because they are literally the same rubber particles as crumb rubber, except that

the surface is activated. In a wet process, 18-25% of crumb rubber is blended with asphalt binder before mixing with aggregate. It is applicable to hot-mix asphalt paving, chip sealing, surface treatment, and as joint and crack sealer. In a dry process, crumb rubber is used as a substitute for a portion of the aggregate. A dry process is not suitable for use in cold mix, chip sealing, or surface treatment (Bressi et al., 2019).

Terminal-blend asphalt is a form of the wet process where crumb-rubber modifier is blended with asphalt binder. This is either done at the refinery or at an asphalt-binder storage and distribution terminal. The major difference with a wet process is that in terminal-blend asphalt, a smaller particle size (<0.25mm) is used at an elevated temperature of 220-260°C for at least 45 minutes; it is claimed to be devulcanized and evenly dispersed in the binder matrix (Bressi et al., 2019; FHWA, 2014). One major drawback of terminal-blend asphalt is that its high-temperature rheological properties are diminished compared to conventional rubberized asphalt because the rubber elasticity is fully lost due to the depolymerization process (Bressi et al., 2019). Although subsequent agitation is reportedly not mandatory for terminal-blend binder to keep the ground-tire-rubber particles evenly dispersed in the binder matrix, segregation is still an issue in terminal-blend binder (Wen et al., 2020).

Surface-activated rubber and microbially desulfurized rubber are best suited to solve the problem of wet processing. Surface activation leads to enhancement of the surface polarity of rubber and hence improves high-temperature properties. It also involves a smaller particle size of rubber, similar to the sizes used in terminal blend. So,

surface-activated rubberized binder is also applicable for use in terminal-blend binder. The SAR and MDR processes are both designed to enhance the interaction between rubber and asphalt binder in a wet process. The effectiveness of these modifications in a dry process has not been studied yet.

It should be noted that to produce SAR, we used heat treatment with microwave radiation. This is a rapid-heating technique with selective heating of materials through differential absorption. To scale the production of SAR, there is a need for a rapid and scalable heat source. It is a fact that large-scale production using microwave processing is complex and requires high technical and economic knowledge (NRC, 1994). Another plausible source of heat could be solar reactors. An alternative solution could be combining the work of microbiomes with bio-chemical treatment. In this study, we used microbial desulfurization without chemical treatment. Batch processing of microbial treatment itself has scalability issues. It is suggested that a continuous reactor be used where sulfate concentration can be removed periodically to avoid toxicity in the microbial community. Microbial desulfurization can be upscaled in a tire landfill by identifying and releasing a selected microbial community to feed on the tire rubber. In that case, the desulfurization rate should be tailored for each recycling site.

8.3 Environmental Effects

SAR and MDR have several environmental effects:

- Microwave treatment of crumb rubber reduces the concentrations of aromatic hydrocarbons and polycyclic aromatic hydrocarbons, which can lower harmful substances in fumes (Liang et al., 2017a).
- The use of carbon-neutral or carbon-negative bio-oils in conjunction with rubber to create surface-activated rubber has additional benefits in terms of carbon sequestration.
- Since microbially desulfurized rubber can be mixed in asphalt at 165°C, which is 15°C lower than the conventional mixing temperature of 180°C used for wet processing, the associated fumes can be up to 60% lower compared with conventional rubberized bitumen (EAPA, 2020).
- The service life of pavements containing SAR or MDR is expected to be extended due to improved rubber-asphalt interactions. This in turn leads to reduced energy consumption associated with construction and rehabilitation.

8.4 Research Conclusions

The findings of this dissertation can be grouped into six areas:

1. Bio-oil from swine manure partially devulcanizes natural rubber.

Intermolecular interactions between the amide-rich bio-oil from swine manure and sulfur-crosslinked rubber were shown to cause partial sulfur devulcanization in rubber. It was observed in laboratory experiments that the treatment of natural rubber with amide-rich bio-binder considerably enhances the performance of natural rubber in asphalt binder in terms of workability and pumpability. The addition of bio-binder to rubberized asphalt enhances the fatigue resistance and could be attributed to cleavage of some of the sulfur crosslinks. The results of this study confirmed that bio-binder has a stronger interaction with natural rubber's S—S bond than with its C—S bond. Furthermore, our model is able to explain the effectiveness of two versions of bio-binder models used (BB1/BB2) during the partial devulcanization of natural rubber. The outcome of this study provides insight into the partial devulcanization phenomenon and plausible mechanisms involved in the surface activation of natural rubber in the presence of amide-based bio-binder.

2. Heat treatment combined with bio-modification enhances surface activation of rubber, which in turn reduces rubber segregation and improves the workability of rubberized asphalt binder.

It was found that heat treatment can enhance the surface activation of rubber; this combined with the bio-modification process led to a hybrid treatment. Crumb-rubber

particles were surface activated via a hybrid process involving microwave irradiation and bio-modification to produce surface-activated rubber (SAR), which was then introduced to the asphalt binder. The efficacy of SAR to address rubber segregation and workability issues was investigated via a combined approach, using experiments, density functional theory (DFT), and thermo-mechanical analysis. FTIR analysis indicated the breakage of the polymer chains of rubber due to irradiation as well as the subsequent crosslinking due to bio-modification, leading to an improvement in the workability of asphalt binder containing SAR. In addition, the segregation index of SAR was reduced. The reduction in segregation was attributed to enhanced interaction between rubber and the asphalt-binder matrix, mainly due to chemical grafting via bio-modification onto the rubber surface; this chemical grafting enhanced the interaction within the bitumen-rubber matrix that prevents segregation. The temperature-dependent results of G* showed that up to 64 °C, surface-activated rubber and crumb-rubber modifier showed very similar values; both were higher than neat and microwave-treated-rubber modifier, which indicates both modifiers are well capable of resisting rutting. Based on the results of this study, the hybrid processing involving microwave irradiation and bio-modification to produce a sustainable surface-activated rubber can alleviate both segregation and workability issues associated with the use of crumb rubber in asphalt, while improving its thermo-mechanical properties. The DFT results show that the reaction pathway of an amidyl radical (RCO-N•H) with a carbon-centered radical is energetically more favorable and stable than the pathway with a sulfur-centered radical. The increased acid-base

component in the treated-rubber scenario indicates successful grafting of highly polar molecules of bio-modifier (such as hexadecanamide) onto the surface of rubber.

3. The chemical composition of a bio-modifier affects its efficacy for surface activation of rubber.

Investigating the merits of surface activation of rubber with various bio-modifiers showed that chemisorption of bio-modifiers can help reduce phase separation of rubber and bitumen. Segregation indices were found to be reduced for all surface-activated rubbers compared to non-activated rubber. The bio-modifier from wood pellets and the bio-modifier from waste vegetable oil both showed the highest adsorption onto the surface of rubber, as evidenced by notable peaks in the FTIR spectra. However, waste vegetable oil, which showed good adsorption to rubber, did not make a strong interaction with the bitumen matrix, leading to a very low percent recovery. The observed desirable performance of wood-based bio-oil was attributed to its higher content of polar aromatics (resin) compared to its counterparts, as evidenced in thin layer chromatography - flame ionization detector (TLC-FID) results. In addition to the physical interactions between polar aromatics of a bio-oil and rubber, our DFT results exhibit reaction pathways for effective interactions between radicals of sulfur and the C=O and C=C bonds of bio-oils. An energetically favorable reaction pathway was also found for the interaction of phenoxyl radicals of a bio-oil with the C=C double bonds of rubber. In terms of moisture susceptibility, all the asphalt binders containing surface-activated rubber except the one

treated with miscanthus oil performed well. The outcome of this study shows how a bio-oil's chemical composition affects its efficacy as a modifier for rubber.

4. Microbial treatment of rubber enhances surface activation of rubber, which in turn reduces rubber segregation and improves the workability of rubberized asphalt binder.

Microbes from wastewater-treatment sludge were collected and used to treat crumb-rubber particles made from scrap tire. The microbial exposure continued for 36 days; during the exposure period, the sulfate concentration was regularly measured. A reduction of disulfide bonds (S-S) in the vulcanized rubber was evidenced in FT-IR. This finding was supported by an increase in the acid-base component of the rubber's surface energy. The increase in surface energy promoted the interaction of rubber particles with bitumen, which reduced the segregation of rubber and bitumen. Unlike surface-activated rubberized asphalt, the reduction in viscosity in microbially desulfurized rubber was not very high in comparison to crumb-rubber modifier. The higher percentage of recovery than crumb-rubber modifier is an indication of better rutting resistance. Overall, the bitumen containing microbially treated rubber showed enhanced rheological properties. Based on the study results, microbially desulfurized rubber (MDR) can be a promising candidate for use in asphalt to improve pavement performance and facilitate recycling and resource conservation.

5. The synergy between bio-modified bitumen and polyphosphoric acid depends on the composition of the bio-modifier.

It was shown that there is a synergistic interaction between polyphosphoric acid (PPA) and a group of renewable bio-modifiers used to upgrade bitumen's properties. The target bio-modifiers are derived from five sources of biomass: waste vegetable oil, wood pellet, miscanthus, corn stover, and castor oil. In a macro-scale evaluation, we evaluated the efficacy of PPA to increase the elasticity and stiffness of bitumen containing each bio-modifier. It was found that the bio-modifier made from wood pellets has the highest synergy with PPA, and the bio-modifier made from waste vegetable has the least synergy with PPA. Given the higher polarity in the content of the wood-based bio-modifier compared to that of waste vegetable oil, a higher phosphorylation is expected for the wood-based bio-modifier when exposed to PPA compared to that of waste vegetable oil. DFT results showed that alkanols (alcoholic OHs) of the wood-based bio-modifier can chemically interact with PPA. In addition, it was found that there are strong interactions between PPA oligomers and the lignin units of the wood-based bio-modifier that can explain the strong synergy between PPA and the wood-based bio-modifier. The study outcome showed that PPA has a high synergy with the wood-based bio-modifier, amplifying the effect of PPA and leading to a modified bitumen with superior performance.

6. The durability of bio-modified rubberized bitumen and the rejuvenation capacity varies depending on the type of modification.

This study showed that not all biomodifiers can improve UV-aging resistance in rubberized bitumen. Wood pellet contains furfural, and it is also high in polar aromatics; these properties may have helped to hinder UV aging in wood-pellet-modified rubberized bitumen. In addition, the presence of carbon black coming from crumb rubber and brown carbonaceous particles of bio-modifiers act as free-radical scavengers and UV blockers. The results obtained after adding 10% rejuvenator showed a decrease in the carbonyl index and the sulfoxide index and activation energy as well as an increase in crossover modulus and crossover frequency. The newly proposed rejuvenating index was able to distinguish well between these bio-modifiers. The study of finding optimum dosage based on crossover modulus and crossover frequency for each modifier shows that the rejuvenation capacity of bio-modified rubberized bitumen depends on the composition of the bio-modifiers. These combined results from various aging indices and their required rejuvenator dosages to restore unaged properties indicate that not every bio-modifier is good against UV aging. The findings of the study provide insights for choosing the best performing bio-modifier for rubberized bitumen to enhance UV resistance in highly solar-irradiated regions as well as for choosing the optimum dosage of rejuvenator to restore the physical properties of aged rubberized asphalt.

8.5 Recommendations for Future Research

This research showed the chemo-mechanics, storage stability, and durability of biomodified rubberized bitumen highly depend on factors such as the chemical composition of the bio-modifier and the surface activation method. Based on the findings of this study, these are recommendations for future research:

- This study mainly focused on bitumen-level characterization. We have showed that surface functionalization of crumb rubber before adding it to bitumen reduces the segregation and enhances the storage stability. It is recommended that performance of bitumen at the mixture level be investigated.
- The surface activation of rubber is designed for enhanced interaction with asphalt binder in a wet process. The effect of this modification has not been studied in a dry process. Due to the surface activation, mixing and compacting at a reduced temperature should be evaluated.
- The microbial desulfurization of crumb rubber should be further investigated to determine if complete removal of sulfur is possible. This study indicated that intoxication of the microbial community may have occurred due to the sulfate release. A DNA sequencing of the microbial community may help to pinpoint the sulfate-releasing bacteria, which may help to investigate field-scale feasibility.
- The synergy between PPA and bio-modified rubberized bitumen has been investigated in terms of rheological properties. It is recommended that aging,

adhesion, low-temperature properties, and moisture susceptibility of PPA and bio-modified rubberized bitumen be investigated.

- The study of aging of surface-activated rubberized asphalt was only performed at the binder level. Since overall aging mechanisms are expected to be impacted by loading dynamics, study at the mixture level is recommended.
- The rejuvenation capacity of bio-modified rubberized bitumen after extensive UV aging was studied, showing that wood-based bio-modifier reduces UV aging and promotes the rejuvenation capacity of bitumen. It is recommended that the efficacy of rejuvenation on field-aged rubberized asphalt be examined.

8.6 References

Caltrans, 2019. Cost Differential Analysis Between Asphalt Containing Crumb Rubber and Conventional Asphalt, Public Resources Code Section 42703. Caltrans.

EIA, 2019. Energy Expplained-Biomass Independent Statistics and Analysis. www.eia.gov/energyexplained/biomass/. 2020).

FHWA, 2020. Average Monthly Asphalt Price. highways.dot.gov/federal-lands/business/escalation-factors-wfl/2020-average-monthly-asphalt-prices. (Accessed 20 June 2020).

Fini, E.H., Kalberer, E.W., Shahbazi, A., Basti, M., You, Z., Ozer, H., Aurangzeb, Q., 2011. Chemical characterization of biobinder from swine manure: Sustainable modifier for asphalt binder. Journal of Materials in Civil Engineering 23(11), 1506-1513.

Fini, E.H., Yang, S.-H., Xiu, S., 2010. Characterization and application of manure-based bio-binder in asphalt industry.

Globenewswire, 2019. Bitumen Market To Reach USD 112.01 Billion By 2026: Reports And Data. https://www.globenewswire.com/news-release/2019/04/11/1802979/0/en/Bitumen-Market-To-Reach-USD-112-01-Billion-By-2026-Reports-And-Data.html. (Accessed 11 April, 2020 2020).

Lei, Z., Bahia, H., Yi-qiu, T., 2015. Effect of bio-based and refined waste oil modifiers on low temperature performance of asphalt binders. Construction and Building Materials 86, 95-100.

Wright, M.M., Daugaard, D.E., Satrio, J.A., Brown, R.C., 2010. Techno-economic analysis of biomass fast pyrolysis to transportation fuels. Fuel 89, S2-S10.

Zhang, R., Wang, H., Gao, J., Yang, X., You, Z., 2017. Comprehensive performance evaluation and cost analysis of SBS-modified bioasphalt binders and mixtures. Journal of Materials in Civil Engineering 29(12), 04017232.

REFERENCES

Brown, R., 1993. Historical Development Crumb rubber modifier workshop notes: Design procedures and construction practices. Federal Highway Administration Washington, DC.

Cao, X.-W., Luo, J., Cao, Y., Yin, X.-C., He, G.-J., Peng, X.-F., Xu, B.-P., 2014. Structure and properties of deeply oxidized waster rubber crumb through long time ozonization. Polymer degradation and stability 109, 1-6.

de Sousa, F.D., Scuracchio, C.H., Hu, G.-H., Hoppe, S., 2017. Devulcanization of waste tire rubber by microwaves. Polymer Degradation and Stability 138, 169-181.

EPA, 2019. “Rubber and Leather: Material-Specific Data.”.

Fan, L.-T., Shafie, M.R., Tollas, J.M., Lee, W.A.F., 2013. Extraction of hydrocarbons from hydrocarbon-containing materials and/or processing of hydrocarbon-containing materials. Google Patents.

Fini, E.H., Hosseinnezhad, S., Oldham, D., Mclaughlin, Z., Alavi, Z., Harvey, J., 2019a. Bio-modification of rubberised asphalt binder to enhance its performance. International Journal of Pavement Engineering 20(10), 1216-1225.

Hansen, K.R., Copeland, A., 2015. Asphalt pavement industry survey on recycled materials and warm-mix asphalt usage: 2014.

Hosseinnezhad, S., Holmes, D., Fini, E.H., 2014. Decoupling the physical filler effect and the time dependent dissolution effect of crumb rubber on asphalt matrix Rheology.

Isayev, A.I., 2005. Recycling of rubbers. In: Mark JE, Erman B, Eirich FR. editors Science and technology of rubber. 3rd ed Elsevier Inc, p. 663e701.

Li, P., Ding, Z., Zou, P., Sun, A., 2017. Analysis of physico-chemical properties for crumb rubber in process of asphalt modification. Construction and Building Materials 138, 418-426.

Liang, H., 2015b. Characterization and surface modification of rubber from recycled tires.

Romero-Sánchez, M.D., Martín-Martínez, J.M., 2006. Surface modifications of vulcanized SBR rubber by treatment with atmospheric pressure plasma torch. International journal of adhesion and adhesives 26(5), 345-354.

Shen, J., Amirkhanian, S., Xiao, F., Tang, B., 2009. Influence of surface area and size of crumb rubber on high temperature properties of crumb rubber modified binders. Construction and Building Materials 23(1), 304-310.

Shulman, V.L., 2019. Tire recycling, Waste. Elsevier, pp. 489-515.

Thodesen, C., Xiao, F., Amirkhanian, S.N., 2009. Modeling viscosity behavior of crumb rubber modified binders. Construction and Building Materials 23(9), 3053-3062.

Tyczkowski, J., Krawczyk, I., Wożniak, B., 2003. Modification of styrene–butadiene rubber surfaces by plasma chlorination. Surface and coatings technology 174, 849-853.

USTMA, 2017. 2017 U.S. Scrap Tire Management Summary. www.ustires.org/system/files/USTMA_scraptire_summ_2017_072018.pdf. (Accessed 6/19 2020).

Way, G.B., Kaloush, K.E., Biligiri, K.P., 2012. Asphalt-rubber standard practice guide. Rubber Pavements Association, Tempe.

Williams, B.A., Willis, J.R., Ross, T.C., 2019. Asphalt Pavement Industry Survey on Recycled Materials and Warm-Mix Asphalt Usage: 2018.

Xiaowei, C., Sheng, H., Xiaoyang, G., Wenhui, D., 2017. Crumb waste tire rubber surface modification by plasma polymerization of ethanol and its application on oil-well cement. Applied Surface Science 409, 325-342.

Yu, G.-X., Li, Z.-M., Zhou, X.-L., Li, C.-L., 2011. Crumb rubber–modified asphalt: microwave treatment effects. Petroleum Science and Technology 29(4), 411-417.

AASHTO-T-313, 2019b. Standard method of test for determining the flexural creep stiffness of asphalt binder using the bending beam rheometer (BBR). American Association of State Highway and Transportation Officials.

AASHTO-T-315, 2019. Standard Method of Test for Determining the Rheological Properties of Asphalt Binder Using a Dynamic Shear Rheometer (DSR).

Adhikari, B., De, D., Maiti, S., 2000. Reclamation and recycling of waste rubber. Progress in Polymer Science 25(7), 909-948.

Alturk, S., Avci, D., Tamer, O., Atalay, Y., 2017. Comparison of different hybrid DFT methods on structural, spectroscopic, electronic and NLO parameters for a potential NLO material. Computational and Theoretical Chemistry 1100, 34-45.

ASTM-D2872, 2019. Standard Test Method for Effect of Heat and Air on a Moving Film of Asphalt (Rolling Thin-Film Oven Test), ASTM International, West Conshohocken, PA.

ASTM-D2872, 2019a. Standard practice for accelerated aging of asphalt binder using a pressurized aging vessel (PAV), USA: Annual Book of ASTM Standards.

ASTM-D6373-16, 2016. Standard Specification for Performance Graded Asphalt Binder. ASTM International, West Conshohocken, PA, 2016, www.astm.org, ASTM International, West Conshohocken, PA, 2016, www.astm.org.

ASTM-D-4402, 2015. Standard test method for viscosity determination of asphalt at elevated temperatures using a rotational viscometer, American Society for Testing and Materials.

Bader, R.F.W., 1990. Atoms in Molecules: A Quantum Theory. Wiley Online Library, Ontario, Canada.

Biegler-Konig, F., Bader, R.F., 2002. AIM 2000, Version 2

Bocoum, A., Hosseinnezhad, S., Fini, E.H., 2014a. Investigating effect of amine based additives on asphalt rubber rheological properties, Asphalt Pavements. CRC Press, pp. 945-956.

Brandenburg, J.G., Alessio, M., Civalleri, B., Peintinger, M.F., Bredow, T., Grimme, S., 2013. Geometrical Correction for the Inter- and Intramolecular Basis Set Superposition Error in Periodic Density Functional Theory Calculations. Journal of Physical Chemistry A 117(38), 9282-9292.

Buckingham, A.D., Fowler, P.W., Hutson, J.M., 1988. THEORETICAL-STUDIES OF VANDERWAALS MOLECULES AND INTERMOLECULAR FORCES. Chemical Reviews 88(6), 963-988.

Burns, L.A., Vazquez-Mayagoitia, A., Sumpter, B.G., Sherrill, C.D., 2011. Density-functional approaches to noncovalent interactions: A comparison of dispersion corrections (DFT-D), exchange-hole dipole moment (XDM) theory, and specialized functionals. Journal of Chemical Physics 134(8).

Cardenas, C., Ayers, P., De Proft, F., Tozer, D.J., Geerlings, P., 2011. Should negative electron affinities be used for evaluating the chemical hardness? Physical Chemistry Chemical Physics 13(6), 2285-2293.

Chai, J.D., Head-Gordon, M., 2008. Long-range corrected hybrid density functionals with damped atom-atom dispersion corrections. Physical Chemistry Chemical Physics 10(44), 6615-6620.

Chritiansson, M., Stenberg, B., Wallenberg, L., Holst, O., 1998. Reduction of surface sulphur upon microbial devulcanization of rubber materials. Biotechnology letters 20(7), 637-642.

Coropceanu, V., Malagoli, M., da Silva Filho, D., Gruhn, N., Bill, T., Brédas, J., 2002. Hole-and electron-vibrational couplings in oligoacene crystals: intramolecular contributions. Physical review letters 89(27), 275503.

De, D., Das, A., De, D., Dey, B., Debnath, S.C., Roy, B.C., 2006. Reclaiming of ground rubber tire (GRT) by a novel reclaiming agent. European Polymer Journal 42(4), 917-927.

Diener, M.D., Alford, J.M., 1998. Isolation and properties of small-bandgap fullerenes. Nature 393(6686), 668-671.

Dubkov, K.A., Semikolenov, S.V., Ivanov, D.P., Babushkin, D.E., Voronchikhin, V.D., 2014. Scrap tyre rubber depolymerization by nitrous oxide: products and mechanism of reaction. Iranian Polymer Journal 23(11), 881-890.

Dumont, R.S., 2014. Effects of charging and polarization on molecular conduction via the source-sink potential method. Canadian Journal of Chemistry-Revue Canadienne De Chimie 92(2), 100-111.

Fini, E., Hajikarimi, P., Rahi, M., and Moghadas Nejad, F., 2015. Physiochemical, Rheological, and Oxidative Aging Characteristics of Asphalt Binder in the Presence of Mesoporous Silica Nanoparticles. J. Mater. Civ. Eng. 28(2), 1-9.

Fini, E.H., Al-Qadi, I.L., You, Z., Zada, B., Mills-Beale, J., 2012. Partial replacement of asphalt binder with bio-binder: characterisation and modification. International Journal of Pavement Engineering 13(6), 515-522.

Fini, E.H., Bocoum, A., Hosseinnezhad, S., Martinez, F.M., 2015. Bio-Modification of Rubberized Asphalt and Its High Temperature Properties.

Fini, E.H., Hosseinnezhad, S., Oldham, D., Mclaughlin, Z., Alavi, Z., Harvey, J., 2019a. Bio-modification of rubberised asphalt binder to enhance its performance. International Journal of Pavement Engineering 20(10), 1216-1225.

Fini, E.H., Kalberer, E.W., Shahbazi, A., Basti, M., You, Z., Ozer, H., Aurangzeb, Q., 2011b. Chemical characterization of biobinder from swine manure: Sustainable modifier for asphalt binder. Journal of Materials in Civil Engineering 23(11), 1506-1513.

Fini, E.H., Oldham, D.J., Abu-Lebdeh, T., 2013. Synthesis and characterization of biomodified rubber asphalt: Sustainable waste management solution for scrap tire and swine manure. Journal of Environmental Engineering 139(12), 1454-1461.

Fletcher, R., 1980. Unconstrained optimization. Practical methods of optimization 1.

Fominykh, O.D., Sharipova, A.V., Balakina, M.Y., 2016. The Choice of Appropriate Density Functional for the Calculation of Static First Hyperpolarizability of Azochromophores and Stacking Dimers. International Journal of Quantum Chemistry 116(2), 103-112.

Froese, R.D.J., Hustad, P.D., Kuhlman, R.L., Wenzel, T.T., 2007. Mechanism of activation of a hafnium pyridyl-amide olefin polymerization catalyst: Ligand modification by monomer. Journal of the American Chemical Society 129(25), 7831-7840.

Fukumori, K., Matsushita, M., Okamoto, H., Sato, N., Suzuki, Y., Takeuchi, K., 2002. Recycling technology of tire rubber. Jsae Review 23(2), 259-264.

Garcia-Hernandez, Z., Flores-Parra, A., Grevy, J.M., Ramos-Organillo, A., Contreras, R., 2006. 2-Aminobenzothiazole phosphorus amides: Molecular and supramolecular structures, hydrogen bonds and sulfur donor-acceptor interactions. Polyhedron 25(7), 1662-1672.

Garza, A.J., Osman, O.I., Asiri, A.M., Scuseria, G.E., 2015. Can Gap Tuning Schemes of Long-Range Corrected Hybrid Functionals Improve the Description of Hyperpolarizabilities? Journal of Physical Chemistry B 119(3), 1202-1212.

Gaussian09, 2020. Optimization

Geerlings, P., De Proft, F., Langenaeker, W., 2003. Conceptual density functional theory. Chemical Reviews 103(5), 1793-1873.

Goldshtein, V., 2002. US Patent, 6 387: 966

Goldshtein, V., 2003. US Patent 6, 541: 526.

Grimme, S., 2006. Semiempirical GGA-type density functional constructed with a long-range dispersion correction. Journal of Computational Chemistry 27(15), 1787-1799.

Hinchliffe, A., 2005. Molecular modelling for beginners. John Wiley & Sons.

Hohenberg, P., Kohn, W., 1964. Inhomogeneous Electron Gas. Physical Review 136(3B), B864-B871.

Honarparvar, B., Pawar, S.A., Alves, C. N., Lameira, J., Maguire, G. E., Silva, J. R., Govender, T, Kruger, H. G., Pentacycloundecane lactam vs lactone norstatine type protease HIV inhibitors: binding energy calculations and DFT study. Journal of Biomedical Science 22(15), 1-15.

Hosseinnezhad, S., Kabir, S.F., Oldham, D., Mousavi, M., Fini, E.H., 2019a. Surface functionalization of rubber particles to reduce phase separation in rubberized asphalt for sustainable construction. Journal of Cleaner Production 225, 82-89.

Isayev AI, 2005. Recycling of rubbers.Science and technology of rubber, Chapter 15,. Elsevier, USA.

Jeong, K.-D., Lee, S.-J., Amirkhanian, S.N., Kim, K.W., 2010. Interaction effects of crumb rubber modified asphalt binders. Construction and Building Materials 24(5), 824-831.

John B. Macleod, M.E.M., Ronald D. Myers, Peter Nicholson, 1995. Rubber devulcanization process, in: Company, E.R.A.E. (Ed.). USA.

Jorgensen, W.L., Madura, J.D., Swenson, C.J., 1984. OPTIMIZED INTERMOLECULAR POTENTIAL FUNCTIONS FOR LIQUID HYDROCARBONS. Journal of the American Chemical Society 106(22), 6638-6646.

Jung, I.H., Lo, W.-Y., Jang, J., Chen, W., Zhao, D., Landry, E.S., Lu, L., Talapin, D.V., Yu, L., 2014. Synthesis and Search for Design Principles of New Electron Accepting Polymers for All-Polymer Solar Cells. Chemistry of Materials 26(11), 3450-3459.

Kabir, S.F., Mousavi, M., Fini, E.H., 2019. Selective adsorption of bio-oils' molecules onto rubber surface and its effects on stability of rubberized asphalt. Journal of Cleaner Production, 119856.

Kanazawa, H., Higuchi, M., Yamamoto, K., 2006. Synthesis and chemical degradation of thermostable polyamide with imine bond for chemical recycling. Macromolecules 39(1), 138–144.

Kemnitz, C.R., Loewen, M.J., 2007. "Amide resonance" correlates with a breadth of C-N rotation barriers. Journal of the American Chemical Society 129(9), 2521-2528.

Kim, K.S., Tarakeshwar, P., Lee, J.Y., 2000. Molecular clusters of pi-systems: Theoretical studies of structures, spectra, and origin of interaction energies. Chemical Reviews 100(11), 4145-4185.

Kleps, T., Piaskiewicz, M., Parasiewicz, W., 2000. The use of thermogravimetry in the study of rubber devulcanization. Journal of Thermal Analysis and Calorimetry 60(1), 271-277.

Knorr, K., 1994. RECLAIM FROM NATURAL AND SYNTHETIC RUBBER SCRAP FOR TECHNICAL RUBBER GOODS. Kautschuk Gummi Kunststoffe 47(1), 54-57.

Kobko, N., Dannenberg, J.J., 2001. Effect of basis set superposition error (BSSE) upon ab initio calculations of organic transition states. Journal of Physical Chemistry A 105(10), 1944-1950.

Kojima, M., Tosaka, M., Ikeda, Y., Kohjiya, S, 2005. Devulcanization of carbon black filled natural rubber using supercritical carbon dioxide. Applied Polymer 95(1), 137–143.

Kojima, M., Tosakaa, M., Ikedab, Y. , 2004. Chemical recycling of sulfur-cured natural rubber using supercritical carbon dioxide. Green Chemistry(6), 84-89.

Kojimaa, M., Kohjiyaa, S., Ikedab,Y. , , 2005. Role of supercritical carbon dioxide for selective impregnation of decrosslinking reagent into isoprene rubber vulcanizate. Polymer 46(7), 2016–2019.

Laidig, K.E., Cameron, L.M., 1996. Barrier to rotation in thioformamide: Implications for amide resonance. Journal of the American Chemical Society 118(7), 1737-1742.

Lameira, J., Alves, C.N., Moliner, V., Silla, E., 2006a. A density functional study of flavonoid compounds with anti-HIV activity. Eur J Med Chem 41(5), 616-623.

Lameira, J., Medeiros, I.G., Reis, M., Santos, A.S., Alves, C.N., 2006b. Structure-activity relationship study of flavone compounds with anti-HIV-1 integrase activity: A density functional theory study. Bioorg Med Chem 14(21), 7105-7112.

Levin, V.Y., Kim, S.H., Isayev, A.I., 1997. Vulcanization of ultrasonically devulcanized SBR elastomers. Rubber Chemistry and Technology 70(1), 120-128.

Li, F., Yan, B., Zhang, Y.P., Zhang, L.H., Lei, T., 2014. Effect of activator on the structure and desulphurization efficiency of sludge-activated carbon. Environmental Technology 35(20), 2575-2581.

Li Feng-Yu, Zhao Ji-Jun 2010. Quantum chemistry PM3 calculations of sixteen mEGF molecules. 1(1), 68-77.

Lo Presti, D., 2013. Recycled Tyre Rubber Modified Bitumens for road asphalt mixtures: A literature review. Construction and Building Materials 49, 863-881.

MacLeod, D., Ho, S., Wirth, R., Zanzotto, L., 2007. Study of crumb rubber materials as paving asphalt modifiers. Canadian Journal of Civil Engineering 34(10), 1276-1288.

Maseras, F., Morokuma, K., 1995. IMOMM - A NEW INTEGRATED AB-INITIO PLUS MOLECULAR MECHANICS GEOMETRY OPTIMIZATION SCHEME OF EQUILIBRIUM STRUCTURES AND TRANSITION-STATES. Journal of Computational Chemistry 16(9), 1170-1179.

Md Abdur Rauf S, A.P.I.A., F., Govender T., Maguire G. E. M., Kruger, H. G., Honarparvar, B., 2015. The effect of N-methylation of amino acids (Ac-X-OMe) on solubility and conformation: a DFT study. Organic & Biomolecular Chemistry 13(39), 9885-10076.

Mohaved, S.O., Ansarifar, A., Nezhad, S.K., Atharyfar, S., 2015. A novel industrial technique for recycling ethylene-propylene-diene waste rubber. Polymer Degradation and Stability 111, 114-123.

Monajjemi, M., Honarparvar, B., Hadad, B.K., Ilkhani, A.R., and Mollaamin, F., 2010. Thermo-chemical investigation and NBO analysis ofsome anxileotic as Nano-drugs. African Journal of Pharmacy and Pharmacology 4 (8), 521-529.

Monajjemi, M., Lee, V.S., Khaleghian, M., Honarparvar, B., Mollaamin, F., 2010. Theoretical Description of Electromagnetic Nonbonded Interactions of Radical, Cationic, and Anionic NH2BHNBHNH2 Inside of the B18N18 Nanoring. Journal of Physical Chemistry C 114(36), 15315-15330.

Morgado, C.A., McNamara, J.P., Hillier, I.H., Burton, N.A., 2007. Density functional and semiempirical molecular orbital methods including dispersion corrections for the accurate

description of noncovalent interactions involving sulfur-containing molecules. Journal of Chemical Theory and Computation 3(5), 1656-1664.

Mosapour Kotena Z, B.A.R., Hashim R., 2014. AIM and NBO analyses on hydrogen bonds formation in sugar-based surfactants (α/β-d-mannose and n-octyl-α/β-d-mannopyranoside): a density functional theory study. Liquid Crystals 41(6), 784-792.

Mosapour Kotena ZB-A, R., Hashim, R., Manickam Achari, V., 2013. Hydrogen bonds in galactopyranoside and glucopyranoside: a density functional theory study. Journal of Molecular Modeling 19(2), 589-599.

Mousavi, M., Hosseinnezhad, S., Kabir, S.F., Burnett, D.J., Fini, E.H., 2019b. Reaction pathways for surface activated rubber particles. Resources, Conservation and Recycling 149, 292-300.

Mousavi, M., Pahlavan, F., Oldham, D., Abdollahi, T., Fini, E.H., 2016. Alteration of intermolecular interactions between units of asphaltene dimers exposed to an amide-enriched modifier. RSC Advances 6(58), 53477-53492.

Mujika, J.I., Matxain, J.M., Eriksson, L.A., Lopez, X., 2006. Resonance structures of the amide bond: The advantages of planarity. Chemistry-a European Journal 12(27), 7215-7224.

Olmsted III, J., Williams, G.M., 1997. Chemistry: the Molecular Science, 2nd Edition ed. Wm.C. Brown.

Pahlavan, F., Mousavi, M., Hungb, A., Fini, E. H. , 2016. Investigating molecular interactions and surface morphology of wax-doped asphaltenes Physical Chemistry Chemical Physics

Paizs, B., Suhai, S., 1998. Comparative study of BSSE correction methods at DFT and MP2 levels of theory. Journal of Computational Chemistry 19(6), 575-584.

Parr, R., Zhou, Z., 1993. Absolute hardness: unifying concept for identifying shells and subshells in nuclei, atoms, molecules, and metallic clusters. Accounts of Chemical Research 26(5), 256-258.

Pearson, R., 1987. Recent advances in the concept of hard and soft acids and bases. Journal of Chemical Education 64(7), 561.

Pearson, R., 1988. Absolute electronegativity and hardness: application to inorganic chemistry. Inorganic Chemistry 27(4), 734-740.

Pearson, R.G., 1989. Absolute electronegativity and hardness: applications to organic chemistry. The Journal of Organic Chemistry 54(6), 1423-1430.

Pearson, R.P., 1997. Chemical hardness: applications from molecules to solids. Wiley-VCH, Weinheim.

Platts, J.A., Maarof, H., Harris, K.D.M., Lim, G.K., Willock, D.J., 2012. The effect of intermolecular hydrogen bonding on the planarity of amides. Physical Chemistry Chemical Physics 14(34), 11944-11952.

Ralph G. Pearson, 1963. Hard and Soft Acids and Bases. J. Am. Chem. Soc. 85(22), 3533–3539.

Rauf, M.A., Arvidsson, P., Albericio, F., Govender, T., Maguire, G. E., Kruger, H. G., Honarparvar, B., 2015. The effect of N-methylation of amino acids (Ac-X-OMe) on solubility and conformation: a DFT study. Organic & biomolecular chemistry 13(39), 9993-10006.

Reed, A.E., Curtiss, L.A., Weinhold, F., 1988. INTERMOLECULAR INTERACTIONS FROM A NATURAL BOND ORBITAL, DONOR-ACCEPTOR VIEWPOINT. Chemical Reviews 88(6), 899-926.

Reed, A.E., Weinhold, F., 1985. Natural localized molecular orbitals. Chemical Physics 83(4), 1736-1740.

Robert G. Parr , Ralph G. Pearson, 1983. Absolute hardness: companion parameter to absolute electronegativity. J. Am. Chem. Soc., 105(26), 7512–7516.

Rooj, S., Basak,G. C., Maji, P. K., Bhowmick, A. K., 2011. New Route for Devulcanization of Natural Rubber and the Properties of Devulcanized Rubber. Journal of Polymers and the Environment 19(2), 382-390.

Sarasia, E.M., Soliman, M.E.S., Honarparvar, B., 2012. Theoretical study on the molecular electronic properties of salicylic acid derivatives as anti-inflammatory drugs. Journal of Structural Chemistry 53(3), 574-581.

Schlegel, H.B., 1984. Estimating the Hessian for gradient-type geometry optimizations. Theoretica chimica acta 66(5), 333-340.

Schlegel, H.B., Binkley, J., Pople, J., 1982. Chent Phys. 1984, 80, 1976-1981. Schlegel, HBJ. Comput. Chem 3, 214-218.

Sutanto, P., Laksmana, F.L., Picchioni, E., Janssen, L.P.B.M., 2006. Modeling on the kinetics of an EPDM devulcanization in an internal batch mixer using an amine as the devulcanizing agent. Chemical Engineering Science 61(19), 6442-6453.

Sutanto, P., Laksmana, F.L. ,Picchioni, F. , Janssen, L.P.B.M., 2006. Modeling on the kinetics of an EPDM devulcanization in an internal batch mixer using an amine as the devulcanizing agent. Chemical Engineering Science 61(19), 6442 – 6453.

Svensson, M., Humbel, S., Morokuma, K., 1996. Energetics using the single point IMOMO (integrated molecular orbital plus molecular orbital) calculations: Choices of computational levels and model system. Journal of Chemical Physics 105(9), 3654-3661.

Szabo Attila. , Ostlund Neil.S., 1989. Modern Quantum Chemistry: Introduction to Advanced Electronic Structure Theory. McGraw Hill, Mineola, New York.

Teixeira, J., 2015. Industrial Devulcanization of Rubber. Kgk-Kautschuk Gummi Kunststoffe 68(1-2), 6-9.

Tsuzuki, S., Uchimaru, T., Tanabe, K., Kuwajima, S., 1994. REFINEMENT OF NONBONDING INTERACTION POTENTIAL PARAMETERS FOR METHANE ON THE BASIS OF THE PAIR POTENTIAL OBTAINED BY MP3/6-311G(3D,3P)-LEVEL AB-INITIO MOLECULAR-ORBITAL CALCULATIONS - THE ANISOTROPY OF H/H INTERACTION. Journal of Physical Chemistry 98(7), 1830-1833.

Udhayakalaa, P., Rajendiranb, T. V., Gunasekaranc, S. , 2012. Theoretical approach to the corrosion inhibition efficiency of some pyrimidine derivatives using DFT method. Journal of Computational Methods in Molecular Design 2(1), 1-15.

Walters, R., Fini, E. H., Abu-Lebdeh, T., 2014. Introducing Combination of Nano-clay and Bio-char to Enhance Asphalt Binder's Rheological and Aging Characteristics. International Journal of Pavement Research and Technology 7(6), 451-455.

Warner, W.C., 1994. METHODS OF DEVULCANIZATION. Rubber Chemistry and Technology 67(3), 559-566.

Weinhold F, Carpenter J.E., 1988. The Structure of Small Molecules and Ions, Plenum, New York.

Wong, K.Y., -Mercader, A.G., Saavedra, L. M., Honarparvar, B., Romanelli, G.P., Duchowicz, P. R., 2014. QSAR analysis on tacrine-related acetylcholinesterase inhibitors. Journal of Biomedical Science 21(84), 1-8.

Xantheas, S.S., 1996. On the importance of the fragment relaxation energy terms in the estimation of the basis set superposition error correction to the intermolecular interaction energy. Journal of Chemical Physics 104(21), 8821-8824.

Zanchet, A., Carli, L.N., Giovanela, M., Crespo, J.S., Scuracchio, C.H., Nunes, R.C.R., 2009. Characterization of Microwave-Devulcanized Composites of Ground SBR Scraps. Journal of Elastomers and Plastics 41(6), 497-507.

Zhao, Y., Gu, F., Xu, J., Jin, J., 2010. Analysis of Aging Mechanism of SBS Polymer Modified Asphalt based on Fourier Transform Infrared Spectrum. Journal of Wuhan University of Technology-Materials Science Edition 25(6), 1047-1052.

Zielinski, T.J., Harvey, E., Sweeney, R., Hanson, D.M., 2005. Quantum states of atoms and molecules. ACS Publications.
AASHTO-T-315, 2019. Standard Method of Test for Determining the Rheological Properties of Asphalt Binder Using a Dynamic Shear Rheometer (DSR).

AASHTO-T315, 2012. Standard method of test for determining the rheological properties of asphalt binder using a dynamic shear rheometer (DSR).

ASTM-D4402, 2015. Standard Test Method for Viscosity Determination of Asphalt at Elevated Temperatures Using a Rotational Viscometer. West Conshohocken, PA.

ASTM-D6723, 2012. Standard Test Method for Determining the Fracture Properties of Asphalt Binder in Direct Tension (DT). ASTM International.

ASTM-D7173, 2014. Standard Practice for Determining the Separation Tendency of Polymer from Polymer Modified Asphalt. ASTM.

Bennert, T., Maher, A., Smith, J., 2004. Evaluation of crumb rubber in hot mix asphalt. Rutgers University, Center for Advanced Infrastructure & Transportation, and Rutgers Asphalt/Pavement Laboratory.

Berry, J., 2017. Molecular Dynamics Simulations on Polymer-Modified Model Asphalts. Journal of Creative Inquiry 1(1).

Bocoum, A., Hosseinnezhad, S., Fini, E.H., 2014b. Investigating effect of amine based additives on asphalt rubber rheological properties. Asphalt Pavements 86, 921-931.

Cai, Y., Jalan, A., Kubosumi, A.R., Castle, S.L., 2015. Microwave-promoted tin-free iminyl radical cyclization with TEMPO trapping: A practical synthesis of 2-acylpyrroles. Organic letters 17(3), 488-491.

CalTrans, 2003. Asphalt Rubber Usage Guide. Division of Engineering Services, Sacramento, CA, 95819-94612.

Cao, X.-W., Luo, J., Cao, Y., Yin, X.-C., He, G.-J., Peng, X.-F., Xu, B.-P., 2014. Structure and properties of deeply oxidized waster rubber crumb through long time ozonization. Polymer degradation and stability 109, 1-6.

Colom, X., Marín-Genescà, M., Mujal, R., Formela, K., Cañavate, J., 2018. Structural and physico-mechanical properties of natural rubber/GTR composites devulcanized by microwaves: Influence of GTR source and irradiation time. J. Compos. Mater., 0021998318761554.

de Sousa, F.D., Scuracchio, C.H., Hu, G.-H., Hoppe, S., 2017. Devulcanization of waste tire rubber by microwaves. Polymer Degradation and Stability 138, 169-181.

Fini, E.H., Kalberer, E.W., Shahbazi, A., Basti, M., You, Z., Ozer, H., Aurangzeb, Q., 2011b. Chemical characterization of biobinder from swine manure: Sustainable modifier for asphalt binder. Journal of Materials in Civil Engineering 23(11), 1506-1513.

Gaweł, I., Piłat, J., Radziszewski, P., Kowalski, K., Król, J., 2011. Rubber modified bitumen, Polymer modified bitumen. Elsevier, pp. 72-97.

Gawel, I., Stepkowski, R., Czechowski, F., 2006. Molecular interactions between rubber and asphalt. Industrial & engineering chemistry research 45(9), 3044-3049.

Gehrke, S., Alznauer, H.T., Karimi-Varzaneh, H.A., Becker, J.A., 2017. Ab initio simulations of bond breaking in sulfur crosslinked isoprene oligomer units. The Journal of chemical physics 147(21), 214703.

Hanson, D.E., 2009. Numerical simulations of rubber networks at moderate to high tensile strains using a purely enthalpic force extension curve for individual chains. The Journal of chemical physics 131(22), 224904.

Hanson, D.E., 2011. The molecular kink paradigm for rubber elasticity: Numerical simulations of explicit polyisoprene networks at low to moderate tensile strains. The Journal of chemical physics 135(5), 054902.

Hanson, D.E., Barber, J.L., 2018. The bond rupture force for sulfur chains calculated from quantum chemistry simulations and its relevance to the tensile strength of vulcanized rubber. Physical Chemistry Chemical Physics 20(13), 8460-8465.

Hanson, D.E., Barber, J.L., Subramanian, G., 2013. The entropy of the rotational conformations of (poly) isoprene molecules and its relationship to rubber elasticity and temperature increase for moderate tensile or compressive strains. The Journal of chemical physics 139(22), 224906.

Hanson, D.E., Martin, R.L., 2009. How far can a rubber molecule stretch before breaking? Ab initio study of tensile elasticity and failure in single-molecule polyisoprene and polybutadiene. The Journal of chemical physics 130(6), 064903.

Hioe, J., Šakić, D., Vrček, V., Zipse, H., 2015. The stability of nitrogen-centered radicals. Organic & biomolecular chemistry 13(1), 157-169.

Hosseinnezhad, S., Bocoum, A., Martinez, F.M., Fini, E.H., 2015a. Biomodification of rubberized asphalt and its high temperature properties. Transportation Research Record: Journal of the Transportation Research Board(2506), 81-89.

Hosseinnezhad, S., Kabir, F., SK., Oldham, D.J., Mousavi, M., Fini, E.H., 2018. Sustainble Surface-Activated Rubber from Scrap Tire for Use in Construction. Journal of Cleaner Production Under Review.

Jana, G., Das, C., 2005. Recycling natural rubber vulcanizates through mechanochemical devulcanization. Macromolecular research 13(1), 30-38.

Klüppel, M., Menge, H., Schmidt, H., Schneider, H., Schuster, R., 2001. Influence of preparation conditions on network parameters of sulfur-cured natural rubber. Macromolecules 34(23), 8107-8116.

Kocevski, S., Yagneswaran, S., Xiao, F., Punith, V., Smith Jr, D.W., Amirkhanian, S., 2012. Surface modified ground rubber tire by grafting acrylic acid for paving applications. Construction and Building Materials 34, 83-90.

Leng, Z., Padhan, R.K., Sreeram, A., 2018. Production of a sustainable paving material through chemical recycling of waste PET into crumb rubber modified asphalt. Journal of Cleaner Production 180, 682-688.

Liang, H., 2015a. Characterization and Surface Modification of Rubber from Recycled Tires. Université Laval.

Liang, M., Xin, X., Fan, W., Ren, S., Shi, J., Luo, H., 2017b. Thermo-stability and aging performance of modified asphalt with crumb rubber activated by microwave and TOR. Materials & Design 127, 84-96.

Lopes, A.R., Constantinides, G.A., 2008. A high throughput FPGA-based floating point conjugate gradient implementation, International Workshop on Applied Reconfigurable Computing. Springer, pp. 75-86.

Manhart, J., Kramer, R., Schaller, R., Holzner, A., Kern, W., Schlögl, S., 2016. Surface Functionalization of Natural Rubber by UV-Induced Thiol-ene Chemistry, Macromolecular Symposia. Wiley Online Library, pp. 32-39.

Markey, S.J., Lewis, W., Moody, C.J., 2013. A new route to α-carbolines based on 6π-electrocyclization of indole-3-alkenyl oximes. Organic letters 15(24), 6306-6308.

McBurney, R.T., Portela-Cubillo, F., Walton, J.C., 2012. Microwave assisted radical organic syntheses. RSC Advances 2(4), 1264-1274.

Mohammadi-Jam, S., Waters, K., 2014. Inverse gas chromatography applications: A review. Advances in colloid and interface science 212, 21-44.

Muchall, H.M., Werstiuk, N.H., Lessard, J., 1999. Computational studies on acyclic amidyl radicals: Π and Σ states and conformations. Journal of Molecular Structure: THEOCHEM 469(1-3), 135-142.

Newell, H.E., Buckton, G., Butler, D.A., Thielmann, F., Williams, D.R., 2001. The use of inverse phase gas chromatography to measure the surface energy of crystalline, amorphous, and recently milled lactose. Pharm. Res. 18(5), 662-666.

Oliveira, J.R., Silva, H.M., Abreu, L.P., Fernandes, S.R., 2013. Use of a warm mix asphalt additive to reduce the production temperatures and to improve the performance of asphalt rubber mixtures. Journal of Cleaner Production 41, 15-22.

Perdew, J.P., Burke, K., Ernzerhof, M., 1996. Generalized gradient approximation made simple. Phys. Rev. Lett. 77(18), 3865.

Portela-Cubillo, F., Scott, J.S., Walton, J.C., 2009. Microwave-promoted syntheses of quinazolines and dihydroquinazolines from 2-aminoarylalkanone O-phenyl oximes. The Journal of organic chemistry 74(14), 4934-4942.

Presti, D.L., Giancontieri, G., Hargreaves, D., 2017. Improving the rheometry of rubberized bitumen: experimental and computation fluid dynamics studies. Construction and Building Materials 136, 286-297.

Presti, D.L., Izquierdo, M., del Barco Carrión, A.J., 2018. Towards storage-stable high-content recycled tyre rubber modified bitumen. Construction and Building Materials 172, 106-111.

Romero-Sánchez, M.a.D., Pastor-Blas, M.M., Martín-Martínez, J.M., 2003. Treatment of a styrene-butadiene-styrene rubber with corona discharge to improve the adhesion to polyurethane adhesive. International journal of adhesion and adhesives 23(1), 49-57.

Romero-Sánchez, M.D., Martín-Martínez, J.M., 2006. Surface modifications of vulcanized SBR rubber by treatment with atmospheric pressure plasma torch. International journal of adhesion and adhesives 26(5), 345-354.

Romero-Sánchez, M.D., Walzak, M.J., Torregrosa-Maciá, R., Martín-Martínez, J.M., 2007. Surface modifications and adhesion of SBS rubber containing calcium carbonate filler by treatment with UV radiation. International journal of adhesion and adhesives 27(6), 434-445.

Schaafsma, Y., Bickel, A., Kooyman, E., 1960. Photolysis of aromatic disulphides. Tetrahedron 10(1-2), 76-80.

Schmidt, U., 1964a. Free Radicals and Free-Radical Reactions of Monovalent and Divalent Sulfur. Angewandte Chemie International Edition 3(9), 602-608.

Shatanawi, K., Biro, S., Thodesen, C., Amirkhanian, S., 2009. Effects of water activation of crumb rubber on the properties of crumb rubber-modified binders. International Journal of Pavement Engineering 10(4), 289-297.

Shu, X., Huang, B., 2014. Recycling of waste tire rubber in asphalt and portland cement concrete: An overview. Construction and Building Materials 67, 217-224.

Treloar, L., 1944. Stress-strain data for vulcanised rubber under various types of deformation. Transactions of the Faraday Society 40, 59-70.

Tyczkowski, J., Krawczyk, I., Wożniak, B., 2003. Modification of styrene–butadiene rubber surfaces by plasma chlorination. Surface and coatings technology 174, 849-853.

Walling, C., Rabinowitz, R., 1959. The Photolysis of Isobutyl Disulfide in Cumene1. Journal of the American Chemical Society 81(5), 1137-1143.

Walton, J.C., 2014. The oxime portmanteau motif: Released heteroradicals undergo incisive EPR interrogation and deliver diverse heterocycles. Accounts of chemical research 47(4), 1406-1416.

Xiang, Y., Xie, Y., Long, G., Zeng, L., 2018. Ultraviolet irradiation of crumb rubber on mechanical performance and mechanism of rubberised asphalt. Road Materials and Pavement Design, 1-14.

Xiaowei, C., Sheng, H., Xiaoyang, G., Wenhui, D., 2017. Crumb waste tire rubber surface modification by plasma polymerization of ethanol and its application on oil-well cement. Applied Surface Science 409, 325-342.

Yu, G.-X., Li, Z.-M., Zhou, X.-L., Li, C.-L., 2011. Crumb rubber–modified asphalt: microwave treatment effects. Petroleum Science and Technology 29(4), 411-417.

Yu, H., Leng, Z., Zhou, Z., Shih, K., Xiao, F., Gao, Z., 2017. Optimization of preparation procedure of liquid warm mix additive modified asphalt rubber. Journal of cleaner production 141, 336-345.

Zhang, X., Lu, C., Liang, M., 2009. Properties of natural rubber vulcanizates containing mechanochemically devulcanized ground tire rubber. Journal of Polymer Research 16(4), 411-419.

Alamawi, M.Y., Khairuddin, F.H., Yusoff, N.I.M., Badri, K., Ceylan, H., 2019. Investigation on physical, thermal and chemical properties of palm kernel oil polyol bio-based binder as a replacement for bituminous binder. Construction and Building Materials 204, 122-131.

ASTM-D3279, 2019. Standard Test Method for n-Heptane Insolubles ASTM International, West Conshohocken, PA.

ASTM-D4541, 2002. Standard Test Method for Pull-Off Strength of Coatings Using Portable Adhesion Testers. pp. 1-13.

ASTM-D7173, 2014. Standard Practice for Determining the Separation Tendency of Polymer from Polymer Modified Asphalt. ASTM.

ASTM-D7405, 2015. Standard Test Method for Multiple Stress Creep and Recovery (MSCR) of Asphalt Binder Using a Dynamic Shear Rheometer. ASTM International, West Conshohocken, PA.

Chailleux, E., Audo, M., Bujoli, B., Queffelec, C., Legrand, J., Lepine, O., 2012. Alternative binder from microalgae: Algoroute project, Workshop alternative binders for sustainable asphalt pavements. pp. pp 7-14.

Cong, P., Xun, P., Xing, M., Chen, S., 2013. Investigation of asphalt binder containing various crumb rubbers and asphalts. Construction and Building Materials 40, 632-641.

Delley, B., 1990. An all-electron numerical method for solving the local density functional for polyatomic molecules. Journal of chemical physics 92(1), 508-517.

Delley, B., 2000. From molecules to solids with the DMol3 approach. Journal of chemical physics 113(18), 7756-7764.

Derakhshandeh, B., Shojaei, A., Faghihi, M., 2008. Effects of rubber curing ingredients and phenolic-resin on mechanical, thermal, and morphological characteristics of rubber/phenolic-resin blends. Journal of applied polymer science 108(6), 3808-3821.

Dong, R., Zhao, M., Xia, W., Yi, X., Dai, P., Tang, N., 2018. Chemical and microscopic investigation of co-pyrolysis of crumb tire rubber with waste cooking oil at mild temperature. Waste Manage. (Oxford) 79, 516-525.

Dong, Z.-j., Zhou, T., Luan, H., Williams, R.C., Wang, P., Leng, Z., 2019. Composite modification mechanism of blended bio-asphalt combining styrene-butadiene-styrene with crumb rubber: A sustainable and environmental-friendly solution for wastes. Journal of cleaner production 214, 593-605.

Duan, S., Muhammad, Y., Li, J., Maria, S., Meng, F., Wei, Y., Su, Z., Yang, H., 2019. Enhancing effect of microalgae biodiesel incorporation on the performance of crumb Rubber/SBS modified asphalt. Journal of Cleaner Production, 117725.

Durairaj, B., Peterson Jr, A., Salee, G., 1989. Novel rubber compounding resorcinolic resins. Google Patents.

Fini, E.H., Kalberer, E.W., Shahbazi, A., 2011. Biobinder from swine manure: Sustainable alternative for asphalt binder.

Fini, E.H., Oldham, D.J., Abu-Lebdeh, T., 2013. Synthesis and characterization of biomodified rubber asphalt: Sustainable waste management solution for scrap tire and swine manure. Journal of Environmental Engineering 139(12), 1454-1461.

Frisch, M.J., Trucks, G.W., Schlegel, H.B., al., e., 2009. GAUSSIAN 09. revision A.1, Gaussian, Inc., Wallingford CT.

Gao, J., Wang, H., You, Z., Mohd Hasan, M., Lei, Y., Irfan, M., 2018. Rheological behavior and sensitivity of wood-derived bio-oil modified asphalt binders. Applied Sciences 8(6), 919.

Hosseinnezhad, S., Fini, E.H., Sharma, B.K., Basti, M., Kunwar, B., 2015. Physiochemical characterization of synthetic bio-oils produced from bio-mass: a sustainable source for construction bio-adhesives. RSC Advances 5(92), 75519-75527.

Hosseinnezhad, S., Kabir, S.F., Oldham, D., Mousavi, M., Fini, E.H., 2019. Surface functionalization of rubber particles to reduce phase separation in rubberized asphalt for sustainable construction. Journal of Cleaner Production 225, 82-89.

Kun, D., Pukánszky, B., 2017. Polymer/lignin blends: Interactions, properties, applications. European Polymer Journal 93, 618-641.

Lattimer, R.P., Kinsey, R.A., Layer, R.W., Rhee, C., 1989. The mechanism of phenolic resin vulcanization of unsaturated elastomers. Rubber chemistry and technology 62(1), 107-123.

Lei, Y., Wang, H., Fini, E.H., You, Z., Yang, X., Gao, J., Dong, S., Jiang, G., 2018. Evaluation of the effect of bio-oil on the high-temperature performance of rubber modified asphalt. Construction and Building Materials 191, 692-701.

Liang, M., Xin, X., Fan, W., Ren, S., Shi, J., Luo, H., 2017. Thermo-stability and aging performance of modified asphalt with crumb rubber activated by microwave and TOR. Materials & Design 127, 84-96.

Liu, W.W., Ma, J.J., Zhan, M.S., Wang, K., 2015. The toughening effect and mechanism of styrene-butadiene rubber nanoparticles for novolac resin. Journal of Applied Polymer Science 132(9).

Moraes, R., Velasquez, R., Bahia, H.U., 2011. Measuring the effect of moisture on asphalt–aggregate bond with the bitumen bond strength test. Transportation Research Record 2209(1), 70-81.

Mousavi, M., Hosseinnezhad, S., Kabir, S.F., Burnett, D.J., Fini, E.H., 2019. Reaction pathways for surface activated rubber particles. Resources, Conservation and Recycling 149, 292-300.

Obrecht, W., Sumner, A., 2004. Rubber gels and rubber compounds containing phenolic resin adducts. Google Patents.

Peralta, J., Williams, R.C., Rover, M., Silva, H.M.R.D.d., 2012. Development of a rubber-modified fractionated bio-oil for use as noncrude petroleum binder in flexible pavements. Transportation Research Circular(E-C165), 23-36.

Perdew, J.P., Burke, K., Ernzerhof, M., 1996. Generalized gradient approximation made simple. Phys. Rev. Lett. 77(18), 3865.

Presti, D.L., Izquierdo, M., del Barco Carrión, A.J., 2018. Towards storage-stable high-content recycled tyre rubber modified bitumen. Construction and Building Materials 172, 106-111.

Schmidt, U., 1964. Free radicals and free-radical reactions of monovalent and divalent sulfur. Angewandte Chemie International Edition in English 3(9), 602-608.

Shatanawi, K., Biro, S., Thodesen, C., Amirkhanian, S., 2009. Effects of water activation of crumb rubber on the properties of crumb rubber-modified binders. International Journal of Pavement Engineering 10(4), 289-297.

Shatanawi, K.M., Biro, S., Geiger, A., Amirkhanian, S.N., 2012. Effects of furfural activated crumb rubber on the properties of rubberized asphalt. Construction and Building Materials 28(1), 96-103.

Shatanawi, K.M., Biro, S., Naser, M., Amirkhanian, S.N., 2013. Improving the rheological properties of crumb rubber modified binder using hydrogen peroxide. Road Materials and Pavement Design 14(3), 723-734.

Sienkiewicz, M., Borzędowska-Labuda, K., Wojtkiewicz, A., Janik, H., 2017. Development of methods improving storage stability of bitumen modified with ground tire rubber: A review. Fuel Process. Technol. 159, 272-279.

Vainio, U., Maximova, N., Hortling, B., Laine, J., Stenius, P., Simola, L.K., Gravitis, J., Serimaa, R., 2004. Morphology of dry lignins and size and shape of dissolved kraft lignin particles by X-ray scattering. Langmuir 20(22), 9736-9744.

Walling, C., Rabinowitz, R., 1959. The Photolysis of Isobutyl Disulfide in Cumene1. Journal of the American Chemical Society 81(5), 1137-1143.

Wang, C., Xue, L., Xie, W., You, Z., Yang, X., 2018. Laboratory investigation on chemical and rheological properties of bio-asphalt binders incorporating waste cooking oil. Construction and Building Materials 167, 348-358.

Xie, J., Yang, Y., Lv, S., Peng, X., Zhang, Y., 2019. Investigation on Preparation Process and Storage Stability of Modified Asphalt Binder by Grafting Activated Crumb Rubber. Materials 12(12), 2014.

Yang, Y., Zhang, Y., Omairey, E., Cai, J., Gu, F., Bridgwater, A.V., 2018. Intermediate pyrolysis of organic fraction of municipal solid waste and rheological study of the pyrolysis oil for potential use as bio-bitumen. Journal of Cleaner Production 187, 390-399.

Yu, G.-X., Li, Z.-M., Zhou, X.-L., Li, C.-L., 2011. Crumb rubber–modified asphalt: microwave treatment effects. Petroleum Science and Technology 29(4), 411-417.

Yu, J., Ren, Z., Gao, Z., Wu, Q., Zhu, Z., Yu, H., 2019. Recycled Heavy Bio Oil as Performance Enhancer for Rubberized Bituminous Binders. Polymers 11(5), 800.

Zeng, M., Li, J., Zhu, W., Xia, Y., 2018. Laboratory evaluation on residue in castor oil production as rejuvenator for aged paving asphalt binder. Construction and Building Materials 193, 276-285.

Zhang, R., You, Z., Wang, H., Chen, X., Si, C., Peng, C., 2018. Using bio-based rejuvenator derived from waste wood to recycle old asphalt. Construction and Building Materials 189, 568-575.

Zhang, X., Lu, C., Liang, M., 2009. Properties of natural rubber vulcanizates containing mechanochemically devulcanized ground tire rubber. Journal of Polymer Research 16(4), 411-419.

AASHTO-T315, 2012. Standard method of test for determining the rheological properties of asphalt binder using a dynamic shear rheometer (DSR).

Adamu, I., Aziz, M., Yeow, Y., Jakarmi, F.M., 2019. Dielectric measurement of bitumen: A review, IOP Conference Series: Materials Science and Engineering. IOP Publishing, p. 012056.

Ahmed, R.B., Hossain, K., 2020. Waste cooking oil as an asphalt rejuvenator: A state-of-the-art review. Construction and Building Materials 230, 116985.

Al-Qadi, I.L., Abauwad, I.M., Dhasmana, H., Coenen, A.R., 2014. Effects of various asphalt binder additives/modifiers on moisture-susceptible asphaltic mixtures. Illinois Center for Transportation.

Alexander, S., 1973. Method of treating asphalt. Google Patents.

ASTMD7175-15, 2015. Standard Test Method for Determining the Rheological Properties of Asphalt Binder Using a Dynamic Shear Rheometer. ASTM International, West Conshohocken, PA, 2015, www.astm.org.

Baumgardner, G.L., Masson, J., Hardee, J.R., Menapace, A.M., Williams, A.G., 2005. Polyphosphoric acid modified asphalt: proposed mechanisms. Journal of the Association of Asphalt Paving Technologists 74, 283-305.

Bonardd, S., Moreno-Serna, V., Kortaberria, G., Díaz Díaz, D., Leiva, A., Saldías, C., 2019. Dipolar glass polymers containing polarizable groups as dielectric materials for energy storage applications. A Minireview. Polymers 11(2), 317.

Bykov, G., Ershov, B., 2010. A sorbent based on phosphorylated lignin. Russian Journal of Applied Chemistry 83(2), 316-319.

Chailleux, E., Audo, M., Bujoli, B., Queffelec, C., Legrand, J., Lepine, O., 2012. Alternative Binder from microalgae: Algoroute project, Workshop alternative binders for sustainable asphalt pavements. pp. pp 7-14.

Chen, M., Leng, B., Wu, S., Sang, Y., 2014. Physical, chemical and rheological properties of waste edible vegetable oil rejuvenated asphalt binders. Construction and Building materials 66, 286-298.

D3279-19, A., 2019. Standard Test Method for n-Heptane Insolubles. ASTM International, www.astm.org, West Conshohocken, PA.

D'Angelo, J.A., 2012. Polyphosphoric Acid Modification of Asphalt Binders: A Workshop. Workshop Summary. Transportation Research E-Circular(E-C160).

Delley, B., 1990. An all-electron numerical method for solving the local density functional for polyatomic molecules. Journal of chemical physics 92(1), 508-517.

Delley, B., 2000. From molecules to solids with the DMol3 approach. Journal of chemical physics 113(18), 7756-7764.

Dupont, J., 2003. VEGETABLE OILS| Dietary Importance.

Eberhardsteiner, L., Füssl, J., Hofko, B., Handle, F., Hospodka, M., Blab, R., Grothe, H., 2015. Influence of asphaltene content on mechanical bitumen behavior: experimental

investigation and micromechanical modeling. Materials and Structures 48(10), 3099-3112.

Edwards, Y., Tasdemir, Y., Isacsson, U., 2006. Rheological effects of commercial waxes and polyphosphoric acid in bitumen 160/220—low temperature performance. Fuel 85(7-8), 989-997.

Ernzerhof, M., Scuseria, G.E., 1999. Assessment of the Perdew–Burke–Ernzerhof exchange-correlation functional. The Journal of chemical physics 110(11), 5029-5036.

Falkiewicz, M., Grzybowski, K., 2004. Polyphosphoric Acid in Asphalt Modification, Western Research Institute Symposium on Pavement Performance Prediction, Laramie, Wyo.

Fini, E.H., Kalberer, E.W., Shahbazi, A., Basti, M., You, Z., Ozer, H., Aurangzeb, Q., 2011b. Chemical characterization of biobinder from swine manure: Sustainable modifier for asphalt binder. Journal of Materials in Civil Engineering 23(11), 1506-1513.

Grimme, S., 2011. Density functional theory with London dispersion corrections. Wiley Interdisciplinary Reviews: Computational Molecular Science 1(2), 211-228.

Hossain, Z., Alam, M.S., Baumgardner, G., 2018. Evaluation of rheological performance and moisture susceptibility of polyphosphoric acid modified asphalt binders. Road Materials and Pavement Design, 1-16.

Hosseinnezhad, S., Fini, E.H., Sharma, B.K., Basti, M., Kunwar, B., 2015b. Physiochemical characterization of synthetic bio-oils produced from bio-mass: a sustainable source for construction bio-adhesives. RSC Advances 5(92), 75519-75527.

Kabir, S.F., Mousavi, M., Fini, E.H., 2019. Selective adsorption of bio-oils' molecules onto rubber surface and its effects on stability of rubberized asphalt. Journal of Cleaner Production, 119856.

Kabir, S.F., Mousavi, M., Fini, E.H., 2020. Selective adsorption of bio-oils' molecules onto rubber surface and its effects on stability of rubberized asphalt. Journal of Cleaner Production 252, 119856.

Kodrat, I., Sohn, D., Hesp, S., 2007. Comparison of polyphosphoric acid-modified asphalt binders with straight and polymer-modified materials. Transportation Research Record: Journal of the Transportation Research Board(1998), 47-55.

Kun, D., Pukánszky, B., 2017. Polymer/lignin blends: Interactions, properties, applications. European Polymer Journal 93, 618-641.

Li, X., Clyne, T., Reinke, G., Johnson, E.N., Gibson, N., Kutay, M.E., 2011. Laboratory evaluation of asphalt binders and mixtures containing polyphosphoric acid. Transportation research record 2210(1), 47-56.

Liu, J., Yan, K., Liu, J., 2018. Rheological properties of warm mix asphalt binders and warm mix asphalt binders containing polyphosphoric acid. International Journal of Pavement Research and Technology 11(5), 481-487.

Liu, J., Yan, K., You, L., Ge, D., Wang, Z., 2016. Laboratory performance of warm mix asphalt binder containing polyphosphoric acid. Construction and Building Materials 106, 218-227.

Loza, R., Dammann, L.G., Hayner, R.E., Doolin, P.K., 2000. Unblown ethylene-vinyl acetate copolymer treated asphalt and its method of preparation. Google Patents.

Maldonaldo, R., Falkiewicz, M., Bazi, G., Grzybowski, K., 2006. Asphalt modification with polyphosphoric acid, PROCEEDINGS OF THE FIFTY-FIRST ANNUAL CONFERENCE OF THE CANADIAN TECHNICAL ASPHALT ASSOCIATION (CTAA): CHARLOTTETOWN, PRINCE EDWARD ISLAND, NOVEMBER 2006.

Martin, J.-V., 2011. Asphalt additive with improved performance. Google Patents.

Masson, J., 2008. Brief review of the chemistry of polyphosphoric acid (PPA) and bitumen. Energy & Fuels 22(4), 2637-2640.

Masson, J., Gagné, M., 2008. Ionic pairs in polyphosphoric acid (PPA)-modified bitumen: insights from model compounds. Energy & fuels 22(5), 3390-3394.

Masson, J., Gagné, M., Robertson, G., Collins, P., 2008. Reactions of polyphosphoric acid and bitumen model compounds with oxygenated functional groups: where is the phosphorylation? Energy & fuels 22(6), 4151-4157.

Mousavi, M., Fini, E.H., 2019. Moderating Effects of Paraffin Wax on Interactions between Polyphosphoric Acid and Bitumen Constituents. ACS Sustainable Chemistry & Engineering 7(24), 19739-19749.

Mousavi, M., Høgsaa, B., Fini, E.H., 2019a. Intermolecular interactions of bio-modified halloysite nanotube within high-impact polystyrene and linear low-density polyethylene. Applied Surface Science 473, 750-760.

Mousavi, M., Oldham, D.J., Hosseinnezhad, S., Fini, E.H., 2019c. Multiscale Evaluation of Synergistic and Antagonistic Interactions between Bitumen Modifiers. ACS Sustainable Chemistry & Engineering 7(18), 15568-15577.

Naher, J., Gloster, C., Doss, C.C., Jadhav, S.S., 2020a. An Automated Tool for Design Space Exploration of Matrix Vector Multiplication (MVM) Kernels Using OpenCL Based Implementation on FPGAs, 2020 IEEE 28th Annual International Symposium on Field-Programmable Custom Computing Machines (FCCM). IEEE, pp. 205-205.

Naher, J., Gloster, C., Doss, C.C., Jadhav, S.S., 2020b. Using Machine Learning to Estimate Utilization and Throughput for OpenCL-Based Matrix-Vector Multiplication (MVM), 2020 10th Annual Computing and Communication Workshop and Conference (CCWC). IEEE, pp. 0365-0372.

Naher, J., Gloster, C., Jadhav, S.S., Doss, C.C., 2020c. Design Space Exploration of an OpenCL Based SAXPY Kernel Implementation on FPGAs.

Naher, J., Sakib, A.S., Jadhav, S.S., Gloster, C., Doss, C.C., 2019. An FPGA based implementation of the Conjugate Gradient Kernels, 2019 4th International Conference on Electrical Information and Communication Technology (EICT). IEEE, pp. 1-6.

Orange, G., Dupuis, D., Martin, J., Farcas, F., Such, C., Marcant, B., 2004. Chemical modification of bitumen through polyphosphoric acid: properties-micro-structure relationship, PROCEEDINGS OF THE 3RD EURASPHALT AND EUROBITUME CONGRESS HELD VIENNA, MAY 2004.

Orlando Jr, C.M., Wirth, J., Heath, D., 1970. Methyl aryl ether cleavage in benzazole syntheses in polyphosphoric acid. The Journal of Organic Chemistry 35(9), 3147-3149.

Perdew, J.P., Burke, K., Ernzerhof, M., 1996. Generalized gradient approximation made simple. Phys. Rev. Lett. 77(18), 3865.

Platonov, V., 2000. Properties of polyphosphoric acid. Fibre Chemistry 32(5), 325-329.

Raouf, M.A., Williams, R.C., 2010. Rheology of fractionated cornstover bio-oil as a pavement material. International Journal of Pavements 9(1-2-3).

Rappoport, D., Crawford, N.R., Furche, F., Burke, K., Wiley, C., 2008. Which functional should I choose? Computational Inorganic and Bioinorganic Chemistry, 594.

Sakakura, A., Katsukawa, M., Ishihara, K., 2005. Selective synthesis of phosphate monoesters by dehydrative condensation of phosphoric acid and alcohols promoted by nucleophilic bases. Organic letters 7(10), 1999-2002.

Sun, Z., Yi, J., Huang, Y., Feng, D., Guo, C., 2016. Properties of asphalt binder modified by bio-oil derived from waste cooking oil. Construction and Building Materials 102, 496-504.

Vainio, U., Maximova, N., Hortling, B., Laine, J., Stenius, P., Simola, L.K., Gravitis, J., Serimaa, R., 2004. Morphology of dry lignins and size and shape of dissolved kraft lignin particles by X-ray scattering. Langmuir 20(22), 9736-9744.

Wen, H., Bhusal, S., Wen, B., 2012. Laboratory evaluation of waste cooking oil-based bioasphalt as an alternative binder for hot mix asphalt. Journal of Materials in Civil Engineering 25(10), 1432-1437.

Xiao, F., Amirkhanian, S., Wang, H., Hao, P., 2014. Rheological property investigations for polymer and polyphosphoric acid modified asphalt binders at high temperatures. Construction and Building Materials 64, 316-323.

Xiu, S., Rojanala, H., Shahbazi, A., Fini, E., Wang, L., 2011. Pyrolysis and combustion characteristics of Bio-oil from swine manure. Journal of thermal analysis and calorimetry 107(2), 823-829.

Yang, X., You, Z.-P., Dai, Q.-L., 2013. Performance evaluation of asphalt binder modified by bio-oil generated from waste wood resources. International Journal of Pavement Research and Technology 6(4), 431-439.

Yang, X., You, Z., Dai, Q., Mills-Beale, J., 2014. Mechanical performance of asphalt mixtures modified by bio-oils derived from waste wood resources. Construction and Building Materials 51, 424-431.

You, Z., Mills-Beale, J., Fini, E., Goh, S.W., Colbert, B., 2011. Evaluation of low-temperature binder properties of warm-mix asphalt, extracted and recovered RAP and RAS, and bioasphalt. Journal of materials in Civil Engineering 23(11), 1569-1574.

Zaumanis, M., Mallick, R.B., Poulikakos, L., Frank, R., 2014. Influence of six rejuvenators on the performance properties of Reclaimed Asphalt Pavement (RAP) binder and 100% recycled asphalt mixtures. Construction and Building Materials 71, 538-550.

Zeng, M., Li, J., Zhu, W., Xia, Y., 2018. Laboratory evaluation on residue in castor oil production as rejuvenator for aged paving asphalt binder. Construction and Building Materials 193, 276-285.

Zeng, M., Pan, H., Zhao, Y., Tian, W., 2016. Evaluation of asphalt binder containing castor oil-based bioasphalt using conventional tests. Construction and Building Materials 126, 537-543.

Zhang, F., Hu, C., Zhang, Y., 2018a. The effect of PPA on performances and structures of high-viscosity modified asphalt. Journal of Thermal Analysis and Calorimetry 134(3), 1729-1738.

Zhang, F., Hu, C., Zhang, Y., 2018b. Influence of poly (phosphoric acid) on the properties and structure of ethylene–vinyl acetate-modified bitumen. Journal of Applied Polymer Science 135(29), 46553.

Zhang, F., Yu, J., 2010. The research for high-performance SBR compound modified asphalt. Construction and Building Materials 24(3), 410-418.

Alavi, Z., Hung, S., Jones, D., Harvey, J., 2016. Preliminary Investigation into the Use of Reclaimed Asphalt Pavement in Gap-Graded Asphalt Rubber Mixes, and Use of Reclaimed Asphalt Rubber Pavement in Conventional Asphalt Concrete Mixes.

Apeagyei, A.K., 2011. Laboratory evaluation of antioxidants for asphalt binders. Construction and Building Materials 25(1), 47-53.

Bahia, H.U., Zhai, H., Rangel, A., 1998. Evaluation of stability, nature of modifier, and short-term aging of modified binders using new tests: LAST, PAT, and modified RTFO. Transportation Research Record 1638(1), 64-71.

Bressi, S., Fiorentini, N., Huang, J., Losa, M., 2019. Crumb rubber modifier in road asphalt pavements: state of the art and statistics. Coatings 9(6), 384.

Caltrans, 2019. Cost Differential Analysis Between Asphalt Containing Crumb Rubber and Conventional Asphalt, Public Resources Code Section 42703. Caltrans.

Cong, P., Xu, P., Chen, S., 2014. Effects of carbon black on the anti aging, rheological and conductive properties of SBS/asphalt/carbon black composites. Construction and Building Materials 52, 306-313.

EAPA, 2020. Warm Mix Asphalt. https://eapa.org/warm-mix-asphalt/. (Accessed July 17 2020).

EIA, 2019. Energy Expplained-Biomass Independent Statistics and Analysis. www.eia.gov/energyexplained/biomass/. 2020).

EPA, 2013. Coking is a refinery process that produces 19% of finished petroleum product exports. https://www.eia.gov/todayinenergy/detail.php?id=9731.

FHWA, 2014. The Use of Recycled Tire Rubber to Modify Asphalt Binder and Mixtures in: Office of Asset Management, P., and Construction (Ed.).

FHWA, 2020. Average Monthly Asphalt Price. highways.dot.gov/federal-lands/business/escalation-factors-wfl/2020-average-monthly-asphalt-prices. (Accessed 20 June 2020).

Fini, E.H., Buabeng, F.S., Abu-Lebdeh, T., Awadallah, F., 2016. Effect of introduction of furfural on asphalt binder ageing characteristics. Road Materials and Pavement Design 17(3), 638-657.

Fini, E.H., Kalberer, E.W., Shahbazi, A., Basti, M., You, Z., Ozer, H., Aurangzeb, Q., 2011b. Chemical characterization of biobinder from swine manure: Sustainable modifier for asphalt binder. Journal of Materials in Civil Engineering 23(11), 1506-1513.

Fini, E.H., Samieadel, A., Rajib, A., 2020. Moisture Damage and Its Relation to Surface Adsorption/Desorption of Rejuvenators. Industrial & Engineering Chemistry Research.

Fini, E.H., Yang, S.-H., Xiu, S., 2010. Characterization and application of manure-based bio-binder in asphalt industry.

Ghasemi-Kahrizsangi, A., Neshati, J., Shariatpanahi, H., Akbarinezhad, E., 2015. Improving the UV degradation resistance of epoxy coatings using modified carbon black nanoparticles. Progress in Organic Coatings 85, 199-207.

Globenewswire, 2019. Bitumen Market To Reach USD 112.01 Billion By 2026: Reports And Data. https://www.globenewswire.com/news-release/2019/04/11/1802979/0/en/Bitumen-Market-To-Reach-USD-112-01-Billion-By-2026-Reports-And-Data.html. (Accessed 11 April, 2020 2020).

He, X., Hochstein, D., Ge, Q., Ali, A.W., Chen, F., Yin, H., 2018. Accelerated aging of asphalt by UV photo-oxidation considering moisture and condensation effects. Journal of Materials in Civil Engineering 30(1), 04017261.

Hosseinnezhad, S., Hung, A.M., Mousavi, M., Sharma, B.K., Fini, E., 2020. Resistance Mechanisms of Biomodified Binders against Ultraviolet Exposure. ACS Sustainable Chemistry & Engineering 8(6), 2390-2398.

Hosseinnezhad, S., Oldham, D., Fini, E.H., Sharma, B.K., Kunwar, B., 2015c. Investigation of effectiveness of liquid rubber as a modifier for asphalt binder.

Hosseinnezhad, S., Shakiba, S., Mousavi, M., Louie, S.M., Karnati, S.R., Fini, E.H., 2019b. Multi-scale Evaluation of Moisture Susceptibility of Bio-Modified Bitumen. ACS Applied Bio Materials.

Hosseinnezhad, S., Zadshir, M., Yu, X., Yin, H., Sharma, B.K., Fini, E., 2019c. Differential effects of ultraviolet radiation and oxidative aging on bio-modified binders. Fuel 251, 45-56.

Hung, A.M., Fini, E.H., 2019. Absorption spectroscopy to determine the extent and mechanisms of aging in bitumen and asphaltenes. Fuel 242, 408-415.

Hung, A.M., Kazembeyki, M., Hoover, C.G., Fini, E.H., 2019a. Evolution of Morphological and Nanomechanical Properties of Bitumen Thin Films as a Result of Compositional Changes Due to Ultraviolet Radiation. ACS Sustainable Chemistry & Engineering 7(21), 18005-18014.

Kabir, S.F., Mousavi, M., Fini, E.H., 2019. Selective adsorption of bio-oils' molecules onto rubber surface and its effects on stability of rubberized asphalt. Journal of Cleaner Production, 119856.

Lei, Z., Bahia, H., Yi-qiu, T., 2015. Effect of bio-based and refined waste oil modifiers on low temperature performance of asphalt binders. Construction and Building Materials 86, 95-100.

Li, Y., Wu, S., Liu, Q., Xie, J., Li, H., Dai, Y., Li, C., Nie, S., Song, W., 2019. Aging effects of ultraviolet lights with same dominant wavelength and different wavelength ranges on a hydrocarbon-based polymer (asphalt). Polymer Testing 75, 64-75.

Liang, M., Ren, S., Fan, W., Wang, H., Cui, W., Zhao, P., 2017a. Characterization of fume composition and rheological properties of asphalt with crumb rubber activated by microwave and TOR. Construction and Building Materials 154, 310-322.

Lu, X., Isacsson, U., 1998. Chemical and rheological evaluation of ageing properties of SBS polymer modified bitumens. Fuel 77(9-10), 961-972.

NRC, 1994. Microwave processing of materials. National Academies Press.

NREL, N.R.E.L., 2020. “Solar Energy and Solar Power in Arizona.”. (Accessed 8 june 2020).

Oldham, D., 2020. Implications of Bio-Modification on Moisture Damage Mechanisms in Asphalt Binder Matrix. Arizona State University.

Oldham, D.J., Rajib, A.I., Onochie, A., Fini, E.H., 2019. Durability of bio-modified recycled asphalt shingles exposed to oxidation aging and extended sub-zero conditioning. Construction and Building Materials 208, 543-553.

Pahlavan, F., Mousavi, M., Hung, A.M., Fini, E.H., 2018. Characterization of oxidized asphaltenes and the restorative effect of a bio-modifier. Fuel 212, 593-604.

Pahlavan, F., Rajib, A., Deng, S., Lammers, P., Fini, E.H., 2020. Investigation of Balanced Feedstocks of Lipids and Proteins To Synthesize Highly Effective Rejuvenators for Oxidized Asphalt. ACS Sustainable Chemistry & Engineering.

Pahlavan, F., Samieadel, A., Deng, S., Fini, E., 2019. Exploiting Synergistic Effects of Intermolecular Interactions To Synthesize Hybrid Rejuvenators To Revitalize Aged Asphalt. ACS Sustainable Chemistry & Engineering 7(18), 15514-15525.

Qin, Q., Schabron, J.F., Boysen, R.B., Farrar, M.J., 2014. Field aging effect on chemistry and rheology of asphalt binders and rheological predictions for field aging. Fuel 121, 86-94.

Rajib, A.I., Pahlavan, F., Fini, E.H., 2020. Investigating Molecular-Level Factors That Affect the Durability of Restored Aged Asphalt Binder. Journal of Cleaner Production, 122501.

Salomon, D., Zhai, H., 2002. Ranking asphalt binders by activation energy for flow. Journal of Applied Asphalt Binder Technology 2(2), 52-60.

Samieadel, A., 2020. Multi-Scale Characterization of Bitumen Doped with Sustainable Modifiers. Arizona State University.

Samieadel, A., Rajib, A.I., Dandamudi, K.P.R., Deng, S., Fini, E.H., 2020. Improving recycled asphalt using sustainable hybrid rejuvenators with enhanced intercalation into oxidized asphaltenes nanoaggregates. Construction and Building Materials 262, 120090.

Sengupta, M., Xie, Y., Lopez, A., Habte, A., Maclaurin, G., Shelby, J., 2018. The national solar radiation data base (NSRDB). Renewable and Sustainable Energy Reviews 89, 51-60.

Sirin, O., Paul, D.K., Kassem, E., 2018. State of the art study on aging of asphalt mixtures and use of antioxidant additives. Advances in Civil Engineering 2018.

Tsoskounoglou, M., Ayerides, G., Tritopoulou, E., 2008. The end of cheap oil: Current status and prospects. Energy Policy 36(10), 3797-3806.

Wang, Q., Li, S., Wu, X., Wang, S., Ouyang, C., 2016. Weather aging resistance of different rubber modified asphalts. Construction and Building Materials 106, 443-448.

Wen, Y., Liu, Q., Chen, L., Pei, J., Zhang, J., Li, R., 2020. Review and comparison of methods to assess the storage stability of terminal blend rubberized asphalt binders. Construction and Building Materials 258, 119586.

Wright, M.M., Daugaard, D.E., Satrio, J.A., Brown, R.C., 2010. Techno-economic analysis of biomass fast pyrolysis to transportation fuels. Fuel 89, S2-S10.

Wu, S., Zhao, Z., Li, Y., Pang, L., Amirkhanian, S., Riara, M., 2017. Evaluation of aging resistance of graphene oxide modified asphalt. Applied Sciences 7(7), 702.

Xiang, L., Cheng, J., Kang, S., 2015. Thermal oxidative aging mechanism of crumb rubber/SBS composite modified asphalt. Construction and Building Materials 75, 169-175.

Xiu, S., Rojanala, H., Shahbazi, A., Fini, E., Wang, L., 2012. Pyrolysis and combustion characteristics of Bio-oil from swine manure. Journal of thermal analysis and calorimetry 107(2), 823-829.

Yang, X., You, Z., Dai, Q., Mills-Beale, J., 2014. Mechanical performance of asphalt mixtures modified by bio-oils derived from waste wood resources. Construction and Building Materials 51, 424-431.

You, Z., Mills-Beale, J., Fini, E., Goh, S.W., Colbert, B., 2011. Evaluation of low-temperature binder properties of warm-mix asphalt, extracted and recovered RAP and RAS, and bioasphalt. Journal of materials in Civil Engineering 23(11), 1569-1574.

Yu, H., Bai, X., Qian, G., Wei, H., Gong, X., Jin, J., Li, Z., 2019. Impact of ultraviolet radiation on the aging properties of SBS-modified asphalt binders. Polymers 11(7), 1111.

Yu, J.-Y., Feng, P.-C., Zhang, H.-L., Wu, S.-P., 2009. Effect of organo-montmorillonite on aging properties of asphalt. Construction and Building Materials 23(7), 2636-2640.

Zadshir, M., Hosseinnezhad, S., Ortega, R., Chen, F., Hochstein, D., Xie, J., Yin, H., Parast, M.M., Fini, E.H., 2018. Application of a Biomodifier as Fog Sealants to Delay Ultraviolet Aging of Bituminous Materials. J. Mater. Civ. Eng. 30(12), 04018310.

Zadshir, M., Ploger, D., Yu, X., Sangiorgi, C., Yin, H., 2020. Chemical, thermophysical, rheological, and microscopic characterisation of rubber modified asphalt binder exposed to UV radiation. Road Materials and Pavement Design, 1-17.

Zeng, W., Wu, S., Pang, L., Chen, H., Hu, J., Sun, Y., Chen, Z., 2018. Research on Ultra Violet (UV) aging depth of asphalts. Construction and Building Materials 160, 620-627.

Zhang, D., Zhang, H., Shi, C., 2017. Investigation of aging performance of SBS modified asphalt with various aging methods. Construction and Building Materials 145, 445-451.

Zhang, H., Chen, Z., Xu, G., Shi, C., 2018. Evaluation of aging behaviors of asphalt binders through different rheological indices. Fuel 221, 78-88.

Zhang, R., Wang, H., Gao, J., Yang, X., You, Z., 2017. Comprehensive performance evaluation and cost analysis of SBS-modified bioasphalt binders and mixtures. Journal of Materials in Civil Engineering 29(12), 04017232.

Zhu, H., Xu, G., Gong, M., Yang, J., 2017. Recycling long-term-aged asphalts using bio-binder/plasticizer-based rejuvenator. Construction and Building Materials 147, 117-129.

Caltrans, 2019. Cost Differential Analysis Between Asphalt Containing Crumb Rubber and Conventional Asphalt, Public Resources Code Section 42703. Caltrans.

EIA, 2019. Energy Expplained-Biomass Independent Statistics and Analysis. www.eia.gov/energyexplained/biomass/. 2020).

FHWA, 2020. Average Monthly Asphalt Price. highways.dot.gov/federal-lands/business/escalation-factors-wfl/2020-average-monthly-asphalt-prices. (Accessed 20 June 2020).

Fini, E.H., Kalberer, E.W., Shahbazi, A., Basti, M., You, Z., Ozer, H., Aurangzeb, Q., 2011. Chemical characterization of biobinder from swine manure: Sustainable modifier for asphalt binder. Journal of Materials in Civil Engineering 23(11), 1506-1513.

Fini, E.H., Yang, S.-H., Xiu, S., 2010. Characterization and application of manure-based bio-binder in asphalt industry.

Globenewswire, 2019. Bitumen Market To Reach USD 112.01 Billion By 2026: Reports And Data. https://www.globenewswire.com/news-release/2019/04/11/1802979/0/en/Bitumen-Market-To-Reach-USD-112-01-Billion-By-2026-Reports-And-Data.html. (Accessed 11 April, 2020 2020).

Lei, Z., Bahia, H., Yi-qiu, T., 2015. Effect of bio-based and refined waste oil modifiers on low temperature performance of asphalt binders. Construction and Building Materials 86, 95-100.

Wright, M.M., Daugaard, D.E., Satrio, J.A., Brown, R.C., 2010. Techno-economic analysis of biomass fast pyrolysis to transportation fuels. Fuel 89, S2-S10.

Zhang, R., Wang, H., Gao, J., Yang, X., You, Z., 2017. Comprehensive performance evaluation and cost analysis of SBS-modified bioasphalt binders and mixtures. Journal of Materials in Civil Engineering 29(12), 04017232.

APPENDIX A

PREVIOUSLY PUBLISHED WORK

Chapters 2, 5, and 6 are all studies that have been submitted for peer review and currently under review.

The materials, which has been published prior to the submission of this dissertation, is Chapter 3 and 4, which was in Journal of Cleaner production and Resource, Conservation and Recycling. They are cited below:

Hosseinnezhad, S., Kabir, S. F., Oldham, D., Mousavi, M., & Fini, E. H. (2019). Surface functionalization of rubber particles to reduce phase separation in rubberized asphalt for sustainable construction. Journal of cleaner production, 225, 82-89.

In this publication, Sk Faisal Kabir prepared all of the samples used for binder testing which includes weighing, surface activating and blending the binder. Faisal also prepared samples for Cigar tube test, performed viscosity and MSCR testing and analyzed them. Faisal also wrote introduction of the paper and relevant sections of analysis.

Kabir, S. F., Mousavi, M., & Fini, E. H. (2019). Selective adsorption of bio-oils' molecules onto rubber surface and its effects on stability of rubberized asphalt. Journal of cleaner production, 119856.

In this publication, Sk Faisal Kabir prepared all of the samples used for binder testing which includes weighing, surface activating and blending the binder. Faisal also performed all tests and analyzed. Faisal also wrote the draft of the paper except for the part of computational modeling.

APPENDIX B

COAUTHOR PERMISSION FOR PREVIOUSLY PUBSLISHED WORK

Co-Authors:

Dr. Masoumeh Mousavi

Dr. Shahrzad Hosseinnezhad

Sk Faisal Kabir

Dr. Daniel J. Burnett

Dr. Ellie H. Fini

Have granted their permission for the use of the following publication to be used for the dissertation of Sk Faisal Kabir.

Mousavi, M., Hosseinnezhad, S., Kabir, S.F., Burnett, D.J., Fini, E.H., 2019. Reaction pathways for surface activated rubber particles. Resources, Conservation and Recycling 149, 292-300.

BIOGRAPHICAL SKETCH

Sk Faisal Kabir grew up in Port city Khulna, Bangladesh with one elder brother. His mother is a housewife and his father is a retired banker. He received his elementary education from Saint Joseph's Infant School and secondary education from Khulna Zilla School. He completed his higher secondary education from Notre Dame College, Dhaka. In 2006, he started an BSc in Civil Engineering program at Bangladesh University of Engineering and Technology (BUET) and graduated in 2011. He then worked for Bangladesh Government as Maintenance Engineer in Public Works Department (PWD) till 2013. He then started his MS in Civil Engineering, at North Carolina A&T State University (NC A&T) in the MS in Civil Engineering program. After finishing his MS in civil engineering in 2015 he started PhD in the Nanoengineering program in 2016. Then he transferred to Civil, Environmental, and Sustainable Engineering Program at Arizona State University in 2019. So far, he has over 5 journal publications, 2 conference posters, 21 citations.

In his personal life he is married to Dr. Jannatun Naher and blessed with a one-year old son Rishav Aditya Faisal.